Idiopathic pulmonary fibrosis:

exploration of aberrant epithelial wound repair

and stem cell-mediated regenerative approaches

Khondoker Mehedi Akram

School of Postgraduate Medicine

Institute for Science and Technology in Medicine

Keele University

Thesis submitted to the Keele University for the degree of

Doctor of Philosophy

February 2013

List of contents

Abstract

Idiopathic pulmonary fibrosis (IPF) is a fatal form of fibrotic lung disease. The pathogenesis of IPF is unclear. An aberrant alveolar epithelial wound repair is likely to be involved in the disease process. Alveolar bronchiolisation, a process where bronchiolar Clara cells migrate into the affected alveoli, is a manifestation of abnormal alveolar wound repair. The role of Clara cells during alveolar injury repair in IPF is controversial. This study was undertaken to investigate the role of Clara cells in alveolar epithelial wound repair and pulmonary fibrosis. Currently, there is no curative treatment for IPF; therefore, stem-cell mediated regenerative therapy has been suggested. In this study, the paracrine role hMSC and hESC on pulmonary epithelial wound repair has also been evaluated.

A direct-contact co-culture *in vitro* model was utilised to evaluate the role of Clara cells on alveolar epithelial cell wound repair. Immunohistochemistry was conducted on IPF lung tissue samples to replicate the *in vitro* findings *ex vivo*. The paracrine role of hMSC and hESC on pulmonary epithelial cells was evaluated by utilising the *in vitro* wound repair system.

This study demonstrates that Clara cells induce apoptosis in AEC through a TRAIL-dependent mechanism, resulting in significant inhibition of wound repair. Furthermore in the IPF lungs, TRAIL-expressing Clara cells were detected within the fibrotic alveoli, together with widespread AEC apoptosis. This study also demonstrates that hMSC enhance AEC and SAEC wound repair via a paracrine mechanism through stimulation of cell migration; whereas, secretory factors of differentiated hESC promote AEC wound repair through stimulation of both cell proliferation and migration.

Through this study I propose a novel hypothesis which implies that the extensive pro-fibrotic remodelling associated with IPF could be driven by TRAIL-expressing Clara cells inducing AEC apoptosis through a TRAIL-dependent mechanism. My study also supports the notion of clinical application of hMSC and hESC or their secretory products as regenerative therapeutic modality for IPF.

Acknowledgements

First of all, I wish to acknowledge and thank to my lead supervisor Dr Nick R Forsyth and co-supervisor Prof. Monica Spiteri for their support that has undoubtedly helped me to become a self confident scientist. Without their guidance, suggestions and numerous revisions the completion of this thesis would not have been possible. I am truly grateful to them. I would also like to thank my advisor Dr Alan Richardson for his suggestion and all the supports that he has given me throughout my PhD course.

I would like to thank to our previous Postdoc Dr Amiq Gazdhar for his help in the early days of my PhD research. My special thank to my colleague Ms Nicola Lomas with whom, collaboration has led to development of a novel hypothesis of this thesis and a fantastic publication. I also thank to my friendly colleague Dr Neil Patel for his encouragement throughout my thesis writing. I would like to thank Dr Heidi Fuller as well for performing mass spectrometry analysis on my samples.

People of Skills Lab- my friends and colleagues have really made my long PhD research period enjoyable and less-stressful. My special thank to Deepak and Angeliki for providing me some reagents and antibodies for some of my experiments. I would also like to thank Hare for her effortless encouragement, Sammy for her amazing graphical ideas for my posters, Richard for his IT specialty that kept my laptop fast and 'hang-free', Sohel for his help as a brother and Kiren for her 'all time good wishes' for me. I also wish to give my cordial thank to Alex, Tina, Mike, Abbey, Jane, Vas, Hu Bin, Rupert, Ling, Feng, Param and Sanya; these people helped me in many ways. I would like to give a big thank to 'good fella' Dr Ian Wimpenny for his helpful suggestions in preparation of my thesis. I am

thankful to all people of Guy Hilton Research Centre, in particular, Steff and Anne who processed all of my purchase orders throughout my PhD.

I would like to thank my parents who provided me the support and encouragement throughout my long academic career that has now reached to the completion stage of my PhD. There is no doubt that without their encouragement, I could not have reached the stage that I am now in; my heartfelt gratitude to them. I am grateful to my loving wife who never complained about my clock-less and weekend-less work schedules. Her support and encouragement pushed me towards a successful end of my thesis. I would like to say, "Thank you; one day I will pay you back for all of your sacrifice."

Finally, I would like to extend my gratitude to my funding bodies, Medical Research Council-Dorothy Hodgkin Postgraduate Award and Chest Fund charity from University Hospital of North Staffordshire. I am also thankful to God for keeping me mentally and physically sound to pursue the hardest research works and completion of my thesis.

Publications

■ ***Peer reviewed journals***

1. Akram KM, Lomas NJ, Spiteri MA, Forsyth NR. "Clara cells inhibit alveolar epithelial wound repair via TRAIL-dependent apoptosis". *Eur Respir J*. **2012 Jul 12.** [Epub ahead of print]. *Work from the Chapter 3*.

2. Lomas NJ, Watts KL, **Akram KM**, Forsyth NR, Spiteri MA. "Idiopathic pulmonary fibrosis: immunohistochemical analysis provides fresh insights into lung tissue remodelling with implications for novel prognostic markers". *Int J Clin Exp Pathol*. **2012**; 5(1) :58-71. [Epub 2012 Jan 7].

■ ***Review/Book Chapters***

1. Akram KM, Samad S, Spiteri M, Forsyth NR. "Mesenchymal stem cell therapy and lung diseases". *Adv Biochem Eng Biotechnol*. **2012 Jul 8.** [Epub ahead of print]. *Work from the Chapter 1*.

Abbreviations

ACTC1	Actin, alpha, cardiac muscle 1
AEC	Alveolar epithelial cell
AECI	Type I alveolar epithelial cell
AECII	Type II alveolar epithelial cell
AFP	Alpha-fetoprotein
AFP	α-Fetoprotein
ALP	Alkaline phosphatase
ATCC	American type culture collection
BAL	Bronchoalveolar lavage
BASCs	Bronchioloalveolar stem cells
bFGF	Basic fibroblast growth factor
BMA	Bone marrow aspirate
CCSP	Clara cell secretory protein
CFU-F	Colony forming unit- fibroblast
COPD	Chronic obstructive pulmonary disease
CT	Computed tomography
CTGF	Connective tissue growth factor
ddH_2O	Double distilled water
dH_2O	Distilled water
DMEM	Dulbeco's Modified Eagle Medium
DMSO	Dimethyl sulfoxide
EB	Embryoid body
EBV	Epstein-Barr-Virus

ECM	Extra cellular matrix
EGF	Epidermal growth factor
EMT	Epithelial-mesenchymal transition
eNOS	Endothelial nitric oxide synthase
ESC	Embryonic stem cells
ET-1	Endothelin-1
FBS	Foetal bovine serum
FGF	Fibroblast growth factor
GAG	Glycosaminoglycan
GvHD	Graft-versus-host disease
hESC	Human embryonic stem cells
HGF	Hepatocyte growth factor
HHV	Human herpesvirus
hMSC	Human mesenchymal stem cells
HRCT	High resolution computed tomography
HSC	Haematopoitic stem cell
hTERT	Human telomerase reverse transcriptase
IGF	Insulin growth factor
IGF-1	Insulin-like growth factor-1
IGFBP-7	Insulin-like growth factor binding protein-7
IIP	Idiopathic interstitial pneumonia
IL	Interleukin
ILD	Interstitial lung disease
iNOS	Inducible nitric oxide synthase
IPF	Idiopathic pulmonary fibrosis

KGF	Keratinocyte growth factor
KO-DMEM	Knock out-Dulbeco's Modified Eagle Medium
KO-SR	Knock out-Serum replacement
MEF-CM	Mouse embryonic fibroblast-conditioned media
MEFs	Mouse embryonic fibroblast
MMP	Matrix metalloproteinase
MSC	Mesenchymal stem cells
NO	Nitric oxide
Oct-4	Octamer-binding protein-4
OSF-2	Osteoblast specific factor-2
pAEpiC	Primary alveolar epithelial cells
PBS	Phosphate-buffered saline
PDGF	Platelet-derived growth factor
PET	Polyethylene terephthalate
PFA	Paraformaldehyde
PGE_2	Prostaglandin-E_2
*pro*SP-C	*pro*Surfactant protein-C
PSA	Penicillin-Streptomycin-Amphotericin B
ROS	Reactive oxygen species
RT	Room temperature
SABM	Small airway basal media
SAEC	Small airway epithelial cells
SAGM	Small airway growth media
SCID	Severe combined immunodeficient
SF-DMEM	Serum-free DMEM

SFTPC	Surfactant protein-C
SOX1	Sex determining region Y-box 1
SSEA-1	Stage-specific embryonic antigen-1
SSEA-4	Stage-specific embryonic antigen-4
TGF-β1	Transforming growth factor-β1
TIMP	Tissue inhibitory metalloproteinase
TNF-α	Tumour necrosis factor-α
TRAIL	TNF-related apoptosis-inducing ligand
TRAIL-R1	TNF-related apoptosis-inducing ligand-Receptor 1
TRAIL-R2	TNF-related apoptosis-inducing ligand-Receptor 2
TUNEL	Terminal deoxynucleotidyl transferase mediated deoxyuridine triphosphate nick end-labelling
UIP	Usual interstitial pneumonia
VEGF	Vascular endothelial growth factor
α-SMA	α-smooth muscle actin

Chapter contents

List of Figures

List of Tables

Dedicated to

The departed soul of my Father

(1947-2006)

Chapter 1

General introduction

1.1. Definition of Idiopathic pulmonary fibrosis

Idiopathic pulmonary fibrosis (IPF) is defined as a specific form of chronic, progressive fibrosing interstitial pneumonia of unknown aetiology, occurring primarily in older adults, limited to the lungs, and associated with the histopathological and/or radiological pattern of usual interstitial pneumonias (UIP) (Raghu et al., 2011). This disease is also referred as cryptogenic fibrosing alveolitis (Selman & Pardo, 2002). The pathophysiology of IPF involves micro-injuries to alveolar epithelium, abnormal wound repair, accumulation of fibroblasts and myofibroblasts, deposition of excessive extracellular matrix, replacement of normal lung tissue with fibrotic scar and alteration of normal lung architecture. IPF is clinically manifested by progressive worsening of dyspnoea, deterioration of lung function and ultimately respiratory failure (Raghu et al., 2011, Gharaee-Kermani et al., 2007).

IPF, which is synonymously known as UIP, is the most common and possibly the fatal form of idiopathic interstitial pneumonias (IIPs). Idiopathic interstitial pneumonias are a group of diffuse parenchymal lung diseases of unknown cause associated with varying degrees of inflammation and fibrosis (Kim et al., 2006, Maher et al., 2007). Mostly affected group are 50 years or older. Unlike the other inflammatory and fibrotic lung diseases, IPF does not significantly response to steroids or any other potent anti-inflammatory drugs. Cytotoxic immunosuppressive agents largely fail to reduce the death rate of patients who are suffering from IPF. The only curative treatment option is lung transplantation (Selman et al., 1998).

1.2. Epidemiology and vital statistics of IPF

To date, there is no large-scale statistical study on IPF; thereby, formal estimation of incidence and prevalence of IPF is difficult (Raghu et al., 2011). The geographical

distribution of IPF is equal across the rural and urban areas, race and ethnicity but mortality has been reported slightly higher in whites than blacks. The mostly affected age-group is over 50 years of age and two-third of them is over 60 years at their presentation of disease. Males are more affected than females (ATS/ERS, 2000, Kim et al., 2006). The median survival of IPF patient is 2.8 years (Bjoraker et al., 1998). A recent study demonstrated that in the United States of America, incidence and prevalence of IPF, on the basis of clinical diagnosis, were 16.3 and 42.7 per 100,000 people respectively. But on the basis of surgical lung biopsy, BAL (Bronchoalveolar lavage) and CT scan confirmatory reports, the incidence and prevalence were 6.8 and 14.0 per 100,000 population respectively (Raghu et al., 2006). Higher incidence was found in the age group of 75 years or older where it was 76.4 per 100,000 people; as compared to age group 18 to 34 years, with 1.2 per 100,000. The prevalence was appeared to be increasing with an approximate rate of 150% in the last decade. An estimated 48,000 new IPF cases are currently diagnosed annually in the USA alone (ATS/ERS, 2000, Raghu et al., 2006).

A European study demonstrated that in Norway, average incidence of clinically diagnosed IPF was 4.3 per 100,000 population with an average prevalence of 21.8 per 100,000 people in a 15-year time period (von Plessen et al., 2003). In that study, the incidence of IPF was significantly higher in old aged people. A study in the United Kingdom reported an overall incidence rate of IPF was 4.6 per 100,000 cases per year with a progressive 11% increment of incidence rate per annum between 1991 to 2003 (Gribbin et al., 2006). According to this study, more than 4,000 new IPF cases are currently being diagnosed each year in the UK.

The evidence suggests that the mortality rate from IPF has increased over the last two decades. In the United States, the mortality rate from IPF has significantly risen from 1992

to 2003 time period, where it was 61.2 deaths per 1,000,000 in men and 54.5 deaths per 1,000,000 for women in the 2003 (Olson et al., 2007). A Japanese study documented 33 deaths in men and 24 in women per 1,000,000 from IPF (Iwai et al., 1994). The mortality rate from IPF has reported to be higher than the deaths from many cancers (Jemal et al., 2007).

1.3. Risk factors of IPF

1.3.1. Acquired risk factors

By definition, IPF is a disease of unknown aetiology, as no specific cause has been strongly identified so far. However, numbers of potential risk factors have been reported which may have some association with development of this disease (Raghu et al., 2011).

■ *Cigarette smoking:* Heavy smoking is believed to be associated with IPF, and this association is related to both familial and sporadic IPF (Baumgartner et al., 1997, Steele et al., 2005, Antoniou et al., 2008).

■ *Environmental exposures:* Exposure to metal dusts, in particular brass, lead and steel as well as wood dust has a significant risk for development of IPF (Hubbard et al., 1996, Miyake et al., 2005, Gustafson et al., 2007). Some occupational hazards related to farming, bird raising, hair dressing, stone cutting/polishing, livestock have also demonstrated association with IPF (Baumgartner et al., 1997).

■ *Microorganisms:* Chronic viral infection, particularly, Epstein-Barr-Virus (EBV) (Egan et al., 1995, Stewart et al., 1999, Tsukamoto et al., 2000, Lok et al., 2001, Kelly et al., 2002) and hepatitis C virus (Ueda et al., 1992, Meliconi et al., 1996) infections are though to have close association with initiation of IPF. A study on 33 IPF patients found evidences of herpesvirus infection including cytomegalovirus, EBV, human herpesvirus (HHV)-7 and human HHV-8 in 97% of IPF cases (Tang et al., 2003). However, in contrast, some

other studies reported no correlation between viral infection and IPF (Wangoo et al., 1997, Zamò et al., 2005). Despite the large number of studies, no definitive conclusion on the role of EBV infection in the development of IPF has been drawn. This is possibly because of high prevalence of viral infection in general population (Raghu et al., 2011).

■ *Gastroesophageal reflux*: Microaspiration in gastroesophageal reflux is thought to have an association with IPF (Tobin et al., 1998, Raghu et al., 2006).

■ *Diabetes mellitus (DM):* A recent study demonstrated that DM could have an association with IPF as well (Gribbin et al., 2009).

1.3.2. Genetic risk factors

1.3.2.1. *Familial idiopathic pulmonary fibrosis:* Mutation in the surfactant protein-C (*SFTPC*) gene has a strong association with familial IPF (Thomas et al., 2002); whereas, this mutation is uncommon in sporadic IPF (Selman et al., 2003, Lawson et al., 2004). The *SFTPC* gene mutation is thought to be one the causes of type II alveolar epithelial cell (AECII) injury (Thomas et al., 2002). A rare mutation in gene encoded for surfactant protein-A2 (*SFTPA2*) has also been reported in familial IPF (Wang et al., 2009). Recent studies identified a mutation in the human telomerase reverse transcriptase (*hTERT*) gene in familial IPF (Armanios et al., 2007, Tsakiri et al., 2007, Alder et al., 2008, Diaz de Leon et al., 2010). This mutation causes telomere shortening which may ultimately result in the alveolar epithelial cell apoptosis (Raghu et al., 2011).

1.3.2.2. *Sporadic idiopathic pulmonary fibrosis:* To date, there is no genetic factor identified that is consistently associated with sporadic IPF (Raghu et al., 2011). However, polymorphisms of genes encoding interleukin (IL)-1α, IL-4, IL-6, IL-8, IL-10, IL-12, tumour necrosis factor-α (TNF-α), transforming growth factor-β1 (TGF-β1), angiotensin

converting enzyme and matrix metalloproteinase-1 (MMP-1) have been detected, although inconsistently, in some cases of sporadic IPF (Riha et al., 2004, Vasakova et al., 2007, Hutyrova et al., 2002, Renzoni et al., 2000, Pantelidis et al., 2001, Xaubet et al., 2003, Whittington et al., 2003, Morrison et al., 2001, Checa et al., 2008).

1.4. Histopathological features

The histopathological hallmark and the cardinal diagnostic criteria of IPF/UIP is the heterogeneous appearance of lung tissue characterised by areas of fibrosis with scarring and honeycomb changes alternating with areas of less affected or healthy-looking lung parenchyma (Raghu et al., 2011). This alternate patchy distribution of affected and unaffected lung tissue is also termed as 'temporal heterogeneity' (Dacic & Yousem, 2003). These histopathological changes mostly affect the subpleural and paraseptal regions of the lung. Inflammation is usually mild and associated with hyperplasia of type II AEC and bronchiolar epithelium. Another consistent histopathologic feature is the presence of fibroblastic foci which are scattered, convex subepithelial foci composed of dense collagen with fibroblasts and myofibroblasts (Figure 1.1). The areas of honeycomb changes are often cystic, frequently lined with bronchiolar epithelium and are filled with mucus which appears relatively late stages of disease progression (ATS/ERS, 2000, Raghu et al., 2011).

The histological pattern of UIP is not unique to IPF; similar features are also found in asbestosis, scleroderma, collagen vascular diseases, drug toxicity, chronic hypersensitivity pneumonitis and Hermansky-Pudlak syndrome; but the uniqueness of IPF is the absence of any definitive cause (ATS/ARS, 2002, Raghu et al., 2008). On the other hand, some biopsy samples of IPF patients may not fulfill the criteria of UIP. In those cases the histological

pattern of IPF are termed as "nonclassifiable fibrosis"; hence the diagnosis in made based on clinical and radiological findings (ATS/ERS 2000, Raghu et al., 2011).

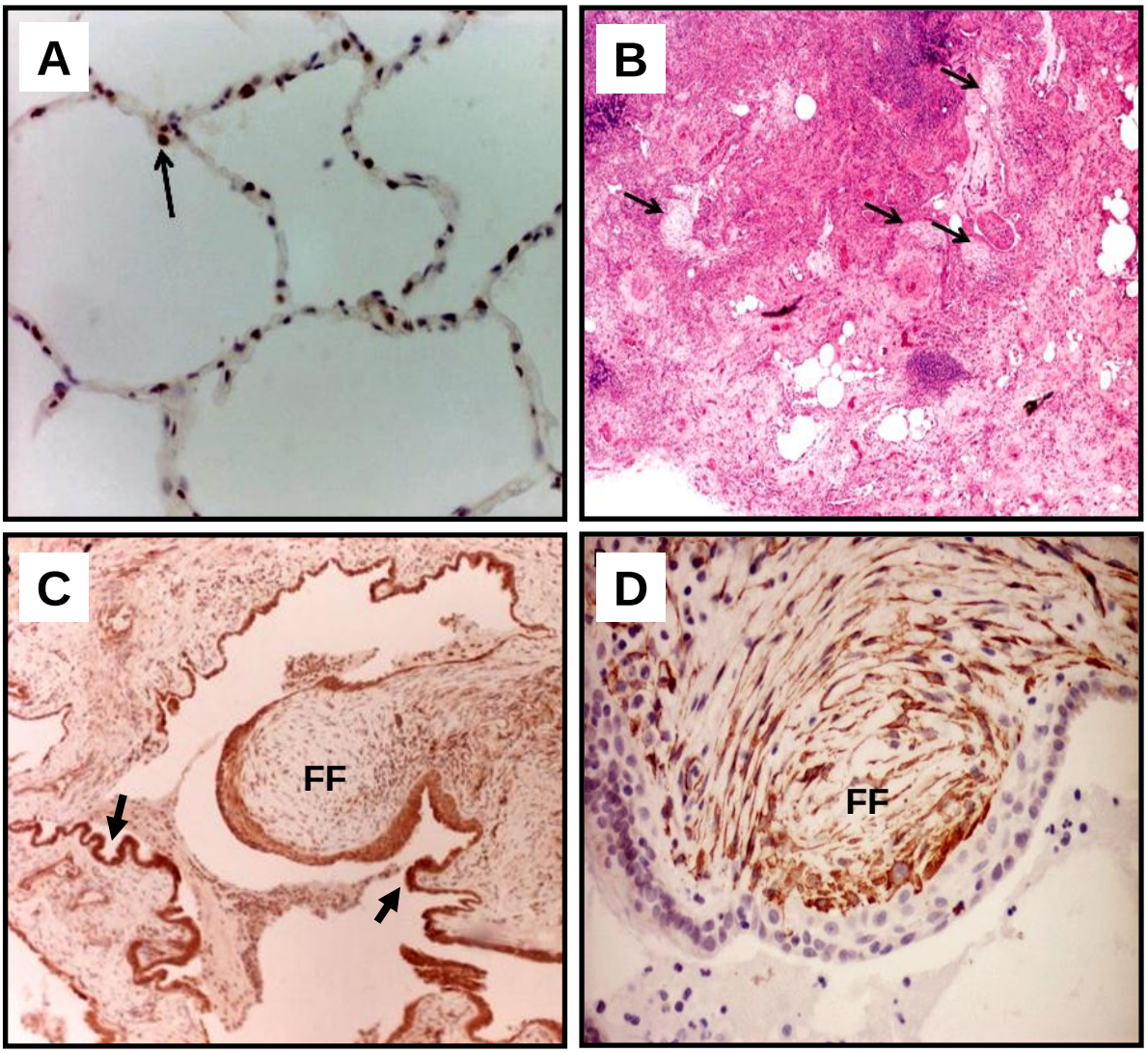

Figure 1.1: Histological slides of normal and IPF lung tissues.

(**A**) Alveolar region of normal human lung tissue, immunostained with antibody against Sp-C showing Sp-C positive AECII cells (arrow) in high magnification (400X). (**B**) Fibroblastic foci are shown (arrows) in the alveolar region of the affected part of an IPF lung in low magnification (100X). (**C**) Fibroblastic foci (FF) and hyperplasia of AECII (arrows) are shown in the alveolar regions of IPF lung. Tissue section stained with antibody against TGF-β; image magnification 200X. (**D**) Myofibroblasts within the fibroblastic foci (FF) are stained with antibody against α-SMA. Image magnification is 400X. (Images are taken from Lomas et al., 2012).

1.5. Clinical features of IPF

Most often patients with IPF suffer for more than 6 months before diagnosis. (ATS/ERS, 2000, Selman et al., 2001). The most common clinical features of IPF are as follows:

■ Nonproductive cough: Gradual onset.

■ Exertional breathlessness: Most prominent and disabling symptom.

■ Paroxysmal dry cough which is not relieved by common antitussives.

■ Inspiratory crackles: Found in more than 80% of patients which is typically 'dry' and 'Velcro' type and initially present at lung bases and afterwards appears in the mid and upper zones in course of disease progression.

■ Digital clubbing: Present in 25% to 50% patients.

■ Cyanosis: Appears in late stage of disease.

■ Cardiac signs: Cor pulmonale, right ventricular heave, accentuated pulmonic second sound and peripheral oedema may be appeared at the late stage of disease.

■ Generalised illness: Weight loss, fatigue and malaise can be noticed but fever is rare. (ATS/ERS, 2000, Selman et al., 2001).

1.5.1. Radiological abnormalities

Virtually all IPF patients present with some degree of chest radiological changes. Typically, bilateral basal reticular opacity is found in the postero-anterior view plain X-ray of chest which is widely non-specific (Figure 1.2A) (ATS/ERS 2000, Strollo, 2003, Misumi & Lynch, 2006). Computed tomography (CT) and high resolution computed tomography (HRCT) have become the mainstay of non-invasive investigation technique for diagnosis of IPF and other ILDs (Interstitial lung diseases) (Strollo, 2003). Presence of patchy, bilateral, predominantly basal and subpleural reticular opacity (80% cases) (ATS/ERS, 2000, Strollo, 2003), peripheral honeycombing (96% cases), minimal degree of

ground-glass opacity (75% cases) (Strollo, 2003, Hartman et al., 1993), traction bronchiectasis and bronchiolectasis in advanced stages (50% cases) are the classical imaging criteria for diagnosis of IPF on HRCT (Strollo, 2003) (Figure. 1.2B).

1.6. Diagnosis of IPF

During diagnosis, it is essential to exclude IPF from other interstitial lung diseases (ILDs) as the prognostic outcome of IPF is worse than other pulmonary fibrosis. Diagnosis of IPF is made on the basis of detailed medical history, physical examination, radiological HRCT investigation and surgical lung biopsy in some special cases (Figure. 1.3). To make a confident diagnosis of IPF, it is essential to take expert opinion of pulmonologists, radiologists, pathologists and thoracic surgeons (Raghu et al., 2008). According to the recent consensus by ATS/ERS the diagnostic criteria for IPF are as follows (Raghu et al., 2011):

1.6.1. Diagnostic criteria

1. Exclusion of other known causes of ILD such as domestic and occupational exposures, connective tissue disorders and drug toxicity.

2. The presence of UIP pattern on HRCT in suspected patients not undergoing surgical biopsy.

3. Presence of specific UIP patterns in HRCT and surgical lung biopsy in patients are subject to surgical lung biopsy.

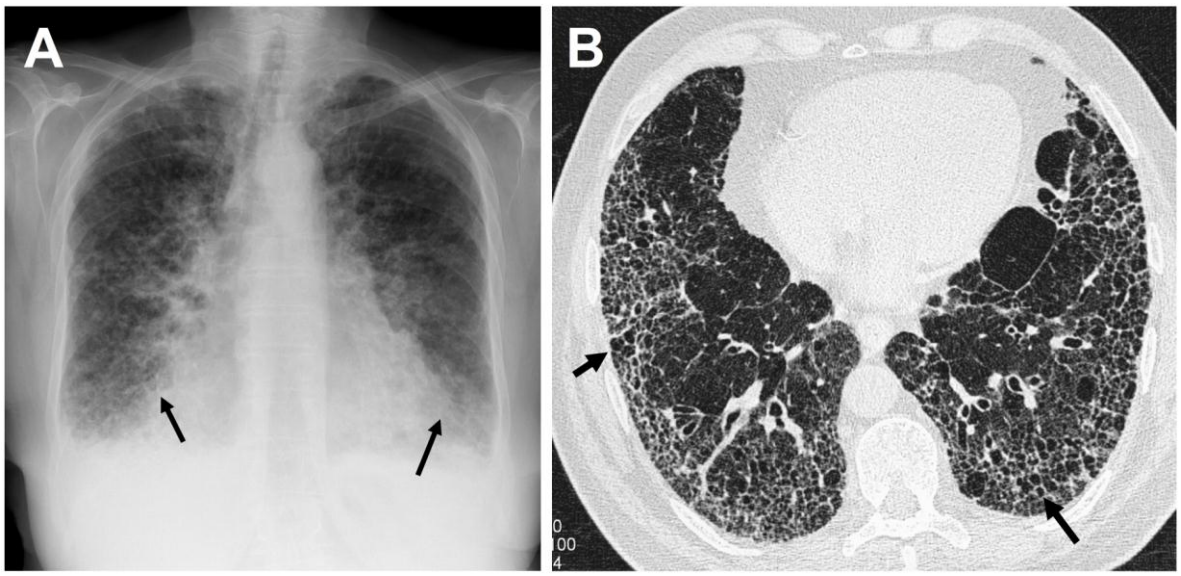

Figure 1. 2: Chest radiographs of a patient with IPF.

(**A**) The PA-view X-ray chest of a male patient with IPF shows bibasilar and peripheral reticular opacity (arrows) with marked reduction of lung volume. (**B**) HRCT of lung of an IPF patient shows subpleural honeycombing (arrows). (The radiographs are kindly provided by Prof. Monica Spiteri, Directorate of Respiratory Medicine, University Hospital of North Staffordshire, Stoke-on-Trent, UK).

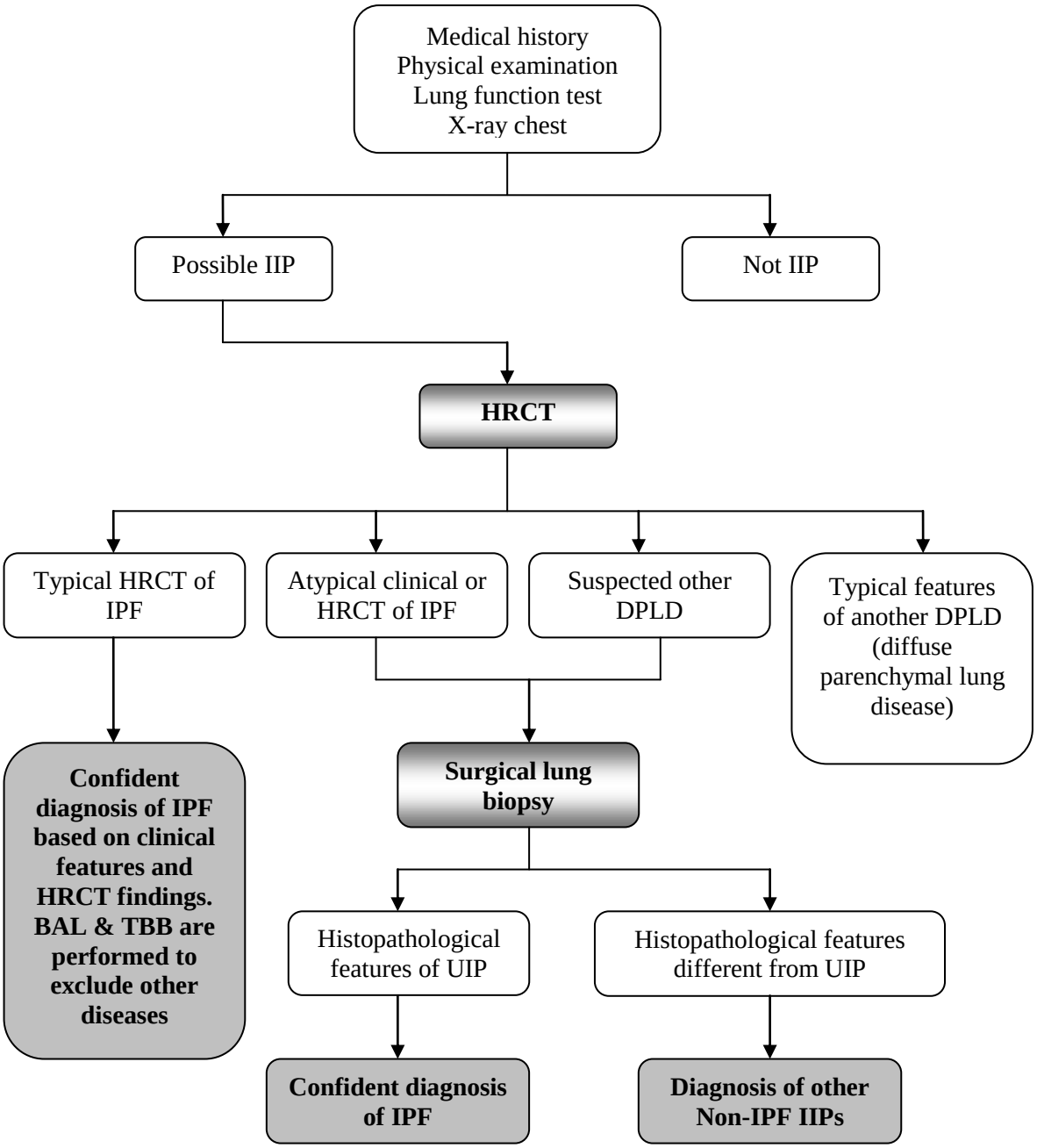

Figure 1.3: Algorithmic flowchart for IPF diagnosis.

Diagnostic algorithm for IPF starts from detailed medical history following radiology to surgical lung biopsy. This chart is modified and simplified from (Raghu et al., 2008).

1.7. Classification of IIP

According to the International Consensus Statement by the American Thoracic Society (ATS) and the European Respiratory Society (ERS) in 2001, IIPs are classified into two groups: one is IPF and another is non-IPF IIPs (Figure 1.4). (ATS/ARS, 2002, Raghu et al., 2008).

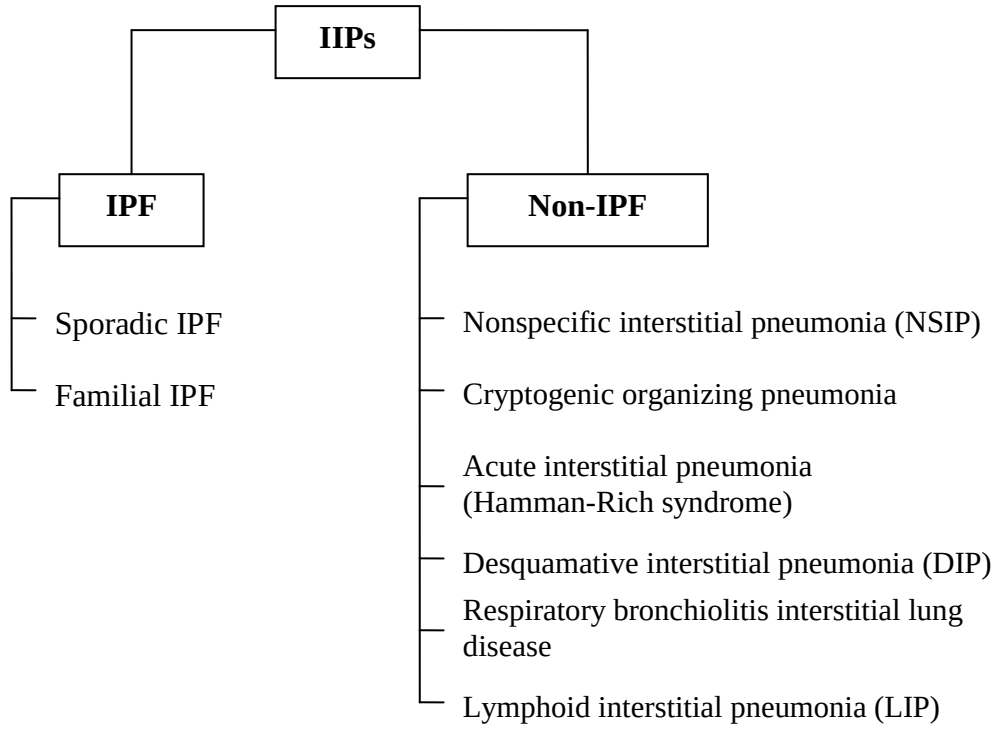

Figure 1.4: Current classification of IIP.

Interstitial pneumonias (IIP) are broadly classified into IPF and Non-IPF IIP. IPF is again divided into two categories, sporadic and familial IPF. Based on clinical features, Non-IPF is divided into six categories.

1.8. Structure of the alveoli

1.8.1. *Alveoli: The functional units of lung*

Alveoli are the functional units of lung. There are approximately 300 million of alveoli present in the adult human lung with over 70 m^2 of gas-exchange surface area. In adult, the alveoli are entirely covered with type I and type II pneumocytes (Figure 1.5). These cells are also referred to as alveolar epithelial cells (AEC). Type I AEC (AECI) are wide-spread squamous-like cells with diameters of up to 100 μm (Selman & Pardo, 2006) covering more than 96% of total alveolar surface area (Gharaee-Kermani et al., 2007). These cells are very thin with an average thickness of 0.1 μm (Bishop, 2004) which provides a thin membrane for gaseous exchange. Type II AEC (AECII) are cuboidal in nature and cover only 4% of alveolar surface area; although they accounts for more than 60% of all alveolar epithelial cells. AECII cells are usually localised in the corners of the alveoli, lying adjacent to the mesenchymal cells. Mesenchymal cells are situated underneath the basement membrane of epithelium (Figure 1.5). AECII are multifunctional and believed to be the defender and progenitor cells of alveoli (Fehrenbach, 2001).

1.8.1.1. Function of AECII

■ *Putative stem/progenitor cells:* Type II AEC are capable of self-renewal and can terminally differentiate into AECI and act as progenitor cells for alveolar regeneration (Fehrenbach, 2001).

■ *Production of surfactant:* AECII cells secret surfactant proteins which primarily regulate alveolar surface tension. Alveolar surfactant contains about 90% of lipids and 10% of proteins. There are different types of surfactant proteins (SP) present in surfactant fluid, named as SP-A, SP-B, SP-C and SP-D. Surfactant also can play role in host defence mechanisms, especially with SP-A and SP-D by opsonising pathogens and presenting them

to the macrophages. Surfactant is also believed to contribute in fluid balance in alveoli and hence prevent alveolar oedema (Fehrenbach, 2001).

■ *Interaction with other cells:* Type II AEC have direct contact with AECI through gap junctions. A contact-inhibition interaction between AECI and AECII regulates AECII proliferation (Kasper & Haroske, 1996). On the other hand, mechanical stimulation of AECI can modulate exocytosis of lamellar bodies and secretion of surfactant by AECII (Ashino et al., 2000). In the alveoli, AECII and fibroblasts remain in close proximity and show both direct and indirect interactions during lung morphogenesis and repair/regeneration process. *In vitro* co-culture experiment demonstrated that fibroblast supernatant increased the alveolar epithelial cell proliferation; whereas, AEC supernatant inhibited the proliferation of fibroblasts. In direct cell-cell contact co-culture, AEC significantly increased fibroblast proliferation (Adamson et al., 1991). In addition AEC can secret interleukin-6 (IL-6) or interleukin-8 (IL-8) which can stimulate neutrophils and thus initiate inflammation. AECII may also play a role as an antigen presenting and immunoregulatory cell of the lung (Fehrenbach, 2001). They secrete TGF-β which indirectly inhibits T-cell activity and proliferation (Zissel et al., 2000). In response to stimuli, AEC can release chemokines which recruit macrophages in the alveoli and stimulate inflammation (O'Brien et al., 1998).

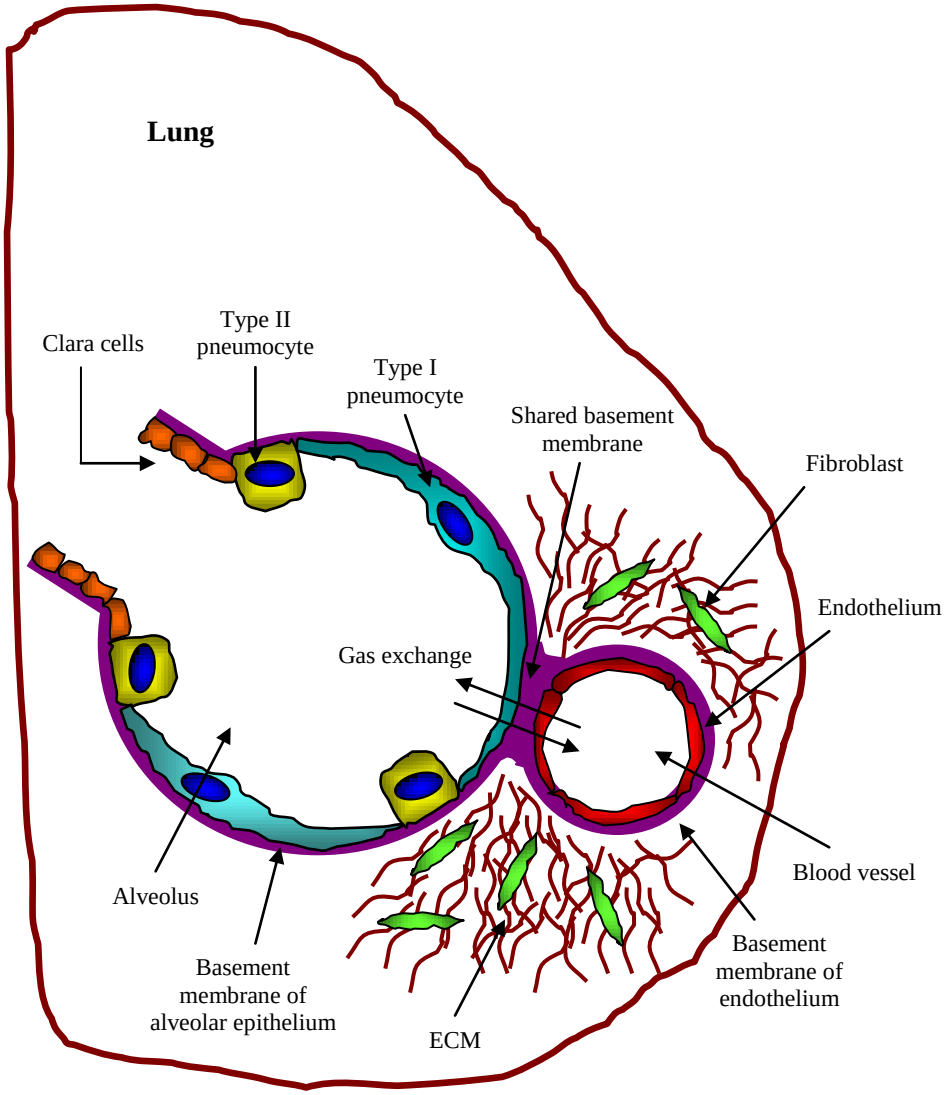

Figure 1.5: Schematic diagram of an alveolus with its adjacent pulmonary blood vessel.
Alveolus is lined with type I and type II pneumocytes. Type I pneumocytes are very flat and cover >95% of surface area while type II pneumocytes are cuboidal and cover <5%. The alveolar duct is lined with non-ciliated, cuboidal, Clara cells. Type II pneumocytes and Clara cells are thought to have progenitor/stem cell properties. Resident fibroblasts are located within the interstitium. Alveolus and pulmonary blood vessel share a common basement membrane which makes the 'respiratory membrane' for gas exchange.

1.9. Alveolar repair and regeneration

1.9.1. Stem cells in alveolar regeneration

Stem cells are capable of self-renewal, are clonogenic and can be described as an unspecialised cell with varying potency which can differentiate into various specialised adult phenotypes. Self-renewal is a characteristic property of stem cells that implies the production of exact duplicates of stem cells with maintenance of all attributes, including the full range of self-renewal of the original. The potency is the capacity of an unspecialised stem cell to differentiate into other specialised cell types. Different stem cell populations are broadly classified as unipotent, multipotent or pluripotent and totipotent by their potency. Unipotent stem cells differentiate into one specialised cell type, multipotent and pluripotent stem cells differentiate into many specialised cell types and totipotent stem cells can differentiate into all cells types (Martin, 1981, Brecher et al., 1993, Thomson et al., 1998).

Undifferentiated multipotent tissue-specific stem/progenitor cells have been identified in almost all tissues and are thought to contribute tissue homeostasis and regeneration (Sueblinvong & Weiss, 2010). The lung is a complex and vital organ and highly exposed to the environment with around 70 m^2 of alveolar surface area making it susceptible to frequent injuries by noxious substances and microorganisms. It is believed that there are numbers of anatomical region-specific stem/progenitor cells present within the lung, such as basal cells in trachea and distal airways (Rock et al., 2009), Clara cells in bronchioles (Stripp & Reynolds, 2008) and type II AEC in alveoli (Evans et al., 1975, Brody & Williams, 1992, Rawlins, 2008). These resident stem/progenitor cells contribute lung regeneration through their differentiation during physiological turnover and injury repair (Selman & Pardo, 2006, Gharaee-Kermani et al., 2007).

By lineage tracing study in transgenic mice models, Rock *et al*. showed that basal cells of trachea differentiated into tracheal lining epithelium during postnatal growth and in the adult during both steady-state and epithelial injury repair (Rock et al., 2009). In the same study, they also demonstrated that mouse and human basal cells isolated from trachea and distal airways could self-renew and were capable of differentiating into ciliated airway epithelial cells (Rock et al., 2009). On the other hand, Clara cells are non-ciliated cuboidal cells, broadly distributed throughout the bronchiolar epithelium which are normally quiescent in steady-state condition, but become activated following injury; proliferate and differentiate into other bronchiolar cells, hence they are termed as facultative progenitor cells (Stripp & Reynolds, 2008, Stripp, 2008). Not all but a subpopulation of Clara cells which are resistant to naphthalene-induced injury are thought to be the bronchiolar progenitor cells which contribute to bronchiolar repair and regeneration (Chen et al., 2009). Lineage tracking in animal models has indicated that Clara cells may not participate in alveolar injury repair or regeneration (Rawlins et al., 2009). A naphthalene resistant population of cells which express both the Clara cell marker CCSP (Clara cell secretory protein, also known as CC10) and type II AEC marker *pro*SP-C (ProSurfactant protein-C) have been identified at the bronchioloalveolar duct junction in mice. These cells can self-renew and give rise to progeny which express CCSP, *pro*SP-C or aquaporin-5 (AQP-5, a type I AEC marker) in culture, hence they have acquired the title of putative bronchioloalveolar stem cells (BASCs) (Kim et al., 2005). However, the role of BASCs in bronchiolar or alveolar repair *in vivo* is unclear and needs to be further elucidated.

For more than 50 years, type II AEC have been described as the stem/progenitor cells in the alveoli and are believed to give rise to type I AEC and participate in alveolar regeneration and repair (Bishop, 2004). Type II AEC can be sub-divided into two groups;

E-cadherin positive and E-cadherin negative. E-cadherin positive cells are quiescent, liable to DNA damage with low level of telomerase activity. Whereas, E-cadherin negative cells are resistant to DNA damage, proliferative, with a high level of telomerase activity. The E-cadherin negative type II AEC are likely to be the progenitor cells of alveoli (Reddy et al., 2004). In late 1960s when Kapanci and colleagues proposed type II AEC as alveolar stem cells, this concept was widely accepted. However, there are arguments around whether type II AEC fulfill all the criteria to be classified as a stem cell.

Recently, Fujino and colleagues isolated MSC-like cells from human lungs which were clonogenic, self-renewing and could differentiate into type II AEC *in vitro* (Fujino et al., 2011). They also demonstrated that this MSC-like cell population, which expressed both mesenchymal stem cell marker CD90 and type II AEC marker *pro*SP-C, were present in the normal human alveolar wall and their number significantly increased in the hyperplastic regions of IPF alveoli, possibly, as a reparative response (Fujino et al., 2011). The authors suggested these CD90/proSP-C dual positive MSC-like cells could be progenitors for type II AEC (Fujino et al., 2011). More recently, an exciting study demonstrated that there are undifferentiated stem cells nested in the niche of distal airways of human lungs which are clonogenic, self-renewing and multipotent in nature (Kajstura et al., 2011). Kajstura and colleagues isolated these stem cells from human lung, particularly from the distal airway regions. They expanded those cells *in vitro* and then transplanted into the injured mouse lungs. They demonstrated that those transplanted stem cells generated bronchioles, alveoli and pulmonary vasculature (Kajstura et al., 2011). This finding has opened a new horizon to manipulate the niche-stem cells to promote lung regeneration as a therapeutic intervention for various lung disorders including IPF.

Apart from endogenous lung stem cells, bone marrow derived haematopoitic stem cells (BM HSC) are thought to be an exogenous stem cell source for maintenance of alveolar epithelium during physiological turnover or injury repair (Bishop, 2004, Hunninghake et al., 2003). This idea is supported by animal model studies that demonstrated that intravenously transplanted bone marrow stem cells were capable of differentiating into type I AEC (Kotton et al., 2001) and type II AEC (Theise et al., 2002). In the radiation induced pneumonitis mouse model, Theise and colleague demonstrated that after injury type II AEC derived from donor bone marrow-transplant and engrafted in the injured alveoli. After 2 months of transplantation the entire alveoli were lined with bone marrow-derived AEC, suggesting that the type I AEC were differentiated from bone marrow derived type II AEC (Theise et al., 2002).

1.9.2. Normal healing process following alveolar injury

The process of alveolar repair is complex and involves interactions along the epithelial-mesenchymal-inflammatory cellular axis, multiple growth factors, cytokines, chemokines, signaling pathways, structural elements and the mechanical environment (Crosby & Waters, 2010). Following alveolar injury, the ensuing inflammatory response induces release of a wide range of soluble factors by neighbouring AEC, fibroblasts, endothelial cells and macrophages which activate the reparative process (Figure 1.6) (Crosby & Waters, 2010). However, our understanding of the interaction between soluble factors and cellular components in regards to alveolar wound repair is mostly based on *in vitro* studies; thereby, the precise mechanism of *in vivo* wound repair remains widely elusive.

In general, after injury the denuded area is covered with neighbouring epithelial cells through epithelial restitution, which involves migration and proliferation to restore the cell

number and differentiation to restore the functions (Puchelle et al., 2006, Zahm et al., 1991). In the airways, after injury to the epithelium the first 12-24 hours of healing process involves epithelial cell spreading and migration as a primary reparative process followed by cell proliferation and differentiation which takes days to weeks (Horiba & Fukuda, 1994). During *in vivo* alveolar injury repair, the proliferation index of type II AEC is considered as a primary indicator of reparative process (Panos et al., 1995, Yee et al., 2006). Whereas, the wound healing process *in vitro* is demonstrated through type II AEC spreading, migration, proliferation and differentiation into type I AEC in wound repair models (Kheradmand et al., 1994, Atabai et al., 2002). The concept of type II AEC spreading and migration as primary events during alveolar wound repair is also supported by observations in other non-alveolar wound repair mechanisms such as in cornea (Danjo & Gipson, 1998), gut (Lotz et al., 2000) and kidney (Fenteany et al., 2000).

Following alveolar injury, AEC, fibroblasts, endothelial cells and inflammatory cells secrete a myriad of growth factors, cytokines, chemokines, prostaglandins and matrix components (Figure 1.6). A critical balance between the milieu of soluble factors and the responses to the cellular components is important for a normal wound healing (Crosby & Waters, 2010). Several growth factors such as epidermal growth factor (EGF), keratinocyte growth factor (KGF), hepatocyte growth factor (HGF), TGF-α and TGF-β play major role during alveolar injury repair. EGF has mitogenic effect on type II AEC and bronchial epithelial cells and facilitates their migration (Ryan et al., 1994, Lesur et al., 1996, Leslie et al., 1997). KGF has a cytoprotective function and plays a vital role in lung development (Panos et al., 1995, Simonet et al., 1995). During wound repair, KGF stimulates type II AEC proliferation and promotes cell spreading, migration and adhesion via an EGF-receptor dependent mechanism (Panos et al., 1995, Atabai et al., 2002, Panos et al., 1993,

Ulich et al., 1994, Galiacy et al., 2003). HGF has a mitogenic property and facilitates alveolar epithelial wound repair by type II AEC proliferation and migration mechanism (Mason et al., 1994, Panos et al., 1996, Furuyama & Mochitate, 2004).

The effects of TGF-β in alveolar wound repair are complex and controversial. The biological functions of this growth factor are diverse and plays crucial roles in development, inflammation, wound repair, fibrosis and tumourigenesis (Crosby & Waters, 2010). It has been demonstrated that TGF-α and TGF-β stimulate type II AEC wound repair *in vit*ro by increasing cell proliferation and migration (Ryan et al., 1994, Buckley et al., 2008, Yu et al., 2008). However, TGF-β has pro-inflammatory and pro-fibrotic properties, and its aberrant expression is believed to be responsible for the development of pulmonary fibrosis through activation of its downstream target CTGF (connective tissue growth factor), collagen and by induction of EMT (epithelial-mesenchymal transition).

Apart from growth factors and cytokines, extracellular matrix (ECM) components also play an important role in the resolution of alveolar injury. In the early stages of airway epithelial wound repair the provisional matrix, which is composed of serum fibronectin and fibrinogen, facilitates cell migration (Perrio et al., 2007). The integrin receptors play a major role in type II AEC migration on fibronectin and type I collagen coated matrix during alveolar wound repair (Kim et al., 1997). Matrix metalloproteinases (MMPs) are a group of enzymes that are believed to play major role during injury repair and ECM remodeling. In particular, MMP-1, MMP-7 and MMP-9 have been shown to increase type II AEC and other airway epithelial cells migration during wound healing (Planus et al., 1999, Parks et al., 2001, Chen et al., 2008b, Legrand et al., 2001).

Aberrations in the orchestration of soluble bioactive cues and cellular responses results in aberrant wound repair and fibrosis. Failure or delayed re-epithelialisation due to impaired migration, proliferation, differentiation and increased AEC apoptosis can stimulate fibroproliferative activities which likely to underpin the pathogenesis of IPF (Selman et al., 2001).

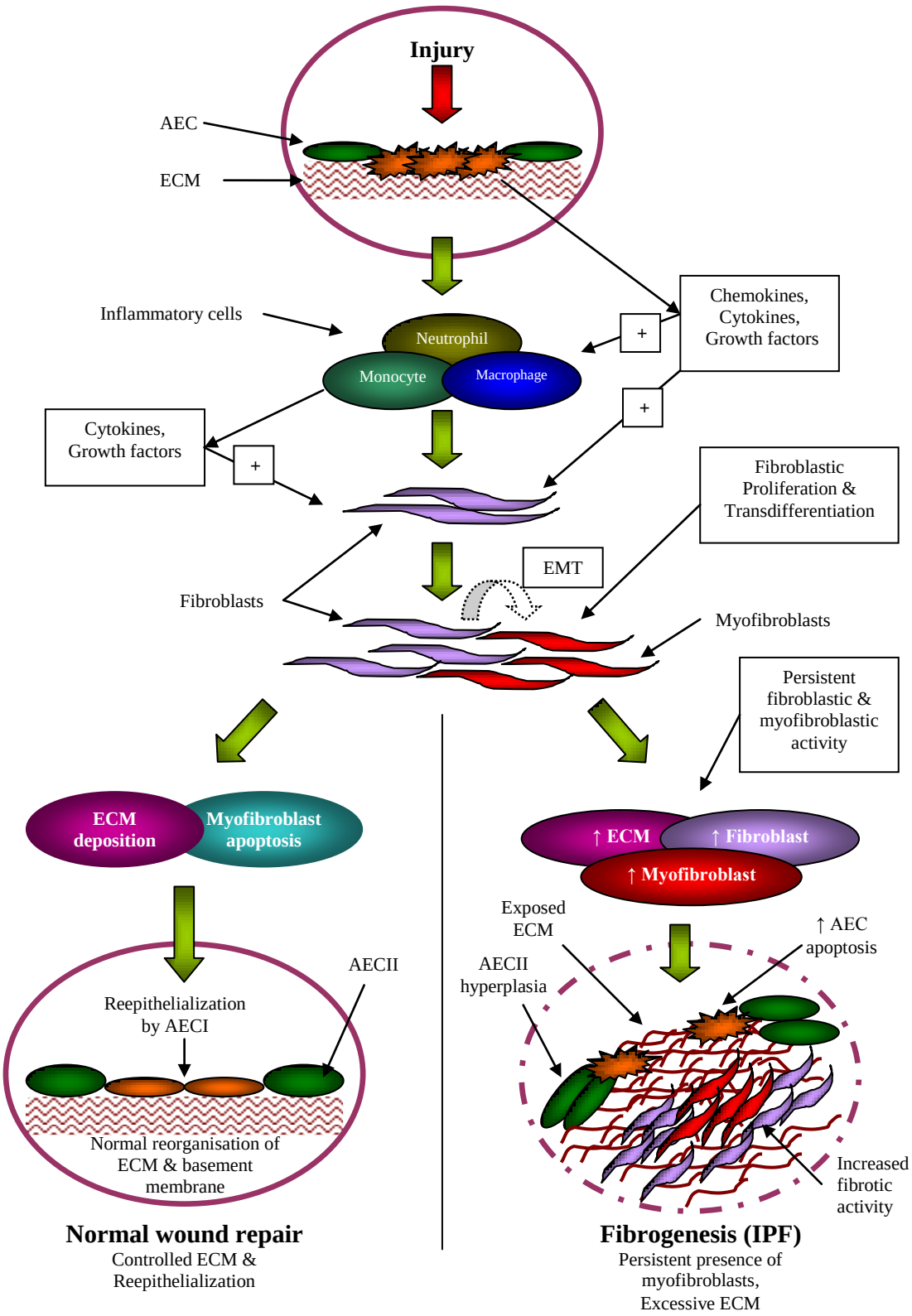

Figure 1.6: Normal and abnormal healing process after alveolar injury.

Injured AEC activate inflammatory cells and fibroblasts through secretory cytokines. Activated inflammatory cells stimulate fibroblasts. Fibroblasts proliferate and differentiate into myofibroblasts which resolve injury by formation of ECM and basement membrane that facilitate alveolar re-epithelialisation. On the other hand, persistence of the fibroproliferative response causes fibrosis.

1.10. Pathogenesis of IPF

Despite intense research effort, the pathogenesis of IPF is still elusive and controversial. Over the last three decades, numbers of hypotheses have been proposed to explain the pathophysiological process of this incurable disease. The inflammatory hypothesis has been abolished, meanwhile, recent hypothesis describes IPF as a consequence of aberrant alveolar wound repair and regeneration due to multiple alveolar epithelial cell injuries, disrupted epithelial-mesenchymal cross-talk, imbalanced immune responses and abnormal activation of coagulation cascaded (Selman et al., 2001, Gharaee-Kermani et al., 2007).

1.10.1. The evolution of hypotheses of IPF pathogenesis

1.10.1.1. Inflammatory fibrosis hypothesis

Previously, it was believed that chronic inflammation played a pivotal role in the pathogenesis of IPF. According to this hypothesis, the disease process is characterized by inflammation and abnormal injury repair of lung due to hyper proliferation of fibroblasts and myofibroblasts and subsequent accumulation of ECM followed by marked alteration of tissue architecture and aberration of functionality of lungs. However, clinical, histological and experimental findings now do not support this hypothesis (Selman et al., 2001, Gharaee-Kermani et al., 2007).

Corticosteroids have been used for the treatment of IPF since the 1950s, but these days, it is widely accepted that steroids and other anti-inflammatory drugs provide a very little or no beneficiary effect in halting the disease progression (Mapel et al., 1996). Even, when steroids are used with potent immunosuppressive drugs, they fail to show any significant response (Selman et al., 1998, Johnson et al., 1989). The histopathological findings also

failed to show significant presence of inflammatory cells at the site of the lesion (Selman et al., 2001).

In addition, inflammation is not always essential to initiate a fibrotic response. A mouse-lung-explant model experiment showed that in a blood-free environment, severe hyperoxic alveolar injury could promote fibrosis without the initiation of inflammation. In that case, the healing process was completed by fibrosis rather than epithelial regeneration (Adamson et al., 1988). This study demonstrated that initiation of the fibrotic response in the absence of inflammation was possible, at least, in a mouse model (Selman & Pardo, 2002). Some other studies showed that in the absence of IL-10, silica-induced inflammation was unable to initiate fibrosis in mice (Huaux et al., 1998) and bleomycin-induced inflammation did not induce significant fibrosis in integrin-αvβ6 deficient mice (Munger et al., 1999). These findings along with clinical features and poor outcome of anti-inflammatory therapy challenge the validity of the 'inflammatory fibrosis' hypothesis in the pathogenesis of IPF.

1.10.1.2. Epithelial injury and abnormal wound repair hypothesis

As the 'inflammation and fibrosis' hypothesis can not clearly explain the pathophysiological process of IPF, Selman *et al*. proposed a new hypothesis. They suggested that, idiopathic pulmonary fibrosis occurs due to multiple epithelial injuries followed by abnormal wound repair without any preceding chronic inflammation (Selman *et al*., 2001; Kaminski *et al*., 2003). They did not deny the association of inflammation in IPF, but they mentioned that '*the inflammatory response neither precedes nor plays a relevant role in its pathogenesis*' (Kaminski *et al*., 2003).

1.10.1.3. Inflammation and immune response followed by fibrosis hypothesis

More recently, a modified hypothesis of IPF has been proposed which implies that, 'inflammation is subsequent to injury and that IPF occurs as a result of polarization of the immune response of the body to repeated injury (multi-hits) to the lung' (Strieter, 2005). This hypothesis is based on the well-established theory of wound healing which implies that injury to any tissue is always followed by inflammation and subsequent repair. Microarray data and HRCT evaluation of IPF patients support this hypothesis. Microarray gene analysis of IPF lung samples showed over-expression of pro-inflammatory cytokines and chemokine genes which encode immunoglobulins that can stimulate chronic B-cell infiltration. However, they did not find any over-expression of acute inflammatory cytokines (Zuo et al., 2002). This finding reflects the presence of chronic inflammation in IPF. Presence of accentuated adenopathy detected by HRCT scan in 55% IPF patients which supports the notion of involvement of abnormal immune responses (Hunninghake et al., 2003). However, this study did not show any histopathological confirmation of the adenopathy.

According to this hypothesis, IPF occurs due to repeated injury or exposure to antigens which leads to an imbalanced response between type-1 and type-2 helper-T cell mediated immunity which subsequently influences fibroblast and myofibroblast proliferation and excessive ECM deposition resulting in failure of re-epithelialisation and fibrosis.

1.10.2. Cellular and humoral events in the development of IPF

1.10.2.1. Role of alveolar epithelial cells

The evolving hypothesis is that multiple alveolar epithelial cell injuries and subsequently aberrant wound healing leads to the development of IPF (Selman et al., 2001). This concept has been accepted by many scientists albeit with lack of sufficient evidence to explain the pathogenesis. According to this hypothesis, fibrosis occurs due to disrupted epithelial-mesenchymal interaction instead of chronic inflammation. In the following sections the contribution of alveolar epithelial cells and fibroblasts in the development of IPF will be briefly discussed.

1.10.2.1.1. Repeated alveolar epithelial cell injuries

Repeated injury to the alveolar epithelial cell is believed to be the initiating trigger for the development of fibrosis. However, the exact cause or mechanism of these multiple injuries are unknown (Selman & Pardo, 2006). Some believe that the initiating cause may be multifactorial and potentially viral. Studies reported the evidence of Epstein-Barr virus (EBV) (Egan et al., 1995), cytomegalovirus, human herpesvirus-7 (HHV-7) and human herpesvirus-8 (HHV-8) (Tang et al., 2003) in the samples of IPF patients. On the other hand, similar study failed to detect any EBV and HHV-8 in IPF lung (Zamò et al., 2005). This contradictory data suggests that there might be no universal involvement of virus in IPF.

Intrinsic abnormalities in AEC may cause alveolar epithelial injury (Selman & Pardo, 2006). In some familial IPF cases, mutation in the SP-C gene was observed which resulted in the accumulation of misfolded surfactant protein within the alveolar epithelia resulting in type II AEC injury (Grutters & du Bois, 2005). This type of intrinsic abnormality is

uncommon in patients with sporadic IPF (Lawson et al., 2004). Cigarette smoking is a major cause in many lung diseases such as chronic obstructive pulmonary disease (COPD), lung carcinomas and some other pulmonary fibrosis. It is speculated that cigarette smoking could be related to IPF; however, to date, there is no firm evidence of the involvement of tobacco smoking in the development of this disease (Selman & Pardo, 2006).

1.10.2.1.2. Increased AEC apoptosis

Apoptosis which is also called programmed cell death can be defined as 'gene-directed cellular self-destruction'. Apoptosis is a normal physiological process required for the development and maintenance of tissue homeostasis. The entire apoptotic process is tightly regulated by a number of genes and their products (Uhal, 2008). Exacerbated apoptosis can be pathological. The persistent presence of increased AEC apoptosis is frequently detected in the lung of IPF patients (Uhal et al., 1998, Kuwano et al., 1999, Barbas-Filho et al., 2001, Uhal, 2008). A significant up-regulation of pro-apoptotic proteins p53, p21, bax and caspase-3 with associated down-regulation of anti-apoptotic protein Bcl-2 was found in IPF alveolar epithelial cells (Plataki et al., 2005). TUNEL positive apoptotic AEC were also detected in IPF lung samples (Plataki et al., 2005). A Fas-FasL mediated pathway has been suggested to be involved in this apoptosis (Maeyama et al., 2001). Electron microscopic and biochemical experiments on lung tissue samples taken from patients with IPF showed significantly increased apoptosis in type II AEC of healthy-looking alveoli of IPF patients comparing non-IPF control lung tissues (Barbas-Filho et al., 2001). These cumulative evidences suggest that type II AEC apoptosis could play a key role in the initial stage of the disease (Barbas-Filho et al., 2001).

Bleomycin-induced pulmonary fibrosis animal model studies demonstrated that pulmonary fibrosis occurred due to apoptosis of AEC via activation of pro-apoptotic Bcl-2 family member Bid (Budinger et al., 2006), activation of angiotensin receptor A1 (AT1) (Li et al., 2003) and through Fas-Fas ligands (Hagimoto et al., 1997a, Hagimoto et al., 1997b). How apoptosis can initiate or propagate fibrogenesis is not clear. In normal circumstances AEC secrete anti-fibrotic factors such as prostaglandin-E_2 (PGE_2), plasminogen activators and metalloproteinase which can inhibit fibroblast proliferation and enhance the degradation of ECM. There is a possibility that the loss of AEC by excessive apoptosis or necrosis could diminish the anti-fibrotic effects of the alveoli and trigger a fibrotic response. The alveolar epithelium acts as a physical barrier between the ECM and the macrophage. Denuded basement membrane and ECM can activate the macrophage and stimulate release of pro-fibrotic factors which can ultimately cause a fibrotic response (Uhal, 2008). Apoptotic loss of AECs can cause delay or failure of re-epithelialisation which is another potential key mediator for fibrosis (Plataki et al., 2005). More recently, it has been reported that severe and chronic endoplasmic reticulum stress in AEC could be an underlying cause of AEC apoptosis, which is likely to be involved with sporadic IPF (Korfei et al., 2008, Lawson et al., 2011, Tanjore et al., 2012).

1.10.2.1.3. Failure of alveolar re-epithelialisation

Re-epithelialisation is an essential step in normal tissue repair process (Selman et al., 2001, Crosby & Waters, 2010). Following alveolar injury, inflammation starts, healing processes proceed and finally repair is accomplished by type II AEC migration, proliferation and differentiation into type I AEC, that subsequently cover the denuded area of alveoli. The alveolar healing process starts with AEC injury and ends with re-epithelialisation. Failure or delay of this re-epithelialisation can cause persistence of reparative responses which can

ultimately result in fibrosis. Supporting this concept, increased AEC death or delayed repair was shown to promote fibroblast proliferation and subsequent fibrosis (Adamson et al., 1990).

In IPF, alveolar re-epithelialisation is likely to be hampered. While the exact mechanism of this failure of epithelial restitution is widely unknown, a possible set of aetiology could be: 1) increased apoptosis, 2) impaired migration and 3) loss of differentiation of AEC (Thannickal et al., 2004). In IPF, hyper-proliferation of type II AEC is common; however, their differentiation into type I AEC is thought to be seriously impaired (Kasper & Haroske, 1996).

1.10.2.1.4. Loss of type II AEC plasticity

Type II AEC can terminally differentiate into type I AEC, and this differentiation process is essential for maintenance of the integrity of alveolar epithelium. Abnormal accumulation of ECM proteins and over-expression of pro-fibrotic growth factors and cytokines are key mediators that are likely to be involved in the impairment of AEC differentiation (Selman & Pardo, 2006). The differentiation of type II AEC depends on the underlying matrix proteins. Studies have demonstrated that culture of type II AEC on collagen I or fibronectin matrix proteins allowed them to differentiate into type I AEC; whereas, culture on laminin-5 supplemented matrix protein interfered this differentiation process (Isakson et al., 2001, Isakson et al., 2002). During differentiation, type II AEC first transdifferentiate into an intermediate type II/type I cell-like phenotype without underlying matrix protein dependence, this intermediate cell can then differentiate into either type I or type II AEC depending on the presence of matrix proteins such as collagen, fibronectin or laminin-5 (Figure 1.7) (Olsen et al., 2005). Like matrix proteins, some growth factors such as KGF

(Fehrenbach et al., 1999) and insulin-like growth factor-1 (IGF-1) and IGF-II (Narasaraju et al., 2006) have important roles in the differentiation of type II AEC into type I cells (Figure 1.7).

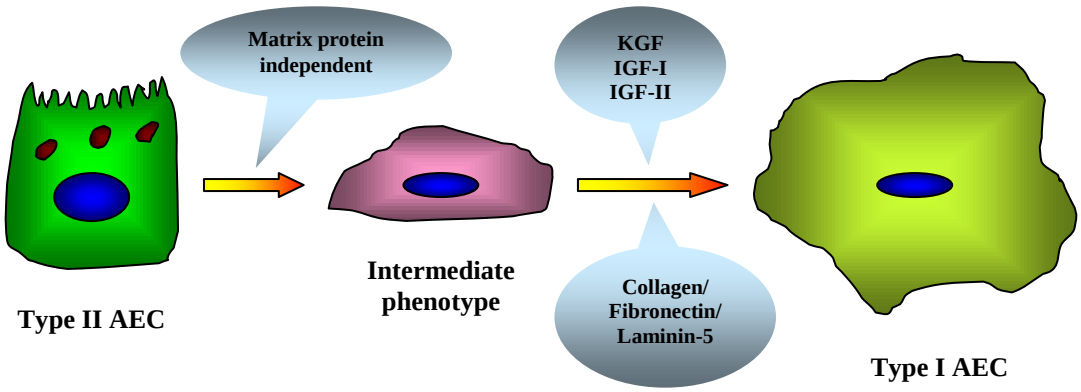

Figure 1.7: Differentiation of type II AEC into type I AEC.
In vitro differentiation of type II AEC into type I AEC occurs through an intermediate phenotypic cell transformation.

1.10.2.2. Disruption of epithelial-mesenchymal cross-talk

A balanced cross-talk between alveolar epithelial cells and fibroblasts is established during the alveolar healing process following injury. This cross-talk takes place either by direct cell-cell contact or via their secreted soluble factors (Geiser, 2003) (Figure 1.8). The epithelial-mesenchymal cross-talk is likely to be interrupted in IPF (Selman et al., 2001). In IPF, activated and/or injured AEC secrete increased levels of TGF-β, TNF-α, PDGF (platelet-derived growth factor), IGF-1, CTGF and ET-1 (endothelin-1). (Khalil et al., 1991, Kapanci et al., 1995, Nash et al., 1993, Antoniades et al., 1990, Pan et al., 2001, Giaid et al., 1993, Noble, 2008). These factors are capable of inducing fibrosis by stimulating growth and proliferation of fibroblasts and myofibroblasts. The sole effect of TGF-β is very critical in development of IPF (Geiser, 2003). TGF-β stimulates proliferation of fibroblasts, activation of myofibroblasts, apoptosis of AEC and induction

of EMT (Willis et al., 2005, Willis & Borok, 2007). CTGF and PDGF are potent mitogens for fibroblasts. ET-1 promotes fibroblast proliferation, myofibroblast differentiation, deposition of ECM and EMT in AEC (Abraham, 2008). IGF-1 can increase proliferation and inhibit apoptosis of fibroblasts and myofibroblasts which enhance fibrogenesis (Wynes et al., 2004) (Figure. 1.8).

During the normal reparative process activated fibroblasts and myofibroblasts synthesize and secrete ECM proteins to create a favorable basement membrane for epithelial migration. After completion of the basement membrane, AEC release an array of inhibitory molecules which suppress fibroblastic activities. One of the well-documented inhibitory factors is PGE_2 which inhibits fibroblast proliferation and collagen synthesis. PGE_2 is decreased in IPF patients (Wilborn et al., 1995, Borok et al., 1991). Another anti-fibrotic factor is NO (nitric oxide) which is released by both epithelial cells and fibroblasts and can suppress fibroblast and myofibroblast activity (Vernet et al., 2002, Wang et al., 1997). NO inhibits proliferation and transdifferentiation of fibroblasts into myofibroblasts resulting in reduction of collagen synthesis via neutralization of ROS (reactive oxygen species) (Vernet et al., 2002). In IPF, AEC derived NO has found to be reduced as well (Thannickal et al., 2004).

However, the precise mechanism of NO reduction in the IPF lung is unknown. TGF-β inhibits iNOS (inducible nitric oxide synthase) synthesis causing inhibition of NO production (Perrella et al., 1994, Finder et al., 1995). Up-regulation of TGF-β in IPF reduces NO by suppression of iNOS. NO has negative feedback effect on myofibroblasts. So, inhibition of NO production increases proliferation of myofibroblasts and subsequent collagen synthesis (Zhang and Phan, 1999). IL-1β is a potent inducer of iNOS and can thus

increase production of NO (Jorens et al., 1992, Lavnikova & Laskin, 1995) and subsequently inhibits fibroblasts and myofibroblasts proliferation and induces apoptosis of these cells via DNA damage (Zhang et al., 1997). TGF-β can completely block the IL-1β-induced apoptosis in fibroblast and myofibroblasts (Zhang and Phan, 1999). Interestingly, TGF-β induces apoptosis in AEC (Lee et al., 2006) but inhibits apoptosis in fibroblasts and myofibroblasts.

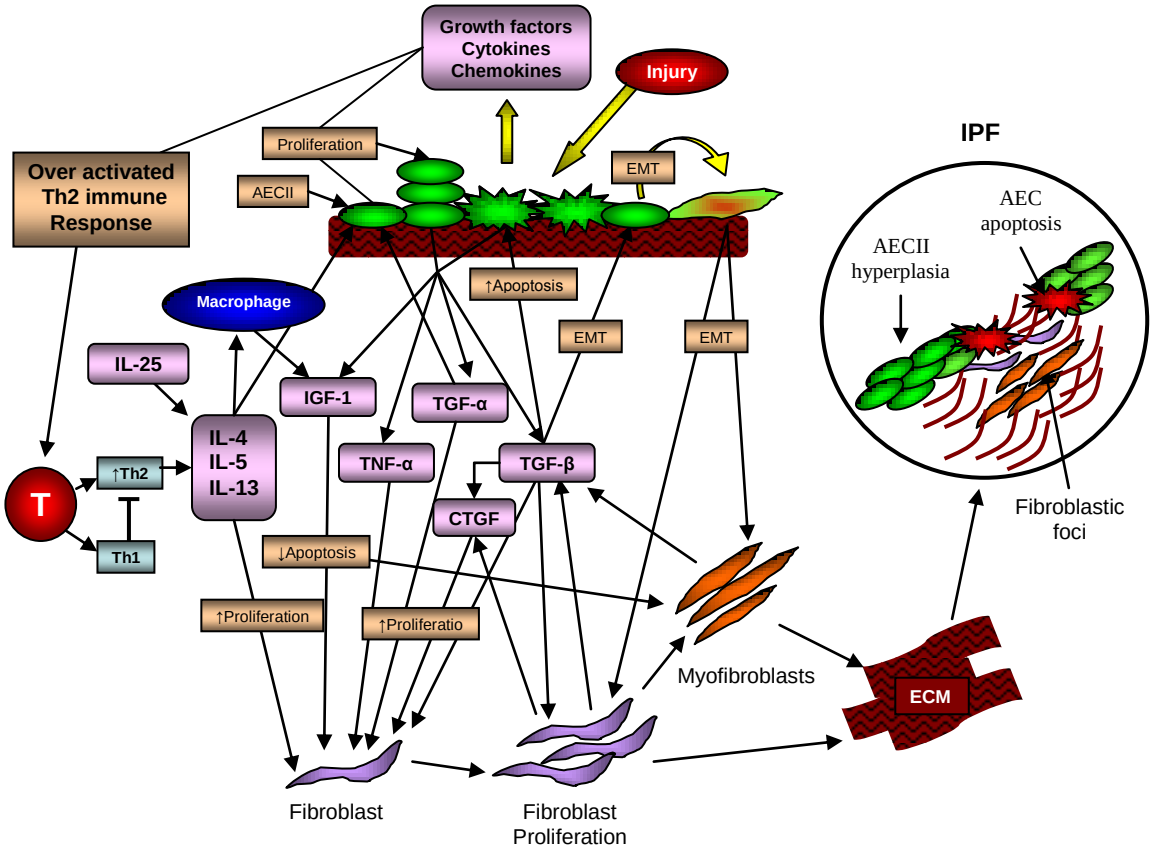

Figure 1.8: Epithelial- mesenchymal cross-talk during pathogenesis of IPF.

Injured AEC secrete bioactive cues that activate the Th2 immune response; which then increase Th2 type cytokines IL-4, IL-5 and IL-13. These interleukins and other growth factors promote fibroblast and type II AEC proliferation. Proliferating type II AEC and fibroblasts then increase secretion of pro-fibrotic growth factors. Among them TGF-β plays vital role by promoting myofibroblast differentiation, increased apoptosis of AEC and EMT. IGF-1 inhibits apoptosis of fibroblasts and myofibroblasts. The cumulative effects of this disrupted cross-talk lead to aberrant accumulation of collagen and other ECM proteins with associated derangement of AEC and subsequent fibrosis.

1.10.2.3. Multi-hits AEC injury: A vicious cycle between alveolar epithelial and mesenchymal cells is established.

While no known exogenous or genetic cause has been identified for the pathogenesis of IPF, it is difficult to explain the mechanism of repeated micro-injuries in AEC which eventually causes fibrosis. Depending on the cytokine and growth factor profile, the speculation is that there might be some active intrinsic factors within the micro-milieu of the fibrotic lesion that can cause repeated AEC injuries in a persistent manner. This speculation is supported by the demonstration that secretory products of fibroblasts isolated from IPF lungs induced apoptosis in cultured AEC (Uhal et al., 1995).

In 2006, Horowitz and Thannickal suggested that dysregulated epithelial-mesenchymal interaction in IPF may promote a '*vicious cycle*' in the pathogenesis of this disease (Figure 1.9) (Horowitz & Thannickal, 2006). Raised levels of pro-fibrotic and pro-apoptotic factors, such as TGF-β, TNF-α, and angiotensin are detected in the microenvironment of the fibrotic lesion. Following injury, TGF-β, TNF-α, angiotensin (Wang et al., 1999) and ROS are released by AEC and mesenchymal cells (fibroblasts and myofibroblasts) resulting in further injury to the AEC by apoptosis or necrosis. A vicious cycle is possibly established through initial AEC injury by unknown factor followed by secretion of cytokines, chemokines and growth factors by AEC and macrophages. These factors then promote fibroblast proliferation and differentiation into myofibroblasts causing additional release of pro-fibrotic and pro-apoptotic factors and accumulation of collagen and other ECM proteins. This combined unfavourable micro-milieu causes further alveolar epithelial cell damage, and epithelial injury again starts the fibrotic response through activation of mesenchymal cells (Figure 1.9).

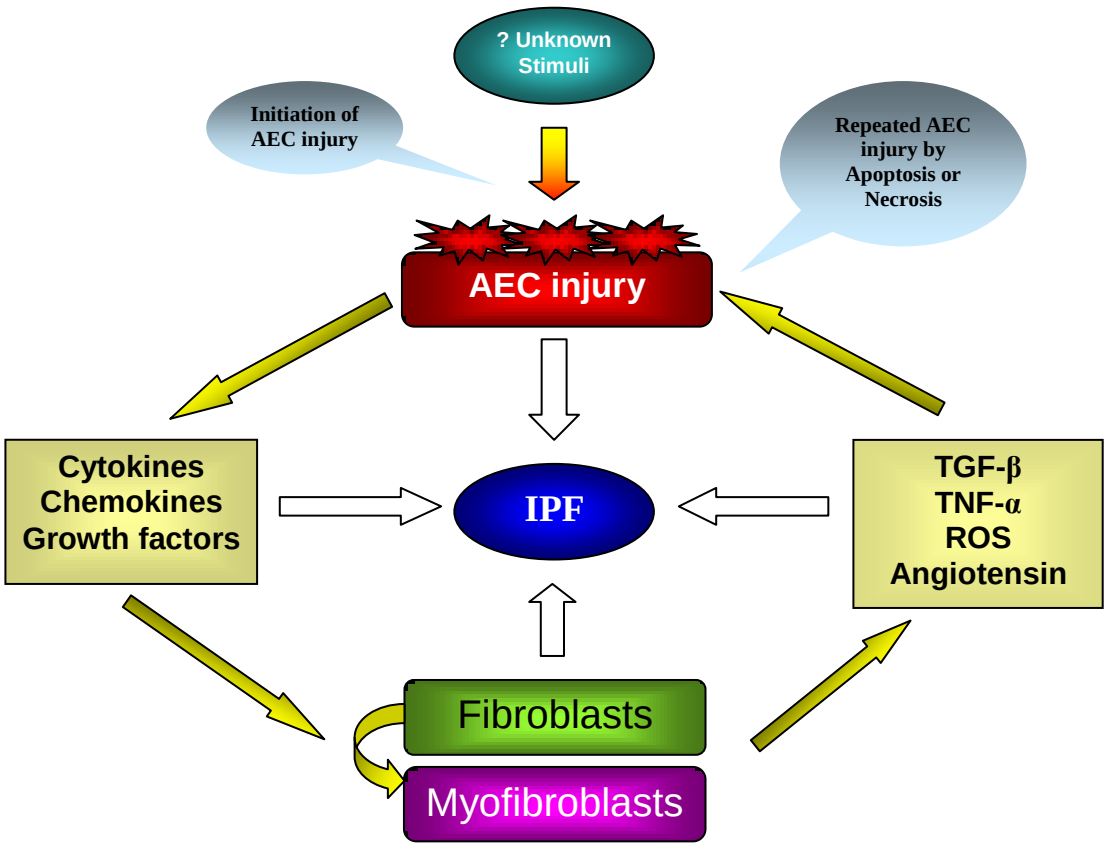

Figure 1.9: Hypothetical '*vicious cycle*' in multiple micro-injuries to AEC in IPF.

The cycle starts following AEC injury by unknown stimuli. After injury, AEC release pro-fibrotic cytokines, chemokines and growth factors which activate fibroblast/myofibroblast-driven fibrotic responses. This combined AEC and mesenchymal cell activation increase pro-fibrotic and pro-apoptotic factor levels in the micro-environment of the lesion. Among them, TGF-β, TNF-α, angiotensin and ROS can induce apoptosis or necrosis in AEC resulting further epithelial injury and thus continues this 'vicious cycle' of AEC injury.

1.10.2.4. Role of fibroblasts and myofibroblasts

The classical feature of IPF is the presence of 'fibroblastic foci' within the alveolar wall at the leading edge of fibrosis (Katzenstein & Myers, 1998, Thannickal et al., 2004, Lomas, et al., 2012). Fibroblasts and myofibroblasts play a pivotal role in the development of IPF. During normal healing process, following injury, inflammation takes place and fibroblasts become activated in an attempt to repair and secrete ECM proteins to form granulation tissue. At later stages, they differentiate into myofibroblasts which help wound contraction and facilitate wound healing. At the end-stage of the healing process, myofibroblasts disappear by apoptosis which is essential for proper wound repair (Desmouliere et al., 1995, Selman & Pardo, 2002). Many studies have shown the persistent presence of myofibroblasts in the active lesion of IPF (Desmouliere et al., 1995, Selman & Pardo, 2002, Lomas et al., 2012). Failure of alveolar re-epithelialisation can cause a continuous fibrotic response through activation of myofibroblasts that further inhibit re-epithelialisation.

Fibroblasts isolated from IPF patient's lungs are pro-fibrotic where their secretory products induce apoptosis in AEC *in vitro* through an angiotensin-dependent mechanism (Uhal et al., 1995, Wang et al., 1999). The *in vitro* proliferation profile of IPF lung fibroblasts is contradictory. One study demonstrated that fibroblasts from IPF lung grew significantly faster than those obtained from normal lung (Jordana et al., 1988); whereas, others have reported the inverse phenomenon (Ramos et al., 2001). Raghu and colleagues showed that fibroblasts isolate from early-fibrotic regions grew faster than those obtained from dense fibrotic regions (Raghu et al., 1988). Very recently, our group reported a low proliferative status of fibroblast/myofibroblasts within the fibroblastic foci of IPF lung which was evaluated based on Ki-67, a cell proliferation marker, expression by an *ex-vivo* study on 21

IPF patients (Lomas et al., 2012). These above findings indicate that the proliferative status of fibrotic fibroblasts is heterogeneous and could be related to the disease status.

Myofibroblasts are thought to play a vital role in the development of IPF. Myofibroblasts express α-SMA (α-smooth muscle actin) and represent an intermediary phenotype between fibroblasts and smooth muscle cells (Darby et al., 1990, Roy et al., 2001). The main function of this mesenchymal cell is synthesis and secretion of ECM proteins, wound contraction and ECM remodeling. The transient appearance and disappearance of myofibroblasts are observed during normal healing and repair process. On the other hand, in IPF, the persistent presence of myofibroblasts is a constant feature (Desmouliere et al., 1995, Selman & Pardo, 2002, Lomas et al., 2012). During activation and proliferation, fibroblasts/myofibroblasts release pro-fibrotic factors such as TGF-β, TNF-α, and angiotensin which can cause AEC damage. These cells also secret MMP-2 (matrix metalloproteinase-2) and MMP-9 which may disrupt the basement membrane, alter the tissue architecture and inhibit alveolar re-epithelialisation (Selman et al., 2000).

Although the presence of myofibroblasts within the fibrotic lesion is apparent, their source remains elusive. There is ample evidence showing that myofibroblasts can be transformed from tissue fibroblasts in presence of TGF-β (Desmoulière et al., 1993) and IL-4 (Mattey et al., 1997) *in vitro*. But *in vivo*, how myofibroblasts are acquired in the site of fibrotic lesion of IPF is largely unknown. Based on their similar cellular kinetics, it is assumed that myofibroblasts are transformed cells from pre-existing resident tissue fibroblasts with the influence of stimulatory cytokines, such as TGF-β (Phan, 2002) (Figure 1.10). Some studies suggested that circulating fibrocytes derived from bone marrow stem cells (MSC) could be an extra-pulmonary source of fibroblasts and myofibroblasts in IPF (Lama &

Phan, 2006, Hashimoto et al., 2004, Phillips et al., 2004, Epperly et al., 2003, Ishii et al., 2005). Another possible source of myofibroblasts in fibroblastic foci is AEC by EMT (Figure 1.10).

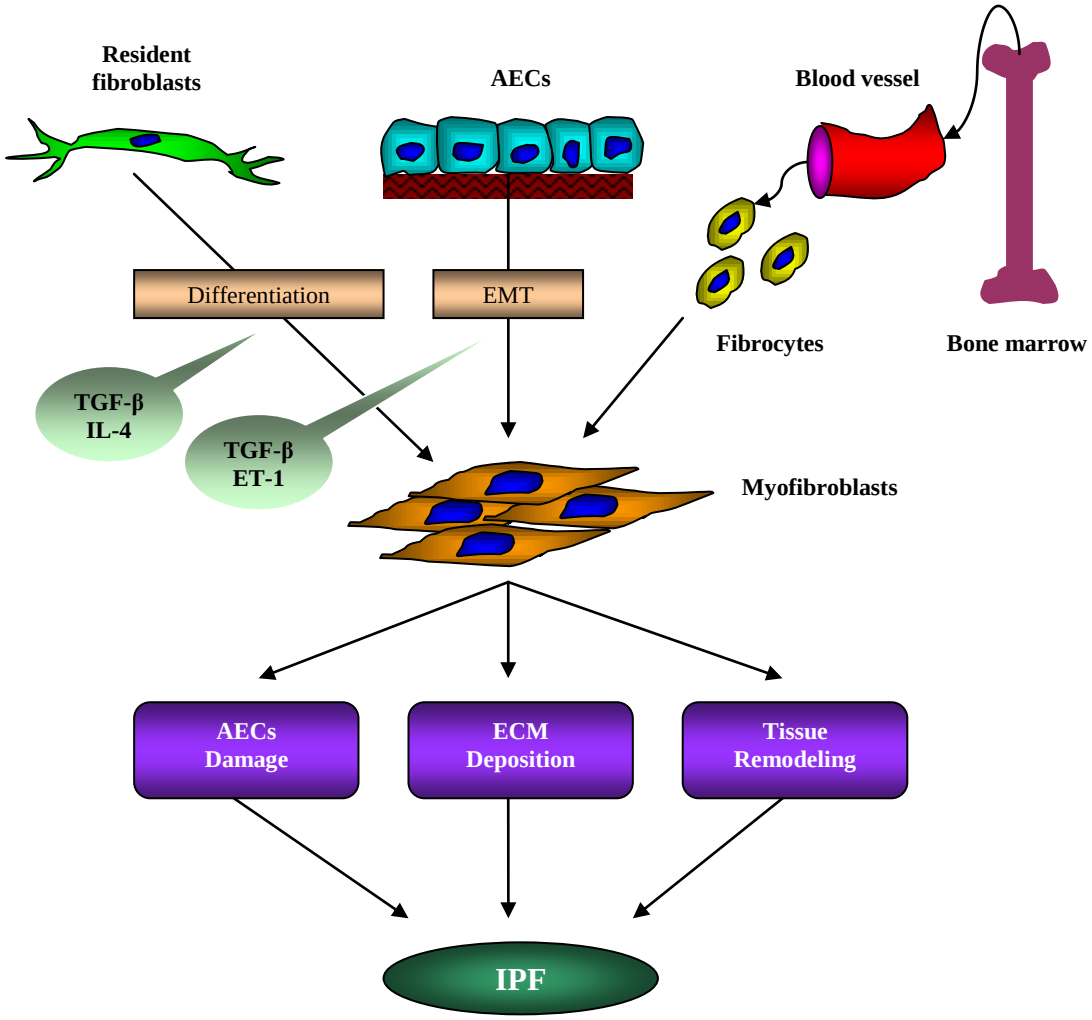

Figure 1.10: The origins of myofibroblasts in IPF lesion.

Schematic diagram demonstrates the acquisition of myofibroblasts from pulmonary and extra-pulmonary sources at the site of fibrotic lesion in IPF and their effects in the pathogenesis. Pulmonary sources are resident fibroblasts and AEC. AEC transformed into fibroblasts/myofibroblasts by EMT driven effects of TGF-β and ET-1. Myofibroblasts are transdifferentiated from tissue fibroblasts by TGF-β and IL-4. Extra-pulmonary source is circulatory bone marrow-derived fibrocytes.

1.10.2.5. Role of EMT in IPF

Epithelial-mesenchymal transition (EMT) is a biological process whereby polarized epithelial cells lose many of their epithelial characteristics and undergo morphological changes to assume a mesenchymal phenotype (Thiery & Sleeman, 2006). The EMT process is frequently observed in IPF lung which suggests that EMT could be involved in the disease process. However, the precise mechanism of EMT in pulmonary fibrosis is not well understood (Selman & Pardo, 2006, Willis et al., 2005, Willis & Borok, 2007, Willis et al., 2006, Kim et al., 2006). *In vitro* studies demonstrated that TGF-β can transform primary human and rat AEC into fibroblast and myofibroblasts (Willis et al., 2005, Kim et al., 2006, Kasai et al., 2005). ET-1 is implicated in the pathogenesis of IPF. A study demonstrated that ET-1 could induce EMT in AEC through production of TGF-β via an ET-A receptor dependent-manner (Jain et al., 2007). Twist, a transcription factor, is not normally expressed in AEC; however, high expression levels have been detected in AEC of IPF lungs with the accompanying EMT features (Pozharskaya et al., 2009). Murine lung fibrosis models and IPF lungs demonstrated that overexpression of Twist in AEC was related to viral infection; thereby, it has been suggested that Twist could be involved in EMT, particularly in viral infected cases (Pozharskaya et al., 2009). Overexpression of Wnt and β-catenin has also been detected in fibroblast/myofibroblast and type II AEC of IPF lung (Konigshoff et al., 2008, Chang et al., 2010). The Wnt/β-catenin pathway was implicated in the regulation of EMT in other cell types (Dissanayake et al., 2007, Medici et al., 2008). It has been suggested that the Wnt/β-catenin signaling pathway could also be involved in the EMT process in IPF (Chang et al., 2010).

1.10.2.6. Role of alveolar bronchiolisation

Alveolar bronchiolisation, a process of abnormal proliferation of Clara and other bronchiolar epithelial cells and their migration into the alveoli, has been documented in both IPF lung tissues and animal models of pulmonary fibrosis (Collins et al., 1982, Kawanami et al., 1982, Fukuda et al., 1989, Kawamoto & Fukuda, 1990, Betsuyaku et al., 2000, Chilosi et al., 2002, Mori et al., 2004, Odajima et al., 2007). A sub-population of these Clara cells behaves as functional bronchiolar progenitor cells with participation in bronchiolar wound repair and regeneration (Evans et al., 1976, Reynolds & Malkinson, 2010). However, lineage tracking in animal model studies has indicated that Clara cells may not take part in alveolar injury repair (Rawlins et al., 2009). Also, in bleomycin-induced murine pulmonary fibrosis, abrogation of alveolar bronchiolisation does not worsen the disease state (Betsuyaku et al., 2000). Despite these findings, alveolar bronchiolisation remains a constant histological feature in IPF lungs albeit that this activated event appears to fail to restore alveolar architecture and functionality (Chilosi et al., 2002, Mori et al., 2004, Odajima et al., 2007). Thus, the role of the alveolar bronchiolisation process in the dynamic between alveolar injury repair on one hand and propagation of fibrogenesis on the other remains unclear (see Chapter-3, Section- 3.4).

1.10.2.7. Basement membrane disruption and ECM remodeling

Basement membrane is a specialized extracellular matrix layer consisting mainly of type IV collagen, laminin, fibronectin, entactin and heparin sulfate proteoglycans produced mainly by epithelial cells, endothelial cells and mesenchymal cells (Yurchenco & Schittny, 1990). Basement membrane provides support for epithelial cells and a suitable surface for their migration, proliferation and differentiation. This membrane also acts as a physical barrier between epithelial and mesenchymal cells. Disruption of this membrane hampers

epithelial cell migration and proliferation but facilitates fibroblast and myofibroblast migration to the epithelial surface which ultimately causes epithelial cell destruction and fibrosis. In IPF, marked disruption of basement membrane is common (Selman et al., 2001).

Bleomycin-induced pulmonary fibrosis animal model experiments demonstrated that, in the early stages of fibrosis, alveolar epithelial basement membrane disruption occurred due to the over activity of MMP-9 (Gelatinase B), and in later stages by MMP-2 (Gelatinase A). Gelatinase B is predominantly localized in inflammatory cells, whereas, Gelatinase A is localized in alveolar epithelial cells (Yaguchi et al., 1998). Gelatinase A and Gelatinase B cause degradation of ECM proteins, specially, collagen IV and elastin. The activities of MMPs are controlled by TIMPs (tissue inhibitory metalloproteinases). Imbalance between MMPs and TIMPs may cause basement membrane disruption and remodeling of ECM and thus may contribute in the pathogenesis of IPF.

1.10.2.8. Imbalanced inflammatory response of T cells

Two types of helper-T cell responses in inflammation take place following an injury. These are called Type-1 and Type-2 helper T cell responses (Th1 and Th2 respectively). Specific types of cytokines are released in different types of helper-T cell response. In the Th1 response, the predominant cytokines are IL-2, IL-12, IL-18 and interferon-γ (INF- γ). On the other hand, the predominant cytokines of Th2 response are IL-4, IL-5, IL-10 and IL-13. In general, the Th1 response regulates cell mediated immunity and injured tissue restoration; whereas, the Th2 type response promotes antibody mediated immunity and persistence of this type of response initiates fibroblast activation and extracellular matrix deposition followed by unresolved fibrosis (reviewed in Keane, 2008). After injury, a

balanced response between Th1 and Th2 is essential for proper tissue restoration. Uncontrolled over activation of Th2 type response may cause excessive fibrosis (reviewed in Keane, 2008). How these two types of immune responses play role in pathogenesis of IPF is not clear.

Along with cytokines, some chemokines and their receptors are essential mediators for regulation of the Th1 and Th2 inflammatory responses (Sallusto et al., 1998). For example, chemokine receptors CXCR3 and CCR5 are predominantly expressed in the Th1 type response; whereas, in Th2 type inflammatory response, CCR3, CCR4 and CCR8 chemokine receptors are predominant (Sallusto et al., 1998) (Keane, 2008). The bleomycin-induced pulmonary fibrosis mouse model experiment showed that levels of chemokines CCL17 and CCL22 and their common receptor CCR4 were significantly raised during the fibrotic process, and that neutralization of CCL17 reduced fibrosis levels (Belperio et al., 2004). CCL17 and its receptor CCR4 do not have any effect on fibroblast proliferation (Belperio et al., 2004). This indicates that CCL17 may follow an alternative pathway in the pathogenesis of pulmonary fibrosis bypassing fibroblast proliferation.

On the other hand, high levels of CCL17 and CCL22 are found in the lung tissue of IPF patients, where they are predominantly expressed on epithelial cells, particularly on the hyperplastic epithelial cells (Belperio et al., 2004). On the basis of cytokine and chemokine profiles of animal model and IPF patient lung tissue, it is postulated that, uncontrolled and exacerbated Th2 type immune responses may play crucial role in the pathogenesis of IPF, especially in the early stage of disease process (Keane, 2008).

1.10.2.9. Oxidative stress

Increased levels of oxidant and decreased glutathione, a potent anti-oxidant, levels have been reported in IPF lung (MacNee & Rahman, 1995, Cantin et al., 1989) which was also associated with systemic oxidant/anti-oxidant imbalance (Rahman et al., 1999). Glutathione neutralizes H_2O_2 and other oxidants and thus prevents oxidative damage of AEC. A deficiency of glutathione or other anti-oxidant in the alveolar lining fluid can make AEC vulnerable to injury. Therefore, an oxidative insult to AEC might cause epithelial cell damage and promote fibrosis. Human lung fibroblasts can release H_2O_2 only when stimulated by TGF-β (Thannickal & Fanburg, 1995). In IPF, raised levels of TGF-β may stimulate fibroblasts to secret H_2O_2. This cytokine-fibroblasts-H_2O_2 interaction is implicated in the pathogenesis of IPF.

1.10.2.10. Genetic abnormalities

The pathogenesis of IPF is complex, so it is unlikely that a single gene abnormality will emerge as being responsible for this disease (Loyd, 2008). Selman and colleagues produced a microarray-based gene expression profile of IPF, hypersensitivity pneumonia and non-specific interstitial pneumonia (NSIP). They demonstrated a distinct gene expression patterns between IPF and the other two diseases (Selman et al., 2006). The upregulated genes in IPF were associated with extracellular matrix remodeling; and adhesion, migration, proliferation and differentiation of AEC and myofibroblasts; whereas, in other two diseases, the gene expression profiles were predominantly inflammation related (Selman et al., 2006). MMP-7 and (Zuo et al., 2002) osteopontin overexpression (Pardo et al., 2005) have also been detected within AEC in most IPF cases. MMP-7 knock-out mice were resistant to bleomycin induced pulmonary fibrosis (Zuo et al., 2002). Osteopontin has been demonstrated to have pro-fibrotic properties by stimulation of

fibroblast migration and proliferation (Pardo et al., 2005). These findings suggest that aberrant expression of MMP-7 and osteopontin could be involved in IPF pathogenesis.

Most of the genetic abnormalities are found in familial IPF where the common anomalies are telomerase shortening and misfolded surfactant protein-C in AEC. In about 8-10% of familial IPF, genetic mutation is found in telomerase related genes *hTERT* and *hTR* (Armanios et al., 2007, Tsakiri et al., 2007). hTERT is a telomerase reverse transcriptase which is an important enzyme for maintenance of telomeres (the end region of linear chromosomes comprised of TTAGGG repeats which prevents inappropriate recognition by DNA damage complexes) and cell proliferation (Loyd, 2008). The *hTR* gene encodes telomerase RNA. Genetic mutation is also found in *SFTPC* gene which encodes surfactant protein-C (SP-C). This mutation results production and accumulation of misfolded protein (SP-C) in type II AEC. However, this type of mutation is rare, only found in 1% in study group (Nogee et al., 2001).

1.11. Treatment strategies for IPF

1.11.1. Current Treatments

1.11.1.1. Anti-inflammatory and immunomodulatory drugs

Currently, there is no effective treatment for IPF. Anti-inflammatory drugs such as corticosteroids are used, but these agents do not show any beneficiary effects to halt the disease progression. Moreover, these drugs have tremendous side effects including osteoporosis, peptic ulcer disease, weigh gain, avascular necrosis, hyperglycaemia, susceptibility to infection and so on. Some immunomodulatory agents like azathioprine, cyclophosphamide and colchicine have also shown to be ineffective (Walter et al., 2006). IPF is no longer an inflammatory disease; rather it is a special type of fibrotic lung disease

that occurs due to multiple alveolar epithelial injuries and abnormal wound healing. Possibly, for this reason anti-inflammatory agents appear to be ineffective.

1.11.2. Future potential treatment options

1.11.2.1. Newer anti-fibrotic agents

Due to poor response of anti-inflammatory drugs to halt fibrogenesis, some newer anti-fibrotic agents have recently been proposed for the treatment of IPF; such as pirfenidone and etanercept. Pirfenidone is an orally bioavailable synthetic molecule that can inhibit activities of TGF-β and TNF-α *in vitro* and suppress fibroblast proliferation and collagen synthesis with subsequent reduction of fibrotic load in animal models of lung fibrosis (Iyer et al., 1995, Iyer et al., 1998, Iyer et al., 1999, Nakazato et al., 2002, Oku et al., 2002, Hirano et al., 2006). Pirfenidone has already undergone phase II and III clinical trials in Japan, USA, Australia, UK and many other countries (Raghu et al., 1999, Nagai et al., 2002, Azuma et al., 2005, Taniguchi et al., 2010, Noble et al., 2011). Cumulative data analysis demonstrated that pirfenidone reduced lung function decline and prolonged progression-free survival of patients with IPF (Noble et al., 2011). Another anti-fibrotic agent etanercept, a recombinant soluble human TNF-α receptor that can bind and neutralise TNF-α (Mohler et al., 1993), has been evaluated in a Phase II clinical trial on IPF patients; however, this showed no statistically significant beneficial effects over placebo (Raghu et al., 2008).

1.11.2.2. Regenerative cell therapy

Regenerative medicine is an emerging therapeutic concept that aims to repair, replace or regenerate cells, tissues or organs to restore impaired function (Daar & Greenwood, 2007). Regenerative medicine-based therapeutic interventions could be effective for the treatment

of specified clinical conditions where currently there is no adequate therapy. Therefore, regenerative therapy offers a rational approach for the treatment of IPF. Delivery of regenerative therapy could be through a tissue engineered intervention or through stem cell-mediated approaches (Daar & Greenwood, 2007). Stem cells are non-specialised self-renewing cells which can differentiate into various specialised cell lineages under appropriate conditions (Martin, 1981, Thomson et al., 1998, Bajada et al., 2008). Broadly, stem cells are divided into two types: 1) Embryonic stem cells (ESC), which are pluripotent and can differentiate into derivatives of all three embryonic germ layers. 2) Non-embryonic stem cells or adult stem cells which are multipotent and can differentiate into limited number of phenotypes (Lee & Hui, 2006). Mesenchymal stem cells (MSC) are one of the widely studied adult stem cells which have shown enormous potential in regenerative medicine. Both MSC and ESC have been suggested for regenerative therapy for IPF.

1.11.2.2.1. Mesenchymal stem cells

Mesenchymal stem cells are a population of adult stem cells which were first discovered within the bone marrow through the pioneering work of Friedenstein and colleagues (Friedenstein et al., 1970). MSC are multipotent, adherent, spindle in shape and form colonies in culture which are known as colony forming unit-fibroblasts (CFU-Fs). The cells of the colony can self-renew and are capable of differentiating into, minimally, osteoblasts, chondrocytes and adipocytes (Friedenstein et al., 1970) (Figure 1.11). These cells are also known as mesenchymal stromal cells. The mesenchyme or stroma as often quoted describes the tissue that provides the structural and functional support for the growth and development of numerous organ systems. In relation to the bone marrow the

mesenchyme forms a layer of cells that delivers the essential support which haematopoietic stem cells require for their self-renewal and differentiation (Strobel et al., 1986).

More recently, MSC-like cells have been discovered in almost all tissues and organs (da Silva et al., 2006). However, their identification and characterisation are challenging due to the lack of any specific biomarkers. To establish a standard of MSC characterisation the International Society for Cellular Therapy has provided a guideline which state that MSC must express CD73, CD90, CD105 and lack of expression of CD34, CD45, CD14, CD11b, CD19 or MHC class II antigen (Figure 1.12) and show capability of tri-lineage differentiation into osteoblasts, chondrocytes and adipocytes (Figure 1.11) (Dominici et al., 2006). MSC also express CD44, CD146 and STRO-1 antigens (Simmons & Torok-Storb, 1991, Pittenger et al., 1999, Colter et al., 2001, Delorme et al., 2009).

Although MSC were first discovered in bone marrow, recently adipose tissue has offered another potential source of MSC for clinical applications (Kuhbier et al., 2010). The advantages of adipose tissue as a source of MSC over bone marrow are 1) relatively easy collection procedure and 2) and high yield of MSC in comparison to bone marrow. The frequency of MSC in the adipose tissue is 1-10 in 100 stromal vascular fraction (Guilak et al., 2006, Oedayrajsingh-Varma et al., 2006) whereas, in bone marrow it is 1-10 in 100,000 of mononuclear cells (Baksh et al., 2007) which provides an advantageous high yield of MSC from adipose tissue when comparing equal volumes of bone marrow (Madonna et al., 2009). Birth-associated tissues such as umbilical cord, umbilical cord blood and Wharton's jelly have also been proposed to be another source of MSC (Ennis et al., 2008). The advantage of birth-associated tissue-derived MSC is their higher proliferative capacity and reduced senescence properties; however, their incapability of differentiating into

adipocytes has been reported (Conconi et al., 2006, Baksh et al., 2007). Despite multiple sources of MSC have been proposed, bone marrow is to date still the gold standard location for MSC isolation and further research must be conducted before the use of alternative locations becomes common practice within the research community. Since discovery of MSC they have amassed significant interest from the medical and scientific community due to their differentiation capacity into various tissues and their tissue repair and regenerative properties.

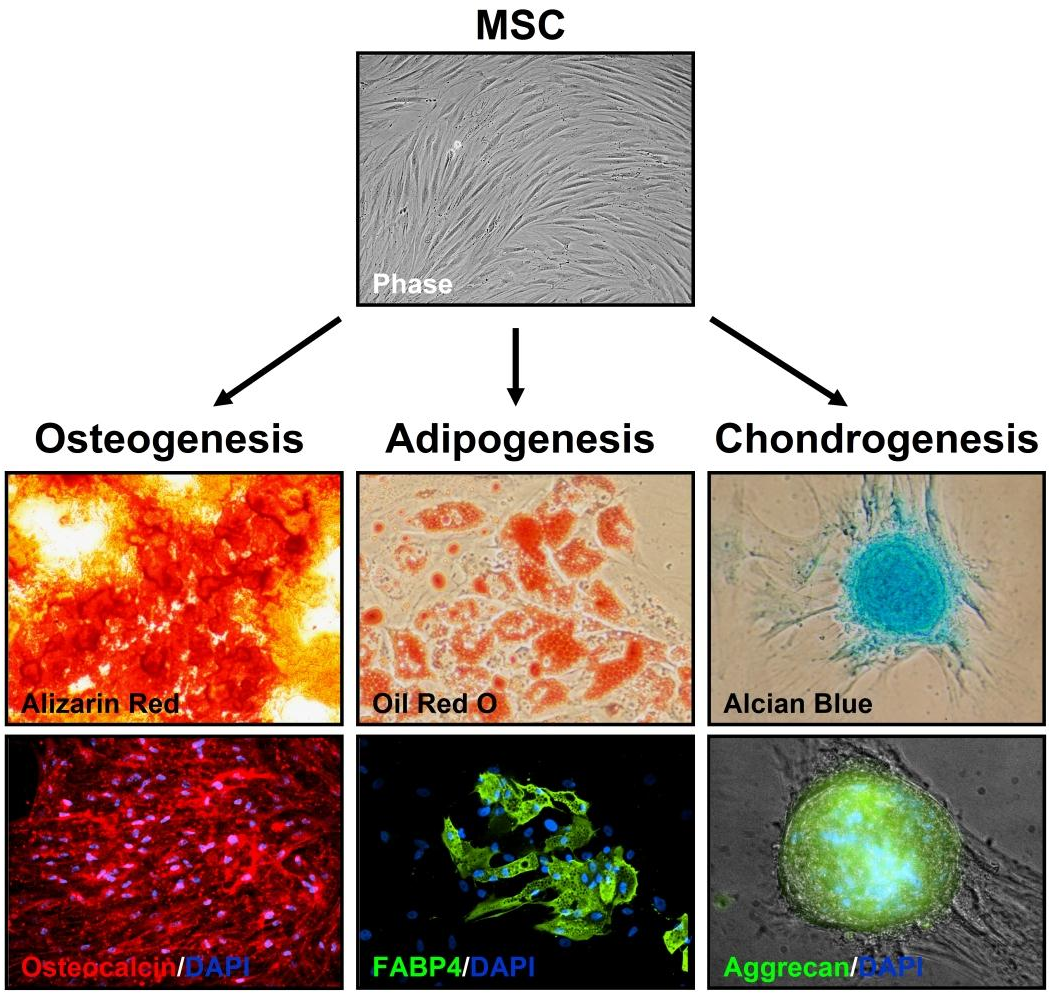

Figure 1.11: Morphology of human MSC and their classical tri-lineage differentiation.
Phase image shows the typical spindle shaped morphology of adherent human MSC. **Osteogenesis;** deposited calcium by differentiated osteoblasts was stained with Alizarin Red and osteocalcin was labelled by anti-osteocalcin antibody. **Adipogenesis;** differentiated adipocytes produce triglyceride which was stained with Oil Red O and adipocytes were stained with anti-FABP4 antibody. **Chondrogenesis;** chondrogenic nodules were stained with Alcian Blue and anti-aggrecan antibody. (Images were taken from Akram et al., 2012).

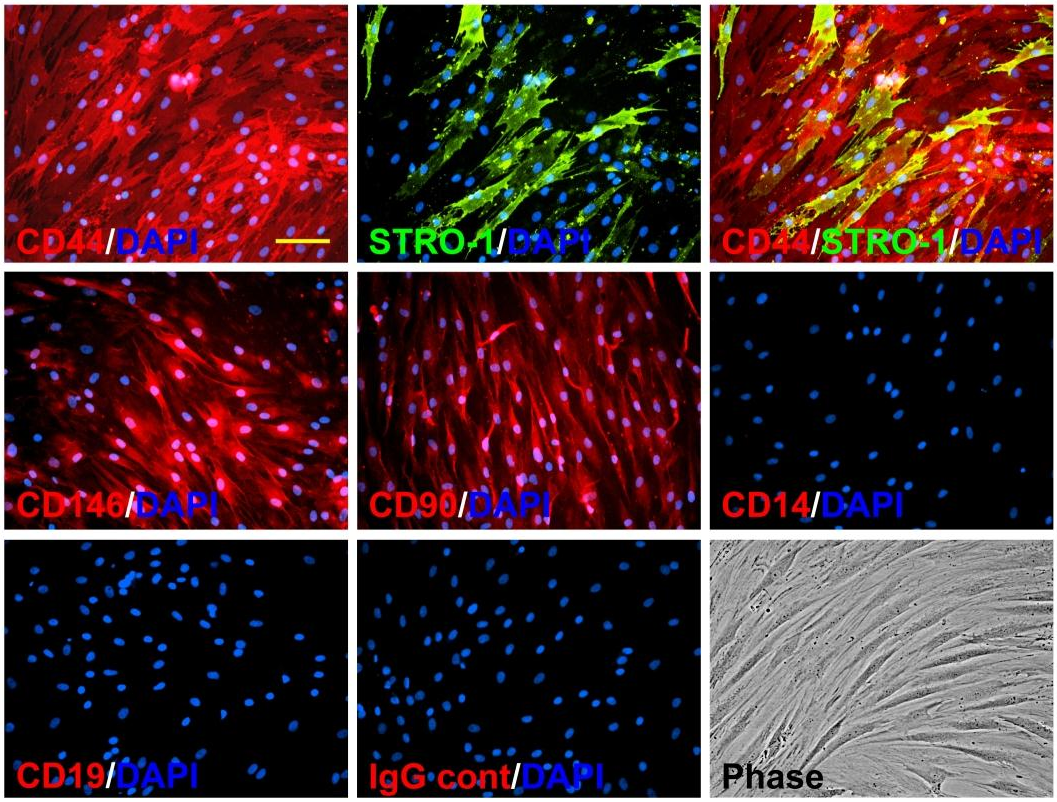

Figure 1.12: Phenotypic antigenic markers of human MSC.

Human MSC demonstrate positive expression of CD44, STRO-1, CD90, CD146 and negative expression to haematopoietic markers CD14 and CD19. Nuclei are stained with DAPI. Phase images show typical morphology of MSC. Scale bar, 100µm. (Images were taken from Akram et al., 2012).

1.11.2.2.1.1. Reparative mechanism of MSC

Pre-clinical studies and clinical trials demonstrated that application of MSC stimulated wound repair and regeneration resulting in efficient amelioration of clinical conditions (Kotton et al., 2001, Berry et al., 2006, Morigi et al., 2004, Rojas et al., 2005) (www.clinicaltrials.gov). However, the precise mechanism of MSC-mediated wound repair and regeneration is not clearly known. One of the unique properties of MSC is their site-specific migration and structural engraftment to the injured tissue. Their differentiation into specific cell types has also been demonstrated through various experimental animal models which suggests their active participation in wound repair and tissue regeneration (Kotton et al., 2001, Morigi et al., 2004, Rojas et al., 2005). On the other hand, some studies

postulated that MSC-secreted paracrine factors play a vital role for wound repair, most likely through their anti-inflammatory, anti-apoptotic, angiogenic and immunomodulatory properties (Ortiz et al., 2007, Zhen et al., 2008, Burdon et al., 2011, Baber et al., 2007, Nemeth et al., 2010). Additional reports also suggest that MSC secretory products are capable of stimulating tissue-specific regional progenitor cells which activate tissue regeneration (Gnecchi et al., 2008, Suzuki et al., 2011).

1.11.2.2.1.1.1. Functional contribution of MSC in tissue repair

MSC classically can differentiate into mesodermal lineages including osteoblasts, chondrocytes and adipocytes (Figure 1.11) (Friedenstein et al., 1970, Pittenger et al., 1999). A rapidly growing number of reports suggest their capacity of differentiation into a further wide range of mesodermal and non-mesodermal adult phenotypes including cardiomyocytes (Toma et al., 2002, Deb et al., 2003), neurons (Dezawa et al., 2004, Zeng et al., 2011), hepatocytes (Sato et al., 2005) and lung epithelial cells (Kotton et al., 2001, Ma et al., 2011). The capacity of MSC to differentiate into distinct cell types is a central phenotypic feature that has attracted significant interest within the scientific community for their application in the field of regenerative medicine.

In 2002, Toma and colleague injected human bone marrow MSC isolated from healthy donors into the myocardium of healthy mice and observed that after a week MSC were differentiated into cardiomyocyte-like cells (Toma et al., 2002). Berry and colleagues injected MSC into the infarct region of cardiac wall of myocardial infarction rat models and demonstrated that MSC treatment improved cardiac function, reduced cardiomyocytes apoptosis and fibrosis scar comparing non-MSC treated control groups (Berry et al., 2006). They also demonstrated that transplanted MSC expressed cardiomyocyte-specific protein

'troponin T' although their phenotypic morphology was unlike cardiomyocyte suggesting a putative paracrine role underpinned the reparative process.

MSC have also been reported to differentiate into type I and type II alveolar epithelial cells *in vivo* (Kotton et al., 2001, Rojas et al., 2005). Studies on bleomycin induced animal lung fibrosis models demonstrated that following intratracheal and intravenous administration of MSC, a small proportion of transplanted cells engrafted into the affected lung and differentiated into AECI and AECII cells with an accompanying amelioration of pulmonary fibrosis (Kotton et al., 2001, Rojas et al., 2005). A recent *in vitro* study also demonstrated that human MSC are capable of differentiating into SP-C (a bio-marker of AECII) -expressing AECII-like cells when co-cultured with foetal lung mesenchymal cells (Ma et al., 2011). In addition, systemic application of murine MSC in a cisplatin-induced acute renal failure mouse model resulted in migration and engraftment to the affected kidneys and differentiation into renal tubular epithelial cells with amelioration of renal dysfunction and augmentation of renal tubular regeneration suggesting MSC as a potential candidate for regenerative cell therapy for the cure of acute renal failure (Morigi et al., 2004).

The differentiation capacity of MSC into hepatocytes was also demonstrated in alcohol-induced chronic liver injury rat models (Sato et al., 2005). Sato and colleagues injected human MSC directly into the alcohol-induced injured part of rat liver and assessed for different hepatocyte-specific bio-markers in different time periods. They revealed that on and after a 7 post-transplant period MSC started to express a set of hepatocyte-specific proteins (hepatocyte bio-markers) namely, human-specific alpha-fetoprotein (AFP), albumin (Alb), cytokeratin-19 (CK-19), cytokeratin-18 (CK-18), and asialoglycoprotein

receptor (AGPR) (Sato et al., 2005). Apart from these, under specific culture conditions MSC have been shown to differentiate into functional neuronal phenotypes (Dezawa et al., 2004, Zeng et al., 2011), retinal pigment epithelial cells (Arnhold et al., 2007) and skin epithelial cells (Nakagawa et al., 2005).

Although increasing reports demonstrated the differentiation potential of MSC into different adult phenotypes, in most of the cases the targeted cell-type differentiation was confirmed based on their cell-type specific biomarkers. It is true that some markers are specific for certain cells; however they do not always have functional relation. In addition these markers are not always unique for characterization of a specific cell type. Empirical analysis on both human and rodent MSC demonstrated that MSC is, by nature, primed for osteogenic, chondrogenic, adipogenic and vascular smooth muscle differentiation and can undergo active differentiation under appropriate culture condition via activation of TGF-β, hedgehog, peroxisome proliferator-activated receptor interaction and MAPK pathways respectively (Delorme et al., 2009). Thereby, precaution must be taken for clinical application of MSC to avoid any unwanted ectopic differentiation.

1.11.2.2.1.1.2. Tissue repair by MSC-mediated paracrine mechanism

A growing body of evidence suggests that the paracrine mechanism of MSC is largely involved in the tissue repair and regenerative process. MSC possesses immunomodulatory functions which have been demonstrated through their therapeutic efficacy in alleviation of graft-versus-host disease (GvHD) and animal model of bronchial asthma through their putative role in modulating Type-1 (Th1) and Type-2 (Th2) immune responses (Nemeth et al., 2010). MSC-secreted factors are cytoprotective as demonstrated in a cardiac injury animal model driven by anti-apoptotic and inotropic effects (Gnecchi et al., 2008). The

MSC-mediated anti-apoptotic effects can be driven by up-regulation of the anti-apoptotic gene, Bcl-2, which was demonstrated in an animal model of emphysema (Zhen et al., 2008) (Figure 1.13). Animal model of myocardial infarction and pulmonary hypertension have demonstrated that transplanted MSC improved cardiac function and pulmonary vasculature by stimulating neovascularisation possibly via their secretory VEGF (vascular endothelial growth factor) and eNOS (endothelial nitric oxide synthase) (Burdon et al., 2011, Baber et al., 2007, Kanki-Horimoto et al., 2006). The anti-inflammatory function of MSC has been documented in many animal model studies. The mechanism is paracrine and more likely *via* blocking of anti-inflammatory cytokines such as TNF-α and IL-1 (Ortiz et al., 2007, Gupta et al., 2007) (Figure 1.13).

1.11.2.2.1.2. Potential MSC-mediated regenerative therapy for IPF

Due to the lack of available curative treatments for IPF and the repeated failure of anti-fibrotic drugs, stem cell-mediated regenerative therapeutic approaches have been proposed. Several animal models of pulmonary fibrosis have been developed (Moore & Hogaboam, 2008). Among them the best characterised and most widely used model is the bleomycin-induced pulmonary fibrosis model (Harrison & Lazo, 1987, Moore & Hogaboam, 2008). Other models include radiation-induced fibrosis (Haston & Travis, 1997), silica-induced fibrosis (Davis et al., 1998) and asbestos-induced lung fibrosis model (Bozelka et al., 1983).

The bleomycin-induced pulmonary fibrosis mouse model was applied in the demonstration of migration and engraftment of endotracheal or systematically transplanted MSC towards the site of injuries of the lung and subsequent attenuation of pulmonary fibrosis (Rojas et al., 2005, Ortiz et al., 2003). Ortiz and colleagues demonstrated that the systemic

administration of bone marrow derived MSC after 4 hours of bleomycin administration attenuated pulmonary inflammation, reduced fibrosis and decreased mortality after 14 days of injury and engraftment of transplanted MSC in the injured alveoli with their differentiation into type II AEC-like phenotype (Ortiz et al., 2003). However, when MSC were administered after 7 days of injury, the MSC-mediated protective function was abrogated (Ortiz et al., 2003). Using the same model, Rojas and colleagues also demonstrated the injury reparative function of MSC and their engraftment potential to injured lung (Rojas et al., 2005). In 2007, Ortiz and colleagues showed that MSC protected bleomycin-induced lung injury and reduced fibrosis by blocking pro-inflammatory cytokines such as TNF-α and IL-1 by MSC-associated IL-1 receptor antagonist (IL-1RN) (Ortiz et al., 2007) (Figure 1.13).

Nemeth and colleagues demonstrated that MSC were stimulated by pro-inflammatory cytokines and endotoxin such as TNF-α and LPS respectively. MSC endotoxin-based activation occurred via toll-like receptor-4 (TLR-4), resulting in increased production of cyclooxygenase-2 and subsequent increased production of potent anti-inflammatory agent PGE_2 by MSC. MSC-secreted PGE_2 drove increased macrophage IL-10 secretion and attenuated sepsis and sepsis-associated lung injury (Nemeth et al., 2009). The explanted human lung model provided the demonstration that MSC enhanced LPS-induced acute lung injury repair had likely occurred in a KGF-dependent manner (Lee et al., 2009a) (Figure 1.13).

The administration of KGF-expressing engineered MSC or HSC in the bleomycin-induced mouse lung fibrosis model was associated with reduced fibrosis via suppression of collagen accumulation (Aguilar et al., 2009). KGF has the established role in the repair of

alveolar epithelium through stimulation of type II AEC proliferation, migration and spreading (Panos et al., 1993, Guo et al., 1998, Yano et al., 2000). This proof-of-concept demonstration that genetically modified MSC or HSC with suitable cytokine/growth factor have added benefit in the repair of lung injury with the potential to be a valid stem cell therapeutic strategy for pulmonary fibrosis (Aguilar et al., 2009).

Although the above pre-clinical studies suggested MSC as a potential candidate for regenerative therapy for IPF, there are some concerns that MSC has fibrotic effects and could deteriorate the pathological condition if they are applied in chronic lung fibrosis (Yan et al., 2007). Yan and colleagues demonstrated that after systemic application of MSC at 4 hours of irradiation-induced lung injury, transplanted cells engrafted in the alveolar and bronchiolar epithelium and differentiated into epithelial phenotype; whereas, when MSC were administered at 60 and 120 days post-injury they localised in the interstitial spaces and differentiated into myofibroblasts, a fibrotic phenotype that plays major role in fibrogenesis (Yan et al., 2007). The authors concluded that the fate of MSC differentiation is controlled by the microenvironment milieu and warned that MSC therapy might be ideal for acute lung injury but may augment fibrosis in chronic lung fibrosis such as IPF.

Supporting the putative pro-fibrotic nature of MSC, an *in vitro* study has demonstrated that human and mouse MSC secrete TGF-β1 and Wnt proteins that can stimulate human and mouse lung fibroblast proliferation and collagen production, the two major hallmarks of lung fibrosis (Salazar et al., 2009). PGE_2 treatment significantly inhibited resident MSC proliferation and collagen secretion and abrogated fibrotic differentiation into myofibroblasts (Walker et al., 2012). If this is true for other MSC from common sources

such as bone marrow and cord blood, PGE_2 could be administered concomitantly with MSC to reduce their putative fibrotic effects.

Conversely, no TGF-β1 expression was detected in MSC isolated from bone marrow of either normal healthy individuals or patients with IPF; and the expression of FGF (fibroblast growth factor) and VEGF were not significantly different in either cases (Antoniou et al., 2010). However, CXCR4, a potent chemokine receptor was significantly over-expressed in IPF. The increased CXCR4 expression by IPF MSC suggests that the bone marrow is probably implicated in the pathophysiology of IPF by mobilising resident MSC in response to preceding lung injury (Antoniou et al., 2010). Further studies are required to confirm whether MSC mobilisation is an attempt to repair lung injury or to solely aggravate fibrosis in IPF.

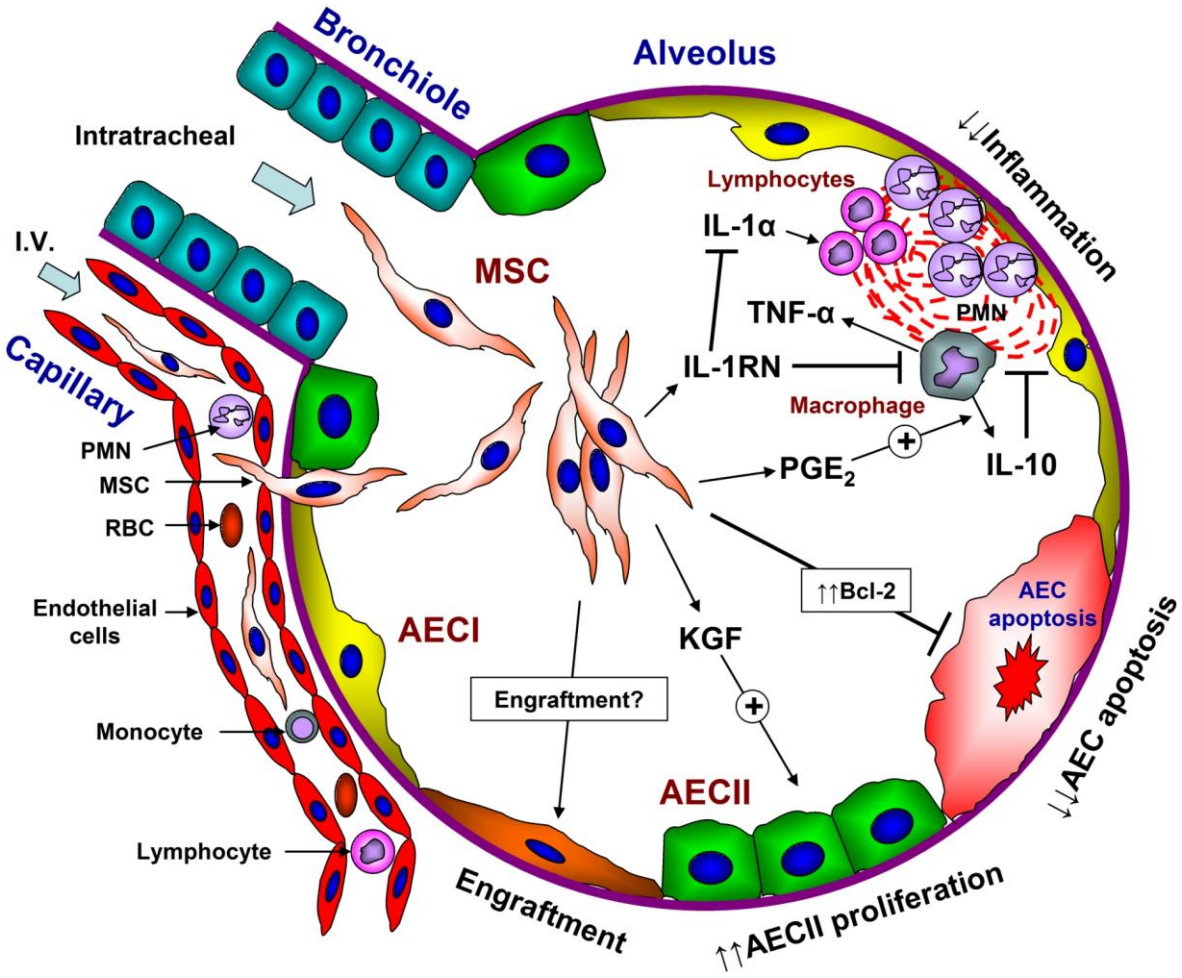

Figure 1.13: MSC-mediated acute alveolar injury repair.

This illustration shows an injured alveolus associated with inflammation and AEC apoptosis. MSC can be delivered via intratracheal or intravenous (I.V) route. MSC can inhibit alveolar inflammation by abrogation of IL-1α-depenednt T-lymphocyte proliferation and suppression of TNF-α secretion by the activated macrophages through MSC-secreted IL-1 receptor antagonist (IL-1RN). Inflammatory environment stimulates MSC to secrete PGE_2 which can stimulate activated macrophages to secrete anti-inflammatory cytokine IL-10. IL-10 can alleviate alveolar inflammatory responses. MSC also can inhibit AEC apoptosis through up-regulation of anti-apoptotic Bcl-2 gene. MSC-secreted KGF can stimulate AECII proliferation and migration propagating alveolar epithelial restitution. Alveolar structural engraftment of MSC is a rare event. (Image was taken from Akram et al., 2012).

1.11.2.2.2. Embryonic stem cells

Embryonic stem cells (ESC) are self-renewing, pluripotent stem cells derived from the inner cell mass of a 5-6 day-old blastocysts and are capable of unlimited, undifferentiated proliferation *in vitro*. Unlike adult stem cells ESC are capable of differentiating into tissues of all three germ layers (Martin, 1981). Murine ESC were first described by Gail Martin in 1981 (Martin, 1981). Thereafter, it took 17 years before the first human ESC line was established in 1998. Since then, at least 225 human ESC (hESC) lines have been created. Pluripotent hESC lines express a set of antigens including SSEA-3, SSEA-4, TRA-1-60, TRA-1-81, alkaline phosphatase, Oct-4 and Nanog transcription factors and high levels of telomerase activity (Thomson et al., 1998, Reubinoff et al., 2000, Henderson et al., 2002, Laslett et al., 2003).

1.11.2.2.2.1. ESC in regenerative therapy for IPF

ESC have been suggested as a suitable source for regenerative cell therapy for lung repair and regeneration due to their potential to differentiate into lung epithelial cells (Weiss & Finck, 2010). For IPF, ESC could be utilised to replace damaged AEC to facilitate alveolar wound repair. Type II AEC have been successfully differentiated from human (Wang et al., 2007) and mouse (Ali et al., 2002, Rippon et al., 2006, Roszell et al., 2009) ESC. More recently, Wang and colleagues have demonstrated that intratracheal administration of ESC-derived type II AEC improved survival and ameliorated pulmonary inflammation and fibrosis in a bleomycin-induced experimental lung injury model (Wang et al., 2010). In this study, structural engraftment of transplanted ESC-derived type II AEC and their differentiation into type I AEC were also noted (Wang et al., 2010). However, attenuation of bleomycin-induced fibrotic responses occurred as early as 24 to 48 hours of ESC-derived type II AEC administration indicating a putative paracrine mechanism involved in

the amelioration of pulmonary fibrosis. Although ESC have a substantial potential differentiation capacity into AEC, the ethical issues of their therapeutic application and potential risk of teratoma formation are the main obstacles that need to be overcome before their clinical application (see Chapter 5, Section- 5.4).

1.12. Aims and objectives of this study

IPF is a disease of aberrant alveolar epithelial wound repair of unknown aetiology where the pathogenesis is widely unknown. A substantial number of studies have been conducted to understand the abnormal epithelial-mesenchymal cross-talk, effects of fibroblasts and myofibroblasts in IPF; whereas, the effect of alveolar bronchiolisation in the aberrant AEC wound repair in IPF remains unexplored. On the other hand, animal model studies have demonstrated that MSC or ESC are capable of attenuating pulmonary fibrosis which suggests a stem cell based regenerative therapeutic approach for IPF. However, the paracrine influence of MSC or ESC on AEC wound repair has yet to be elucidated.

Aim 1: Through this study, efforts have been taken to understand the role of Clara cells in the alveolar epithelial cell wound repair in the context of alveolar bronchiolisation. The paracrine role of Clara cells on AEC wound repair has been investigated by using *in vitro* wound repair assay; whereas, a direct-contact *in vitro* wound repair model has been developed to evaluate the Clara cell direct-contact effect on AEC wound repair mimicking the scenario of alveolar bronchiolisation.

Aim 2: Whilst the majority of studies have highlighted anti-inflammatory and anti-fibrotic effects of MSC, here a set of experiments have been undertaken to explore the paracrine role of human MSC on AEC and small airway epithelial cell wound repair *in vitro*. In

addition, the influence of secretory products obtained from different stages human ESC differentiation has been tested on AEC *in vitro* wound repair model. Understanding the paracrine effects of hMSC/hESC and the identification of effective secretory factor(s) are definitive advancement towards development of novel acellular stem cell-mediated regenerative therapy for IPF and other incurable lung diseases.

Chapter 2:

Materials and Methods

2.1. Cell lines

The primary cell and the cell lines that were used in the experiments are tabulated below (Table 2.1). All other cell culture materials that used in this study are tabulated in Table S1, Appendix-1.

Table 2.1: Primary cells and cell lines

Cell lines	Description	Origin
A549	Human type II alveolar epithelial cell line originated from human lung	ATCC, Rockville, MD, USA
H441	Human Clara cell line originated from human lung	ATCC, Rockville, MD, USA
SAEC	Human primary small airway epithelial cells isolated from human lung	Lonza, USA
hMSC	Human mesenchymal stem cells isolated from bone marrow aspirates	Human bone marrow aspirates from Lonza, USA
SHEF-2	Human embryonic stem cell line	Sheffield University, UK; used under license from UK Stem Cell Bank
MEFs	Mouse embryonic fibroblasts isolated from 12.5-13.5 days gravid uteri of black CB1 hybrid mice	Keele University small animal facilities
CCD-8Lu	Normal human lung fibroblasts	ATCC, Rockville, MD, USA
pAEpiC	Human primary alveolar epithelial cells	ScienceCell Laboratory, USA

2.2. Cell culture condition

2.2.1. A549 and H441 cell culture

Cells were cultured according to the supplier instruction. A549 and H441 cells were stored in the liquid nitrogen at -190^0C in cryovials in freeze-media comprised of 10% DMSO (Dimethyl sulfoxide) in FBS (Foetal bovine serum). Cells in cryovials were thawed

quickly (within a minute) in water bath at 37^0C and resuspended in 10 ml of complete culture media that composed of DMEM (Gibco, Invitrogen, USA) supplemented with 10% FBS (Lonza, Belgium), 1% L-glutamine (Lonza, Belgium) and 1% NEAA (Non-essential amino acid) (Lonza, Belgium). Cell suspension was then centrifuged for 3 minutes at 1200 rpm, a cell pellet formed at the bottom of the centrifuge tube. Supernatant was discarded and pellets of A549 and H441 cells were resuspended in 10 ml of complete culture media by gentle pipetting. A549 and H441 cell suspensions were then passaged into T75 tissue culture flasks separately in total 15-18 ml of complete culture media and incubated in the humidified incubator at 37^0C in presence of 5% CO_2 and 95% air. On the next day, media was replaced with 15-18 ml of fresh complete culture media. After recovery, the A549 cells became confluent within 2-3 days and H441 cells took a week for confluency. Both of these cell lines were maintained in a continuous subculture throughout the whole experimentation period. New vials of A549 and H441 cells were thawed as required.

For subculture, A549 and H441 cells were harvested by trypsinisation and passaged at a split ratio of 1:4 to 1:8 in T75 culture flasks in 15-18 ml of complete culture media. The trypsinisation process was as follows: a confluent T75 flask of cells was rinsed once with 10 ml of warm PBS (Phosphate-buffered saline) (pre-equilibrated at 37^0C) and 5 ml of 0.05% trypsin/EDTA solution (Lonza, Cat No- BE02-007E) was added to the cells and incubated at room temperature for 3-5 minutes. Trypsinised cell were checked under microscope, when they appeared rounded and detached from each other the flask was rapped against the palm to dislodge the cells completely from their adherent culture surface (Figure 2.1). Same volume (5 ml) of complete media was added to the cells to neutralise the trypsin. Cell suspension was taken into a 15 ml centrifuge tube and centrifuged at 1200 rpm for 3 minutes to get cell pellet. Supernatant was discarded and cell pellet was

resuspended for passage. Media was replaced twice in a week during the whole period of culture.

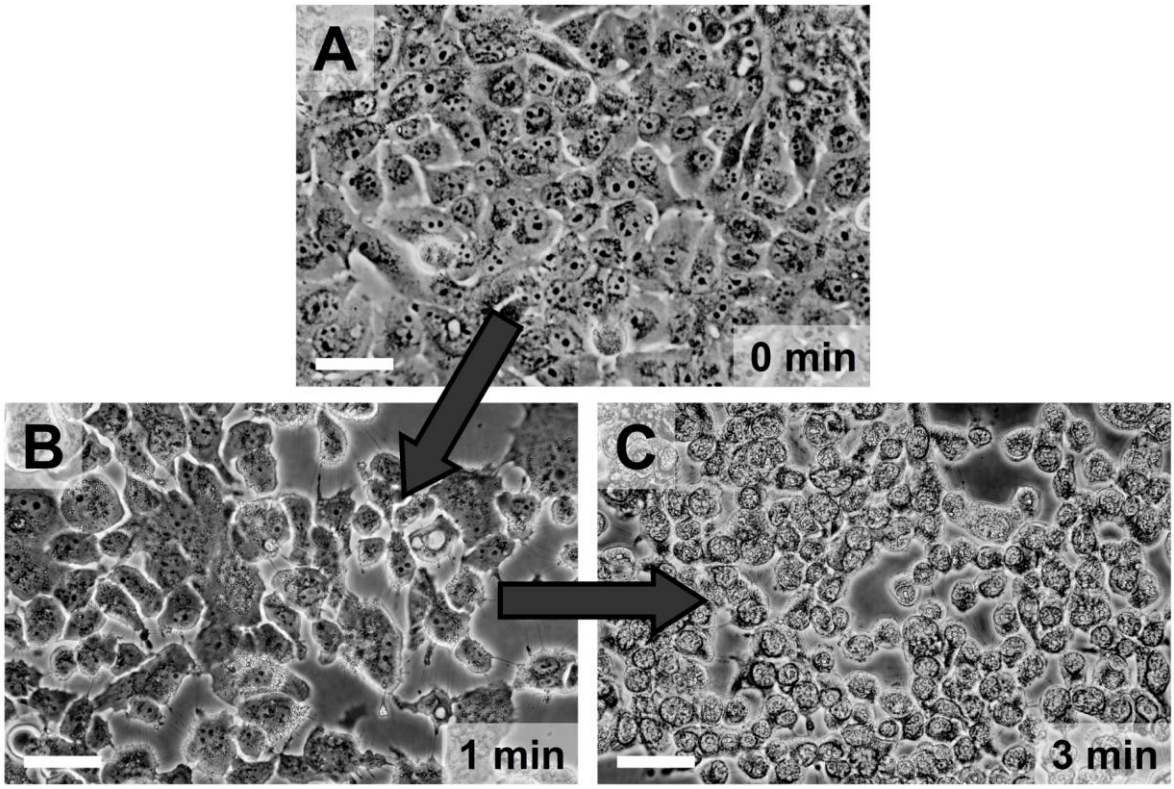

Figure 2.1. Trypsinisation of H441 cells.

(**A**) Just after adding trypsin/EDTA solution in confluent monolayer of H441 cells. (**B**) Cells start to detach from each other. (**C**) Cells appear round-up after 3-5 minutes of adding trypsin. Original magnification 400X. Scale bar, 50 µm.

2.2.2. SAEC culture

Cell recovery: Primary human small airway epithelial cells (SAEC) were purchased from Lonza, USA (Cat. No. CC-2547, Lot. No. 0000105938). Cryopreserved SAEC (5×10^5) (P-2) in a vial were transported in dry ice; upon receipt cells were stored in liquid nitrogen at -190^0C. Cells were recovered and subcultured following the manufacturer's instruction using recommended culture media (SAGM Bullet Kit, Lonza, USA) and subculture reagent pack (Reagent Pack, Lonza, USA). A vial of cryopreserved SAEC ($\geq 5 \times 10^5$ cells)

were thawed quickly in water bath at 37^0C and resuspended in 8 ml of complete SAGM (Small airway growth media) which was prepared using SABM (Small airway basal media) supplemented with 1% of BSA-FAF (Bovine serum albumin-Fatty acid free), 0.4% of BPE (Bovine pituitary extract), 0.1% of rhEGF (Recombinant human epidermal growth factor), 0.1% of transferrin, 0.1% of triiodothyronine (T3), 0.1% of retinoic acid, 0.1% of insulin, 0.1% of epinephrine, 0.1% of hydrocortisone and 0.1% of GA (Gentamicin and Amphotericin-B) (All from Lonza, USA). Five ml of pre-equilibrated SAGM at 37^0C was taken in each of total 8 T25 tissue culture flasks (Corning, NY, USA). 1 ml of SAEC suspension that contains ≥62,500 cells (Recommended seeding density was 2,500 cells/cm^2) was passaged into each T25 flask and incubated in the humidified incubator at 37^0C in presence of 5% CO_2 and 95% air. On the next day, each flask of SAEC was replenished with 6 ml of fresh SAGM. Media was changed on every alternate day and cells became 70-80% confluent in 7 days (Figure 2.2). SAEC have a tendency to undergo irreversible contact-inhibition once they become confluent. To avoid the loss of proliferation capacity, SAEC were never allowed reaching confluency during subculture.

Subculture: For subculture, 70-80% confluent T25 flasks of SAEC were harvested by trypsin/EDTA and passaged into T25 flasks at a cell-seeding concentration of 2,500 cells/cm^2 in 6 ml of complete SAGM per flask using Reagent Pack (Lonza) that includes trypsin/EDTA solution, trypsin neutralisation solution (TNS) and HEPES buffered saline solution (HEPES-BSS). For trypsinisation cells were washed once with HEPES-BSS (4 ml/T25 flask) and then 2.5 ml of trypsin/EDTA solution was added to the cells and incubated for 2-5 minutes at room temperature. Trypsinised cells were examined under the microscope, when >90% cells became rounded up cells were dislodged from the culture surface by gently rapping the flask against the palm. When >95% of cells were dislodged,

5 ml of TNS was added to neutralise the action of trypsin. Cell suspension was then taken into a 15 ml centrifuge tube and centrifuged for 3 minutes at 1200 rpm to form a cell pellet at the bottom of the tube. Supernatant was discarded and the cell pellet was resuspended in 5 ml of complete SAGM (pre-equilibrated at 37^0C). Before passaging, cells were counted using trypan blue and haemocytometer. Total yield of SAEC from a T25 flask ranged from 8×10^5 to 1×10^6 cells depending on their passage number and confluency with >95% viability. Approximately 62,500 cells were seeded per T25 flask in 6 ml of complete SAGM and cultured in standard condition until they became ready for next passage. Cells were growing well up to passage 5; at passage 6 SAEC appeared to be quiescent/senescence. During the whole culture period media was changed on alternate days.

Cell cryopreservation: SAEC were cryopreserved using recommended freeze-media. The freeze-media was composed of 80% SAGM, 10% FBS and 10% DMSO. SAEC (P-3) were harvested by trypsinisation as described above. Cell pellet was formed from cell suspension by centrifugation. Cell pellets were then resuspended in 1 ml of freeze-media and taken into a cryovial. 1 T25 flask of 70-80% confluent cells was stored in each cryovial. Cells were frozen using Mr Frosty at -80^0C in first 24 hours. Frozen cells were then transferred into liquid nitrogen cell storage reservoir at -190^0C for long term preservation.

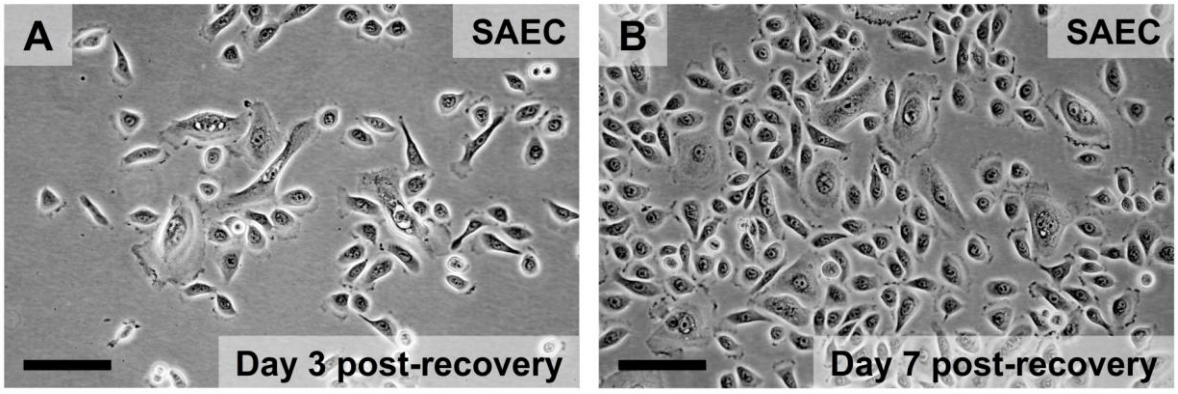

Figure 2.2: SAEC recovery.

SAEC are in 3 days (A) and 7 days (B) of post-recovery phases. Original magnification 200X. Scale bar, 100 µm.

2.2.3. hMSC culture

hMSC isolation: hMSCs were isolated and expanded from human bone marrow aspirates (BMA) by plastic adherent culture technique following previously published methodology (D'Ippolito *et al*. 2004, Wimpenny *et al*. 2010). A total of 3 human bone marrow aspirates (BMA) from 3 different donors which were aspirated from iliac crest were purchased from Lonza, USA and processed for experimentation (Table 2.2). Whole bone marrow was seeded at a density of 10^5 mononuclear cells/cm^2 on 10 ng/ml fibronectin-coated (Cat. No. F0895, Sigma) T-75 tissue culture flasks in 20 ml of DMEM supplemented with 5% FBS, 1% L-glutamine, 1% NEAA and 1% PSA (Penicillin-Streptomycin-Amphotericin B) and incubated at 37^0C in presence of 5% CO_2 and 95% of air. For fibronectin coating, 10 ml of 10 ng/ml fibronectin solution in PBS was added in each T75 flask and incubated 2 hours at room temperature. Before use, fibronectin solution was discarded and the culture media was added. The whole bone marrow cells containing non-adherent (mononuclear cells) and adherent cells (MSC) were maintained in a continuous culture for three weeks in a humidified incubator at 37^0C in the presence of 5% CO_2 and 95% air. After 7 days of culture half of media was removed and replaced with antibiotic-free fresh DMEM culture

medium as above. On the second week, whole media was discarded, cells were rinsed once with PBS and complete fresh media was added (20 ml/T75 flask). At the end of third week MSC-colony formed (also known as CFU-F, colony forming unit- fibroblast). Cells of some T75 flasks were fixed with 95% ethanol for 30 min at room temperature then washed twice with PBS. Giemsa stain was added (12 ml/T75 flask) and incubated at room temperature for 2 hours on a rocker. Then washed with tap water till clear. CFU-F, and cell morphology were observed under light microscope (Figure 2.3). The adherent hMSC population was harvested with trypsin as described above and subsequently passaged for expansion. Before expansion, hMSC were plated on 24-well plates for their functionality characterisation and immunophenotyping which is described below in Section- 2.2.3.1, Section- 2.12.3, and Section- 2.12.2 respectively.

hMSC expansion: hMSC were expanded up to passage 4 by subculturing. For subculture, confluent T75 flasks of hMSC were split at 1:4 to 1:6 ratios and passaged to T75 tissue culture flasks. Cells were harvested by trypsin/EDTA as described above. During subculture the DMEM was supplemented with 5% FBS, 1% L-glutamine and 1% NEAA (complete culture media). Media was changed twice a week. Passage 1-3 hMSC were utilised for all of experimentation procedures.

hMSC cryopreservation: After isolation from BMA, substantial number of hMSC at Passage-1 were cryopreserved for future use. For cryopreservation, confluent T75 flasks of hMSC were harvested by trypsinisation and stored in liquid nitrogen using 10% DMSO in FBS freeze media as described above. One confluent T75 flask of hMSC was stored in each cryovial in 1 ml of freeze media.

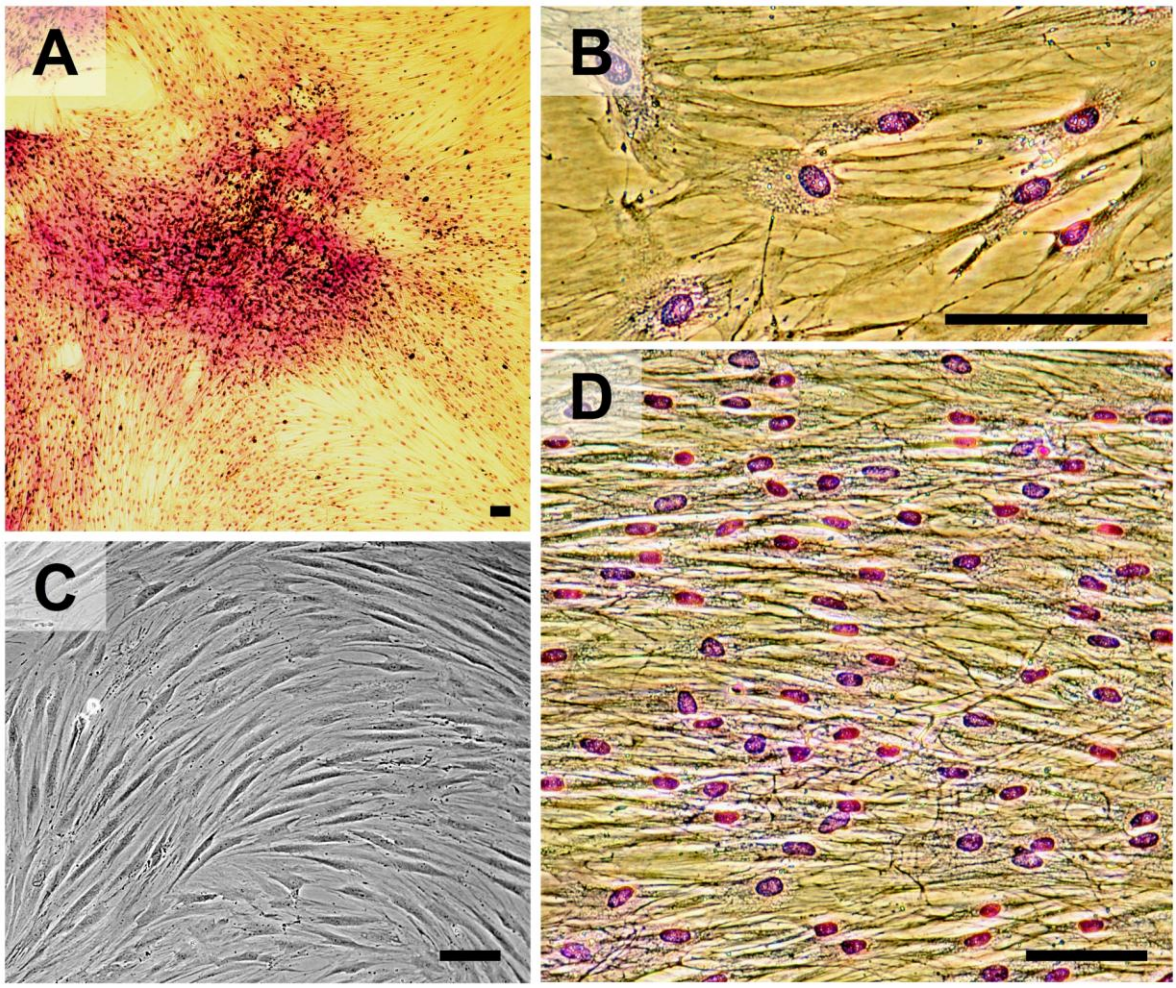

Figure 2.3. Recovered hMSC from bone marrow aspirate after 3 weeks.

(**A**) CFU-F of hMSC forms after 3 weeks of culture, stained with Giemsa. Light microscopic image at 40X. (**B**) High magnification image at 400X. Purple nuclei stained with Giemsa. (**C**) Un-fixed and un-stained light image of hMSC after 3 weeks at 100X. (**D**) Image at 200X, stained with Giemsa. Scale bar, 100 µm.

Table 2.2: Donor details of human bone marrow aspirates.

No	BMA label	Donor description	Supplier
1	BMA-8	Human Bone Marrow, Male, Age-35 years	Lonza, MD, USA
2	BMA-11	Human Bone Marrow, Female, Age-26 years	Lonza, MD, USA
3	BMA-12	Human Bone Marrow, Male, Age-32 years	Lonza, MD, USA

2.2.3.1. Functional characterisation of hMSC by tri-lineage differentiation

Differentiation protocol

To evaluate the multipotency of hMSC, the isolated human bone marrow derived MSC were differentiated into osteogenesis, adipogenesis and chondrogenesis lineages using StemPro hMSC differentiation kits following the manufacturer instruction (Cat. No- A10072-01, A10070-01 and A10071-01; Gibco, Invitrogen, USA). For osteogenesis and adipogenesis, 2 x 10^4 hMSC (P-1) were seeded on each well of 24-well plates and grown 60-70% confluence in 72 hours using complete culture media. Cells were washed with PBS once and SF (Serum-free)-DMEM once to remove serum. hMSC were then cultured for three weeks in StemPro® Osteogenic differentiation media (Cat. No- A10072-01) and StemPro® Adipogenic differentiation media (Cat. No- A10070-01) (600 µl/well each) with media changes every two days. For control, hMSC were cultured in complete growth media (600 µl/well) for same duration, with media changes every two days.

For chondrogenesis, the micromass culture system was used according to the manufacturer's instruction. Briefly, 8 x 10^4 hMSC were resuspended in 7 µl of complete media and dropped in the centre of a 24-well plate as a micromass and cultured for 2 hours in the humidified incubator in the standard culture condition allowing them to adhere with the culture surface. Micromasses were then replenished with StemPro® Chondrogenic

differentiation media (Cat. No- A10071-01) (600 µl/well) and cultured in standard culture conditions for three weeks with media change every two days. For control, micromasses were cultured with complete growth media for same duration.

Evaluation of tri-lineage differentiation

After three weeks, the differentiated hMSC lineage was confirmed by histological staining and immunocytochemistry. Immunocytochemistry evaluation is described below (Section-2.12.3). The mineral deposition by differentiated osteoblasts, lipid accumulation in adipocytes and proteoglycan-rich matrix accumulation in chondrocytes was detected by classical histological stains; Alizarin Red, Oil Red O and Alcian Blue respectively, following standard protocols.

Alizarin Red staining

Preparation of 1% Alizarin Red solution: 0.5g of Alizarin Red powder (Cat. No- A5533, Sigma) was dissolved in 50 ml of dH_2O. The pH of this solution was maintained ~4 by adding 0.1M HCl acid to allow Alizarin Red to bind with deposited extracellular calcium only. Solution was filtered with 0.4 µm porous filter paper before use.

Staining procedure: Osteogenic differentiated samples and controls were fixed with 10% formaldehyde for 30 minutes. After washing once with dH_2O, 800 µl of Alizarin Red solution was added to each well and incubated for 10 minutes at RT (Room temperature). Samples were then washed three times with dH_2O to remove excess dye. Images were acquired by an inverted light microscope (Nikon Eclipse TS100, Japan) attached with a colour CCD camera (Canon, Japan).

Oil Red O staining

Preparation of Oil Red O solution: Stock Oil Red O solution was prepared by dissolving 0.35g of Oil Red O powder (Cat. No- O-0625, Sigma) in 100 ml of 100% isopropanol (Cat. No- I-0398, Sigma). Stock solution was filtered with 0.2 µm filter paper. Oil Red O working solution was prepared by adding 6 ml of stock solution with 4 ml of ddH_2O.

Staining procedure: To detect triglyceride produced by differentiated adipocytes, samples were stained with Oil Red O. Adipogenic differentiated samples were fixed with 10% formalin for 10 minutes at RT. The formalin was removed and again added with fresh 10% formalin and incubated for 1 hour at RT. Samples were then washed with ddH_2O twice and twice with 60% isopropanol for 5 minutes. Samples were then completely air dried. Oil Red O working solution was then added in each sample (800 µl/well) and incubated for 10 minutes at RT. After incubation, Oil Red O was discarded and samples were washed with ddH_2O four times. Images were acquired by an inverted light microscope attached with a colour CCD camera.

Alcian Blue staining

Preparation of 1% Alcian Blue solution: 1g of Alcian Blue 8GX (Cat. No- A-3157, Sigma) was dissolved in 100 ml of 3% acetic acid (Cat. No- A-9967, Sigma) to prepare 1% Alcian Blue solution (pH 1.5). Solution was filtered using 0.2 µm porous paper filter.

Staining procedure: To detect the glycosaminoglycan (GAG) produced by the differentiated chondrocytes, cells were stained with 1% Alcian Blue. Samples were fixed with 10% formalin for 30 minutes. After fixation samples were washed twice with dH_2O then 1% Alcian Blue was added (800 µl/well) and incubated overnight at RT. Samples were washed with dH_2O three times to remove excess stain and images were captured by an inverted light microscope attached with a colour CCD camera.

2.2.4. hESC culture

Human embryonic stem cell (hESC) line SHEF-2 cells were obtained from the UKSCB after donation by the University of Sheffield, UK and cultured on feeder-free matrigel coated tissue culture flasks (T25 flasks) using mouse embryonic fibroblasts (MEFs) conditioned media (MEF-CM) following the protocol described by Xu et al. 2001.

MEFs conditioned media (CM) preparation: 12.5 to 13.5-day pregnant black CB1 hybrid mice were sacrificed by cervical dislocation and gravid uterine horns were isolated through lower abdominal V-shape incision following aseptic protocol at small animal facilities, Keele University (Figure 2.4). Segmented uteri were separated and transferred to the flow hood at cell culture facilities for further processing. Eight to ten embryos were collected from each pair of uteri. Viscera and heads were removed from the embryos using sharp tip forceps. Embryos were then washed three times in 1% PSA containing PBS to remove the remnants of viscera and blood clots. Embryonic fibroblasts were isolated from mouse embryos by trypsin digestion. For this process, 5 embryos were taken into each 7 ml Bijou bottle in 5 ml of trypsin/EDTA solution and incubated for 10 minutes in the incubator at 37^0C. Trypsinised embryos were vortexed twice at 5 minutes interval during the incubation period. After incubation cell supernatants were collected and resuspended in 10 ml of DMEM supplemented with 10% FBS, 1% L-glutamine, 1% NEAA and 1% PSA in 15 ml sterile centrifuge tube. Cell suspensions were then centrifuged at 1200 rpm for 3 minutes. Supernatants were discarded and cell pellets were resuspended in 10 ml of the above mentioned DMEM. 2 ml of MEFs cell suspension was seeded into T75 culture flasks in 18 ml culture media and incubated at 37^0C in presence of 5% CO_2 and 95% air in a humidified cell culture incubator. On the next day, media was replaced with antibiotic-free

complete culture media and media was changed twice weekly until the MEFs became confluent.

A confluent MEF T75 was split into 8 T75 tissue culture flasks at 1:8 split ratio and cultured to 50-60% confluency. To prepare MEF-CM, 50-60% confluent MEFs were washed once with warm PBS and 30 ml of KO (Knock out)-DMEM (Gibco, Invitrogen) supplemented with 20% KO-SR (KO-Serum replacement) (Gibco, Invitrogen), 1% L-glutamine, 1% NEAA, 0.1 mM β-mercaptoethanol and 4 ng/ml human bFGF (Basic fibroblast growth factor) added and cultured for 24 hours. MEF-CM was collected and used fresh or stored at -20^{0}C before use. MEF-CM was collected on three consecutive days from a single T75 flask. Prior to use, MEF-CM was further supplemented with human bFGF (4 ng/ml) and sterile filtered with 0.20 µm porous Millipore filtration unit (Millipore). This media was labelled as 'hESC culture media' and used for hESC culture.

Matrigel coating: Culture surfaces of T25 tissue culture flasks were coated with 1:100 diluted matrigel (BD Matrigel Matrix™, BD, Bedford, MA, USA; Cat No-354234) in ice cold KO-DMEM. 4 ml of ice cold diluted matrigel solution was added into each T25 flask (160µl/cm^2) and incubated at room temperature for 2 hours. Before use, matrigel containing flasks were incubated at 37^{0}C for 30 minutes in the incubator, after incubation the matrigel media was discarded and hESC culture media was added. Prepared matrigel coated culture flasks were stored at 4^{0}C for later use.

hESC culture: A cryovial of SHEF-2 (P-28) was taken from liquid nitrogen cell storage reservoir and thawed in water bath within a minute with a gentle agitation. Cells were stored in 10% DMSO in KO-SR solution. Thawed cells were then added into 6 ml of pre-

equilibrated 37^0C hESC culture media in a matrigel coated T25 tissue culture flask and incubated at 37^0C in presence of 5% CO_2 and 95% air in the humidified incubator. On next day, media was replaced by fresh hESC culture media. The cells which attached with the culture surface were allowed to grow to 70-80% confluency with a daily media change by 6 ml of fresh media (Figure 2.5). 70-80%-confluent hESC were harvested by trypsinisation and passaged into 2 to 4 T25 flasks at a split ratio of 1:2 to 1:4. For trypsinisation, cells were washed once with PBS and 2 ml of trypsin/EDTA solution was added and incubated for 1-3 minutes at RT. Cells were dislodged by rapping the flask with palm of the hand gently. When 70-90% of cells were dislodged, same volume of hESC culture media was added and the solution was taken in 15 ml centrifuge tube and centrifuged for 3 minutes at 1200 rpm to get cell pellet. Cell pellet was then resuspended in 10 ml of hESC culture media and passaged as above split ratio. Cells were passaged every 3 to 7 days and maintained in a continuous culture during the whole experimentation period. New vials of cells were thawed as required.

hESC cryopreservation: 80-90% confluent T25 flask of hESC were harvested by trypsinisation and stored in the liquid nitrogen using 10% DMSO in KO-SR freeze media. 1 T25 of hESC were stored in each cryovial.

2.2.5. CCD-8Lu cell culture

Cells were cultured according to the supplier instruction. CCD-8Lu cells (P-7, P-8, P-10) were stored in the liquid nitrogen at -190^0C in cryovials in freeze-media comprised of 10% DMSO in FBS. Cells in cryovials were thawed quickly in water bath at 37^0C and resuspended in complete media and washed once by centrifugation as described Section-2.2.1. Cells were then passaged into T75 tissue culture flasks in 15-18 ml of complete

culture media and incubated in the humidified incubator at 37^0C in presence of 5% CO_2 and 95% air. Media was changed every two days. Cells were maintained in a continuous culture upto passage 14. New cells were thawed as required.

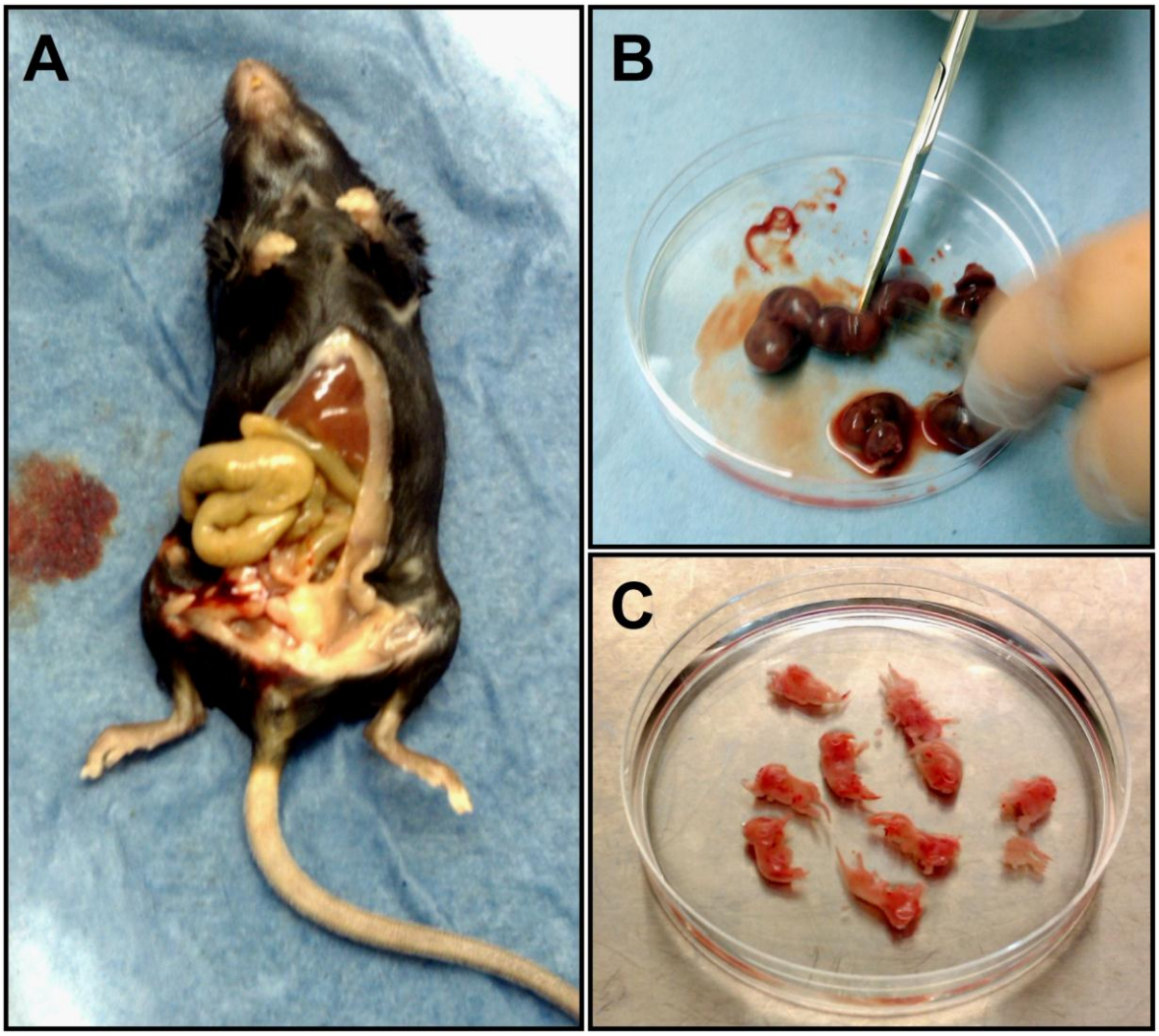

Figure 2.4: Embryos isolation from 13-day pregnant black CB1 hybrid mouse.

(**A**) Black CB1 hybrid mouse, gravid uteri were isolated from pelvic viscera by opening the lower abdomen. (**B**) Embryos were isolated from segmented gravid uteri (horns). (**C**) Head and abdominal viscera were removed from embryos and ready for trypsin digestion. **A** and **B** steps were performed at small animal facilities, Keele University; **C** step was performed in the flow-hood at central cell culture facility, Guy Hilton Research Centre, Keele University.

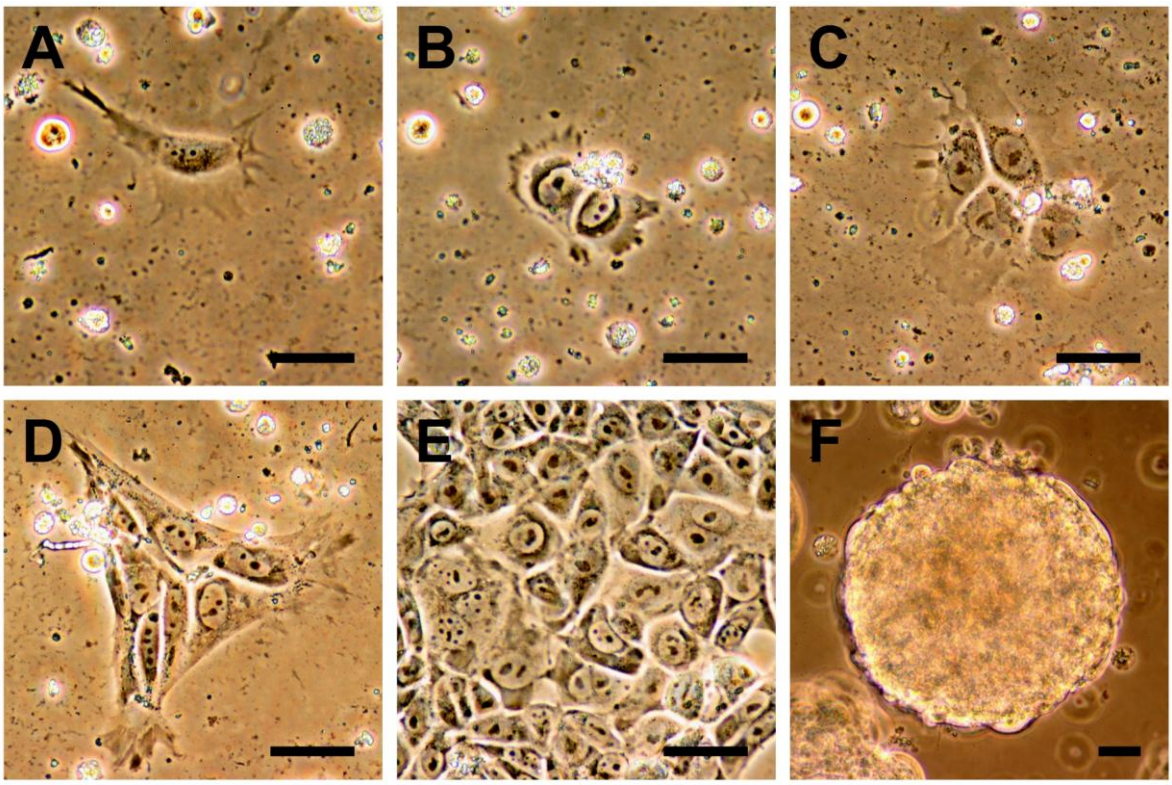

Figure 2.5: Recovery of hESC from cryopreservation and in vitro culture.

(**A**) hESC attached to the matrigel coated culture surface after 24 hours of seeding. (**B**) Cells are dividing. (**C**) Start of colony formation was observed from 3rd -4th day post seeding. (**D**) A small colony of hESC on day 5. (**E**) Typical morphology of hESC with high nucleus: cytoplasm ratio on adherent culture. (**F**) hESC formed embryoid body (EB) in 3D suspension culture. Light microscopic images at 400X (A, B, C, D, E) and 200X (F). Scale bar, 50 µm.

2.2.6. pAEpiC culture

Human primary alveolar epithelial cells (pAEpiC) were purchased from ScienceCell Research Laboratories, USA and cultured on poly-L-lysine (Sigma-Aldrich, MO, USA) coated culture flasks in alveolar epithelial cell media (AEpiCM) supplemented with epithelial cell growth supplements (EpiCGS) (ScienceCell Research Laboratory, USA) following the manufacturer protocol.

2.3. Optimisation of cell seeding density for wound repair assay

For *in vitro* wound repair assay and other experimentation, different size-format well-plates were used ranging from 24-well plate, 48-well plate and 96-well plate including transwells. Other than SAEC, confluent monolayers for experimentation were formed within 24 hours of initial cell seeding. The seeding densities of A549 cells and H441 cells required to form a confluent monolayer in 24 hrs were determined by seeding cells with various densities in different size-format well plates. In 24-well plate, seeding densities explored for A549 and H441 cells were 9.4×10^3, 1.87×10^4, 3.75×10^4, 7.5×10^4, 1.5×10^5 and 3×10^5 cells/well in 1 ml of complete DMEM media for each well (Figure 2.6A). Cells were grown for 24 hours in normal culture condition. After 24 hours, wells were examined under an inverted light microscope and images captured with a CCD camera (Canon, Japan) attached to a microscope (Nikon Eclipse TS100, Japan). Afterwards, cells were fixed with 95% ethanol for 30 minutes then stained with Giemsa stain as described before (Section 2.2.3). Well-plates were then air dried before capturing images of whole well-plates by GeneSnap (Syngene) (Figure 2.6A). Confluent monolayers formed for A549 cells at 1.5×10^5 cells/well and for H441 cells at 3×10^5 cells/well initial seeding densities after 24 hours in 24-well plate format (Figure 2.6B).

Following the same protocol the initial seeding density for A549 cells was determined for 48-well plate and 96-well plate which were 10^5 cells/well and 5×10^4 cells/well, respectively, that formed confluent monolayers after 24 hours. For 24-well plate-format transwells the seeding density for A549 cells was 10^5 cell/transwell and for H441 2×10^5 cells/transwell (under surface) that formed confluent monolayers after 24 hours.

The initial seeding density for SEAC was determined in 48-well plate and 96-well plate. For 48-well plate, 2.5 x 10^4 and 5 x 10^4 cells/well were seeded in 500 µl/well of complete SAGM. SAEC monolayers were formed after 48 hours when the initial seeding density was 5 x 10^4 cells/well. For 96-well plate, SAEC form confluent monolayers with an initial seeding density of 2 x 10^4 cells/well in 48 hours.

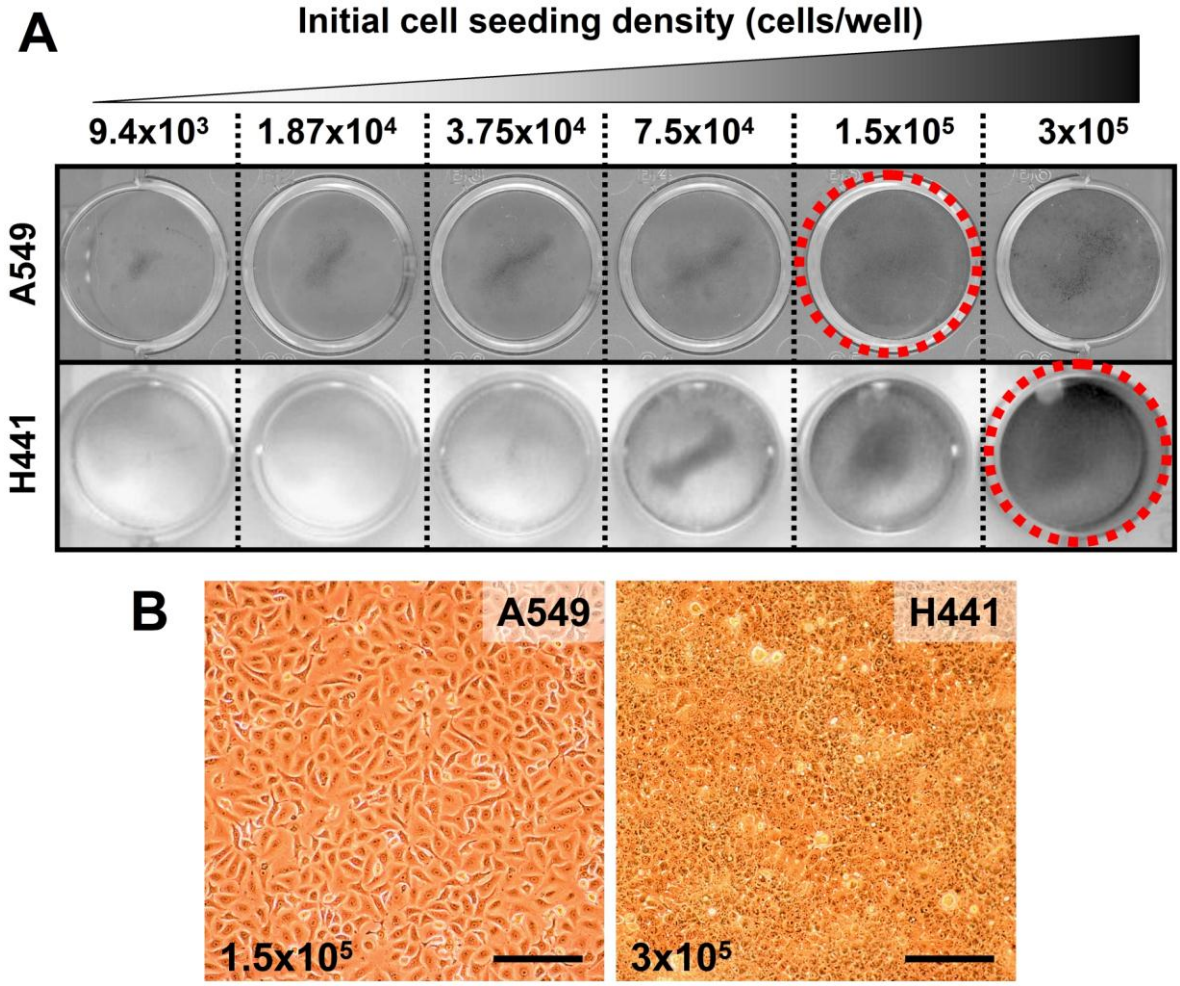

Figure 2.6: Optimisation of A549 and H441 cell seeding density for 24-well plate.

(**A**) A549 and H441 cells were grown on 24-well plates for 24 hours with a range of different initial cell seeding concentration. Cells were fixed and stained with Giemsa and image were captured by GeneSnap (Black & white image). Red circled wells indicate formation of confluent monolayers. (**B**) Light microscopic images of A549 cell confluent monolayer at 1.5 x 10^5 cells/well seeding density and H441 cell confluent monolayer at 3 x 10^5 cells/well seeding density. Original image magnification was 100x (B). Scale bar, 200 µm.

2.4. Preparation of conditioned media (CM)

To evaluate the paracrine influence and for proteomics study, CM were prepared from A549 cells, H441 cells, hMSC, CCD-8Lu and hESC culture.

2.4.1. Preparation of serum-free CM of wounded and unwounded A549 and H441 cells

For preparation of serum-free CM (SF-CM), A549 and H441 cells were grown separately to form confluent monolayers on 24-well plates with an initial seeding density of 1.5 x 10^5 cells/well and 3 x 10^5 cell/well, respectively, in complete DMEM media. To prepare SF-CM from unwounded A549 and H441 cells, unwounded monolayers were washed twice with PBS and then SF-DMEM was added (1 ml/well) and cultured for 24 hours in the incubator at 37^0C in presence of 5% CO_2 and 95% air. To prepare SF-CM from wounded A549 and H441 cells, monolayers were wounded with 200µl plastic pipette tip in a criss-cross pattern followed by two PBS washes before being replenished with SF-DMEM (1 ml/well) and cultured for 24 hours as described above. SF-CM were collected and, centrifuged to remove any cell debris and stored at -80^0C. In most instances, fresh SF-CM was used. Prior to use, all SF-CM were sterile filtered using 0.2 µm Cellulose Acetate syringe filter.

2.4.2. Preparation of SF-CM of hMSC

hMSC (P-2 to P3) were grown to 80-90% confluency in T75 tissue culture flasks in complete hMSC culture media comprised of DMEM supplemented with 5% FBS, 1% L-glutamine and 1% NEAA. To prepare SF-CM for testing on A549 cells (SF-MSC CM^{DMEM}), SF-DMEM and for testing on SAEC (SF-MSC CM^{SABM}), SF-SABM (Small airway basal media, Lonza) was used. Preliminary studies demonstrated that SAEC did not

grow properly in SF-DMEM and developed a squamous type morphology but did maintain their characteristic morphology in Lonza recommended SABM. hMSC grew properly in SAGM with no visible abnormality in cell morphology detectable via microscopy after 24 hours of culture in this media. For SF-CM (SF-MSC CM^{DMEM} or SF-MSC CM^{SABM}) preparation, 80-90% confluent hMSC were washed twice with PBS and once with SF-basal media and 12 ml (0.16 ml/cm^2 of culture surface) of SF-DMEM or SF-SABM (SABM was un-supplemented) added and incubated for 24 hours in normal culture condition (37^0C, 5% CO_2 and 95% air). After 24 hours of culture, media was collected in 15 ml centrifuge tube. To remove cell debris (if any) from SF-CM media was centrifuged for 3 minutes at 1200 rpm and supernatant was collected and stored at -80^0C. Prior use, SF-CM was sterile filtered with 0.2 µm Cellulose Acetate syringe filter.

2.4.3. Preparation of SF-CM of normal lung fibroblast CCD-8Lu

Normal human lung fibroblasts CCD-8Lu (P10 to 12) were grown 80-90% confluent in T25 tissue culture flasks in complete DMEM supplemented with 10% FBS, 1% L-glutamine and 1% NEAA. Cells were then washed twice with PBS and once with SF-DMEM. Following washes, 4 ml of SF-DMEM was added into each T25 flask (0.16 ml/cm^2 of culture surface) and incubated for 24 hours in normal culture conditions. After incubation, SF-CM was collected, centrifuged as above to remove any cell debris and stored at -80^0C. Prior use SF-CM was sterile filtered with 0.2 µm Cellulose Acetate syringe filter.

2.4.4. Preparation of CM from hESC

2.4.4.1. CM from undifferentiated hESC

hESC (SHEF-2, P-32) were grown 60-70% confluent using hESC culture media in T25 culture flasks following the hESC culture protocol described above (Section- 2.2.4). Three sets of media were conditioned on undifferentiated SHEF-2: KO-DMEM supplemented with 20% KO-SR and 4 ng/ml bFGF (+SR +bFGF), 20% KO-SR but no bFGF (+SR –bFGF) and KO-DMEM without any KO-SR or bFGF (-SR –bFGF). All of these above media were supplemented with 1% L-glutamine, 1% NEAA and 0.1 mM β-mercaptoethanol. 6 ml each of these above media were cultured for 24 hours on 60-70% confluent undifferentiated SHEF-2 (P-32) cells in standard culture condition. Before conditioning, cells were washed once with PBS and once with basal KO-DMEM. After incubation, conditioned media (hESC-CM) was collected, centrifuged to remove any cell debris as described above and stored at -80^{0}C. Prior use, CM was sterile filtered with 0.20 µm porous, 33 mm cellulose acetate syringe filter.

2.4.4.2. Preparation of CM from different stages (time points) of differentiated hESC through embryoid body (EB) culture

SHEF-2 cells were differentiated towards endodermal lineages with treatment of recombinant human Activin A (Peprotech, USA) through EB culture for 22 days. During differentiation, CM was collected from EB culture in different time points as follows (Table 2.4).

Formation of EBs (Day 0-1): Three T25 flasks of 80-90% confluent undifferentiated hESC, SHEF-2 (P-38) cells were pooled by trypsinisation and seeded on a 90 mm diameter non-adherent petri dish (Sterilin, UK) in 20 ml of complete hESC culture media and

cultured for 24 hours. Two dishes of EBs were formed, one was for Activin A treatment differentiation protocol and another was untreated differentiation protocol. After 24 hours, a number of EBs formed. EBs along with media were transferred in 50 ml centrifuge tubes and allowed to stand vertically for 10 minutes at RT in the flow-hood allowing EBs to settle down at the bottom of the tube. The supernatant (0-1 day CM) was carefully collected without disturbing EBs and stored at -20^{0}C.

EB suspension culture with 10% FBS (Day 1-3.5): The EBs from Day-1 were then transferred into a new 90 mm non-adherent petridish and replenished with 20 ml of KO-DMEM supplemented with 10% FBS, 1% L-glutamine, 1% NEAA, and 0.1 mM β-mercaptoethanol and cultured for 2½ days (Day 1 to 3.5) without media change in normal culture condition. During this phase of differentiation EBs became more compact. At the end of day 3.5, EB culture supernatant (1-3.5 day CM) was collected and stored as described above.

EB suspension culture with human Activin A (Day 3.5-8): After Day 3.5, one dish of collected EBs were treated with 100 ng/ml human Activin A in 20 ml of KO-DMEM supplemented with 10% SR, 1% L-glutamine, 1% NEAA and 0.1 mM β-mercaptoethanol and cultured in 90 mm non-adherent petridish for 4½ days (Day 3.5 to 8) without any media change. Another dish of EBs was not treated but cultured with above mentioned media for same duration. During this phase EBs were increasing in size. At the end of Day 8 EB culture supernatant (3.5-8 day CM) was collected and stored as described above.

EB suspension culture (Day 8-11): At the end of Day 8, collected EBs were cultured in 20 ml of KO-DMEM supplemented with 10% SR, 1% L-glutamine, 1% NEAA and 0.1

mM β-mercaptoethanol in a 90 mm non-adherent petridish for 3 days (Day 8-11) without any media change in standard culture condition. At the end of Day 11, EB supernatant (8-11 day CM) was collected and stored as described above.

EB suspension culture (Day 11-22): EBs were then cultured in 20 ml of KO-DMEM supplemented with 10% SR, 1% L-glutamine, 1% NEAA and 0.1 mM β-mercaptoethanol in a non-adherent petridish for 11 days in the standard culture condition. During this phase CM was collected on Day 16 (11-16 day CM) and EBs were replenished with fresh media and cultured for further 6 days. At the end of Day 22 of EB culture supernatant (16-22 day CM) was collected and stored as described above and EB culture was terminated.

Three separate experiments were performed with 3 different passages of SHEF-2 (P-37, P-38 and P-46) to collect EB conditioned media for wound repair experiments and secretome analysis.

Table 2.3: SHEF-2 differentiation protocol through EB formation.

Steps	Culture protocol	Culture media composition	Time line
Formation of EBs	3 T25 flasks of SHEF-2 cells were pooled into 90 mm non-adherent petridish in 20 ml of complete hESC media.	Complete hESC culture media: KO-DMEM + 20% SR + 8 ng/ml bFGF + 0.1 mM β-mercaptoethanol + 1% L-glutamine + 1% NEAA.	Day 0-1
FBS treatment of EBs	EBs were cultured in 20 ml of 10%FBS supplemented KO-DMEM.	KO-DMEM + 10% FBS + 0.1 mM β-mercaptoethanol + 1% L-glutamine + 1% NEAA.	Day 1-3.5
Activin A treatment of EBs	EBs were treated with 100 ng/ml human Activin A	KO-DMEM + 10% SR + 100 ng/ml human Activin A + 0.1 mM β-mercaptoethanol + 1% L-glutamine + 1% NEAA.	Day 3.5-8
EB suspension culture	EBs were cultured in KO-DMEM	KO-DMEM + 10% SR + 0.1 mM β-mercaptoethanol + 1% L-glutamine + 1% NEAA.	Day 8-11
EB suspension culture	EBs were cultured in KO-DMEM. CM was collected on day 16 and day 22.	KO-DMEM + 10% SR + 0.1 mM β-mercaptoethanol + 1% L-glutamine + 1% NEAA.	Day 11-22

2.5. Secretome analysis by mass spectrometry

Secretome (secretory proteome) analysis was performed in CM collected from hMSC and hESC by using LC-MS/MS mass spectrometry. The mass spectrometry was performed by Dr Heidi Fuller at Keele University Mass Spectrometry Facilities, Oswestry.

Serum-free MSC-CM, 0.2% FBS supplemented MSC-CM and 0.2% FBS supplemented DMEM were concentrated (10 times) using Amicon Ultra-15 centrifugal filter device (3 kDa MW cut off; Millipore) following manufacturer's instruction. Briefly, 10 ml of CM samples were aliquoted into the upper column of the Amicon Ultra-15 and centrifuged at 5,000g in the Beckman ultracentrifugation machine (Model J2-21) using a fixed angle rotor (JA-20) for 1 hours at 8^0C. Approximately 1 ml of concentrated sample was collected

and stored at -80^{0}C before sending to the Mass Spectrometry facility. CM collected from hESC EB culture at Day 11 (8-11 day-CM), and Day 22 (16-22 day-CM) of differentiation; along with 10% KO-SR supplemented KO-DMEM (un conditioned media as control) was concentrated and stored in a similar way as described above. Samples were transferred to the Mass Spectrometry facility on dry ice for analysis.

In the Mass Spectrometry centre, samples were reduced and alkylated with 1 µL of 1M DTT for 1 hour at 45^{0}C and 25 µL of 200 mM iodoacetamide for 30 minutes at room temperature in the dark followed by overnight digestion with porcine sequencing grade trypsin (2 µg per sample, Promega). The digested samples were then separated by liquid chromatography (LC). Peptides were eluted for 40 minutes over a 2%-50% MeCN gradient, followed by further elution for 10 minutes at 90% MeCN. Samples were spotted onto a MALDI plate and analyzed in both MS and MS/MS modes on a 4800 MALDI TOF/TOF (Matrix assisted laser desorption/ionization Time-of-Flight) (Applied Biosystems). Data was searched against the non-redundant Human NCBI Protein Database. Proteins that were matched with >95% total ion score C.I% and more than 2 peptides were considered as significant. MSC-CM from three independent donors and hESC-CM from two separate experiments were evaluated.

2.6. Calculation of population doubling time for A549 and H441 cells

Doubling time of A549 and H441 cells in serum-free and 10% FBS supplemented DMEM was calculated by cell counting method and using the following formula:

PD = t x Log2/(LogC2-LogC1)

[Here, PD = Population doubling time, t = 24 hours (interval of cell count), Log = 10 based Log, C1 = 1st cell count, C2 = 2nd cell count].

For calculation of doubling time in 10% FBS supplemented DMEM, 10^5 A549 cells or H441 cells were seeded in T25 tissue culture flask in 10% FBS supplemented DMEM (complete media) and cultured for 5 days with media change every alternate days. Cells were harvested by trypsinisation and counted by haemocytometer every 24 hours from Day 1 to Day 5. For calculation of doubling time in serum-free DMEM, 10^5 A549 or H441 cells were seeded in T25 culture flasks in complete DMEM media and grown for 24 hours then cells were washed with PBS twice and serum-free DMEM was added into each flask and allowed to grow for further 4 days in normal culture condition. Cells were harvested and quantified as above every 24 hours from Day 2 to Day 5. None of the above cells recovered properly after seeding in serum-free DMEM, this is why for serum-free sample cells were initially recovered in complete media. Population doubling (PD) time was calculated every 24 hours using the above formula from Day 1 to Day 5 for 10% FBS supplemented DMEM sample and from Day 2 to Day 5 for serum-free DMEM sample. The mean PD of each time point was determined as the population doubling time for each cell-type in each culture condition. A total of three individual experiments were performed.

2.7. *In vitro* epithelial wound repair experiments

To explore the effects of various chemical stimuli on epithelial wound repair, I utilised a widely used *in vitro* scratch wound repair system (Figure 2.7A, Figure 2.8) (Kheradmand et al., 1994, Atabai et al., 2002, Galiacy et al., 2003, Chen et al., 2008b, Savla & Waters, 1998, Geiser et al., 2000, Geiser et al., 2004, Sonar et al., 2010, Curley et al., 2012). I also developed a novel direct and indirect-contact co-culture wound repair system to investigate the direct and paracrine influence of one cell-type to another (Figure 2.7B, 2.7C).

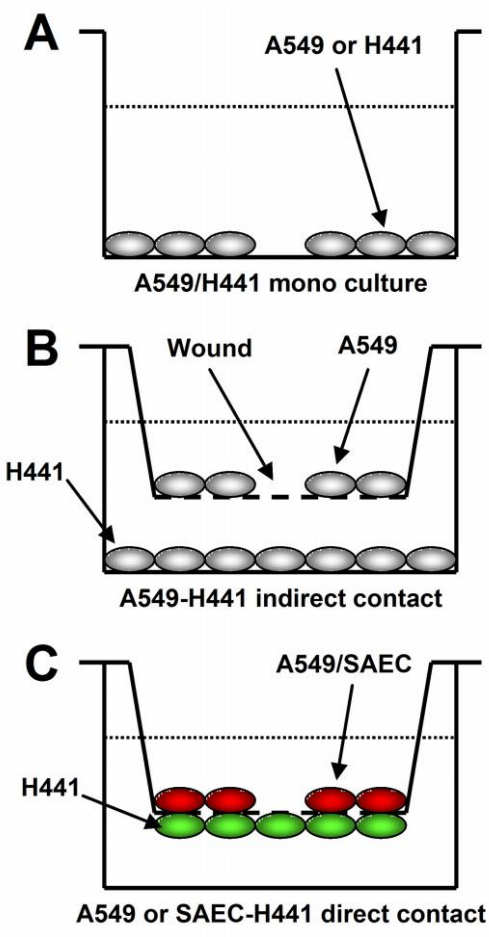

Figure 2.7. *In vitro* epithelial cell wound repair and co-culture system.
(**A**) Scratch wound on A549 or H441 cell monolayer on 24-well plate. (**B**) Indirect-contact co-culture model: wounded A549 on 0.4 μm porous PET membrane of transwell (upper layer) with H441 cells (bottom layer); the gap between two cell layers is 0.8 mm. (**C**) Direct-contact co-culture model: DiI-labelled wounded A549 cells or SAEC (upper layer) with un-wounded DiO-labelled H441 cells (bottom layer) grown on 3 μm porous transwell PET membrane.

2.7.1 Principle of scratch wound repair model

A breach of continuity of an intact epithelial layer is defined as epithelial wound or injury. After injury, a reparative process starts *in vivo* which is complex (Crosby & Waters, 2010). The index of epithelial wound repair assessment *in vivo* is the degree of epithelial cell proliferation (Panos et al., 1995, Yee et al., 2006); however, the index of *in vitro* epithelial wound repair includes cell migration, proliferation and differentiation (Kheradmand et al., 1994, Atabai et al., 2002). Due to the context of our targeted disease, IPF, my primary

focus was to investigate the paracrine and direct influence of Clara and stem cells on alveolar epithelial cell migration and proliferation during wound repair. In the airways, after injury to the epithelium the first 12-24 hours of healing process involves epithelial cell spreading and migration as a primary reparative process followed by cell proliferation and differentiation which takes days to weeks (Horiba & Fukuda, 1994). Therefore, I limited the observation of wound repair upto 24 hours to evaluate the cell migration, which is the early effect during epithelial restitution. Lung epithelial cell (A549, H441 and SAEC) monolayers were formed on well-plates and transwell membranes and injury was made on intact epithelial layers by mechanical scratches introduced by a plastic pipette tip. The wound was then treated with various conditioned media and recombinant proteins to investigate their effects on epithelial wound repair. The degree of wound gap closure which represents the wound repair was monitored after 24 hours. Images were captured just after wounding (0 hour) and after 24 hours of treatment with a CCD camera at the same target point of the wound (Figure 2.8, 2.9) and the area measured manually using Image J software (NIH, USA). The percentage of wound repair was calculated after 24 hours using the following formula:

Wound repair (%) = $\frac{Y1-Y2}{Y1} X100$

Here,

0 hour wound size = Y1

24-hour wound size = Y2

Wound size change = Y1 - Y2 (where Y1 > Y2).

2.7.2. Direct and indirect-contact co-culture wound repair system

To evaluate the direct-contact effect of Clara cells on alveolar epithelial cell wound repair a novel direct-contact wound repair model was developed. A transwell system was utilised. Transwell provides an infrastructure of two compartments which are separated by a porous PET membrane. Alveolar A549 cells were grown monolayer on the upper surface of the PET membrane to make an alveolar compartment. H441 Clara cells were grown monolayer on the opposite surface of the PET membrane to provide a bronchiolar compartment where the porous PET membrane (3 µm pore size) allowed cell migration from one compartment to another (Figure 2.7C). Mechanical injury was made on Alveolar A549 cells and responses of Clara and A549 cells were monitored. This direct-contact model was also replicated in similar SAEC-H441 direct-contact wound repair model. To evaluate the influence of hMSC on alveolar epithelial wound repair, this direct-contact wound repair model was utilised.

An indirect-contact wound repair model was developed using 0.4 µm porous transwell system to evaluate the paracrine role of Clara cells on alveolar epithelial wound repair within a close proximity (Figure 2.7B). In this setting, alveolar A549 cells monolayer was formed on the upper surface of transwell PET membrane and H441 Clara cells were grown on the bottom surface of companion well-plate maintaining a distance of 0.8 mm between these two cell layers. The 0.4 µm porous transwell PET membrane allows free movement of secretory proteins from one chamber to another; therefore, provides a suitable interface for study of paracrine cross-talk between Clara and alveolar epithelial cells.

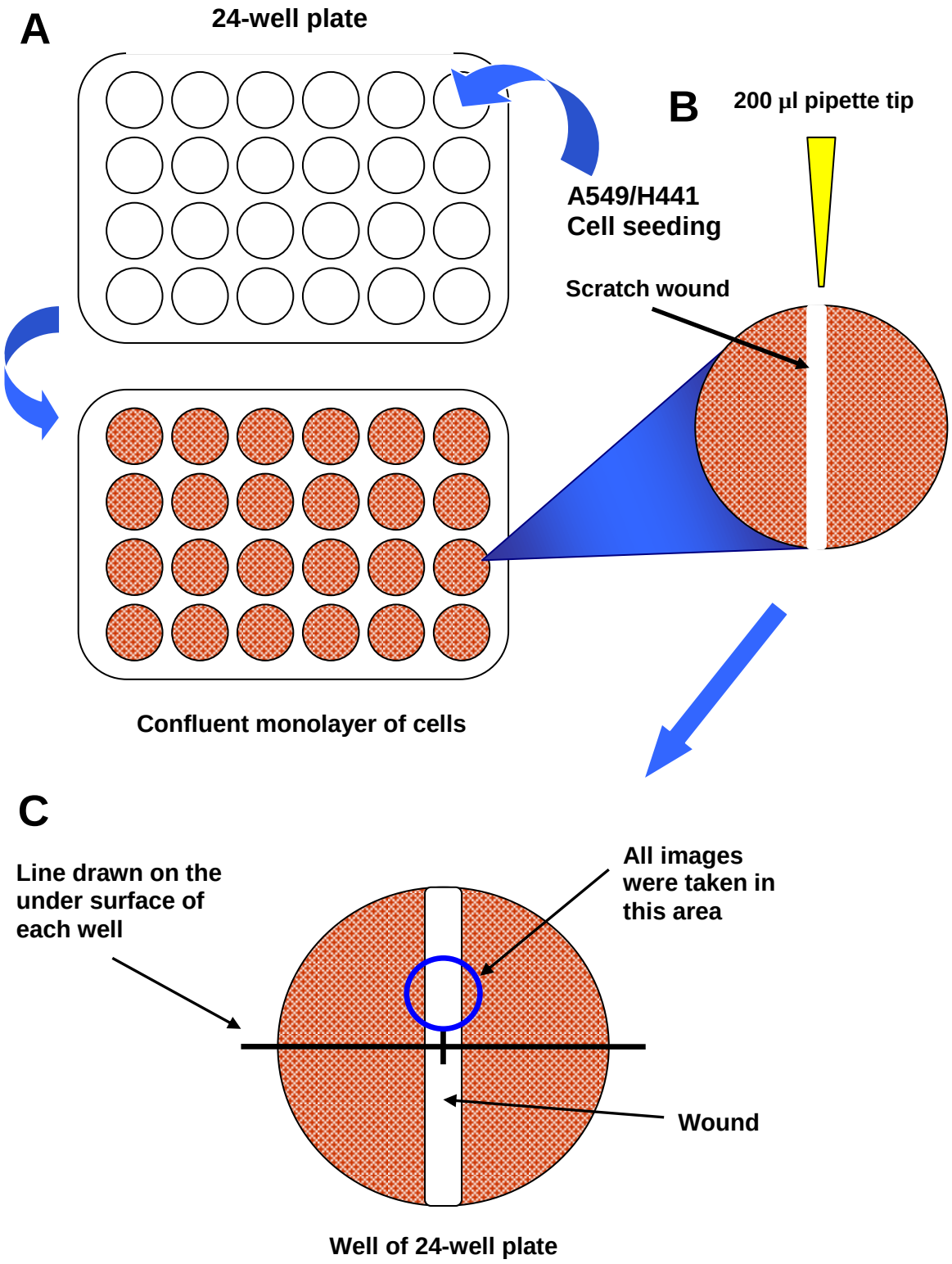

Figure 2.8: Schematic diagram of in vitro wound repair system.

This diagram shows cell seeding and formation of confluent monolayers (**A**); making scratch wound (**B**) and capturing images (**C**).

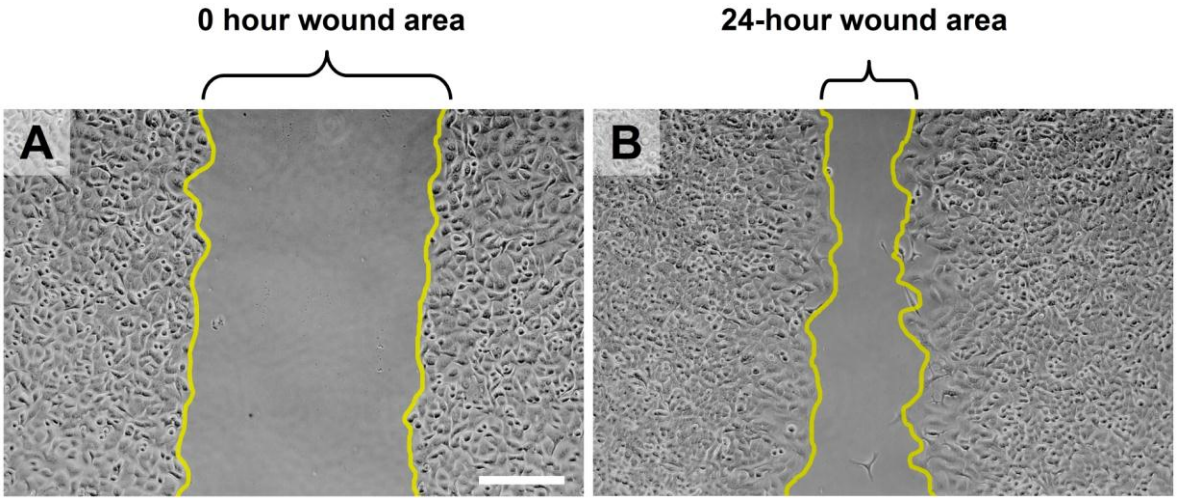

Figure 2.9: Epithelial cell wound area measurement by Image-J software.

The areas of scratch wounds (yellow borders) at 0 hour (A) and after 24 hours (B) of wounding. The wound was made on A549 cell monolayer by 200 µl pipette tip. Images were captured by CCD camera attached with an inverted light microscope. Image magnification 100X. Scale bar, 200µm.

2.7.3. Alveolar A549 cell and H441 (Clara) cell wound repair assay with SF-DMEM, 10% FBS supplemented DMEM and SF-CM

1.5 x 10^5 A549 cells and 3 x 10^5 H441 cells were seeded on each well of 24-well plates (Nunclon) and cultured for 24 hours in DMEM supplemented with 10% FBS, 1% L-glutamine and 1% NEAA (complete growth media) to confluence as monolayers under standard culture conditions. Linear scratch wounds were made on cell monolayers with a 200 µl plastic pipette tip (Figure 2.7, 2.8, 2.9) followed by a wash with pre-heated PBS and once with pre-heated SF-DMEM to remove cell debris and serum. Then samples were replenished with 1 ml of either SF-DMEM or 10% FBS supplemented DMEM or SF-CM obtained from wounded or unwounded A549 or H441 cells (Section- 2.4.1) and cultured for 24 hours. Wound images were recorded with a CCD digital camera (Canon, Japan) attached to an inverted light microscope (Nikon Eclipse, TS100, Japan) at 0 and after 24 hours of wounding. Circumferential wound gaps were measured by Image J software

(NIH, USA) (Figure 2.9) and percentage of wound repair after 24 hours was calculated as described in the Section- 2.7.1.

2.7.4. Alveolar A549 cell wound repair assay with hMSC CM and CCD-8Lu CM

10^5 A549 cells were seeded on each well of a 48-well plate and cultured to confluence as monolayers as described above. Linear scratch wounds were made on A549 cell monolayers as above and treated with SF-MSC CM^{DMEM} (500 µl/well) or with serum-supplemented MSC CM for 24 hours in standard culture condition. SF-MSC CM was supplemented with different concentration (0.1%, 0.2%, 0.3%, 0.4%, 0.5%, 1%, 2%, 5% and 10%) of serum (FBS). For negative and positive control, samples were treated with SF-DMEM or 10% FBS supplemented DMEM respectively. To compare the wound repair effect of MSC-CM with that of fibroblast CM, the similar wound repair assay was replicated on A549 cells with CM obtained from CCD-8Lu. Wound images were recorded at 0 and 24 hours. Image analysis and wound repair calculation were performed as described in the Section- 2.7.1, 2.7.3.

2.7.5. SAEC wound repair assay with hMSC CM

5 x 10^4 SAEC (P-3) were seeded into each well of a 48-well plate in 500 µl of SAGM (complete growth media) and cultured in standard culture condition for 48 hours to achieve confluent monolayers. Linear wounds were made on SAEC monolayers and washed with preheated PBS and SABM (basal media) to remove cell debris. Wounds were then treated with SF-MSC CM^{SABM} (500µl/well) for 24 hours. For negative and positive control, samples were treated with serum-free SABM and complete SAGM respectively. Images were captured at 0 and 24 hours of wounding. Wound repair was calculated as described in the Section- 2.7.1, 2.7.3.

2.7.6. Alveolar A549 cell wound repair assay with hESC CM

1.5 x 10^5 A549 cells were seeded into each well of a 24-well plate and cultured to confluence as monolayers as described above. Linear scratch wounds were made on A549 cell monolayers and treated for 24 hours with three sets of CM (1 ml/well) obtained from undifferentiated hESC. CM was named according to composition: $^{+SR+bFGF}$CM (contains 20% KO-SR and 4ng/ml bFGF), $^{+SR-bFGF}$CM (contains 20% KO-SR but no bFGF) and $^{-SR-bFGF}$CM (contains no KO-SR or bFGF). Corresponding paired controls were similar culture media but un-conditioned (Un-CM).

To evaluate the effects of CM obtained from different stages of Activin-directed or Activin-free hESC differentiation (Section- 2.4.4.2), A549 wounds were treated with 3.5-8 day-CM (collected on 3.5th day), 8-11 day-CM (collected on 11th day), 11-16 day-CM (collected on 16th day) and 16-22 day-CM (collected on 22nd day) for 24 hours (media volume 1 ml/well). For positive and negative controls, wounds were treated with 10% KO-SR supplemented KO-DMEM and SR-free KO-DMEM respectively. Images were captured at 0 and 24 hours of wounding and wound repair calculation was done as described in the Section- 2.7.1, Section- 2.7.3.

2.7.7. A549 cell and SAEC wound repair assay with recombinant human proteins

Plasma Fibronectin, Lumican, Periostin, and IGFBP-7 recombinant human proteins (Table 2.4) were assessed on the A549 and SAEC (P-3 to P-4) *in vitro* wound repair system. A549 and SAEC monolayers were formed on 48-well plate as described in the Section-2.3. Linear wounds were made on A549 cell confluent monolayers and treated with proteins in soluble form in either SF-DMEM or 0.2% FBS supplemented DMEM at different concentrations (1 pg/ml to 100 µg/ml) (Table 2.4). SAEC wounds were treated with the

above mentioned proteins in SF-SABM for 24 hours. Recombinant human Gelatinase-A was assessed on A549 cell wound repair only. For negative control (NC), wounded A549 cells were treated with SF-DMEM or 0.2% FBS supplemented DMEM and SAEC were treated with supplement-free basal SABM for 24 hours. For positive control (PC), wounded A549 cells were treated with 10% FBS supplemented DMEM and SAEC were treated with complete SAGM. Individual positive controls were run for SF and 0.2% FBS supplemented A549 wound samples. PC and NC were included in each experiment to confirm specificity of response. The percentage of wound repair after 24 hours was calculated as described in the Section- 2.7.1, Section- 2.7.3.

Table 2.4: Proteins tested with the *in vitro* wound repair system.

Protein name	Description	Company
Fibronectin	Human plasma Fibronectin Source: Human plasma. Molecular weight 220 kDa	Cat. No. F0895 Sigma-Aldrich, USA
Lumican	Recombinant human protein Source: Murine myeloma cell line. NSO-derived Asn22-Gln836 C-terminal 6-His tag Molecular weight 37.5 kDa	Cat. No- 2846-LU R & D System, USA
Periostin	Recombinant human protein Source: Murine myeloma cell line. NSO-derived Gln19-Asn338 C-terminal 6-His tag Molecular weight 91.7 kDa	Cat. No- 3548-F2 R & D System, USA
IGFBP-7	Recombinant human protein Source: Murine myeloma cell line. NSO-derived Asp30-Leu282 N-terminal 10-His tag Molecular weight 27.5 kDa	Cat. No- 1334-B7 R & D System, USA
Gelatinase A	Recombinant human protein Source: *E. coli* Entire catalytic N-terminal and C-terminal Molecular weight 62.0 kDa	Cat. No-66-96-206 First Link UK Ltd, UK

2.7.8. Direct and indirect-contact co-culture wound repair assays

2.7.8.1. A549-H441 and SAEC-H441 and A549-CCD 8Lu cell direct and indirect-contact co-culture wound repair and cell migration assay

For direct-contact co-culture wound repair experiments (Figure 2.7C), 2 x 10^5 DiO-labeled (Vybrant™ Multicolor Cell Labeling Kit, Cat. No- V22889, Invitrogen, USA) H441 cells were grown on inverted 24-well plate-format 3 µm porous transwell PET (polyethylene terephthalate) membranes (up side down) (BD Bioscience, NJ, USA) in 100µL complete growth media for 4 hours in a humidified incubator at 37^0C allowing them to adhere with the PET transwell membrane (Figure 2.10B, 2.10C, 2.10E). After 4 hours of incubation the transwells were reverted and placed back into the companion well plate (BD Bioscience, NJ, USA) and then 10^5 A549 or 1.5 x 10^5 SAEC (P-3 to P-4) DiI-labeled (Vybrant™ Multicolor Cell Labeling Kit, Invitrogen, USA) cells were seeded onto the upper surface of the transwell PET membrane and sufficient complete growth media (10% FBS supplemented DMEM for A549-H441 direct contact and complete SAGM media for SAEC-H441 direct contact) added (300µl media on upper chamber and 700µl in the lower chamber of the transwell) (Figure 2.10D). For A549-CCD8 Lu direct-contact co-culture, 10^5 DiO-labelled CCD8-Lu (P-14) cells were grown on inverted 24-well plate-format 3 µm porous transwell PET transwell membranes instead of H441 cells as described above.

Cells were labelled with DiO or DiI live-cell label following the manufacturer's instructions. Briefly, adherent cells were harvested by trypsinisation and washed with PBS once by centrifugation technique to remove serum. 10^6 cells were resuspended in 1 ml of pre-heated (pre-equilibrated at 37^0C) SF-DMEM for A549 or H441 or CCD-8Lu and SABM for SAEC. 5 µl of DiO or DiI solution was added in the cell suspension and mixed with gentle pipetting. This cell suspension was then incubated in the incubator at 37^0C for

15 minutes in the dark. During incubation cells were gently agitated every 5 minutes to avoid cell clump formation. After incubation cells were washed once with PBS and once with SF-DMEM or SABM by centrifugation and resuspended in the required volume of complete culture media (complete DMEM for A549 or H441 or CCD-8Lu and complete SABM for SAEC) to seed on transwell.

For indirect-contact co-culture, 10^5 A549 cells were grown on the upper surface of 0.4 μm porous PET membrane of 24-well plate format transwells (BD Bioscience, NJ, USA) and 3 x 10^5 H441 cells or 2 x 10^5 CCD-8Lu cells (un-labelled) on the bottom surface of the companion well plate in complete growth media (Figure 2.7B). Cells of both direct and indirect-contact co-culture were grown in standard culture condition for 24 hours to achieve confluent layers. Linear wounds were made on A549 cell or SAEC monolayers using 10 μl plastic pipette tip followed by washing (once with PBS and once with SF-media) to remove cell debris and serum. H441 or CCD-8Lu cells were also washed to remove all serum. Wounded A549 cells or SAEC along with their accompanying H441 or CCD-8Lu cells were then cultured in SF-DMEM for A549-H441 and A549-CCD 8Lu co-culture or SABM basal media for SAEC-H441 co-culture for a further 24 hours.

Prior to imaging the direct-contact co-culture H441 or CCD-8Lu cells were removed carefully from the undersurface of the PET membrane with a wet cotton swab and washed with warm PBS. The cells of the upper surface of PET membrane were then fixed with 4% paraformaldehyde (4% PFA) (Fisher Scientific, UK) for 30 minutes. The PET membranes were cut from transwell housing and mounted on glass slides and fixed with cover slips for microscopy. Images of direct-contact co-culture were acquired with a laser scanning confocal microscope (Olympus Fluoview, Japan) at both 0 and 24 hours of wounding.

Images of indirect-contact co-culture wounds were taken by an inverted light microscope as described above. Wound gap measurement and wound repair analysis were performed as previously. For negative and positive controls A549 or SAEC monolayers were wounded and cultured in SF-DMEM or SF-SABM and complete 10% FBS supplemented DMEM or complete SAGM, respectively. Control cells were grown on the respective PET membranes specific to the direct or indirect contact co-culture model used.

For assessment of H441 cell migration in A549-H441 or SAEC-H441 cell direct-contact co-culture, DiO-labelled H441 cells and DiI-labelled A549 cells or SAEC were counted at the respective wound sites at 0 and 24 hours after wounding. Confocal Z-scanning was performed to confirm the migration.

2.7.8.2. A549-MSC direct contact co-culture wound repair and migration assay

10^5 DiI-labeled A549 cells and 10^5 DiO-labeled hMSC were grown to confluency in complete culture media on the contra-lateral surfaces of 3 μm porous PET membranes of the 24-well plate format transwell over 24 hours as described in Section- 2.7.8.1. Linear wounds were made on A549 cell monolayers as described in Section- 2.7.8.1. Wounded cells were then cultured in SF-DMEM for 24 hours. Prior to imaging hMSC were removed carefully with a wet cotton swab from the undersurface of the PET membrane. Cells on the upper surface of the PET membrane were then fixed with 4% PFA. Images were acquired with a laser scanning confocal microscope at both 0 and 24 hours. Wound gap measurement and wound repair analysis were performed as described in Section- 2.7.8.1.

For assessment of hMSC migration to A549 wound sites in A549-MSC direct-contact co-culture DiO-labelled hMSCs were counted at the A549 wound gaps and their juxta-wound

monolayers at 0 and after 24 hours of wounding. Confocal Z-scanning was performed to confirm the migration. A minimum of three fields were counted per sample.

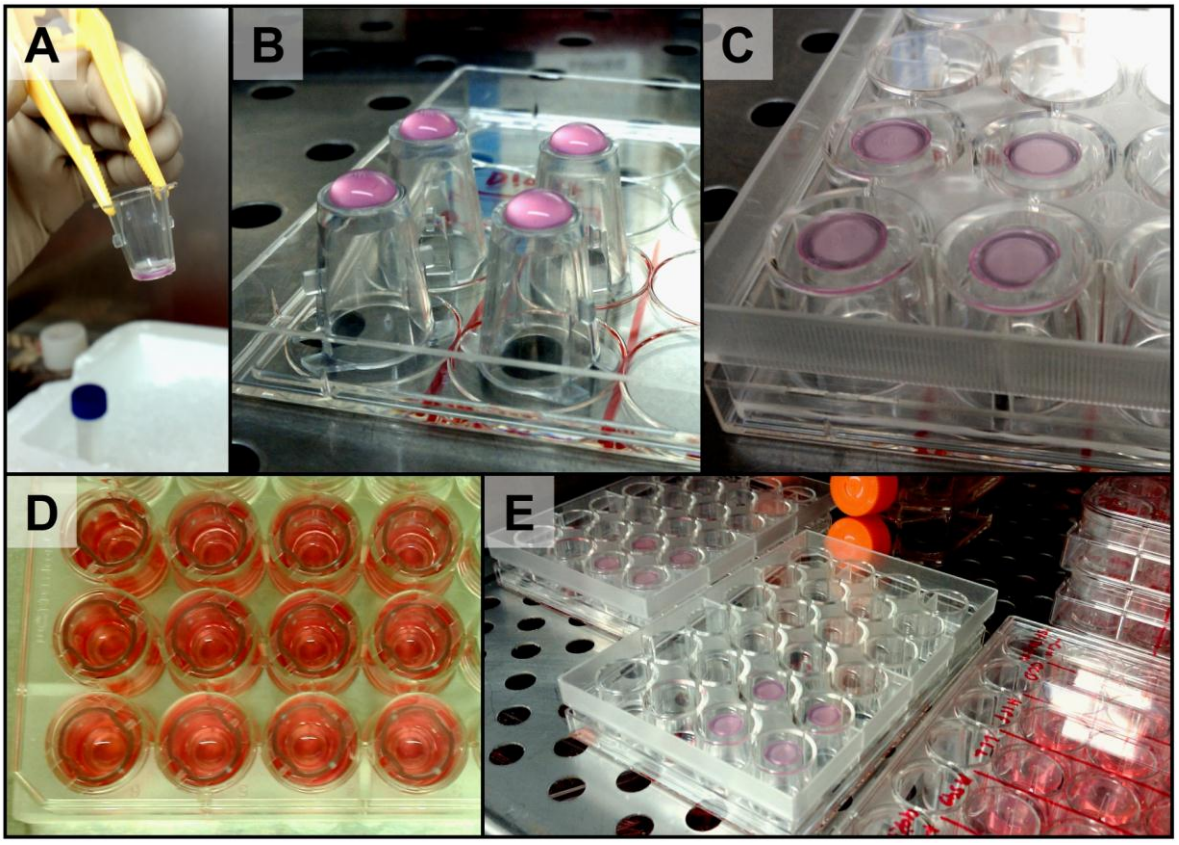

Figure 2.10: Direct-contact co-culture wound repair technique using transwell system.
(**A**) A 24-well plate-format transwell. (**B**) DiO-labelled H441 cells were seeded on 3 µm porous PET membrane on inverted transwells in 100µl complete DMEM. (**C**) Inverted transwells were covered with their accompanying well plate in up side down position. (**D**) After H441 cells had adhered to the under surface of transwell membrane, the transwells were reverted and placed in their accompanying well plate the in original position and A549/SAEC were seeded on the upper surface of PET membrane with adequate media. (**E**) Cells were grown in the incubator.

2.8. Measurement of internuclear distances

To measure the relative migration of A549 cells during wound repair, internuclear distances between migrated A549 at wound margins were measured after 24 hours of wounding using Image J software. Three measurements were taken per migrated cell which was adjacent to the wound margins (Figure 2.11). The distance was measured between nuclei of the cells. A total 18 measures were recorded per wound.

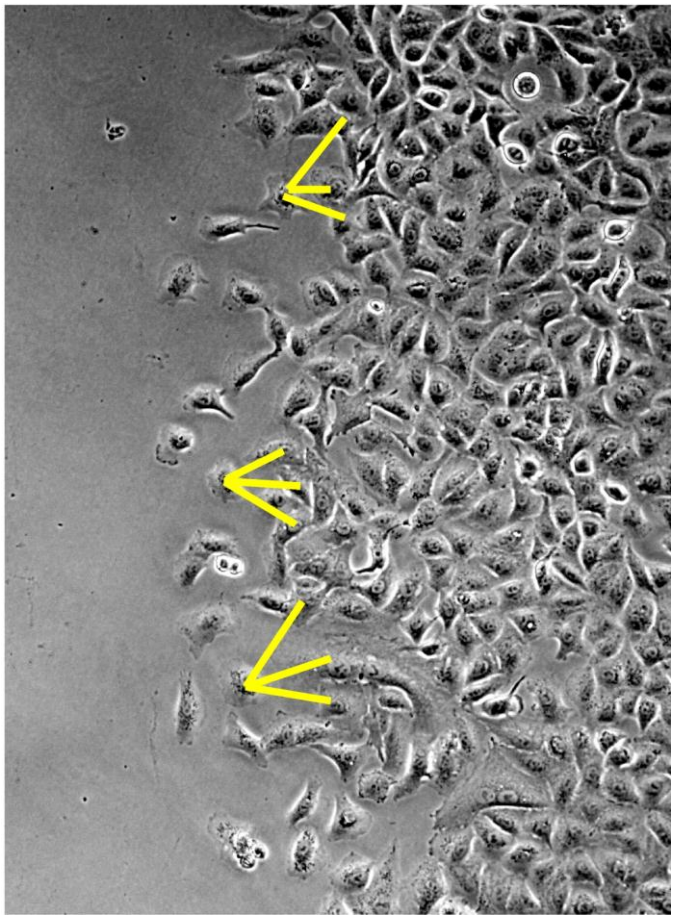

Figure 2.11: Measurement technique of internuclear distances.
Inverted light microscopic images of A549 cell wound repair after 24 hours with SF-MSC CM. Image magnification 100X.

2.9. MTT cell proliferation assay

To evaluate the effects of MSC-CM, CCD-8Lu CM, hESC-CM and recombinant proteins on alveolar A549 cell proliferation during wound repair, the MTT (3-(4,5-dimethylthiazol-2-yl)-2,5-diphenyltetrazolium bromide) cell proliferation assay was performed using the MTT reagent Thiazolyl Blue Tetrazolium Bromide (Sigma, Cat No- M5655) following manufacturer's instructions (Plumb et al., 1989). Briefly, 10^5 A549 cells were grown to confluence on each well of a 48-well plate in 24 hours and wounds were made as described is Section-2.3, Section- 2.7.6. For a 0 hour reading, MTT was performed immediately after wounding. Wounded monolayers were washed and 300 µl of 0.5 mg/ml MTT reagent containing SF-DMEM solution was added to each well and incubated at 37^0C for 2 hours. After incubation, MTT solution was discarded and washed twice with pre-heated PBS. The formazan was extracted by 100% DMSO (250 µl/well) incubation for 10 minutes in the incubator at 37^0C. 200 µl of extracted formazan-DMSO solution was then loaded in each well of 96-well plate and absorption measured with a micro-plate reader (BioTek, Synergy 2) at a 630 nm wavelength. For 24 hours readings, wounded A549 cell monolayers were treated with either SF-MSC CM, 2% FBS supplemented MSC-CM, SF-CCD 8Lu CM, 0.2% FBS supplemented CCD 8Lu CM, or hESC-CM (3.5-8 day-CM, 8-11 day-CM, 16-22 day-CM) for 24 hours in the incubator at 37^0C with standard culture condition. For negative control (NC), wound samples were treated with SF-DMEM or SF-KODMEM or 0.2% FBS supplemented DMEM and for positive controls (PC), wounded samples were treated with 10% FBS supplemented DMEM, or 10% KO-SR supplemented KO-DMEM for 24 hours. After 24 hours of incubation, media was discarded and the MTT assay performed as above. Triplicate experiments were performed for each sample. Data presented as percentage increase of optical density (OD) reflecting degree of cell proliferation after 24 hours.

2.10. TUNEL assay for evaluation of apoptosis

2.10.1. Ligand induced apoptosis

To assess ligand-induced apoptosis in wounded A549 cell monolayers, 5 x 10^4 DiI-labelled A549 cells were seeded into each well of a 96-well plate and grown to confluence over 24 hours using complete culture media. Linear wounds were made as described in Section-2.7.3 and wounded monolayers were treated with recombinant human soluble TRAIL (200 ng/ml, 400 ng/ml, 800 ng/ml) or FasL (200 ng/ml, 400 ng/ml, 800 ng/ml, 1.6 µg/ml, 3.2 µg/ml) (Peprotech, NJ, USA) for 24 hours in SF-DMEM. Ligand-induced apoptosis was blocked through pre-incubation of A549 cells with TRAIL-R1 (HS101, 1µg/ml, 5 µg/ml, 10 µg/ml) and/or TRAIL-R2 (HS201, 1µg/ml, 5 µg/ml, 10 µg/ml); and Fas (SM1/23, 10 µg/ml) receptor blocking antagonistic monoclonal antibodies (mAbs) (Enzo Life Science, Switzerland). For induction of apoptosis in SAEC with soluble TRAIL, 5 x 10^4 SAEC cells were seeded into each well of 96-well plate and grown to confluency over 24 hours in complete SAGM growth media. After 24 hours cells were treated with different concentration of soluble TRAIL (200 ng/ml, 400 ng/ml, 800 ng/ml, 1.6 µg/ml) in SF-SABM for 24 hours. For positive control, wounded monolayers were treated with 200 µM H_2O_2 (Cat. No- H-1009; Sigma, MO, USA) in SF-DMEM for A549 cells and SF-SABM for SAEC for 24 hours. For negative control, samples were treated with SF-DMEM or SF-SABM.

Apoptosis induction was evaluated with the TUNEL (terminal deoxynucleotidyl transferase mediated deoxyuridine triphosphate nick end-labelling) method using an *In Situ* Cell Death Detection Kit, Fluorescein (Roche Applied Science, USA) according to the manufacturer's protocol. Briefly, cells were fixed with 4% PFA for 30 minutes. Cells were then permeabilised with 0.1% Triton X-100 (Sigma, MO, USA) for 2 minutes and washed

twice with PBS. TUNEL reagent (a mixture of Enzyme solution and Label solution) was then added in each well (50 µl/well) and incubated at 37^0C in the incubator for 1 hour in the dark. After incubation, samples were washed three times with PBS and images were captured on a laser scanning confocal microscope.

2.10.2. Direct contact induced apoptosis

To assess H441 or CCD-8Lu cell direct-contact induced apoptosis in alveolar A549 cells or SAEC, DiI-labelled A549 cells or SAEC were cultured in direct-contact with un-labelled H441 or CCD-8Lu cells using 3 µm porous transwell for 24 hours in complete growth media as described above in Section- 2.7.8.1. Linear wounds were made on A549 cell and SAEC confluent monolayers and cultured for an additional 24 hours in serum-free basal media (SF-DMEM for A549-H441 or A549-CCD-8Lu and SF-SABM for SAEC-H441 co-culture) as described above in Section- 2.7.8.1. To block apoptosis, samples were treated with either Fas (SM1/23, 10µg/ml) or TRAIL-R1/R2 (HS101, HS201; 10 µg/ml) receptor blocking antagonistic mAbs throughout the entire co-culture wound repair period. After 24 hours of incubation, H441 or CCD-8Lu cells were removed from the under-surface of the PET membrane and the remaining cells on the upper surface were fixed with 4% PFA for 30 min and permeabilised with 0.1% Triton X-100 for 2 minutes as described above. PET membranes were cut from the transwell housing and placed on the pockets of Glastic® Slide-10 cell counting chamber (Cat. No-87144, Kova, USA) (Figure 2.12). 50 µl of TUNEL reagent was added in each pocket covering the entire PET membrane properly and incubated for 1 hour as described above in Section- 2.10.1. For positive control, apoptosis was induced in A549 or SAEC monoculture by 200 µM H_2O_2 treatment in SF-DMEM/SABM respectively for 24 hours. For negative control, cells were cultured (monoculture) in serum-free basal media (SF-DMEM/SABM). All control cells were

cultured on identical cultures surfaces that were used for respective experimentation. Images were acquired with a laser scanning confocal microscope. TUNEL positive cells were quantified along the wound margins and data were standardised against positive control and presented as percentage of apoptosis.

2.10.3. Apoptosis evaluation in patient tissue samples

The TUNEL assay was performed alongside Ms. Nicola Lomas at the Histopathology lab of University Hospital of North Staffordshire and at Central Cell Culture Lab of Guy Hilton Research Centre. For combined TUNEL assay and immunohistochemistry with *pro*SP-C antibody on lung tissue, formalin-fixed, paraffin-embedded lung tissue samples were cut to 3 µm thick sections. Sections were deparaffinised and pre-treated for heat mediated antigen retrieval in citrate buffer (pH 6). Samples were stained on a Dako autostainer using Dako REAL detection kit (Dako, Denmark) according to the manufacturer protocol. Samples were first treated with *pro*SP-C primary antibody over night at 4^0C (polyclonal, ab40879, dilution 1:1500; Abcam). For visualisation, samples were treated with anti-rabbit IgG-NL557 secondary antibody (R & D systems). Afterwards, TUNEL was performed as described before (Section- 2.10.1). Samples were examined under the fluorescence microscope and TUNEL positive nuclei were counted. Briefly, 100 *pro*SP-C labelled cells were counted in the above mentioned areas of IPF lung tissue samples and dual *pro*SP-C/TUNEL labelled cells were recorded. Same was performed in control sample. Data was presented as percentage of dual *pro*SP-C/TUNEL positive cells with ± SEM per case.

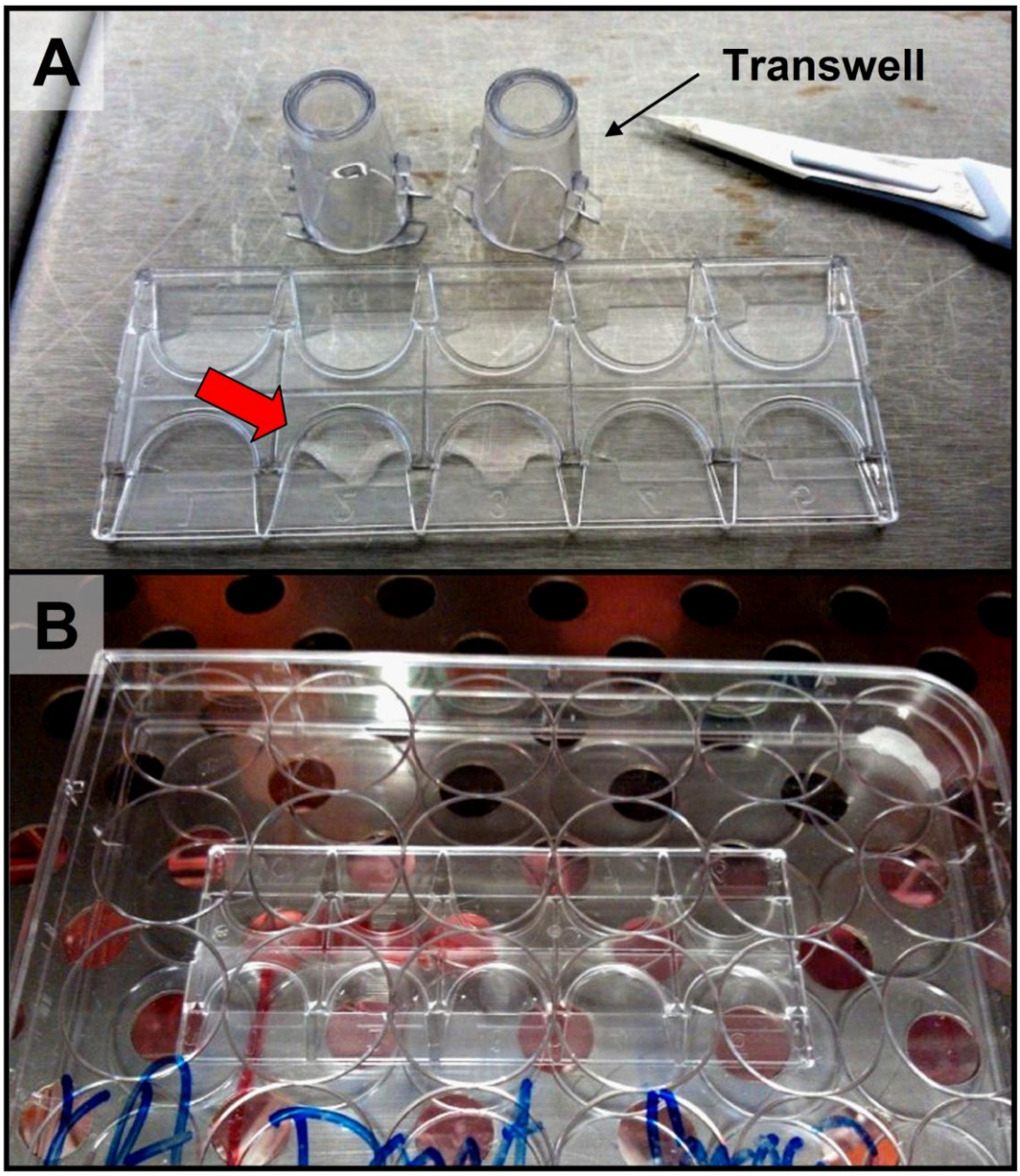

Figure 2.12: TUNEL assay on direct contact co-culture.

(**A**) PET membranes were cut from transwell and placed on the pockets of Glastic® Slide-10 (on reversed surface) and TUNEL reagent was added (red arrow). (**B**) Sample incubation in the incubator in a plastic box.

2.11. Reverse transcription-PCR (RT-PCR)

Semi-quantitative RT-PCR was performed to determine the mRNA expression of TRAIL, TRAIL-R1 and TRAIL-R2 in A549 and H441 cells; and Oct-4, Nanog, hTERT, AFP, ACTC1, SOX1 in hESC. The primers were designed using human gene sequences from NCBI Map Viewer or Ensemble Genome Browser and Primer 3. Designed primers were evaluated in NCBI Primer-BLAST to check specificity. Customised primer sets were purchased from Invitrogen, USA. Primers are tabulated below (Table 2.5). RT-PCR was performed with a one-step protocol.

RNA extraction

Total RNA was extracted using the QIA RNeasy Mini Spin Column (Qiagen, Germany) according to the manufacturer protocol. Briefly, adherent A549, H441 and hESC were harvested by trypsinisation and hESC-EBs collected from suspension culture. Cells were washed with PBS once and pellets were formed by centrifugation. Cell pellets were then lysed with RLT lysis buffer (350 µl RLT buffer + 3.5 µl β-mercaptoethanol per sample). Cell lysates were transferred into the upper column of the QIA Shredder and centrifuged for 3 minutes at 13,000 rpm. Cell lysates were collected in the collection tube and stored at -80^{0}C. For RNA extraction, cell lysates were thawed on ice and 350 µl of 70% ethanol added. Cell lysate-ethanol solution (700 µl total) was then transferred into the upper column of QIA RNeasy Mini Spin Column and centrifuged for 25 seconds at 6000 rpm (13.2 g). Flowthrough was discarded and 700 µl of RW1 buffer was added and centrifuged for 25 seconds at same speed. Flowthrough was again discarded and 500 µl of RPE buffer added into the upper column and centrifuged for 25 seconds. This step was repeated with 2 minutes of centrifugation. The collection along with the collecting tube was discarded and the upper column was transferred into a fresh collection tube and centrifuged for 1 minute

without adding anything. Finally, the upper column was transferred into a fresh eppendorf and 20 µl of RNAse/DNAse-free dH_2O was added onto the membrane of the upper column and allowed to stand vertically for 1 minute before centrifugation for 1 minutes at 13.2 g, this step was repeated once for maximum yield of RNA. The extracted RNA was collected into the eppendorf. The quality and quantity of RNA yield were determined by measurement of absorption at 260 and 280 nm using NanoDrop ND-1000 spectrophotometer (NanoDrop, USA). The ratio of optical density at 260 and 280nm was >1.8 in all cases.

One-step RT-PCR

One-step RT-PCR was performed using SuperScript® III One-Step RT-PCR System with Platinum® *Taq* High Fidelity kit (Invitrogen, CA, USA) and amplified in DNA Engine® Thermal Cycler (MJ Research, MA, USA) in a single tube according to the manufacturer protocol. In short, 10 ng RNA of each sample was mixed with 6.25 µL 2X Reaction Mix, 3 µL RNAse-free water, 1 µL of each primer (10 µM) and 0.25 µL of Platinum® *Taq* polymerase enzyme. The thermal cycling protocol comprised an initial reverse transcription at 50^0C for 30 minutes, pre-denaturation at 94^0C for 2 minutes followed by 30 cycles of denaturation at 94^0C for 15 seconds, annealing at 53-56^0C (depending on primers) for 30 seconds and extension at 68^0C for 1 minute followed by a final extension at 64^0C for 5 minutes. The PCR fragments were separated by electrophoresis on 2% agarose gel (Fisher Scientific, NJ, USA) and visualized by staining with ethidium bromide (Sigma, MO, USA) under UV light. Primers for β-actin were used as a loading control. All primers were obtained from Invitrogen, USA (Table 2.5).

Agarose gel preparation

The PCR products were separated by electrophoresis on 2% agarose gel. 2 g of agarose powder (Fisher Scientific, NJ, USA) was dissolved in 100 ml of 1X TAE (Tris Acetate-EDTA) buffer in the microwave oven. When agarose had completely dissolved 5 µl of ethidium bromide (10 mg/ml) was added and mixed properly. The hot agarose solution was then immediately poured onto an agarose gel case and a comb was placed to make pockets. After 45 minutes at room temperature, the gel formed and became ready to use.

Gel electrophoresis protocol

The agarose gel was placed on the electrophoresis machine (Bio-Rad DNA Sub Cell) and immersed in 1X TAE buffer. Each PCR product (sample) was mixed with 2 µl of loading buffer. 6 µl of PCR product was then loaded per well. 6 µl of DirectLoad™ wide range DNA marker (Cat. No- D7058-1VL; Sigma) was loaded into two wells to determine product size after electrophoresis. Electrophoresis was performed for 45 minutes with 100 volts constant current.

Table 2.5: Primer sequences.

Official name is listed in gene column with alternative name in parentheses. Forward and reverse primers are listed in 5' to 3' orientation.

Gene	Primers (5'-3')		Annealing temp (^{0}C)	Amplicon size (bp)
TNFSF10 (TRAIL)	F	CTGCAGTCTCTCTGTGTGG	55	196
	R	TCTTTCTAACGAGCTGACG		
TNFRSF10A (TRAIL-R1)	F	CAAAGAATCAGGCAATGG	55	196
	R	GTGAGCATTGTCCTCAGC		
TNFRSF10B (TRAIL-R2)	F	CACCAGGTGTGATTCAGG	53	220
	R	CCCACTGTGCTTTGTACC		
POU5F1 (Oct-4)	F	GCAATTTGCCAAGCTCCTGAAGCAG	55	536
	R	CATAGCCTGGGGTACCAAAATGGGG		
NANOG (Nanog)	F	GGTGGCAGAAAAACAACTGGC	55	300
	R	TGCAGGACTGCAGAGATTCC		
TERT (hTERT)	F	GCAGCTCCCATTTCATCAGC	53	343
	R	CAGGATGGTCTTGAAGTCTG		
AFP	F	CAGAAAAATGGCAGCCACAGC	54	399
	R	TGGCAGCATTTCTCCAACAGG		
ACTC1	F	CATCCTGACCCTGAAGTATCCCATC	56	315
	R	CCCTCATAGATGGGGACATTGTGAG		
SOX1	F	CCAGGAGAACCCCAAGAGGC	56	206
	R	CGGCCAGCGAGTACTTGTCC		
ACTB (β-actin)	F	GCCACGGCTGCTTCCAGC	55	477
	R	AGGGTGTAACGCAACTAAGTC		

2.12. Fluorescent immunocytochemistry

Basic protocol: Samples were fixed with 4% PFA (Fisher Scientific, UK) for 30 minutes. Samples were washed with PBS once and permeabilised with 0.5% Triton-X 100 (Sigma) for 5 minutes at RT. Samples were then washed with PBS twice and blocked with 3% BSA (unless otherwise mentioned) for 1 hour at RT. After blocking, samples were washed once with PBS and treated with primary antibodies (Table S2, Appendix-1) in 0.1% BSA in PBS buffer for 24 hours at 4^0C. After primary antibody incubation, samples were washed twice with PBS and secondary antibodies were added and incubated for 2 hours in the dark at RT. For secondary antibody control, samples were treated with secondary antibody (IgG) only. Samples were washed once with PBS and before being immersed in DAPI (Sigma) solution at (1:500 in PBS), for nuclear counter staining, for 10 minutes in the dark at RT. Samples were then washed three times with PBS and examined under a fluorescent microscope.

2.12.1. Fluorescent immunocytochemistry profiling of *pro*SP-C, TRAIL, TRAIL-R1 and TRAIL-R2 in A549 cells H441 cells and SAEC

For immunocytochemistry, either 2.5 x 10^4 A549 cells, 5 x 10^4 H441 cells, or 2.5 x 10^4 SAEC were seeded into each well of 48-well plate and grown to sub-confluence over 24 hours in complete culture media. Cells were fixed, permeabilised and blocked as described above (Section 2.12). Expression of *pro*SP-C in A549 and SAEC cells was determined by immunostaining with anti-*pro*SP-C primary antibody (polyclonal, ab40879, dilution 1:250; Abcam, Cambridge, UK) and visualised by secondary antibody anti-rabbit IgG-NL493 (dilution 1:200, NorthernLights, R & D System, MN, USA) according to manufacturer's instructions protocol as described above in Section- 2.12. TRAIL, TRAIL-R1 and TRAIL-R2 expression were detected in unwounded A549 and H441 cells using anti-TRAIL

primary antibody (polyclonal, ab2435, dilution 1:100; Abcam) and TRAIL-R1 (monoclonal, HS101, 10µg/ml) and TRAIL-R2 (monoclonal, HS201, 10µg/ml) (both Enzo Life Science, Switzerland) according to the manufacturer's protocol. Anti-rabbit IgG-NL493 secondary antibody (1:200) against TRAIL antibody (ab2435) and anti-mouse IgG-NL557 (1:200) against TRAIL-R1 and –R2 antibodies were used (NorthernLights, R & D System). TRAIL evaluation was also conducted on unwounded SAEC. All primary antibody (Table S2, Appendix-1) treatment incubation was for 24 hours at 4^0C and secondary treatment was for 2 hours at room temperature. DAPI was used for nuclear counterstaining (Sigma or Invitrogen, USA). Images were acquired by a fluorescent microscope (Olympus Fluoview, Japan or Nikon Eclipse Ti-ST, Japan).

2.12.2. Characterisation of hMSC

5 x 10^4 hMSC (P-1, P-4) were plated on each well of a 24-well plate and grown to 80-90% confluency for immunophenotyping. Cells were fixed with 4% PFA, permeabilised with 0.5% Triton-X 100 and blocked with 3% BSA as described above (Section 2.12). Fixed hMSC cells were characterised using the human MSC characterisation kit containing anti-human mouse anti-CD44, anti-CD90, anti-CD146, anti-CD14, anti-CD19 and anti-STRO-1 primary antibodies at 1:500 dilution (Cat. No. SCR067, Millipore). Cells were incubated with primary antibodies at 4^0C overnight. Secondary antibodies were anti-mouse IgG-NL557 for all except STRO-1 and anti-mouse IgM-NL493 for STRO-1 (both at 1:200 dilutions) (NorthernLights, R & D System). DAPI was used for nuclear staining. Images were acquired by a fluorescent microscope (Nikon Eclipse Ti-ST, Japan).

2.12.3. Functional characterization of differentiated hMSC

hMSC (P-1) were differentiated into osteoblasts, adipocytes and chondrocytes using StemPro differentiation media in 24-well plates (Section- 2.2.3.1). The tri-lineage differentiation of hMSC was characterised with the Human Mesenchymal Stem Cell Functional Identification Kit containing anti-human mouse anti-Osteocalcin for osteoblasts, goat anti-FABP-4 for adipocytes and goat anti-Aggrecan for chondrocytes at 1 µg/100µl concentration (250 µl/well) (Cat. No. SC006, R & D System). Cells were incubated with primary antibodies at 4^0C overnight. Secondary antibodies were anti-mouse IgG-NL557 for Osteocalcin and anti-goat IgG-NL493 for FABP-4 and Aggrecan (both at 1:200 dilutions) (NorthernLights, R & D System). DAPI was used for nuclear staining. Images were acquired by a fluorescent microscope (Nikon Eclipse Ti-ST, Japan).

2.12.4. Characterisation of hESC

2.5 x 10^4 SHEF-2 (P-44) cells were plated on each well of a 48-well plate and grown to 70-80% confluency for evaluation of embryonic stem cell pluripotent markers by immunocytochemistry. Cells were fixed with 4% PFA, permeabilised with 0.5% Triton-X 100 and blocked with 3% BSA as described above (Section 2.12). Fixed SHEF-2 cells were characterised using the "Human Embryonic Stem Cell Marker Antibody Panel" kit containing anti-human mouse anti-alkaline phosphatase (ALP), goat anti-Oct-4, goat anti-Nanog, mouse anti-SSEA-1 and mouse anti-SSEA-4 primary antibodies at 1µg/100µl concentration (150 µl/well) (Cat. No. SC008, R & D System). Cells were incubated with primary antibodies at 4^0C for 24 hours. Secondary antibodies were anti-goat IgG-NL493 (1:200, NorthernLights, R & D System) for Oct-4 and Nanog; and TRITC-conjugated anti-mouse IgG (1:200, ab6787, Abcam) for ALP, SSEA-1 and SSEA-4. DAPI was used for

nuclear staining. Images were acquired by a fluorescent microscope (Nikon Eclipse Ti-ST, Japan).

2.12.5. Evaluation of pluripotent markers in differentiated EBs

SHEF-2 cells were differentiated with Activin A through EB suspension culture as described above. EBs were fixed with 4% PFA for 1 hours on day 1 and day 11 of differentiation. More than 100 EBs were fixed per well. EBs were permeabilised with 0.5% Triton X-100 for 20 minutes and then washed twice with PBS. EBs which were subject for visualisation with donkey secondary antibody were blocked with 3% BSA and 1% donkey serum; and those EBs which were subject for visualisation with goat secondary antibody were blocked with 3% BSA and 1% goat serum for 2 hours at RT. EBs were treated with Human Embryonic Stem Cell Marker Antibody Panel kit containing anti-human mouse anti-alkaline phosphatase (ALP), goat anti-Oct-4, goat anti-Nanog, mouse anti-SSEA-1 and mouse anti-SSEA-4 primary antibodies at 1µg/100µl concentration (150 µl/well) (Cat. No. SC008, R & D System) for 24 hours at 4^0C as described above. EBs were washed three times with PBS and treated with secondary antibodies and incubated for 2 hours at RT as described above. DAPI was used for nuclear staining. Images were acquired by a fluorescent microscope (Nikon Eclipse Ti-ST, Japan).

2.12.6. Immunohistochemistry on lung tissue samples

This section of study was conducted alongside Ms. Nicola Lomas at Histopathology lab of the University Hospital of North Staffordshire. Experiments were performed by Ms Nicola Lomas and analysis performed jointly.

Formalin-fixed, paraffin embedded lung tissue samples were cut to 3 µm thick sections. Sections were deparaffinised and pre-treated for heat mediated antigen retrieval in citrate buffer (pH 6). Samples were stained on a Dako autostainer using Dako REAL detection kit (Dako, Denmark) according to the manufacturer protocol. Type II AEC and Clara cells were differentiated by dual immunostaining of samples with *pro*SP-C antibody (polyclonal, ab40879, dilution 1:1500; Abcam) and CC10 antibody (polyclonal, ab40873, dilution 1:200; Abcam). For dual immunostaining with TRAIL and CC10 antibodies samples were first treated with TRAIL primary antibody (polyclonal, ab2435, dilution 1:80; Abcam) and visualised by DAB followed by second antibody treatment by CC10 antibody and visualised by VIP (Very Intense Purple, Lab Vision, UK) in dual immunostaing and by DAB in mono-staining. For dual-immunohistochemistry staining an avidin biotin block was performed after completion of the first antibody labelling to prevent cross reaction with the detection kit. The Negative controls included omission of the primary antibody. Sections were counterstained using haematoxylin Z (CellPath, UK).

Sections were reviewed by two independent pathologists for expression of the above mentioned markers at the sites of interest in IPF and control lung tissues. For quantification of CC10, TRAIL and CC10/TRAIL stained cells within the vicinity of fibrotic regions of IPF lung samples, 100 epithelial cells were counted and the number of cells expressing each marker (or dual marker) was recorded. The same was performed at the alveolar regions of the control samples. Data was presented as percentage of specified marker expressing cells with ± SEM per case.

2.13. Collagen drop cell migration assay

To evaluate the effect of identified hMSC secretory proteins on alveolar A549 cell migration as substrate components, I developed a cell migration assay tool where 5 x 10^4 A549 cells were resuspended in 10 µl of 1 mg/ml concentration of rat tail collagen I (BD Bioscience) in 0.2% FBS supplemented DMEM. The cell/collagen solution was dropped (10 µl/drop) on different concentration of Fibronectin or Lumican or Periostin coated 24-well plates. Well-plates were coated with proteins by adding 500 µl of different concentrations of proteins (in PBS) and incubating them at 4^0C over night. After incubation, solution was discarded and wells were air dried before plating the collagen drop. Acidity of collagen was neutralised using 1M NaOH buffer. A single drop (10 µl) was placed at the centre of each well and incubated for 30 minutes in the humidified incubator at 37^0C allowing the drops to form into gel. Following gel formation, 20% FBS supplemented DMEM was added to each well to provide a chemoattractant-bias for the promotion of cell migration out of the gel barrier (Figure 2.13). After 24 hours migratory cells were quantified microscopically using inverted light microscope. The radius of each drop was measured by Image J software and the circumference of each drop was calculated. Results were expressed as mean migration through per millimeter of circumference of collagen-drop barrier.

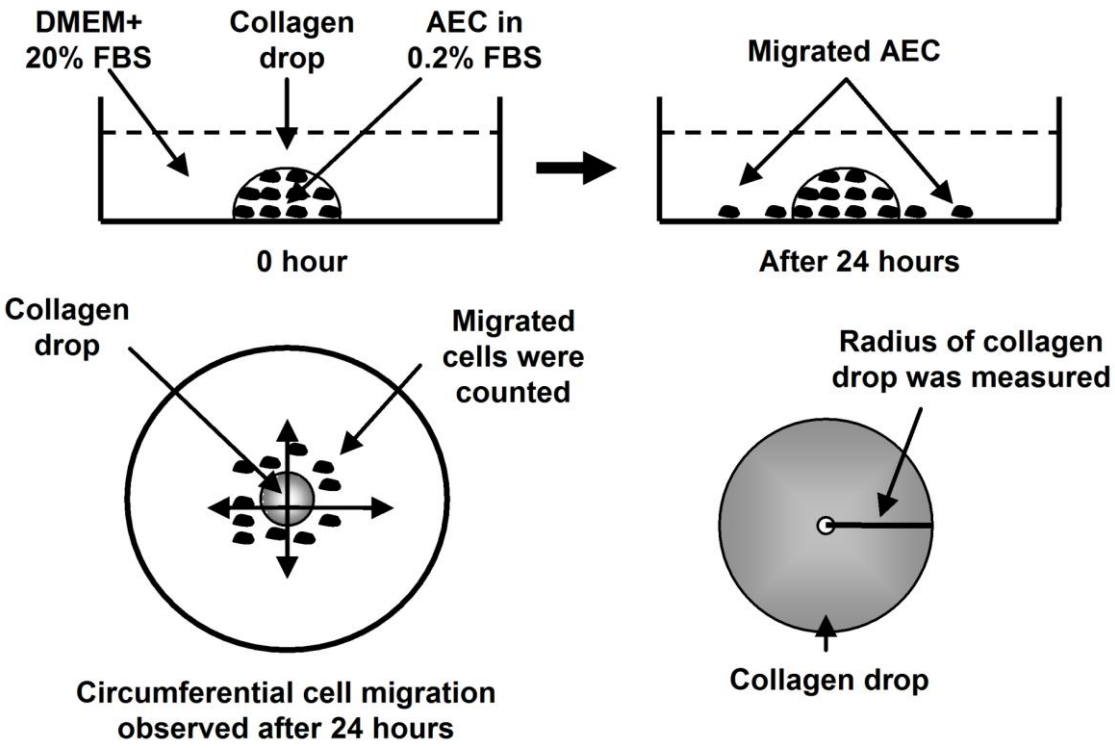

Figure 2.13: Collagen drop cell migration assay.

2.14. Statistical Analysis

The significance of difference between two groups was determined by paired, two-tailed Student t-test. Differences between three or more groups were analysed by one-way ANOVA with Post-hoc Tukey's Multiple Comparison analysis (unless otherwise mentioned). Patient data were analysed by Wilcoxon matched-pairs signed rank test or Mann Whitney U test. Correlation analysis between different doses of proteins and wound repair responses was conducted by Spearman rank correlation coefficient test (Moine et al., 1997, Park et al., 2011). Correlation data were presented in logarithmic scale for better presentation (Moine et al., 1997). A 'p' value less than 0.05 was considered to indicate statistical significant. *In vitro* data are presented as mean ± standard deviation (SD) and patient data presented as mean ± standard error of mean (SEM). For *in vitro* studies, at least three separate assays were performed for each experimental setting which is represented as 'n' number and replicate number per assay is mentioned as 'replicates per n'. 'n' numbers are mentioned throughout the manuscript at the figure legends. All data were processed and analysed using Microsoft Excel of Microsoft Office XP® software (Microsoft Corporation, USA). Statistical analysis was conducted using GraphPad Prism® version 5.00 software for Windows (GraphPad Software, San Diego California USA).

2.15. Study approval

Human tissue research was approved by the South Staffordshire Local Research Ethics Committee (08/H1203/6).

Chapter 3

Clara cells inhibit alveolar epithelial wound repair via TRAIL-dependent apoptosis: a potential novel mechanism for pulmonary fibrogenesis

3.1. Background

Idiopathic pulmonary fibrosis (IPF) is a chronic, progressive fibrosing interstitial pneumonia of unknown aetiology occurring primarily in older adults, and limited to the lungs (Raghu et al., 2011). The pathophysiological process of this disease is not well understood. However, recently it has been hypothesised that multiple micro-injuries to alveolar epithelial cells (AEC), imbalanced immune response and abnormal wound repair are the key mediators of IPF pathogenesis where inflammation may not be an initiating trigger (Selman et al., 2001, Kaminski et al., 2003, Strieter, 2005). After injury, the restoration of alveolar integrity and functionality through rapid re-epithelialisation of the denuded alveolar basement membrane through AEC migration, proliferation and differentiation is essential. In IPF this healing process seems to be impaired (Selman et al., 2001); whilst the precise mechanism for this remains uncertain, it is likely to involve multifactorial interactive processes of repeated injury and substantial type I AEC loss (Corrin et al., 1985, Selman et al., 2001), increased AEC apoptosis (Uhal et al., 1998, Kuwano et al., 1999, Barbas-Filho et al., 2001), dysregulated epithelial-mesenchymal cross-talk (Selman & Pardo, 2002), polarised immune response (Strieter, 2005) and alveolar bronchiolisation (Chilosi et al., 2002, Odajima et al., 2007).

Alveolar bronchiolisation, a process of abnormal proliferation and alveolar migration of Clara and other bronchiolar epithelial cells, has been documented in both IPF lung tissues and animal models of pulmonary fibrosis (Odajima et al., 2007, Chilosi et al., 2002, Kawanami et al., 1982, Mori et al., 2004, Betsuyaku et al., 2000, Kawamoto & Fukuda, 1990, Fukuda et al., 1989, Collins et al., 1982). A sub-population of these Clara cells behaves as functional bronchiolar progenitor cells with participation in bronchiolar wound repair and regeneration (Evans et al., 1976, Reynolds & Malkinson, 2010). However,

lineage tracking in animal model studies has indicated that Clara cells may not take part in alveolar injury repair (Rawlins et al., 2009). Also, in bleomycin-induced murine pulmonary fibrosis, abrogation of alveolar bronchiolisation does not worsen the disease state (Betsuyaku et al., 2000). Despite these findings, alveolar bronchiolisation remains a constant histological feature in IPF lungs accompanied by failed alveolar architecture and functionality restoration (Odajima et al., 2007, Chilosi et al., 2002, Mori et al., 2004). I hypothesise that with the onset of IPF, the activated migration of Clara cells towards the alveolar regions and their interaction with *in situ* AEC is pivotal to the consequent aberrant repair response and ensuing fibrotic tissue remodelling. Elucidation of this key Clara cell-AEC interaction could unravel exploitable targets for pharmacological manipulation beneficial to IPF, a disease for which there is still no efficacious treatment.

3.1.1. Aim of this study

The aim of this study was to evaluate the role of Clara cells in the aberrant alveolar epithelial wound repair in the pathogenesis of IPF, particularly, during alveolar bronchiolisation process.

3.2. Study design

Before approaching to the major experimentation, the growth and wound repair rates of human type II AEC cell line A549 cells and human Clara cell line H441 cells were evaluated (Section- 2.6, Section- 2.7.3) (See Chart 3.1). Next, the paracrine role of Clara cells on alveolar A549 cell wound repair was evaluated by testing conditioned media (CM) obtained from wounded and unwounded H441 cells and tested on alveolar A549 cell wound repair system (Section- 2.7.1, Section- 2.7.3). An indirect-contact co-culture wound repair system was developed to investigate the cross-talk between Clara cells and alveolar A549 cells during A549 cell wound repair (Section- 2.7.2, Section- 2.7.8.1). To explore the direct-contact effects of Clara cells on AEC wound repair, a novel A549-H441 direct-contact co-culture wound repair system was developed (Section- 2.7.2). Using this direct-contact model the migratory aspect of Clara cells towards alveolar A549 cell wounds was investigated (Section- 2.7.8.1). The direct-contact effect of Clara cells on alveolar A549 cell wound repair was assessed by measurement of wound repair rate and TUNEL apoptosis assay (Section- 2.7.8.1, Section- 2.10.2). The Clara cell direct-contact effect on human primary small airway epithelial cells (SAEC) was also evaluated using the similar SAEC-H441 direct-contact wound repair model (Section- 2.7.8.1). Apoptosis pathway was determined by using Fas and TRAIL-receptor blocking antagonistic monoclonal antibodies (Section- 2.10.1, Section- 2.10.2). The *in vitro* finding was translated on human IPF lung tissue through determination of Clara cell localisation by immunohistochemistry with CC10 antibody and AEC apoptosis by TUNEL assay (Section- 2.12.6, Section- 2.10.3). The experimental data was analysed using the Excel programme of Microsoft Office XP. The statistical analysis was performed using the software GraphPad Prism version 5.00 (Section- 2.14). A conclusion was drawn according to the outcome of the experimental results (See Chart 3.1).

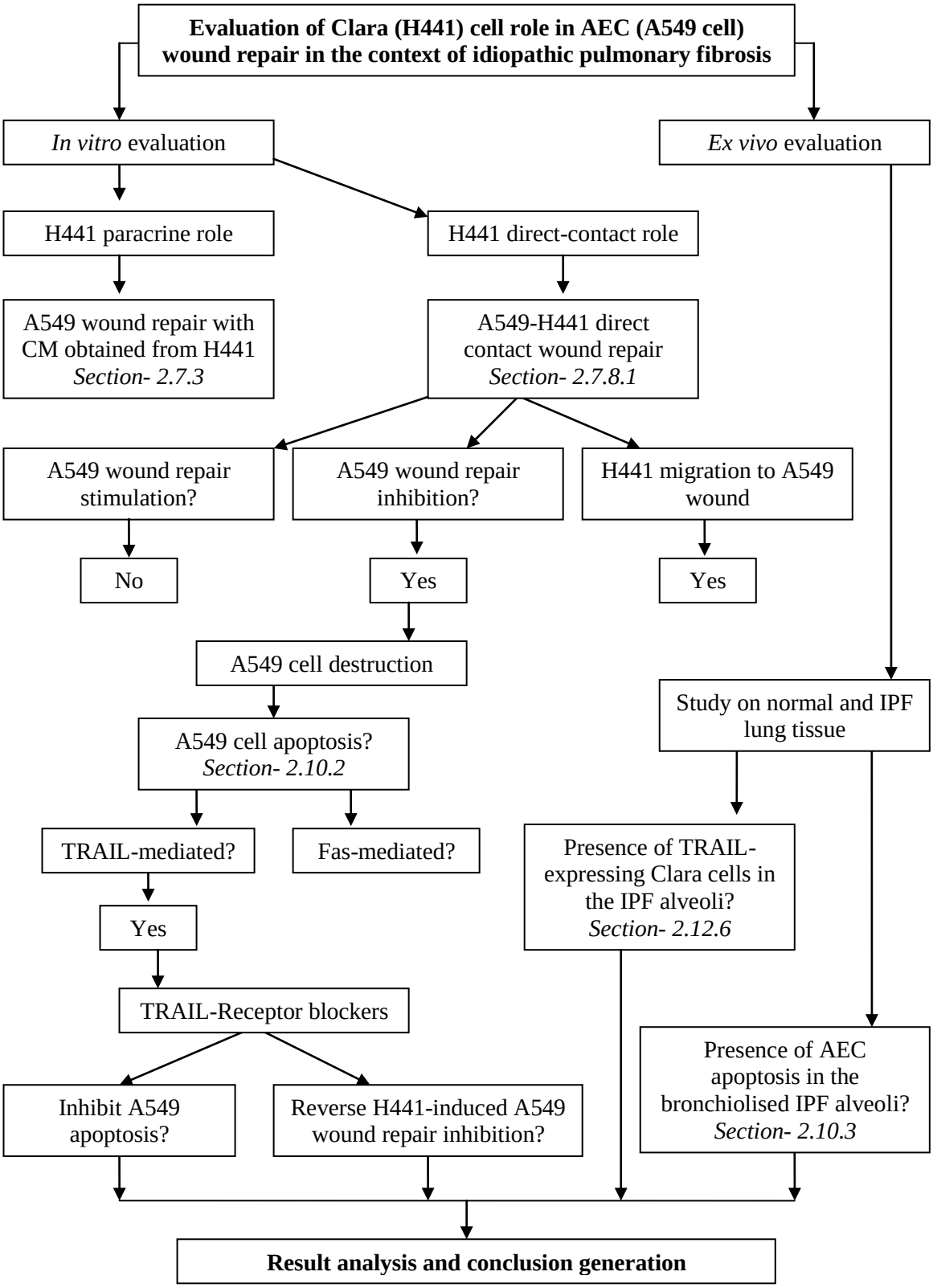

Chart 3.1: Major study plan steps. A detailed description is provided in the methodology section.

3.3. Results

3.3.1. Determination of initial cell seeding density to form monolayer

For the *in vitro* wound repair assay, the formation of a uniform epithelial cell monolayer is a key prerequisite. Prior to approaching the major experiments designed to test my hypothesis, I performed a set of feasibility tests on my selected cohort of human lung epithelial cells (Table 2.1) to establish whether they were capable of forming monolayer in my *in vitro* wound repair and culture system (Section 2.3). I also determined the cell seeding density of those cells for various well-plates (Section 2.3). The human type II AEC line, A549 cells and human Clara cell line, H441 cells formed confluent monolayers on well-plates (Figure 3.1A, 3.1B). In addition, human primary small airway epithelial cells (SAEC) also formed uniform monolayers on well-plates (Passage 3-4) (Figure 3.1C). However, despite multiple approaches and attempts the human primary AEC (pAEpiC) obtained from ScienceCell Research Laboratory, USA failed to form monolayers and did not provide evidence of an epithelial morphology in the recommended culture condition (Figure 3.1D). Therefore, pAEpiC were considered as 'unsuitable' for my *in vitro* wound repair experiments and discontinued from further experimentation. Alveolar A549 cells formed uniform monolayers in 24 hours on 24-well plate, 48-well plate and 96-well plate with initial cell seeding densities at 1.5 x 10^5, 10^5 and 5 x 10^4 cells/well respectively (Section- 2.3). 3 x 10^5 H441 cells formed monolayers on 24-well plate in 24 hours. SAEC (P-3 to P-4) formed monolayers on 48-well plate and 96-well plate in 48 hours when initial cell seeding densities were 5 x 10^4 and 2 x 10^4 cell/well respectively (Section-2.3).

3.3.2. Alveolar A549 cells express *pro*SP-C

SP-C is the definitive antigenic marker for type II AEC (Zhou et al., 1996). In my culture conditions, alveolar A549 cells expressed *pro*SP-C protein as detected through

immunocytochemistry (Section-2.12.1). The SAEC, which are by origin small airway epithelial cells, did not express *pro*SP-C (Figure 3.2).

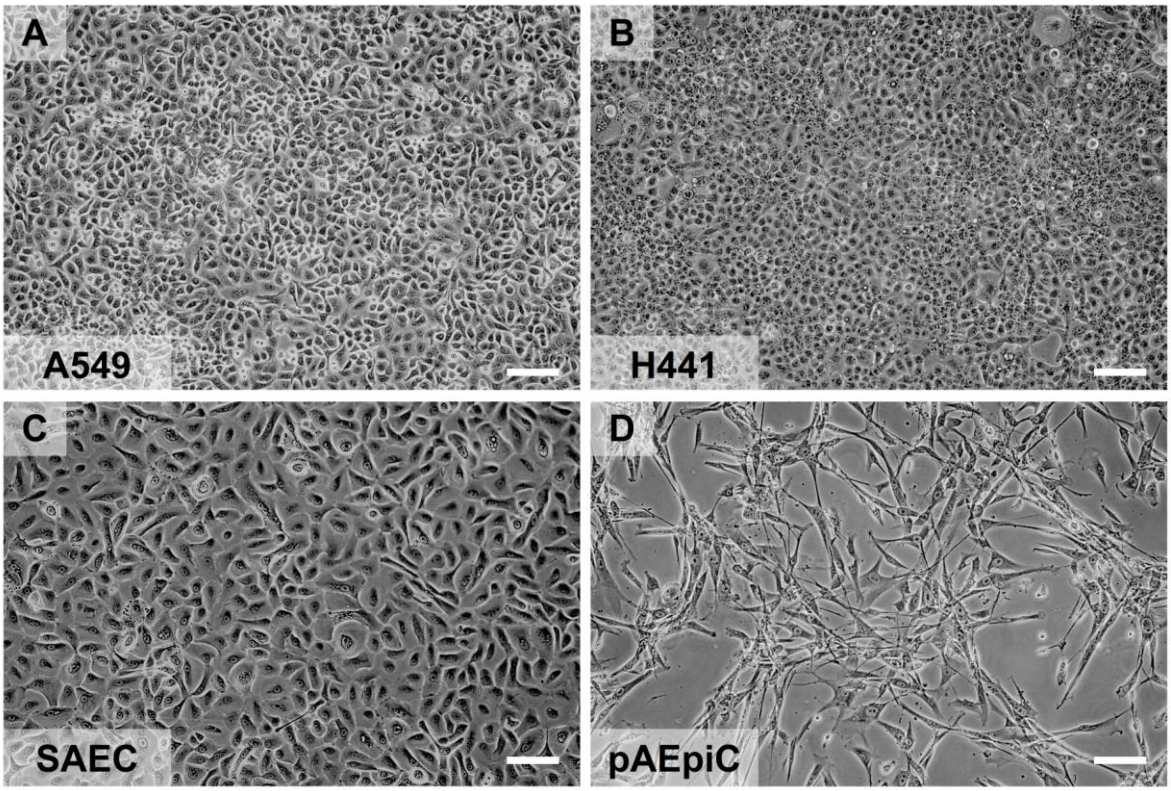

Figure 3.1: Formation of monolayers *in vitro* with human lung epithelial cells.

Inverted light microscopic images show A549 cells (**A**), H441 cells (**B**) and SAEC (**C**) formed uniform monolayers on well-plates. (**D**) pAEpiC did not form perfect monolayers. Image magnification 100X for all cell types. Scale bar, 100 µm.

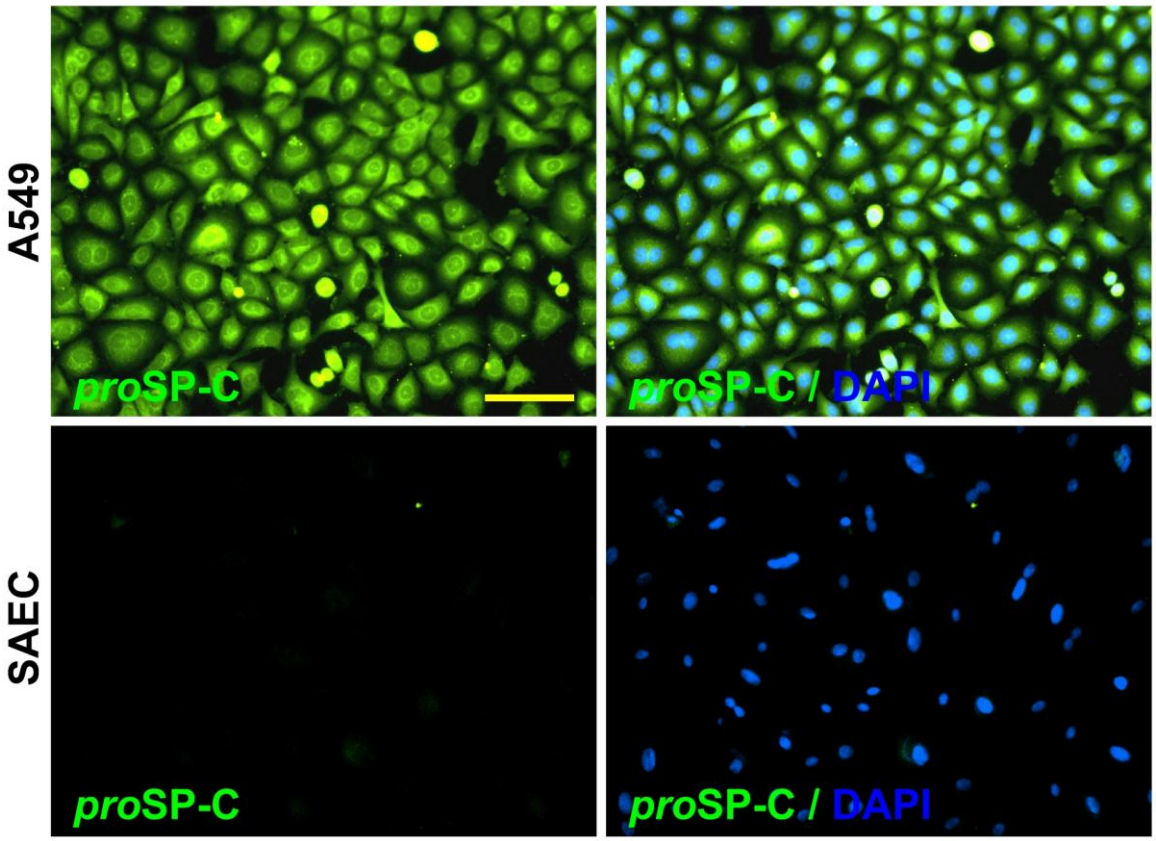

Figure 3.2: *pro*SP-C expression profile in A549 and SAEC.

Immunocytochemistry with anti-*pro*SP-C antibody on A549 cells and SAEC. Nuclear staining was done with DAPI. Image magnification 200X. Scale bar, 100 µm.

3.3.3. H441 (Clara) cells do not stimulate alveolar A549 cell wound repair through paracrine factors

To establish evidence of cross-talk between secretory products of alveolar and bronchiolar cells, I first investigated the wound repair patterns of A549 and H441 cells using an *in vitro* wound repair model (Kheradmand et al., 1994, Atabai et al., 2002, Galiacy et al., 2003, Chen et al., 2008b, Savla & Waters, 1998, Geiser et al., 2000, Geiser et al., 2004, Sonar et al., 2010, Curley et al., 2012) (Section-2.7, Section- 2.7.1, Section- 2.7.3). The H441 cells are slow-growing in comparison to A549 cells in both serum-free (SF) and 10% serum supplemented DMEM (Figure 3.3A, 3.3B) (Section- 2.6). The calculated doubling times of alveolar A549 and H441 cells in SF media were 22 ± 4.97 hours and 100 ± 9.83

hours, respectively, and in 10% FBS supplemented media 18 ± 1.71 hours and 50 ± 8.66 hours, respectively (Figure 3.3C) (Section- 2.6).

In spite of this difference, in the presence of 10% serum, no significant differences in the wound repair patterns of A549 and H441 cells were observed (Figure 3.4A, 3.4B). However, in SF media, the rate of H441 cell wound repair was 2.5-fold higher than that seen for A549 cells (65 ± 11.32% H441 vs. 26 ± 2.65% A549; $p<0.001$) (Figure 3.4A, 3.4B) (Section- 2.7.3).

Next, I tested SF-CM (serum-free conditioned media) obtained from wounded and un-wounded H441 and A549 cell monolayers on A549 cell wound repair (Section- 2.4.1, Section- 2.7.3). SF-CM from both wounded and unwounded H441 cells did not affect A549 cell wound repair (32 ± 2.52% wounded SF-CM vs. 38 ± 9.02% SF-Negative control, 44 ± 3.06% un-wounded SF-CM vs. 38 ± 9.02% SF-Negative control respectively) (Figure 3.5A, 3.5C). Likewise, SF-CM from alveolar A549 cells, irrespective of wounding, did not stimulate any effects on A549 cell wound repair after 24 hours of wounding (Figure 3.5B).

On the other hand, SF-CM of unwounded A549 cells inhibited H441 cell wound repair after 24 hours; whereas, SF-CM of wounded A549 cells did not (47 ± 2.65% unwounded SF-CM vs. 65 ± 7.37% Negative control, $p<0.05$) (Figure 3.6). Taken together, this indicates that Clara cells (H441 cells) can auto-stimulate wound repair in serum-free conditions but not stimulate repair of AEC wounds. In addition, uninjured A549 cells have a negative effect on Clara cell (H441 cells) wound repair *in vitro*.

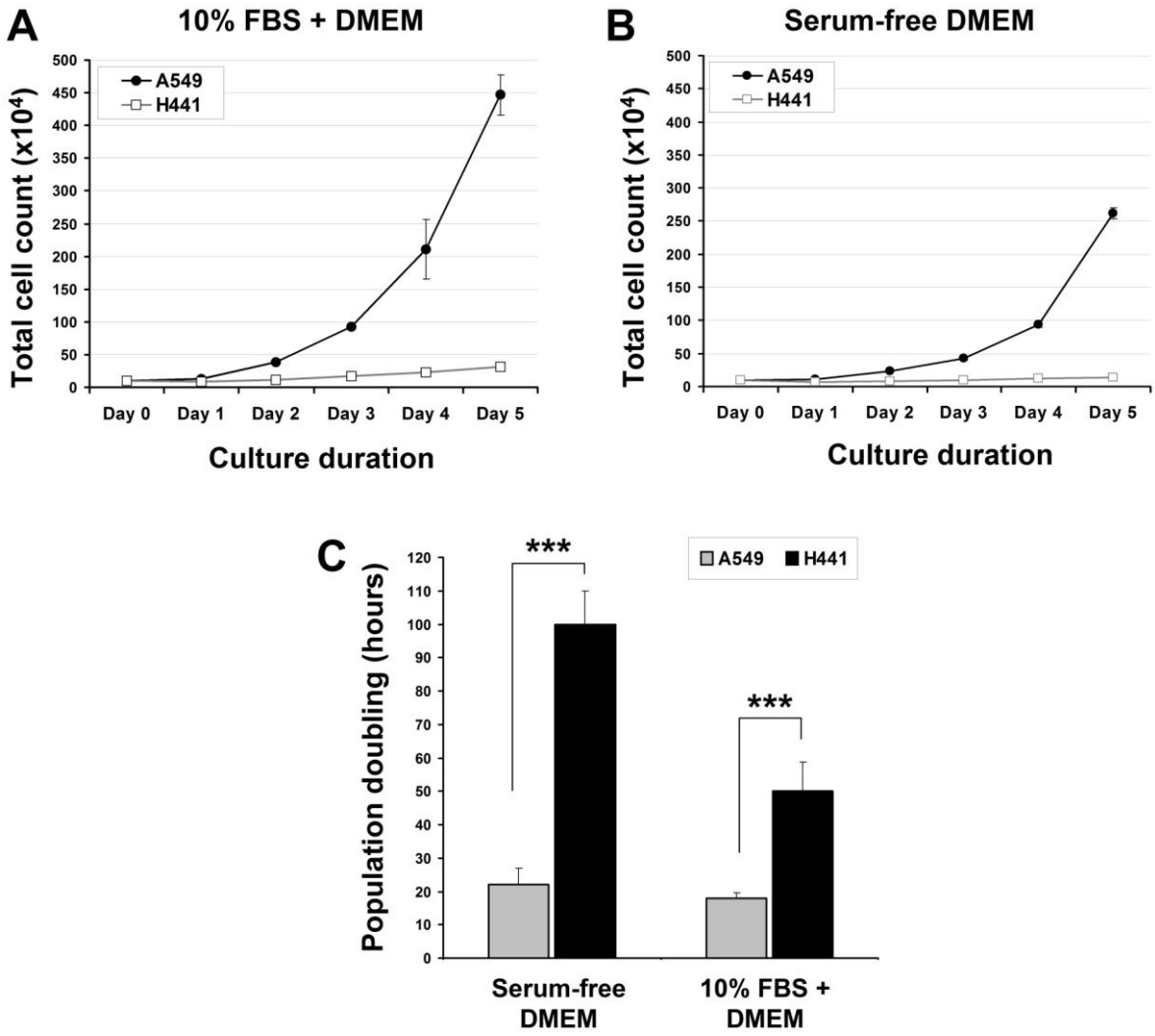

Figure 3.3: A549 and H441 cell growth and population doubling time.

(**A**) A549 and H441 cell growth in 10% FBS serum supplemented complete DMEM culture media. (**B**) A549 and H441 cell growth in serum-free DMEM. (**C**) Population doubling time (PD) of A549 and H441 cell lines in serum-free and 10% FBS supplemented DMEM. n = 3 independent experiments. Data presented as mean ± SD. ***$p<0.001$.

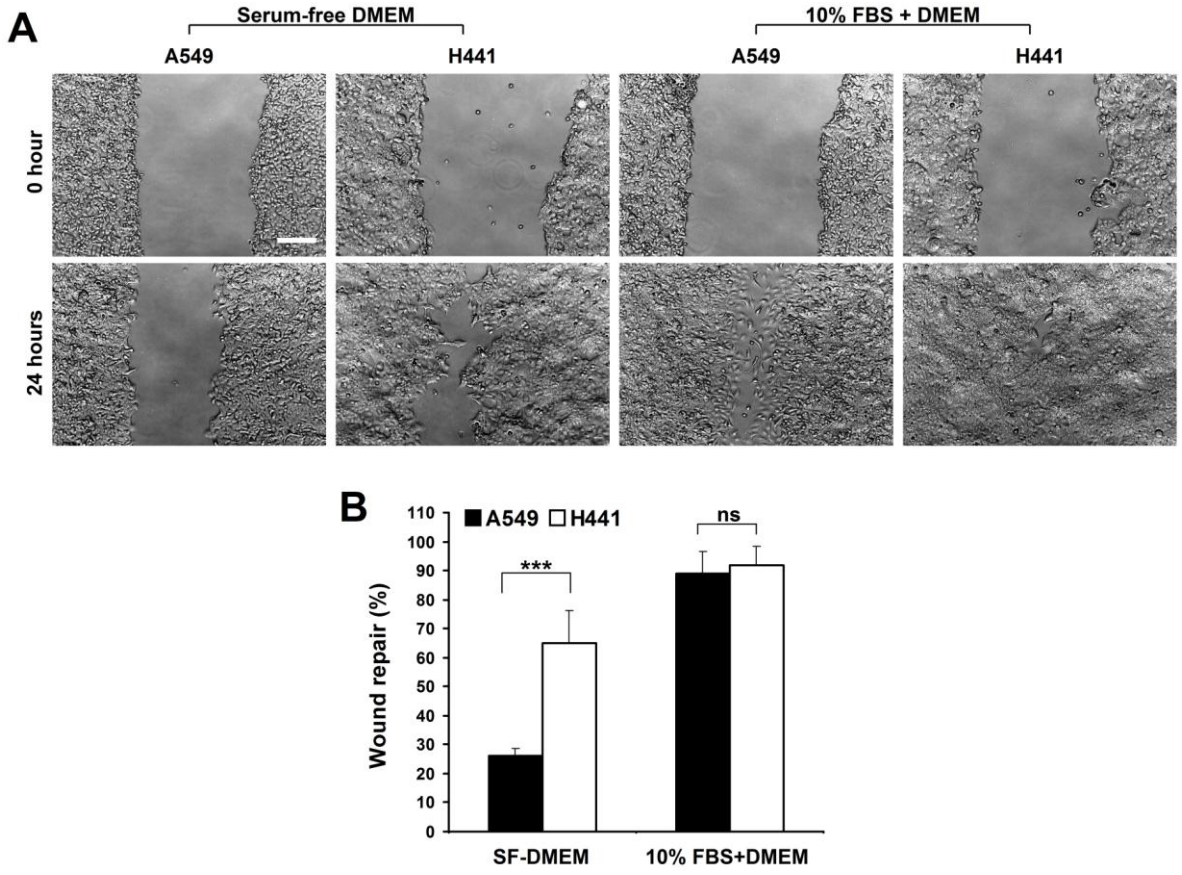

Figure 3.4: A549 and H441 cell *in vitro* wound repair.

(**A**) Inverted light microscopic images of A549 and H441 cell wound repair with SF-DMEM and 10% FBS supplemented DMEM at 0 and after 24 hours. (100X magnification). (**B**) Wound repair of alveolar A549 cells and H441 cells in serum-free and 10% FBS supplemented media after 24 hours. (n = 4 independent experiments, ≥5 replicates per n). Data presented as mean ± SD. ***p<0.001, ns = not significant. Scale bar, 200 µm.

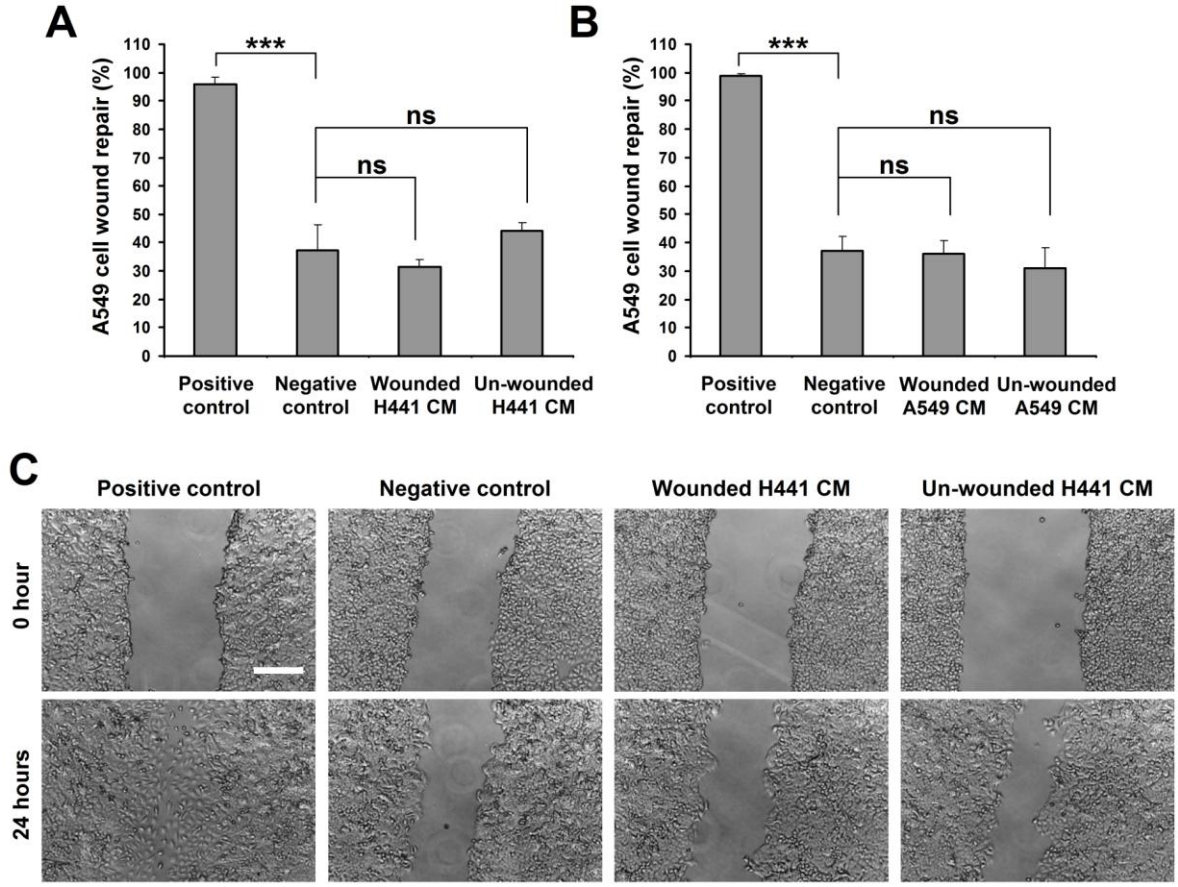

Figure 3.5: A549 cell *in vitro* wound repair with H441 and A549 CM.

(**A**) A549 cell wound repair after 24 hours with serum-free CM of wounded and un-wounded H441 cells. (n = 3 independent experiments, 4 replicates per n). (**B**) A549 cell wound repair after 24 hours with serum-free CM of wounded and un-wounded A549 cell (n = 3 independent experiments, 3 replicates per n). (**C**) Inverted light microscopic images of A549 cell wound repair. Positive and negative controls represent wound repair with 10% FBS supplemented and serum-free media respectively. Data presented as mean ± SD. ***p<0.001, ns = not significant. Scale bar, 200 µm.

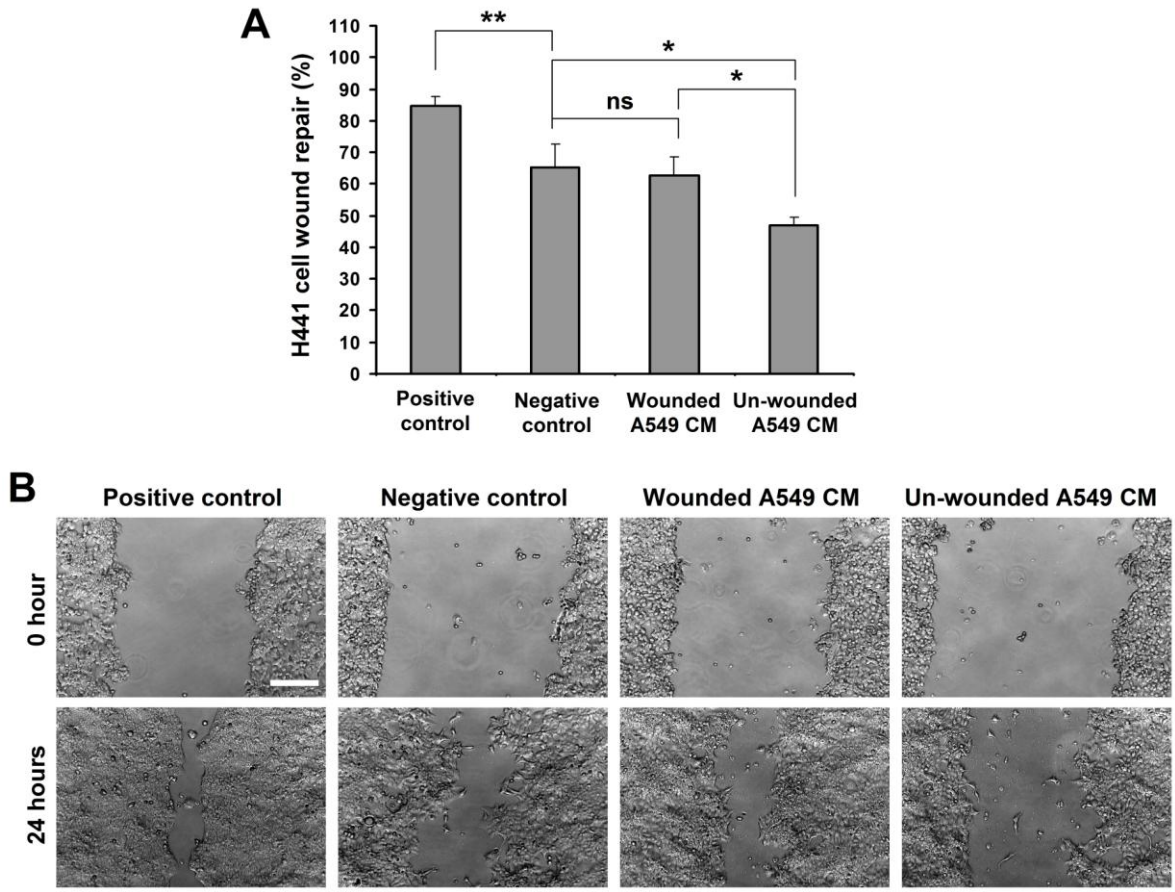

Figure 3.6: H441 cell wound repair.

(**A**) H441 cell wound repair after 24 hours with SF-CM obtained from wounded and un-wounded A549 cell monolayers (n = 3 independent experiments, 3 replicates per n). Positive and negative controls represent wound repair with 10% FBS supplemented and serum-free media respectively. (**B**) Inverted light microscopic images of H441 cell wound repair. Data presented as mean ± SD. **p<0.01. Scale bar, 200 μm.

3.3.4. H441 cells inhibit alveolar A549 cell wound repair in A549-H441 cell co-culture wound repair system

To further explore the role of H441 cells in alveolar A549 cell wound repair, I developed a direct and indirect-contact co-culture wound repair system (Figure 3.7) (Section- 2.7.2, Section- 2.7.8.1). Direct and indirect-contact co-culture of H441 cells with wounded A549 monolayers significantly reduced A549 cell wound repair rates after 24 hours (11 ± 5.89% Direct-contact vs. 36 ± 8.96% Negative control, $p<0.01$, and 20 ± 5.38% Indirect-contact vs. 36 ± 8.96% Negative control, $p<0.05$) (Figure 3.8A, 3.8D, 3.8E).

Coupled to the reduction of repair rate in A549 cell wounds, I also observed substantial H441 cell migration into the wounded A549 cell monolayers, where a 4.25-fold greater number of migrated H441 cells were located at the juxta-wound monolayer sites in comparison to the wound gap itself (234 ± 39.13 cells/field juxta-wound monolayers vs. 55 ± 27.34 cells/field wound-gaps, $p<0.001$) (Figure 3.8B, 3.8E). Coupled to this migration, a 55% reduction of A549 cells at the juxta-wound monolayers was also noted after 24 hours of wounding (700 ± 61.10 A549 cells at 0 hr. vs. 318 ± 40.54 A549 cells at 24 hrs., $p<9x10^{-4}$) (Figure 3.8C, 3.8E). H441 cells did not migrate into the uninjured AEC monolayer in a similar direct-contact co-culture experiment (Figure 3.9A, 3.9B, 3.9C); and in the absence of A549 cells, H441 cell migration after 24 hours was negligible (Figure 3.9D, 3.9E).

In contrast, normal human lung fibroblasts CCD-8Lu cells did not inhibit A549 cell wound repair in A549-CCD 8Lu direct and indirect-contact co-culture (30 ± 3.49% Direct-contact, 29 ± 3.23% In-direct-contact and 37 ± 15.97% Negative control) (Figure 3.10A, 3.10B) (Section- 2.7.8.1). Moreover, CCD-8Lu cell migration to the A549 cell wound site in

direct-contact model was negligible (Figure 3.10B). No apparent reduction A549 cell numbers from the wound margins and 24 hours of direct-contact co-culture with CCD-8Lu was noted (Figure 3.10B). Taken together, these results suggest that H441 (Clara) cells but not normal lung fibroblasts inhibit alveolar A549 cell wound repair in a proximity dependent manner, where at least for the direct-contact model, wound repair inhibition was due to direct interruption and destruction of AEC population.

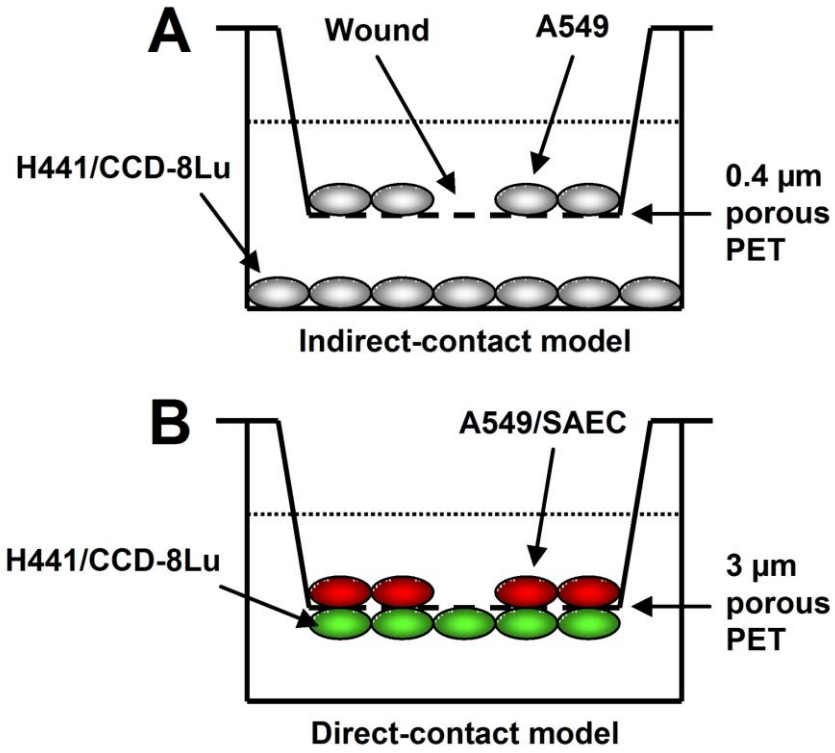

Figure 3.7: *In vitro* direct and indirect-contact co-culture wound repair system.
(**A**) Indirect-contact co-culture wound repair model: wounded A549 cells on 0.4 µm porous PET membrane of transwell (upper layer) with H441 or CCD-8Lu cells (bottom layer); the gap between these two cell layers was 0.8 mm. (**B**) Direct-contact co-culture wound repair model: DiI-labelled wounded A549 cells or SAEC (upper layer) with un-wounded DiO-labelled H441 or CCD-8Lu cells (bottom layer) grown on 3 µm porous transwell PET membrane. After wounding the direct and indirect-contact samples were cultured in serum-free basal media for 24 hours.

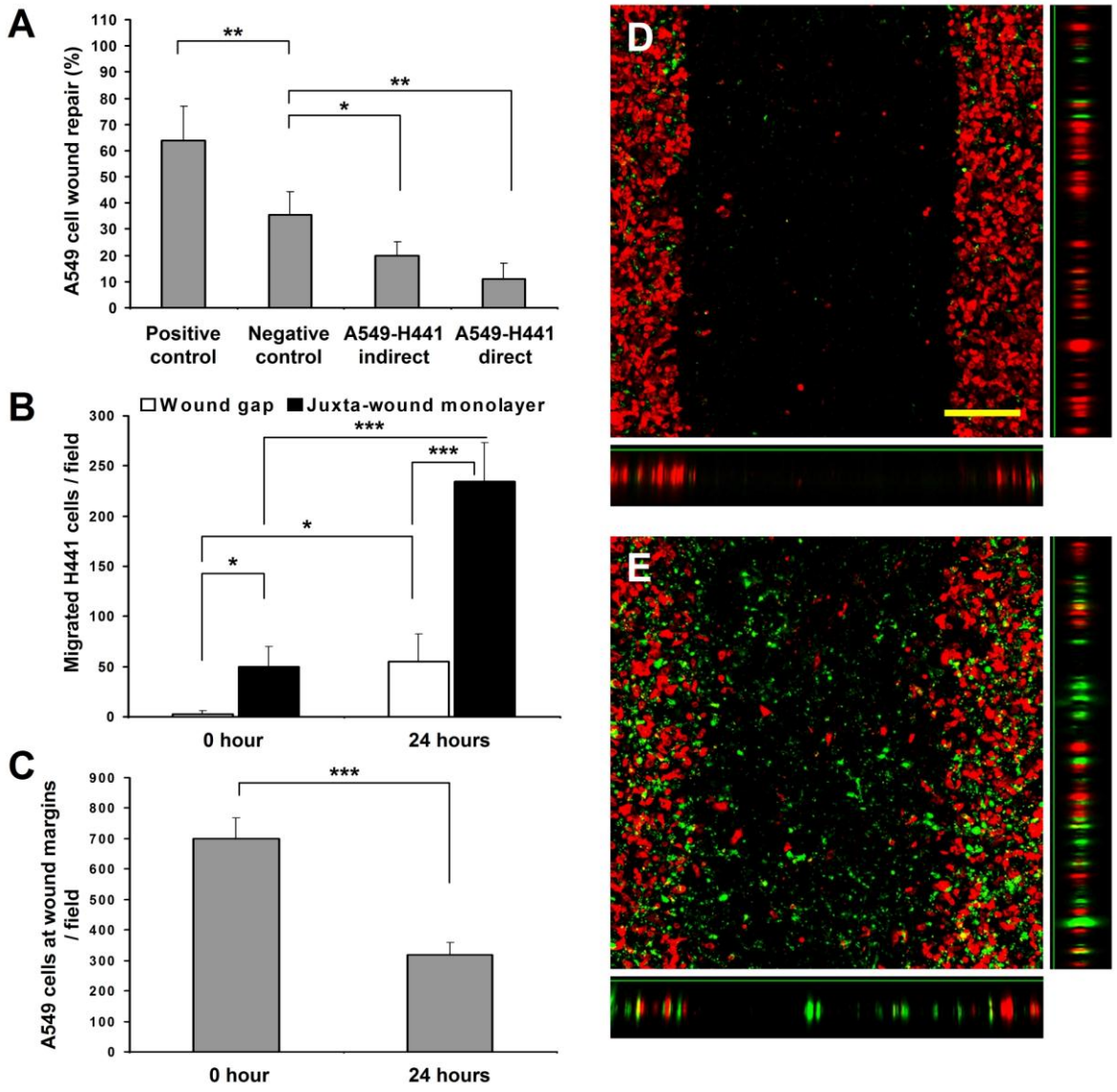

Figure 3.8: A549-H441 direct and indirect-contact co-culture wound repair.

(**A**) A549 cell wound repair after 24 hours in direct and indirect-contact co-culture with H441 cells. Positive and negative control represent the wound repair with 10% FBS supplemented and serum-free media respectively (n = 4 independent experiments, 3 replicates per n). (**B**) Migration of H441 cells into the A549 juxta-wound monolayers and wound gaps (n = 5 independent experiments). (**C**) Number of A549 cells per field at the juxta-wound monolayers in direct-contact co-culture with H441 cells after 24 hours (n = 5 independent experiments). (**D, E**) Laser scanning confocal microscopic images (100X) of A549-H441 direct-contact co-culture at 0 and 24 hours respectively. DiI-labelled red cells are A549 and DiO-labelled green cells are H441 cell. Vertical side bars represent Z-slicing through the corresponding juxta-wound monolayers whereas horizontal bars represent Z-slicing through wound gaps. A significant proportion of migrated H441 cells were noted at the juxta-wound monolayers of A549 cells after 24 hours of wounding (E). *$p<0.05$, **$p<0.01$, ***$p<0.001$. Data presented as mean ± SD. Scale bar, 150 µm.

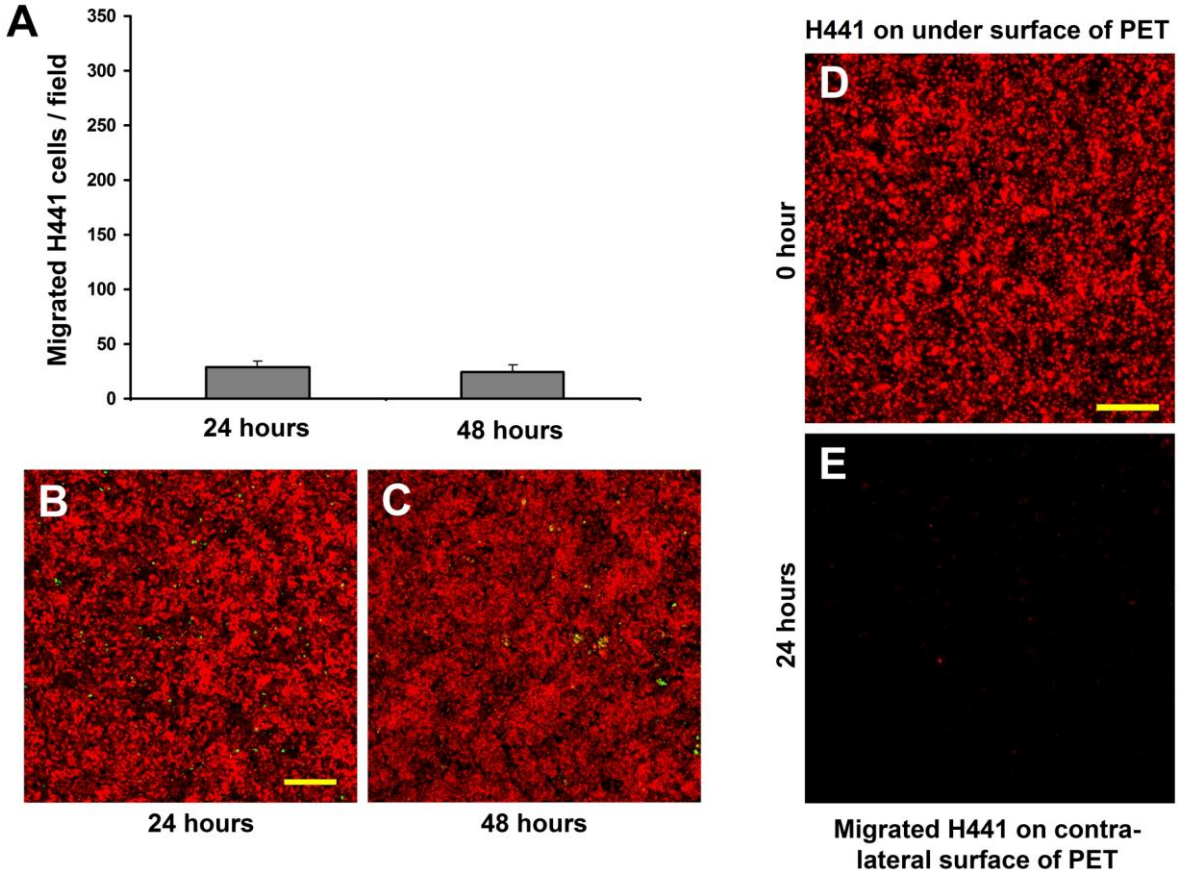

Figure 3.9: H441 cell migration in absence of wound in A549 cells in the A549-H441 direct contact model.

(**A**) Number of migrated H441 cells at unwounded A549 cell layer at 24 hours (equivalent duration of 0 hour wound) and 48 hours (equivalent duration of 24 hours wound) of A549-H441 direct-contact co-culture (n = 3 independent experiments). (**B, C**) Laser scanning confocal microscopic images show migrated DiO-labelled H441 cells (Green) at DiI-labelled A549 cell layer (Red) at 24 (B) and 48 (C) hours of A549-H441 direct-contact co-culture. (**D, E**) Migration of H441 cells to the contra-lateral surface of transwell PET membrane in absence of A549 cells. Laser scanning confocal microscopic images show DiI-labelled H441 cells (Red) on the under-surface of PET membrane at 0 hours (**D**) and on the contra-lateral surface of PET membrane after 24 hours of culture (**E**). Data presented as mean ± SD. Scale bar, 200 µm.

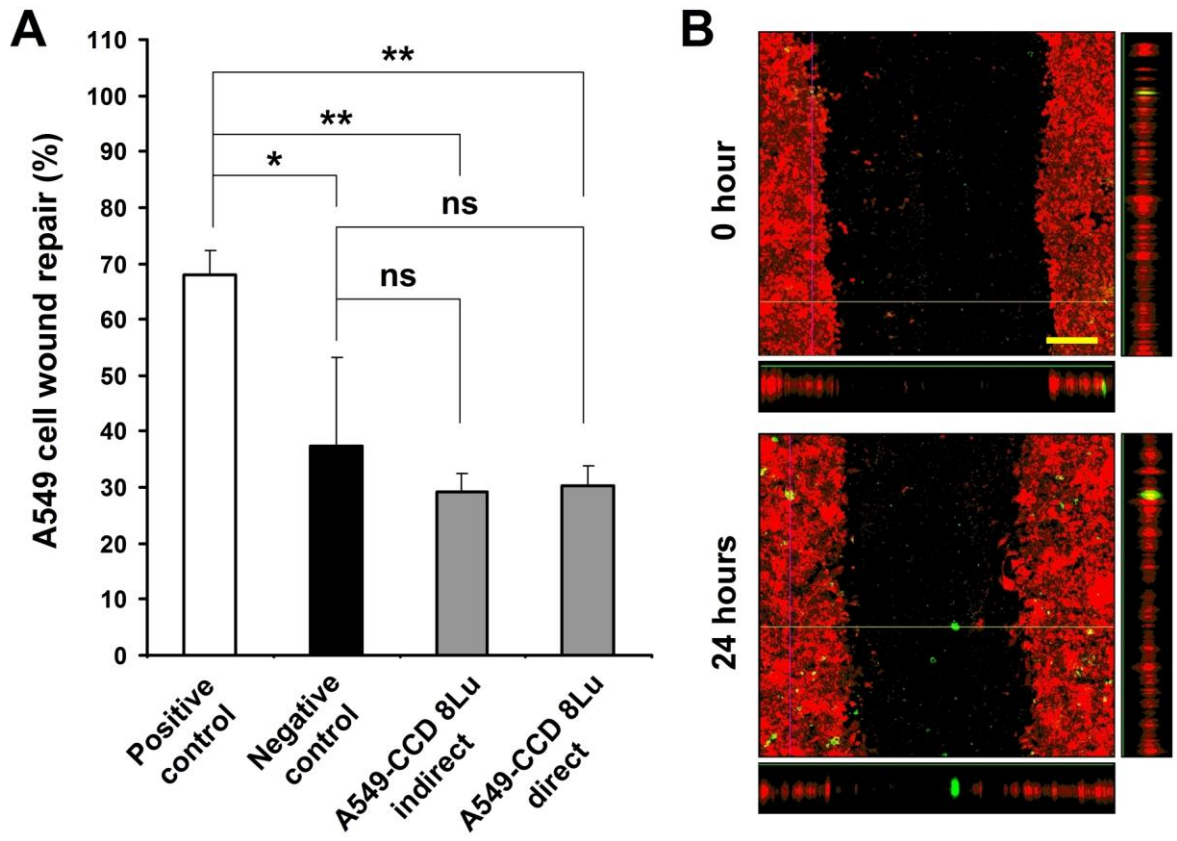

Figure 3.10: A549-CCD 8Lu cell direct and indirect-contact co-culture wound repair.

(**A**) A549 cell wound repair after 24 hours in direct and indirect-contact co-culture with CCD-8Lu cells. Positive and negative control represent the A549 cell wound repair with 10% FBS supplemented and serum-free media respectively in monoculture (n = 3 independent experiments). (**B**) Laser scanning confocal microscopic images (100X) of A549-CCD 8Lu direct-contact co-culture at 0 and 24 hours. DiI-labelled red cells are A549 cells and DiO-labelled green cells are migrated CCD-8Lu cells. Vertical side bars represent Z-slicing through the juxta-wound monolayers and horizontal bars represent Z-slicing through wound gaps. A negligible number of CCD-8Lu cells migrated to the A549 wound sites after 24 hours of wounding (B). *$p<0.05$, **$p<0.01$, ns = not significant. Data presented as mean ± SD. Scale bar, 150 µm.

3.3.5. Soluble TRAIL and FasL induce apoptosis in A549 cells

I hypothesized that the reduction in A549 cell numbers at juxta-wound sites in A549-H441 direct-contact co-culture could be due to H441-induced apoptosis. To test this hypothesis, I first examined the sensitivity of A549 cells to established apoptosis-inducing ligands; TRAIL and FasL (Pan et al., 1997, Walczak et al., 1997, Sheridan et al., 1997, Griffith et al., 1995) (Section- 2.10.1). Significant apoptosis was induced in A549 cell monolayers with either soluble TRAIL or FasL at 800 ng/ml or 3.2 µg/ml, respectively (57 ± 2.17% apoptosis with TRAIL 800ng/ml, 21 ± 6.19% apoptosis with FasL 3.2 µg/ml, 2 ± 0.83% apoptosis with SF-DMEM (0 ng/ml); $p<0.001$ vs SF-DMEM) (Figure 3.11A, 3.11B). 100% of apoptosis was observed in A549 cells (Positive control) following 24 hours of H_2O_2 treatment (Figure 3.11B).

The specificity of TRAIL and FasL-induced apoptosis was established by blocking the apoptotic response using their corresponding receptor blockers anti-TRAIL-R1, -R2 and anti-Fas antagonistic mAbs (Section- 2.10.1). A549 cell pretreatment with 10µg/ml anti-TRAIL-R1 and/or anti-TRAIL-R2 antagonistic mAbs significantly blocked TRAIL (800 ng/ml)- induced apoptosis (6 ± 1.03% anti-TRAIL-R1 mAb, 2 ± 0.89% anti-TRAIL-R2 mAb, 3 ± 1.10% TRAIL-R1+R2 mAbs; $p<0.001$ vs TRAIL-induced apoptosis) (Figure 3.12A, 3.12C). FasL-induced apoptosis specificity was demonstrated via the use of 10 µg/ml anti-Fas antagonistic mAb (2 ± 0.49% anti-Fas mAb, $p<0.001$ vs FasL-induced apoptosis) (Figure 3.12B, 3.12D). This indicated the presence of functional Fas and TRAIL receptors on alveolar A549 cells.

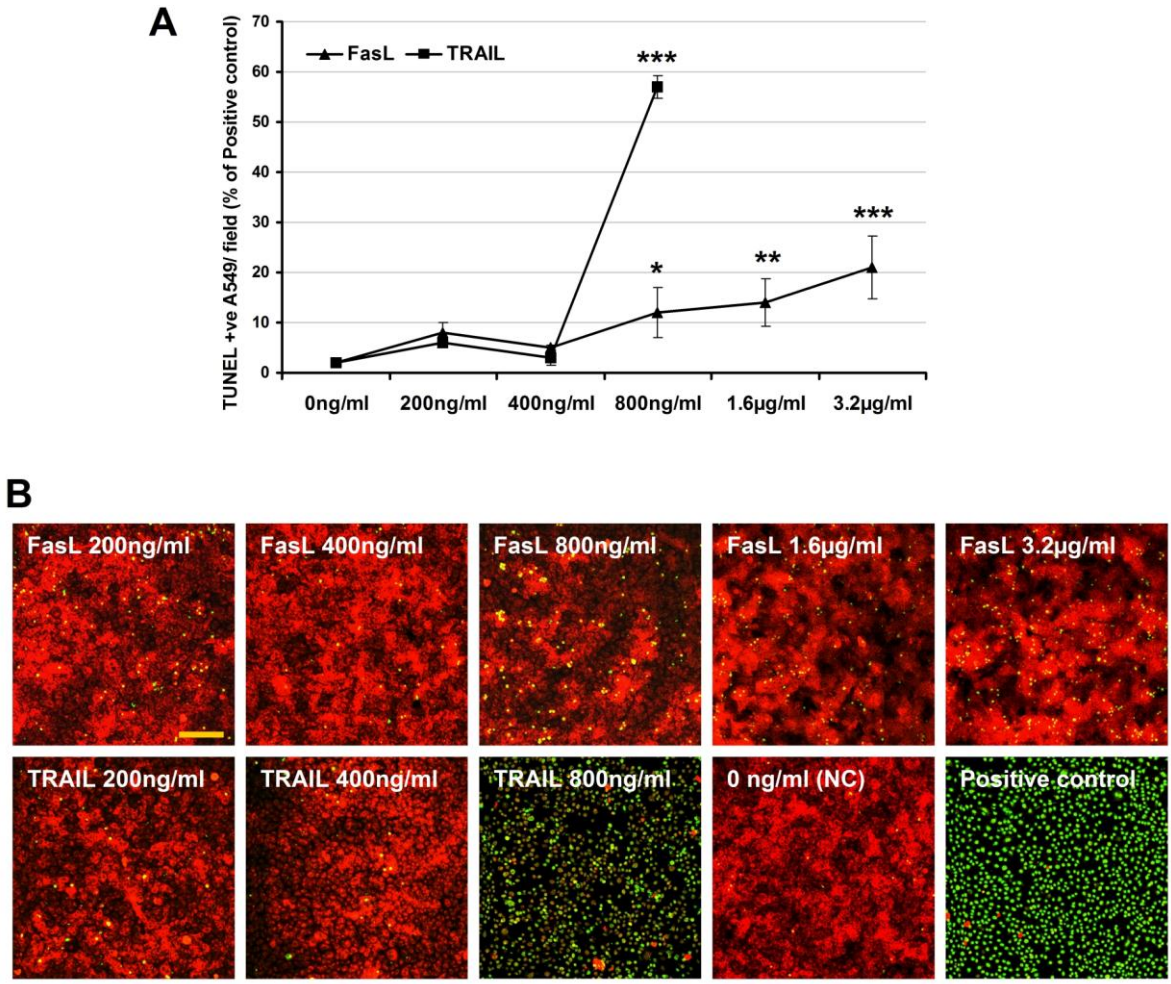

Figure 3.11: Assessment of apoptosis in alveolar A549 cell monolayers.

(**A**) Dose response of apoptosis induction in A549 cells with soluble FasL and TRAIL (n = 3 independent experiments). Results were standardised against positive control where apoptosis was induced in A549 cells with treatment of 200 µM H_2O_2 for 24 hours. (**B**) Laser scanning confocal microscopic images of FasL and TRAIL induced apoptosis in DiI-labelled A549 cells (red) after 24 hours. Green nuclei are TUNEL positive nuclei. *p<0.05, **p<0.01, ***p<0.001 vs 0 ng/ml (negative control, NC). Data plots represent mean experiment values ± SD. Scale bar, 200 µm.

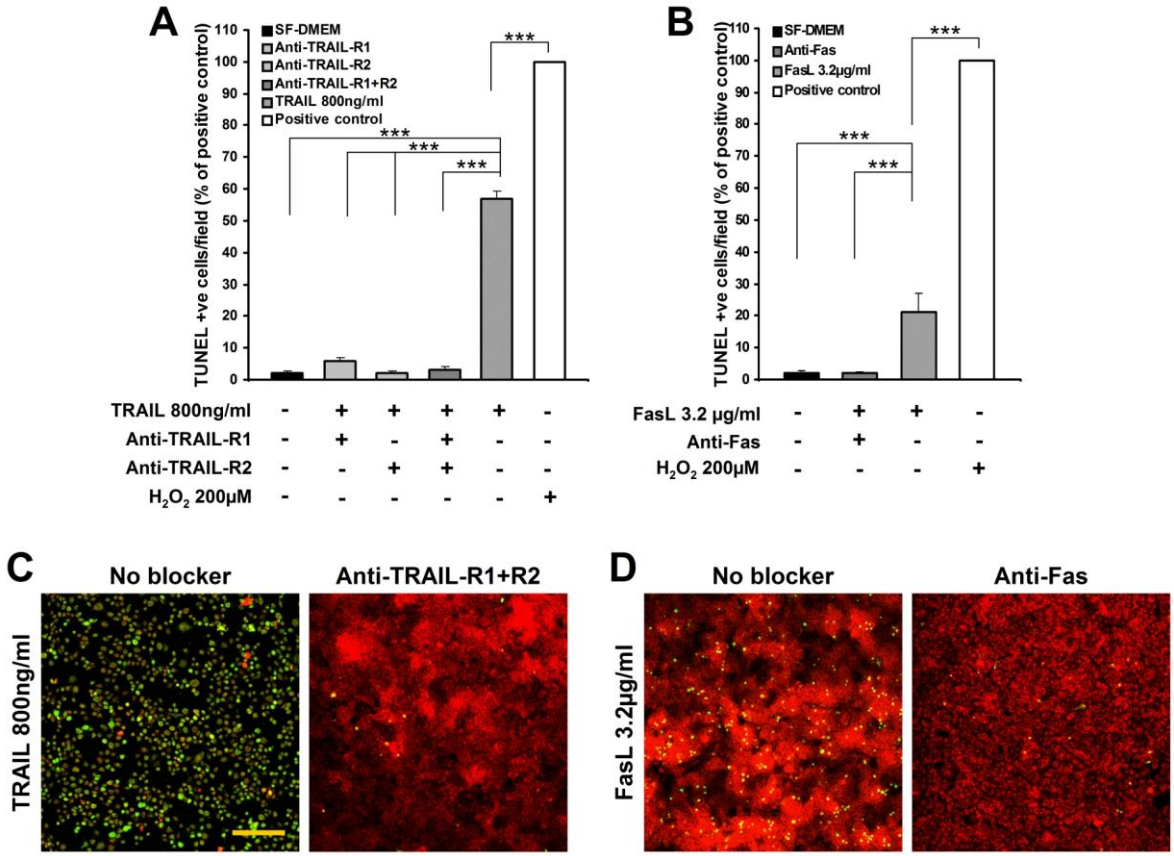

Figure 3.12: Blocking of ligand-induced apoptosis in A549 cell monolayers.

(**A**) Blocking of TRAIL-induced apoptosis in A549 cells by anti-TRAIL-R1 or anti-TRAIL-R2 or combined mAbs (10 µg/ml each) (n = 3 independent experiments). (**B**) Blocking of soluble FasL induced apoptosis in A549 cells with anti-Fas mAb (10 µg/ml) (n = 3 independent experiments). Positive controls represent apoptosis in A549 cells induced by 200 µM H_2O_2. (**C, D**) Laser scanning confocal microscopic images show TRAIL (C) and FasL (D) induced apoptosis in DiI-labelled A549 cells in presence or absence of their corresponding receptor blockers. Green nuclei are TUNEL positive nuclei. ***p<0.001. Data presented as mean ± SD. Scale bar, 200 µm.

3.3.6. Direct-contact of H441 cells induces apoptosis in A549 cells through TRAIL-dependent mechanism

To confirm my earlier hypothesis, I performed the TUNEL assay to evaluate apoptosis on alveolar A549 cell wounds in the direct-contact model with H441 cells (Section- 2.10.2). I observed a significant rate of apoptosis in A549 cells in the juxta-wound margins (52 ± 13.86% normalized to positive control vs. 1 ± 0.31% A549 monoculture, $p<0.001$) (Figure 3.13A). Migratory H441 cells did not stain positively for TUNEL and were therefore considered not to be apoptotic (Figure S3.1, Appendix-2). In a similar A549-CCD8 Lu direct-contact wound repair setting, CCD-8Lu cells did not induce apoptosis in A549 cells (Figure S3.2, Appendix-2).

Next, I investigated whether blocking of either TRAIL-receptors or Fas could block the H441 cell direct-contact induced apoptosis in A549 cells (Section-2.10.2). Pre-incubation of A549 cells with a blocking antibody specific to Fas (anti-Fas mAb, 10 µg/ml), prior to seeding into the direct-contact model with H441 cells, failed to block the apoptotic response in A549 cells (39 ± 3.14% Direct-contact vs. 31 ± 6.80% Direct-contact with anti-Fas mAb) (Figure 3.13B, 3.13D, 3.13F). However, pre-incubation of A549 cells with anti-TRAIL R1/R2 mAbs (10 µg/ml) completely blocked H441-induced apoptosis in the direct-contact model (39 ± 3.14% Direct-contact vs. 1 ± 0.54% Direct-contact with anti-TRAIL-R1/R2 mAbs, $p<0.001$) (Figure 3.13B, 3.13D, 3.13E).

I next sought to investigate whether the TRAIL receptor blocker could reverse the H441 cell direct-contact induced A549 cell wound repair inhibition. I observed that following addition of anti-TRAIL-R1/R2 mAbs (10 µg/ml) to the A549-H441 direct-contact wound repair system, the A549 cell wound repair was significantly improved after 24 hours over

untreated counterpart (32 ± 7.45% anti-TRAIL-R1/R2 mAbs treated vs. 8 ± 1.57% untreated sample; $p<0.05$) (Figure 3.14A, 3.14B). These results demonstrate that H441 cells induce apoptosis in wounded alveolar A549 cells and inhibit wound repair through a TRAIL-dependent mechanism in a direct-contact co-culture wound repair system.

3.3.7. TRAIL, TRAIL-R1 and –R2 expression profile in H441 and A549 cells

I evaluated the expression profile of TRAIL and its receptors TRAIL-R1 and TRAIL-R2 in A549 and H441 cells at transcriptional level by RT-PCR (Section- 2.11) and translation by immunocytochemistry (Section- 2.12.1). Transcriptional analysis confirmed TRAIL, TRAIL-R1 and TRAIL-R2 mRNA expression in both unwounded H441 and A549 cells where the band density for TRAIL was faint in the A549 sample in comparison to H441 (Figure 3.15A). Immunocytochemistry detected a higher level of TRAIL-R1 and –R2 expression in unwounded alveolar A549 cells than H441 cells. The TRAIL protein expression was high in unwounded H441 cells; whereas, TRAIL expression was barely detected in unwounded A549 cells (Figure 3.15B).

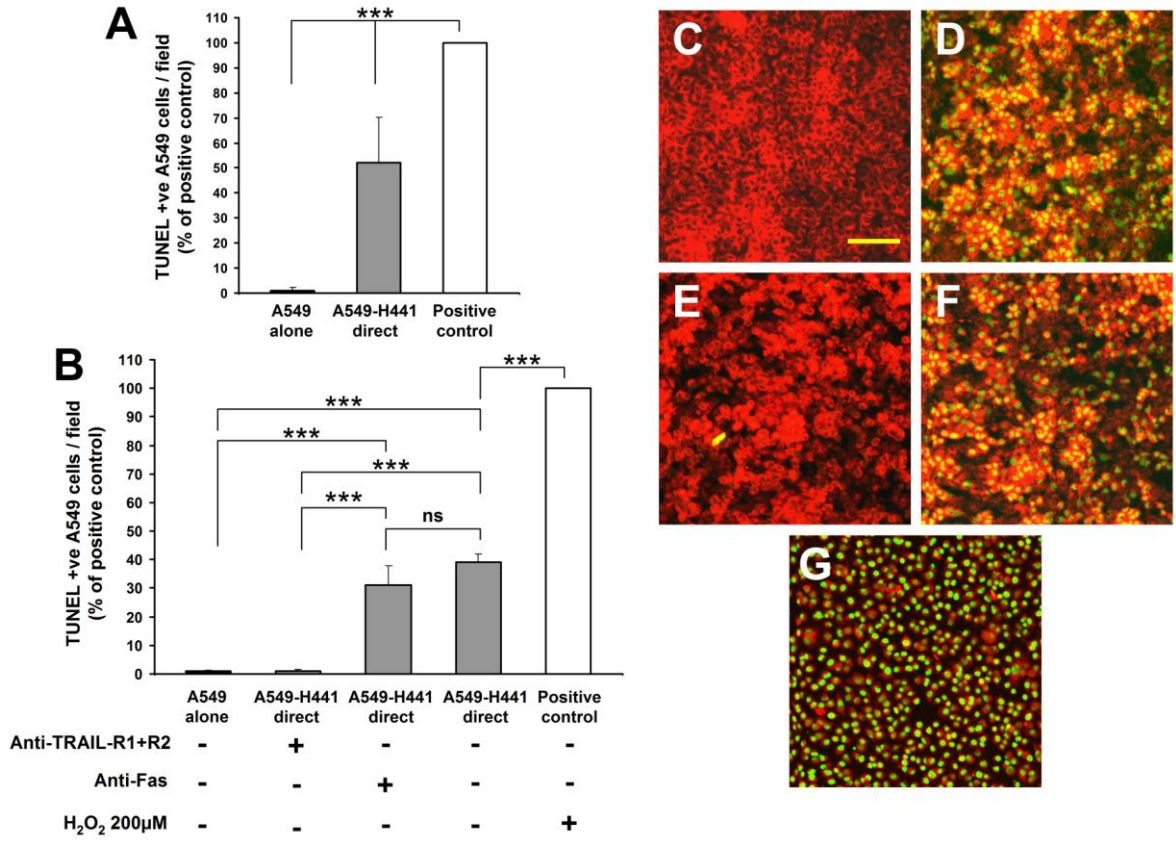

Figure 3.13: Assessment of apoptosis in A549-H441 direct-contact co-culture.

(**A**) Apoptosis in A549 cells at juxta-wound monolayers after 24 hours in A549-H441 direct-contact co-culture wound repair (grey bar) (n = 3 independent experiments). (**B**) A549-H441 direct-contact co-culture induced apoptosis blocking with anti-TRAIL-R1+R2 and anti-Fas mAbs (10 µg/ml each). For positive control, apoptosis was induced in A549 cell monolayers by 200 µM H_2O_2 and for negative control (A549 alone), A549 monolayers were treated with SF-DMEM only. (n = 3 independent experiments). (**C-G**) Laser scanning confocal microscopic images of TUNEL assay on A549-H441 direct-contact co-culture (300X). Red cells are DiI labelled A549 cells and green nuclei are TUNEL positive A549 cell nuclei. (**C**) A549 cell monoculture (as negative control). (**D**) A549-H441 cell direct-contact co-culture without any blockers. (**E**) A549-H441 direct-contact co-culture with anti-TRAIL-R1 and –R2 mAbs. (**F**) A549-H441 direct-contact co-culture with anti-Fas mAb. (**G**) Positive control: apoptosis induced in A549 monoculture with 200 µM H_2O_2. ***p<0.001. ns = not significant. Data presented as mean ± SD. Scale bar, 100 µm.

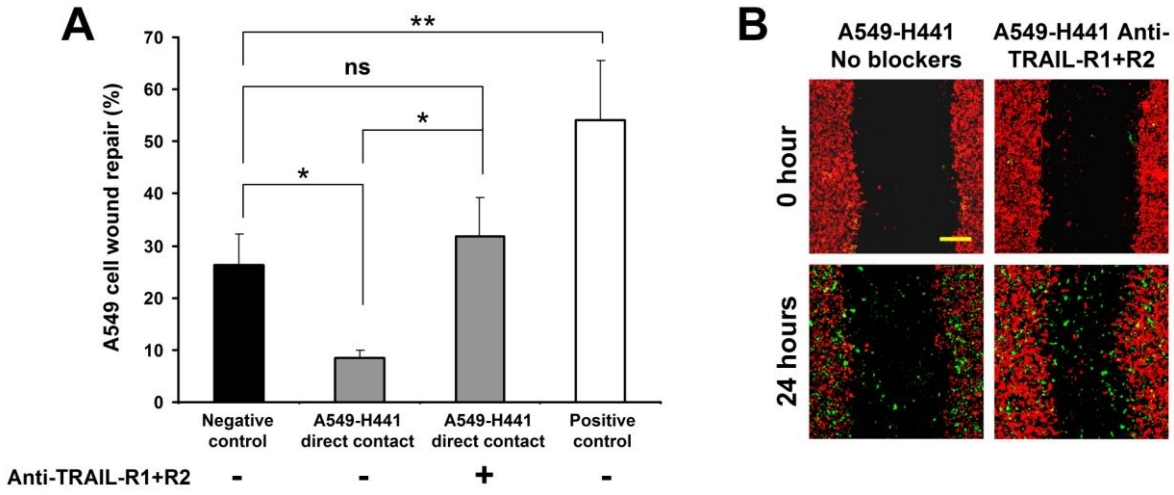

Figure 3.14: Assessment of A549 cell wound repair in A549-H441 direct-contact co-culture with TRAIL blockers.

(**A**) Alveolar A549 cell wound repair in presence and absence of anti-TRAIL-R1+R2 mAbs (10µg/ml) in A549-H441 direct-contact co-culture after 24 hours. Negative and positive controls represent A549 cell wound repair on transwell membrane in monoculture with serum-free and 10% FBS containing DMEM respectively (n = 3 independent experiments). (**B**) Representative laser scanning confocal microscopic images (100X) of A549-H441 direct-contact co-culture wound repair. DiI-labelled red cells are A549 and DiO-labelled green cells are migrated H441 cells *p<0.05, **p<0.01. ns = not significant. Data presented as mean ± SD. Scale bar, 150 µm.

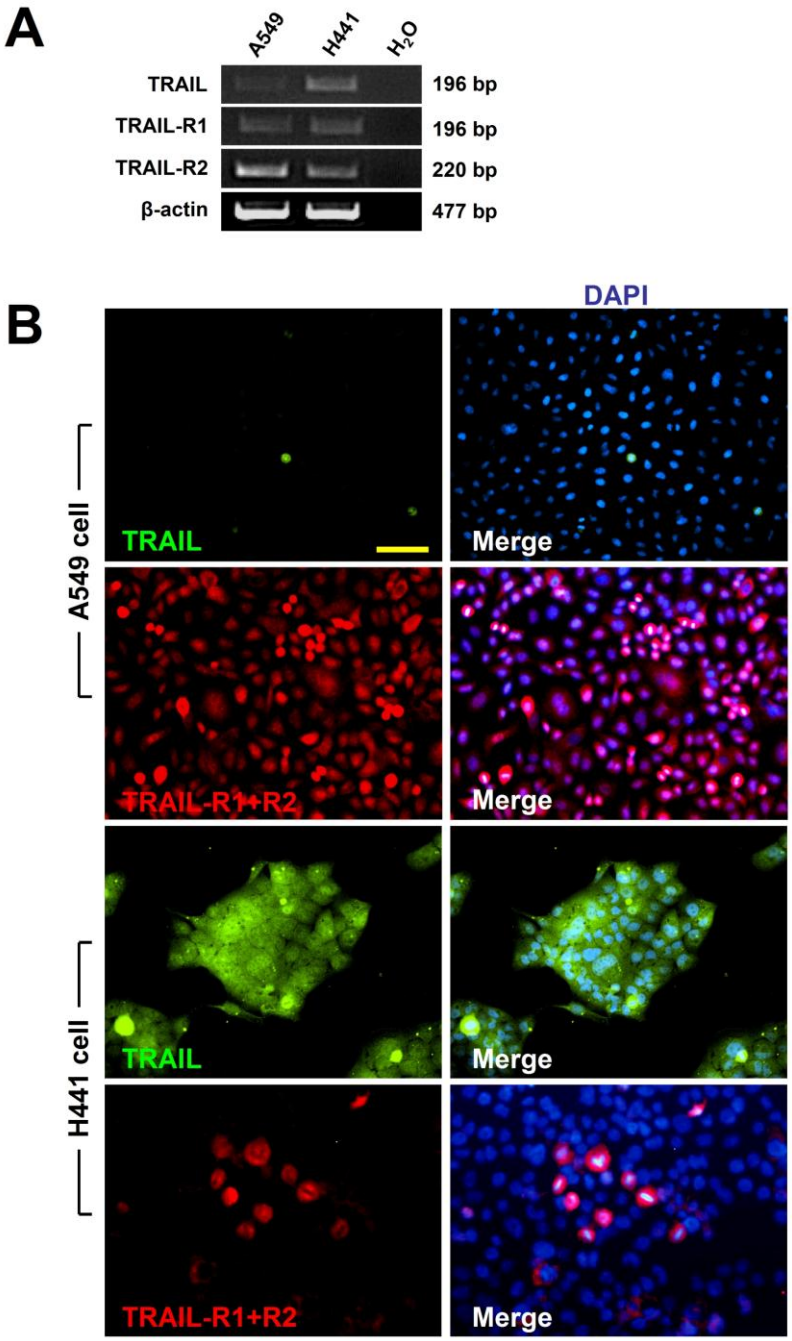

Figure 3.15: TRAIL and TRAIL receptor expression profile in A549 and H441 cells.

(**A**) RT-PCR of TRAIL, TRAIL-R1, and TRAIL-R2 of A549 and H441 cells. (**B**) Fluorescent immunocytochemistry for TRAIL, TRAIL-R1 and TRAIL-R2 in A549 and H441 cells. DAPI was used for counter staining of nuclei. Scale bar, 50 µm.

3.3.8. H441 cells migrate to SAEC wound sites and induce apoptosis in SAEC in SAEC-H441 direct contact co-culture wound repair system

Although SAECs are *pro*SP-C negative (Figure 3.2) and do not represent type II AEC, due to their suitability for wound repair model (O'Toole et al., 2009) and biological relevance to my experiments I replicated a set of major experiments that were conducted using A549 cells to exclude the potential of cancer cell line related bias in our results (Section-2.7.8.1). First, I assessed the migratory properties of H441 cells towards wounded SAEC monolayers. Interestingly, my experiments recapitulated the observations noted in the A549-H441 direct-contact co-culture model. A significant proportion of H441 cells migrated to the SAEC wound sites after 24 hours of wounding, where a 7.25-fold greater number of migrated H441 cells were located at the juxta-wound monolayers in comparison to the wound gap (58 ± 7.51 cells/field vs 8 ± 5.03 cells/field, $p<0.001$) (Figure 3.16A, 3.16B, 3.16C).

The TRAIL-ligand induced an apoptotic response in SAEC in a dose-dependent manner (Section- 2.10.1) which though reduced in comparison to A549 cells was demonstrably significant when compared to the relevant control (Figure 3.17A, 3.17B, 3.17C). Similarly, TRAIL-expressing H441 cells induced significant apoptosis in wounded SAEC in SAEC-H441 direct-contact co-culture when compared to SAEC monoculture (9.54 ± 1.90% vs 0.38 ± 0.11%, $p<0.001$) (Figure 3.18A, 3.18B, 3.18C). Confocal microscopy confirmed that TUNEL positive nuclei were SAEC and not migrated H441 cells (Figure S3.3, Appendix-2).

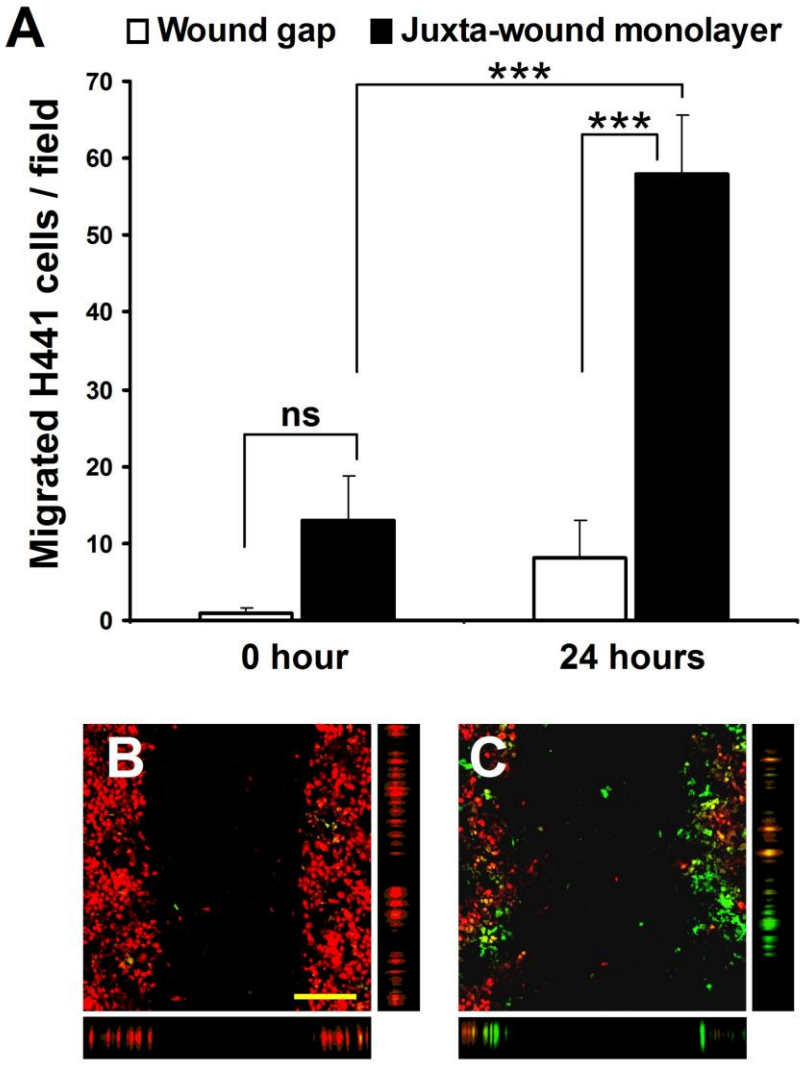

Figure 3.16: H441 cell migration in SAEC-H441 direct-contact co-culture wound repair.

(**A**) Migration of H441 cells into the SAEC juxta-wound monolayers and wound gaps (n = 3 independent experiments). (**B, C**) Laser scanning confocal microscopic images (100X) of SAEC-H441 direct-contact co-culture at 0 (B) and 24 hours (C) respectively. DiI-labelled red cells are SAEC and DiO-labelled green cells are H441 cells. Vertical side bars indicate Z-slicing through the corresponding juxta-wound monolayers and horizontal bars indicate Z-slicing through the wound gap. ***p<0.001. Data presented as mean ± SD. Scale bar, 200 µm.

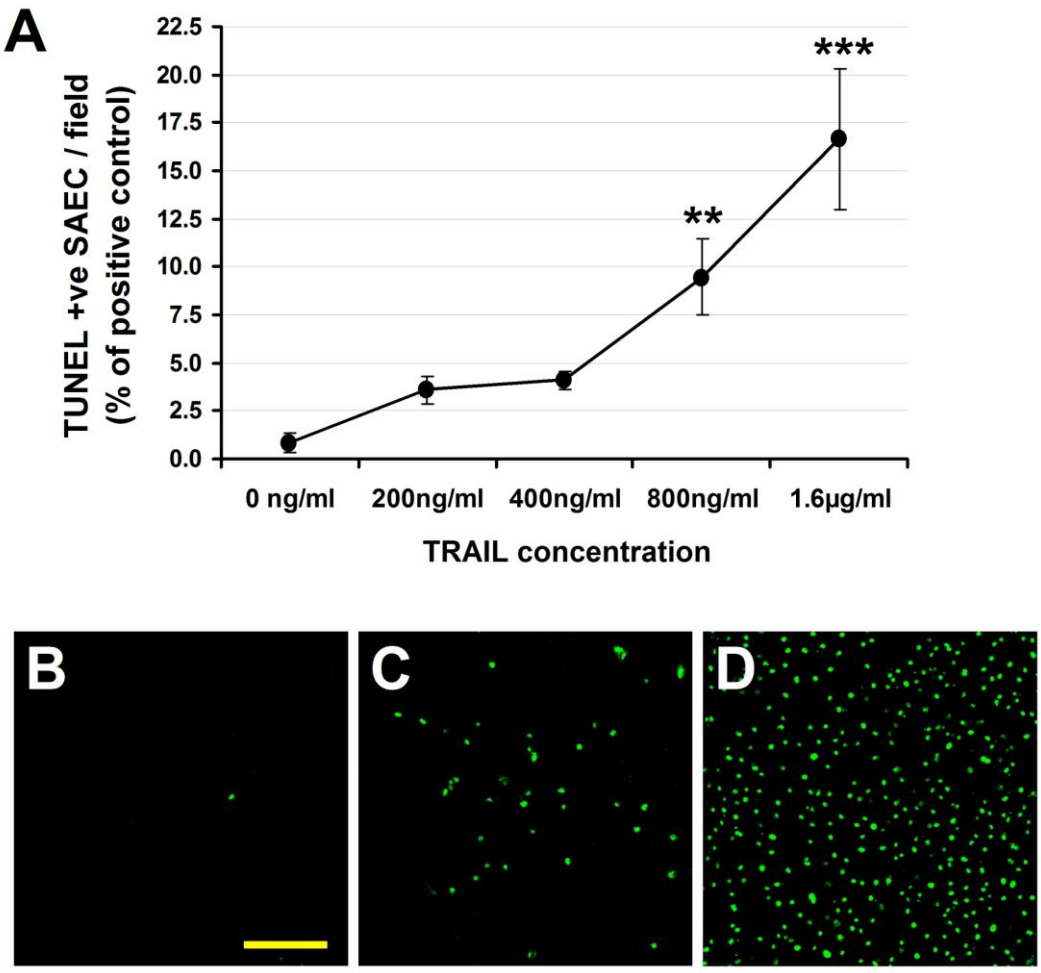

Figure 3.17: Induction of apoptosis in SAEC with soluble TRAIL.

(**A**) Dose response of apoptosis induction in SAEC monoculture with different concentration of soluble TRAIL treatment for 24 hours (n = 3 independent experiments). (**B, C, D**) Laser scanning confocal microscopic images of TUNEL positive SAEC in negative control (cells were treated with serum-free basal media) (B), 1.6µg/ml of soluble TRAIL-treated sample (C) and positive control (cells were treated with 200 µM H_2O_2) for 24 hours (D). Data plots represent mean ± SD. **p<0.01, ***p<0.001. Scale bar, 150 µm.

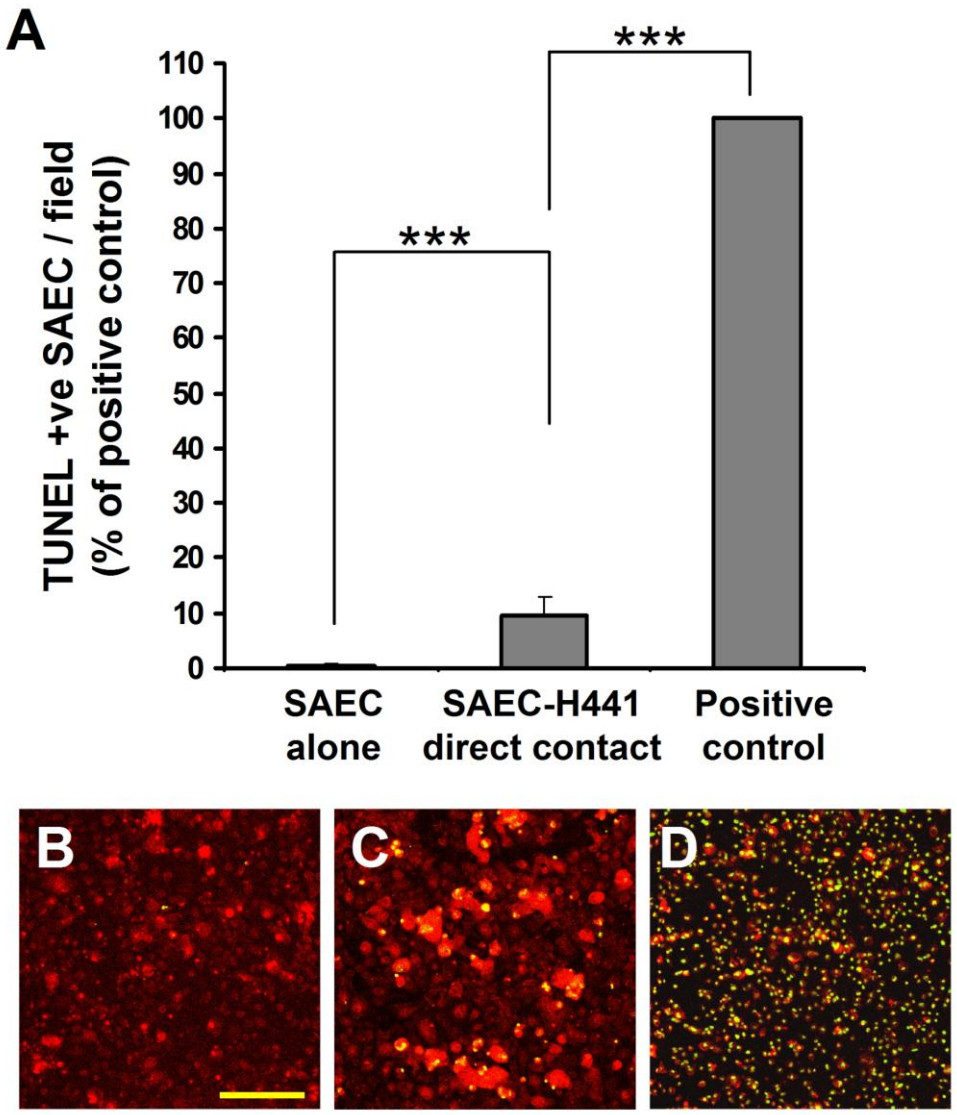

Figure 3.18: Assessment of apoptosis in SAEC-H441 direct-contact co-culture.

(**A**) Apoptosis in SAEC at juxta-wound monolayers after 24 hours in SAEC-H441 direct-contact co-culture wound repair (n = 3 independent experiments). For positive control, apoptosis was induced in SAEC monolayers by treatment of 200 µM of H_2O_2 for 24 hours and for negative control, SAEC monolayers were treated with serum-free SABM only (SAEC alone). (**B, C, D**) Laser scanning confocal microscopic images of TUNEL assay on SAEC-H441 direct-contact co-culture (200X). Red cells are DiI-labelled SAEC and green nuclei are TUNEL positive SAEC nuclei. (**B**) Negative control, SAEC monoculture. (**C**) SAEC-H441 cell direct-contact co-culture wound repair. (**D**) Positive control. ***$p<0.001$. Data presented as mean ± SD. Scale bar, 200 µm.

3.3.9. TRAIL-expressing Clara cells are detected in the fibrotic alveoli of IPF lungs with associated AEC apoptosis

Histologically all IPF biopsy samples showed features in keeping with Usual Intestinal Pneumonia (UIP); specifically a pathognomonic patchwork of normal unaffected lung alternating with remodelled fibrotic lung involving type I pneumocyte destruction, type II pneumocyte hyperplasia in the presence of fibroblastic foci and collagen type scaring. The fibroblastic foci are recognised to reflect sites of active ongoing fibrogenesis.

Localisation of TRAIL-expressing Clara cells in the alveolar regions of control and IPF lung tissues was investigated by dual immunohistochemistry with CC10 (Clara cell marker) and TRAIL antibodies (Section- 2.12.6). Dual-labelled CC10/TRAIL Clara cells were not detected in the alveolar regions of control lungs (Figure 3.19A) but were observed in the bronchiolar walls (Figure 3.19B, arrows). However, CC10/TRAIL-positive Clara cells were readily detected within the hyperplasic alveolar epithelial regions (Figure 3.19D, arrow) and in the alveolar epithelium directly overlying fibroblastic foci (Figure 3.19E, arrow) in 18 out of 21 IPF cases. Quantitative analysis displayed an average of 15 ± 2.66% CC10/TRAIL-positive epithelial cells within the specified areas per IPF case. ($p=0.0004$; Figure 3.19I).

Dual *pro*SP-C/TUNEL labelling was performed to identify the presence and localisation of apoptotic AEC in IPF lungs and control lung tissue (Figure 3.19F, 3.19G, 3.19H) (Section-2.10.3). Increased numbers of TUNEL-labelled *pro*SP-C positive AEC cell were detected in the regions of fibroblastic foci and remodelled fibrotic areas in IPF lungs (37 ± 6.79% of proSP-C/TUNEL cells per IPF case vs. 11 ± 7.53% in control; p=0035) (Figure 3.19J). Ten out 12 control cases did not demonstrate TUNEL-labelled AEC; however, two cases

displayed a high number of TUNEL-positive *pro*SP-C-labelled calls for an unknown reason that skewed the mean value towards 11% (Figure 3.19J). Taken together, these observations demonstrate evidence for a potential association of AEC apoptosis and TRAIL-expressing Clara cells with an involvement in the propagation of fibrogenesis in pulmonary fibrosis.

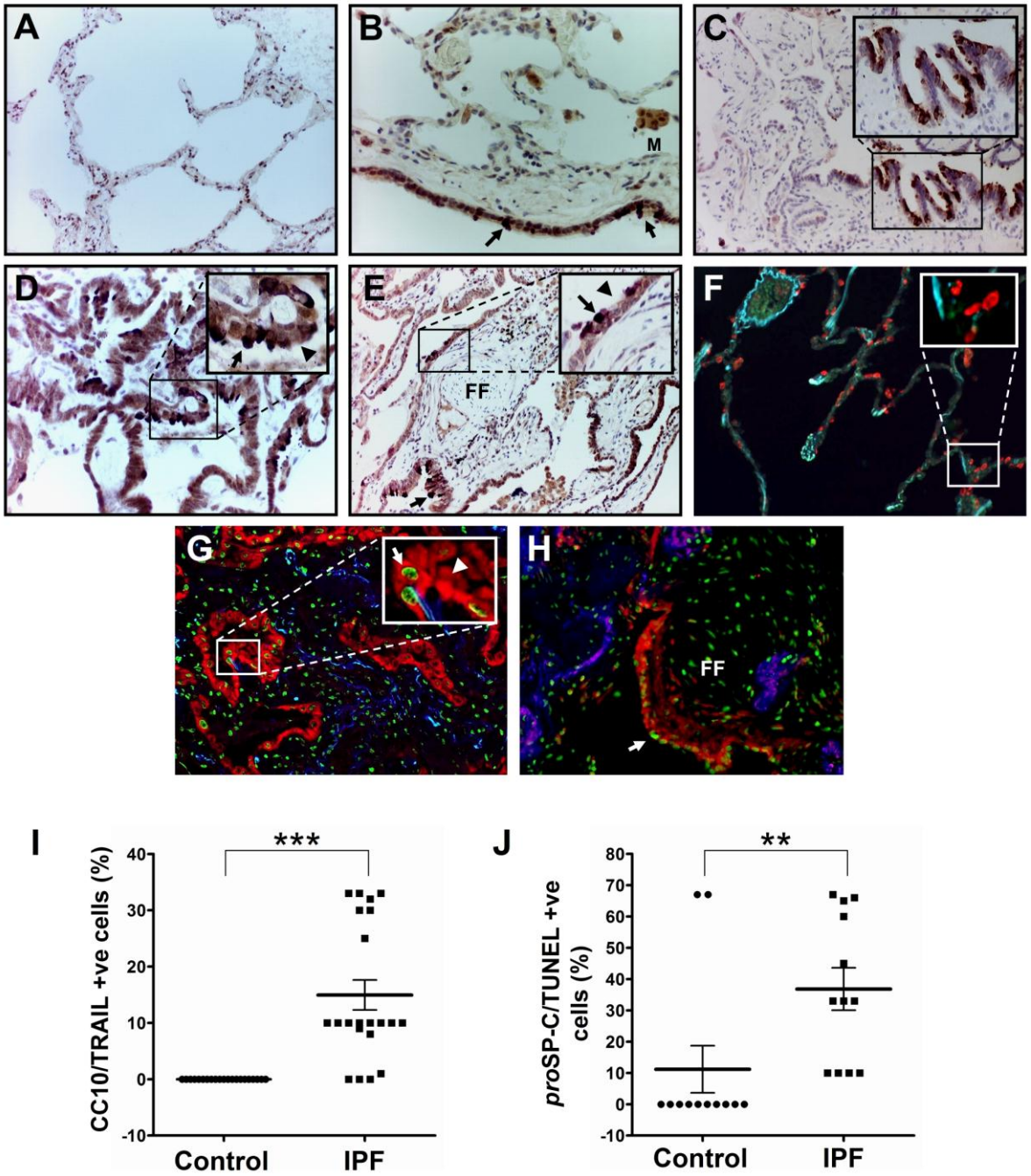

Figure 3.19: TRAIL and CC10 immunohistochemistry and TUNEL assay in normal control and IPF lung tissue samples.

(**A**) Alveolar region of control lung dual stained with CC10/TRAIL antibodies. No CC10-labelled Clara cells were detected in the alveolar region. AEC were negative to TRAIL. (**B**) Dual immunostaining with CC10/TRAIL of bronchioloalveolar region of normal control lung shows CC10-labelled Clara cells in the bronchiolar epithelium (arrows, visualised with VIP, Very Intense Purple). Clusters of macrophages were positively labelled with TRAIL which was visualised with DAB (M). No AEC was labelled with TRAIL. (**C**) Clara cells were labelled with CC10 antibody

within epithelium of hyperplastic alveolar regions of IPF lung (visualised with DAB). (**D**) Dual labelled CC10/TRAIL Clara cells were detected in the hyperplastic alveolar region of IPF lung (arrows, stained with both DAB for TRAIL and VIP for CC10). Type II AEC also showed positive to TRAIL immunostaining but negative to CC10 (arrow heads). (**E**) CC10/TRAIL dual labelled Clara cells were detected in the epithelium overlying the fibroblastic foci (FF) and hyperplastic regions (arrows). AEC were TRAIL positive and CC10 negative (arrow heads). (**F**) *pro*SP-C/TUNEL dual staining of control lung. TUNEL positive green nuclei were not detected in *pro*SP-C positive type II AEC (red fluorophore labelled). (**G**) *pro*SP-C/TUNEL dual labelled cells were detected in the hyperplastic regions of IPF lung tissue (arrow, green apoptotic nuclei within red cytoplasm). A heterogeneous pattern of TUNEL positive AEC was observed. Arrow head (inset) indicates non-apoptotic type II AEC. Notable numbers of inflammatory cells in the interstitial spaces were also TUNEL positive. Magnification was 200X for all images. (**H**) Apoptosis was detected in AEC overlying the fibroblastic foci in IPF lung (arrows). (**I**) Quantitative analysis of CC10/TRAIL dual-positive cells in the alveolar region of normal and IPF lungs (21 IPF patients and 19 controls). (**J**) Quantification of *pro*SP-C/TUNEL positive cells in the alveolar regions of IPF and healthy control lungs (12 IPF and same number of control). **p=0.0004, ***p=0.0035. Data are presented as mean ± SEM.

3.4. Discussion

The precise role of Clara cells in the repair of alveolar epithelial injury in IPF remains unknown. A reparative role is unlikely due to failed restoration of normal architecture and lung function after apparent proliferation and migration into injured alveoli in IPF (Chilosi et al., 2002, Odajima et al., 2007). In this study, I have clarified a likely role of Clara cells in AEC wound repair by using an *in vitro* wound repair model and implicated the Clara cells in the pro-fibrogenic process. This first demonstration that Clara cells induce apoptosis in AEC through a TRAIL-dependent mechanism provides evidence of a previously undiscovered cell behavior with implications for lung pathophysiology. I further demonstrate that TRAIL-expressing Clara cells not only induced apoptosis in an AEC line but also in primary human small airway epithelial cells. Clara cell behavior towards AEC were cell-type specific as demonstrated via the contrasting behavior of normal lung fibroblasts on AEC. In addition, the observation that alveolar bronchiolised Clara cells express TRAIL and are associated with AEC apoptosis in IPF lungs suggests that Clara cells may drive the aberrant alveolar wound repair event cascade and propagate the ensuing fibrogenesis through TRAIL-mediated apoptosis induction in AEC. Preliminary in-house studies have demonstrated a significant up-regulation of TRAIL-R1 and –R2 receptors in AEC of IPF lungs (data not presented in this thesis), further supporting a potential involvement of TRAIL-mediated apoptosis in AEC in IPF.

Clara cells are non-ciliated cuboidal cells, broadly distributed throughout the bronchiolar epithelium which are normally quiescent in steady-state condition but become activated following injury and proliferate/differentiate into other bronchiolar cells, hence are termed as facultative progenitor cells (Stripp & Reynolds, 2008, Stripp, 2008). Not all but a subpopulation of Clara cells which are resistant to naphthalene-induced injury are thought

to be the bronchiolar progenitor cells which contribute to bronchiolar repair and regeneration (Chen et al., 2009). H441 cells are originated from human Clara cells and have widely been used for Clara cell functional study (Gazdar et al., 1990, Kulaksiz et al., 2002, Wong et al., 2010). Due to unavailability of primary human Clara cells, the H441 cell line was chosen for my study.

Idiopathic pulmonary fibrosis is characterised as a consequence of aberrant alveolar wound repair potentially due to; apoptosis, dysregulated epithelial-mesenchymal homeostasis, basement membrane disruption, imbalanced immune response, AEC loss, and alveolar bronchiolisation (Selman & Pardo, 2002, Selman et al., 2001, Strieter, 2005, Uhal et al., 1998, Kuwano et al., 1999, Barbas-Filho et al., 2001, Odajima et al., 2007, Chilosi et al., 2002, Corrin et al., 1985). The role of alveolar bronchiolisation in aberrant wound repair and the precise nature of the interaction between the Clara cells and AEC are both relatively undefined. Bronchiolisation has been postulated as an indicator of aberrant alveolar wound repair in chemically-induced pulmonary fibrosis and human IPF lung tissue (Odajima et al., 2007, Chilosi et al., 2002, Plantier et al., 2011).

During fibrogenesis in IPF, Clara and other bronchiolar cells appear in the alveolar regions of established fibrotic areas and directly contact with AEC. While the precise mechanism is unknown, animal model and *ex vivo* studies on IPF tissue suggest that down-regulation of caveolin-1 (a membrane protein that suppresses epithelial proliferation) stimulates bronchiolar and Clara cell proliferation (Odajima et al., 2007) and up-regulation of MMP-9 (matrix metalloproteinase-9) facilitates their migration into the affected alveoli resulting in alveolar bronchiolisation (Betsuyaku et al., 2000). A recent study has suggested an NRG1α-dependent ectopic mucus cell differentiation involvement in the process of

bronchiolisation and lung remodeling in IPF lungs (Plantier et al., 2011). The migratory aspect of Clara cell behavior was confirmed in our model where H441 cells migrated to the wounded alveolar A549 cell and SAEC layers, most likely driven by a chemotactic mechanism as in the absence of A549 or SAEC, Clara cell migration was not observed. This migration was accompanied by an inhibitory effect on AEC wound repair via TRAIL-mediated apoptosis of AEC.

TRAIL (TNF-related apoptosis-inducing ligand, also known as Apo2L), a member of the TNF superfamily, can induce apoptosis through interaction with the TRAIL-R1 and TRAIL-R2 receptors (alternatively known as DR4 and DR5 respectively) (Pan et al., 1997, Walczak et al., 1997, Sheridan et al., 1997). TRAIL is a type 2 transmembrane protein which also can be released as a soluble form after being proteolytically cleaved from cell surface. In humans, TRAIL interacts with four membrane receptors which belong to the TNF receptor (TNFR) gene superfamily. TRAIL-R1 and TRAIL-R2 have conserved cytoplasmic death domain motifs, and can transduce apoptotic signals. Whereas, the other two receptors, namely DcR1 (TRAIL-R3) and DcR2 (TRAIL-R4) have truncated death domains and are incapable of transmitting apoptotic signal, hence are called decoy receptors. There is another soluble decoy receptor called osteoprotegerin (OPG) has relatively lower affinity of binding with TRAIL. TRAIL-mediated apoptosis occurs by engagement with and homotrimerisation of TRAIL-R1 or TRAIL-R2 receptor via a mitochondrial independent or/and dependent signaling pathways depending on cell types (Figure 3.20). The decoy receptors and the intracellular proteins, anti-apoptotic Bcl-2 and cFLIP are negative regulators of TRAIL-mediated apoptosis (reviewed in LeBlanc & Ashkenazi, 2003). However, the role of cFLIP in the regulation of TRAIL-mediated apoptosis is controversial.

Although expression of TRAIL and its receptors are detected in many steady-state human cell types (Daniels et al., 2005), their physiological function is poorly understood. However, TRAIL has been shown to play an important role in T-cell mediated immunomodulatory function and intestinal epithelium homeostasis (Falschlehner et al., 2009, Rimondi et al., 2006). Here, the observation that Clara cells can induce apoptosis in alveolar A549 cells provides support for my hypothesis of the involvement of TRAIL-expressing Clara cell in the aberrant alveolar wound repair found in IPF.

Pathologically, IPF is characterised by its regional and temporal heterogeneity. Affected alveolar regions in proximity to the fibroblastic foci and collagen deposition displayed increased numbers of TRAIL expressing Clara cells (as compared to control healthy lung biopsies) and were associated with elevated AEC apoptosis. Furthermore in IPF lungs, TRAIL-positive AEC were notably present in areas of hyperplastic cuboidalised alveoli and in epithelia overlying fibroblastic foci. In contrast, AEC of control lungs did not express TRAIL. However, in contradictory with our findings, a recent non-quantitative immunohistochemistry study showed a relatively low TRAIL expression in IPF alveolar epithelial cells and high TRAIL-expression in control lung (McGrath et al., 2012). I however, observed TRAIL expression in bronchiolar epithelial cells of healthy control lung. The reason of this contradictory results is undetermined; however, the McGrath et al. evaluation was on 3 control and 5 IPF lung whereas, our quantitative analysis was on 19 control and 21 IPF cases. It is possible that the TRAIL-expression in IPF AEC is heterogeneous within the affected population.

TRAIL-mediated apoptosis has been reported in other chronic disease states. For instance in chronic pancreatitis the pancreatic stellate cells overexpress TRAIL and directly

contribute to the acinar regression through induction of apoptosis in parenchymal cells via TRAIL-receptor mediated apoptosis mechanism (Hasel et al., 2003). TRAIL-mediated apoptosis has been reported as a key mediator for progression of human diabetic nephropathy where TRAIL-overexpression in renal tubular epithelial cells is associated with severe tubular atrophy and interstitial fibrosis (Lorz et al., 2008). Other studies have demonstrated up-regulation of TRAIL in intestinal epithelial cells associated with epithelial cell destruction through TRAIL-mediated apoptosis and progression of inflammatory bowel disease like ulcerative colitis and Crohn's disease while down-regulation is associated with the refractory stages of the disease (Begue et al., 2006, Brost et al., 2010). Chronic endoplasmic reticulum stress and Fas-FasL mediated apoptosis in alveolar epithelial cells and their association in aberrant alveolar wound repair in IPF have been reported previously (Kuwano et al., 1999, Korfei et al., 2008). Combining the literature evidence with our study findings, here I suggest that TRAIL-mediated apoptosis could play a crucial role in AEC apoptosis and fibrogenesis propagation in IPF; this is likely mediated via activated TRAIL-expressing Clara cells consequent on alveolar bronchiolisation (Figure 3.20). These findings unravel critical targets for further investigation towards development of novel therapeutic agents for IPF.

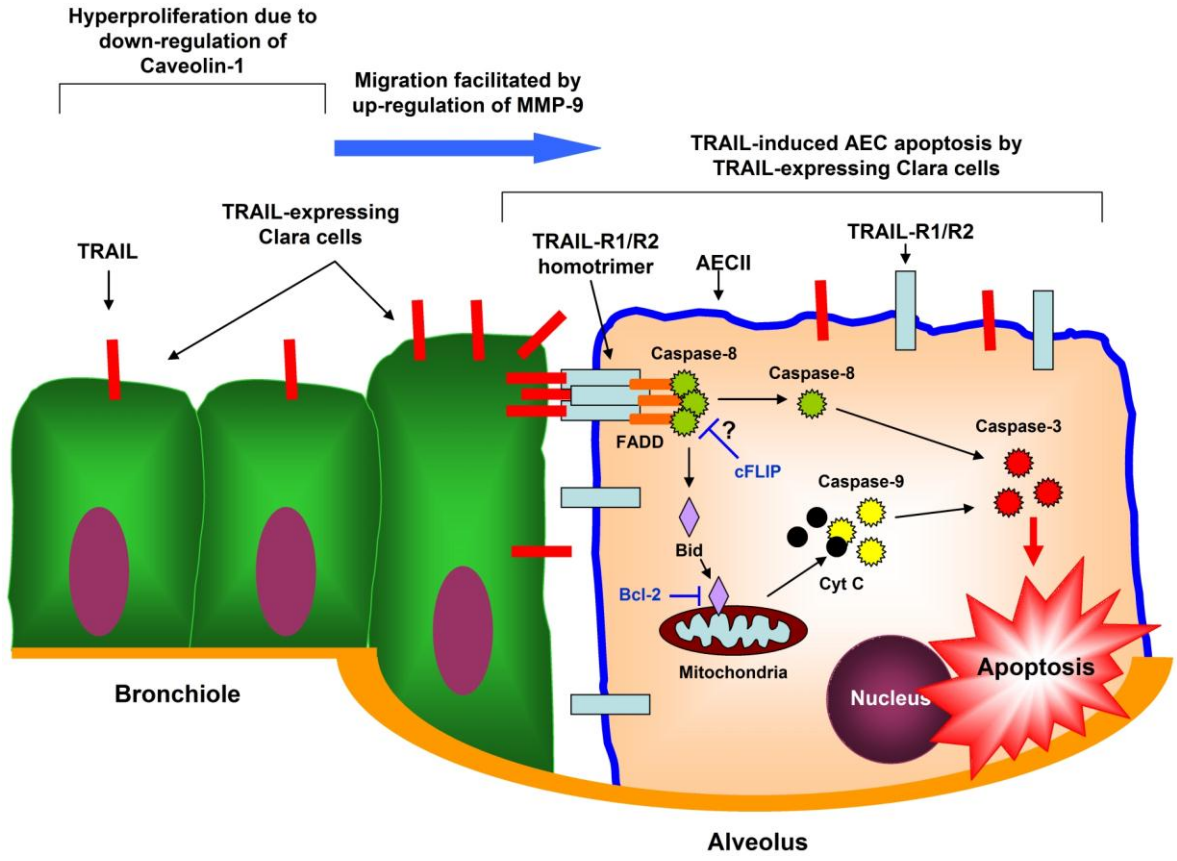

Figure 3.20: The graphical summary of TRAIL-expressing Clara cell induced AEC apoptosis. The ongoing pathognomonic events in alveolar bronchiolisation, particularly in IPF, are complex and largely unknow. Here is a proposed, hypothetical chain of events that takes place during alveolar bronchiolisation in IPF. Down-regulation of caveolin-1 in bronchiolar/Clara cells promotes their proliferation and up-regulation of MMP-9 facilitates their migration into the affected alveoli, a process called alveolar bronchiolisation. TRAIL-expressing Clara cells come in direct-contact with AEC within the alveoli and induce TRAIL-mediated apoptosis in AEC through their membranous TRAIL. TRAIL engages with TRAIL-R1/R2 receptors and makes homotrimer complex. This ligand-receptor complex then recruits the intracellular proteins to their death-domain to form DISC (death-inducing signaling complex). The TRAIL/DISC complex, which resembles to FADD (Fas-associated death domain), activates apoptotic inducer caspase-8. The caspase-8 then triggers apoptosis through proteolytic activation of caspase-3 via a mitochondrial-independent pathway (Cell-extrinsic pathway). Activated caspase-8 also can cleave Bid and translocate them to the mitochondria that augment proapototic Bax protein which stimulates release of cytochrome C (Cyt C). The Cyt C then activates caspase-9 and thus caspase-3 triggering apoptosis (Cell-intrinsic pathway) (LeBlanc & Ashkenazi, 2003).

Chapter 4

Mesenchymal Stem Cells promote Alveolar Epithelial Cell wound repair through distinct migratory and paracrine mechanisms

4.1. Background

Bone marrow derived mesenchymal stem cells (MSC) classically can differentiate into mesodermal lineages including osteoblasts, chondrocytes, adipocytes, and cardiomyocytes (Pittenger et al., 1999, Deb et al., 2003, Toma et al., 2002). Numerous reports also suggest that MSC can differentiate into other, non-mesodermal lineages including neurons (Dezawa et al., 2004, Zeng et al., 2011), hepatocytes (Sato et al., 2005) and lung epithelial cells (Liechty et al., 2000, Kotton et al., 2001, Ma et al., 2011). This evidence provides a strong rational for the potential application of hMSC in regenerative therapeutic approaches in many diseases including those of the lung where effective treatment options are limited, such as idiopathic pulmonary fibrosis. IPF is a chronic, progressive fibrotic lung disorder of unknown aetiology and the most common and lethal form of interstitial lung diseases with a post diagnosis median survival time of 3-5 years irrespective of its treatment status (Raghu et al., 2011).

Hypothetically, the pathophysiology of IPF is most likely associated with multiple alveolar injuries, failure or delayed alveolar re-epithelialisation, abnormal immune responses and subsequent fibrosis (Selman et al., 2001, Strieter, 2005, Kaminski, 2003). Studies involving the bleomycin-induced pulmonary fibrosis mouse model, a widely used animal model of pulmonary fibrosis (Harrison & Lazo, 1987), demonstrated the migration and homing of endotracheal or systematically transplanted MSC towards the site of injury and attenuation of pulmonary fibrosis (Ortiz et al., 2003, Rojas et al., 2005). However, the magnitude of the amelioration of fibrosis appeared out of proportion to the numbers of engrafted MSC which had differentiated into AEC indicating the involvement of other mechanisms in this MSC-mediated reparative process. An emerging consensus is that paracrine mechanisms could be associated with MSC-mediated wound repair and tissue

regenerative process (Weiss & Finck, 2010). However, the identity of these paracrine factors with a putative role in alveolar injury repair and regeneration is not clear.

A wide range of different growth factors, cytokines and extracellular matrix proteins (ECM) have been identified as constituents of the *in vitro* cultured MSC secretome (Chen et al., 2008a, Estrada et al., 2009). Many of these secretory proteins are biologically active with anti-inflammatory, anti-fibrotic and immunomodulatory functions (Meirelles et al., 2009, Nauta & Fibbe, 2007). The immunomodulatory function of MSC has been demonstrated through their therapeutic efficacy in alleviation of graft-versus-host disease (GvHD) and animal model of bronchial asthma through their putative role in modulating Type-1 (Th1) and Type-2 (Th2) immune responses (Nemeth et al., 2010). MSC-secreted factors are cytoprotective as demonstrated in a cardiac injury animal model driven by anti-apoptotic and inotropic effects (Gnecchi et al., 2008). The MSC-mediated anti-apoptotic effect can be driven by up-regulation of anti-apoptotic gene, Bcl-2, which was demonstrated in an animal model of emphysema (Zhen et al., 2008).

Animal model of myocardial infarction and pulmonary hypertension have demonstrated that transplanted MSC improved cardiac function and pulmonary vasculature by stimulating neovascularisation possibly via their secretory VEGF (vascular endothelial growth factor) and eNOS (endothelial nitric oxide synthase) (Burdon et al., 2011, Baber et al., 2007, Kanki-Horimoto et al., 2006). The anti-inflammatory function of MSC has been documented in many animal model studies. The mechanism is paracrine and more likely via blocking of anti-inflammatory cytokines such as TNF-α and IL-1 (Ortiz et al., 2007, Gupta et al., 2007). Previous reports have demonstrated that conditioned media obtained from MSC culture improved cutaneous wound healing (Chen et al., 2008a, Walter et al.,

2010) and cardiac repair (Nguyen et al., 2010). However, data supporting the role of MSC-secreted paracrine factors in the mediation of alveolar epithelial cell wound repair is absent.

4.1.1. Aims and objectives of the study

The aim of this study was to evaluate the likely role of hMSC on alveolar and small airway epithelial wound repair. I utilised an *in vitro* scratch wound repair system (Kheradmand et al., 1994, Atabai et al., 2002, Galiacy et al., 2003, Chen et al., 2008b, Savla & Waters, 1998, Geiser et al., 2000, Geiser et al., 2004, Sonar et al., 2010, Curley et al., 2012) to evaluate the paracrine effects of hMSC on AEC and SAEC wound repair and developed a novel direct-contact co-culture wound repair system to investigate their migratory property of hMSC towards epithelial wound (Section- 2.7.2, Section- 2.7.8.2).

4.2. Study design

To investigate the paracrine influence of hMSC on alveolar A549 cell and SAEC wound repair, SF-CM was obtained from hMSC culture and tested on A549 and SAEC wound repair system (Section- 2.4.2, Section- 2.7.4, Section- 2.7.5) (See Chart 4.1). The effect of hMSC-CM on the alveolar A549 cell wound repair was evaluated with different concentration of serum supplementation as well (Section- 2.7.4). The internuclear distances of A549 cells at wound margins were measured to evaluate cell migration (Section- 2.8). The MTT cell proliferation assay was performed to investigate the A549 cell proliferation in response to hMSC-CM treatment during wound repair (Section- 2.9). CM obtained from human lung fibroblast cell line CCD-8Lu was also tested on A549 cell wound repair model to compare and contrast the observed effects by hMSC-CM (Section- 2.4.3, Section- 2.7.4). The migratory property of hMSC was evaluated through utilisation of A549-MSC direct-contact *in vitro* wound repair model (Section- 2.7.8.2). The secretory proteins of hMSC-CM were identified by LC-MS/MS mass spectrometry (Section- 2.5). A cohort of hMSC secretory proteins were selected based on their abundance in the CM and biological relevance to wound repair to test on the alveolar A549 and SAEC wound repair model (Section- 2.7.7). A group of selected proteins were tested to investigate their substrate-effect on A549 cell migration by developing a novel 'Collagen drop cell migration assay' (Section- 2.13). The experimental data was analysed using the Excel programme of Microsoft Office XP. The statistical analysis was performed using the GraphPad Prism version 5.00 software (Section- 2.14). A conclusion was drawn according to the outcome of the experimental results (See Chart 4.1).

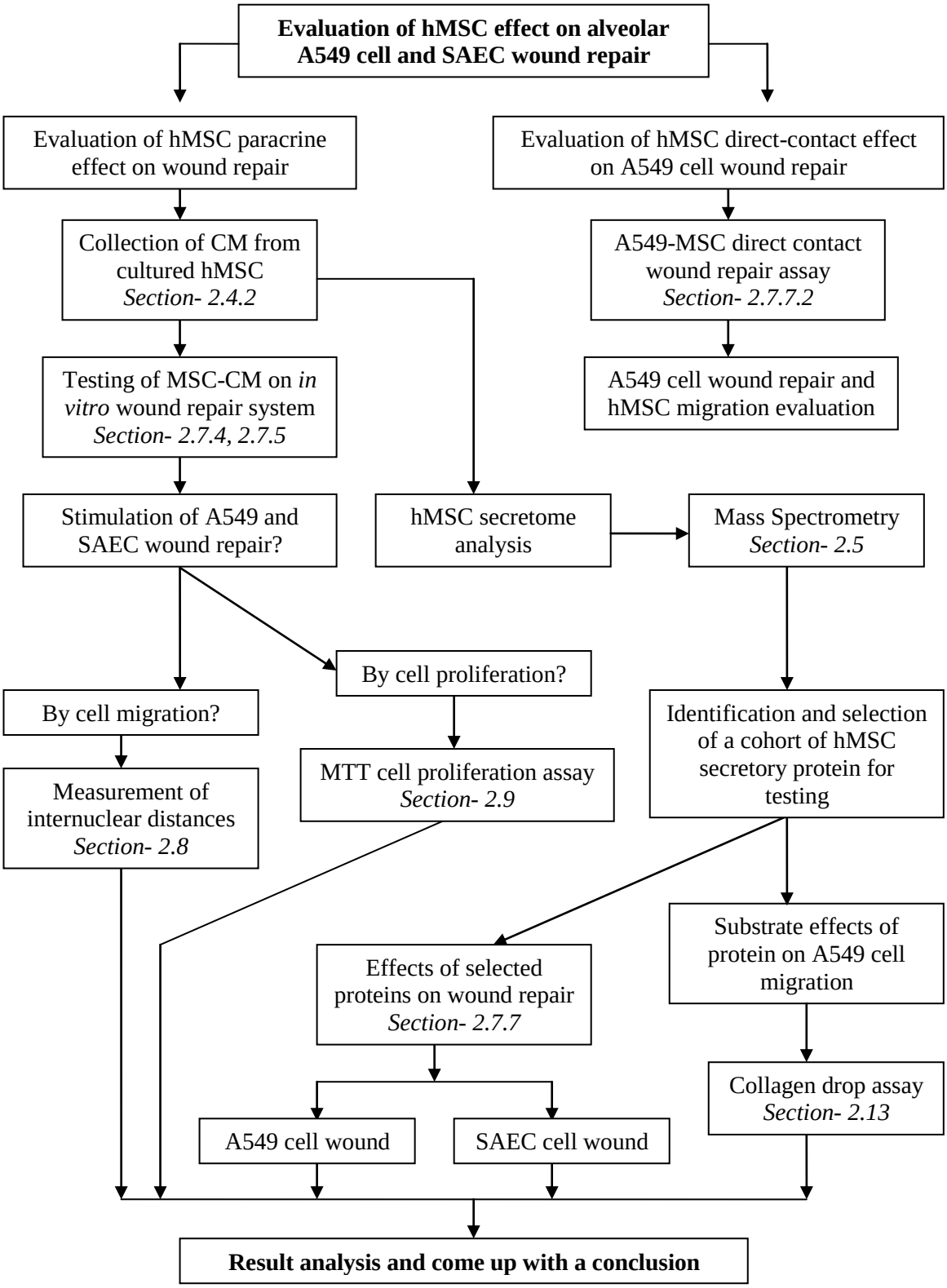

Chart 4.1: Major steps of the study plan.

4.3. Results

4.3.1. Assessment of hMSC phenotypic markers and their multipotency

hMSC were isolated from bone marrow aspirates following the previously described methodology (D'Ippolito et al., 2004, Wimpenny et al., 2010) (Section- 2.2.3). Prior to experimentation, the phenotypic surface markers of hMSC were confirmed by immunocytochemistry (Section- 2.12.2) and their multipotency was confirmed by tri-lineage differentiation (Section- 2.2.3.1, Section- 2.12.3). The hMSC surface markers were detected on passage-1 cells isolated from 3 different donors. Isolated hMSC were positive for surface antigens CD44, CD90, CD146, STRO-1 and negative for haematopoietic markers CD14 and CD19 (Figure 4.1).

The isolated hMSC were also capable of differentiating into tri-lineage mesodermal derivatives; osteoblasts, chondrocytes and adipocytes, which were demonstrated through histological staining and immunocytochemistry (Figure 4.2) (Section- 2.2.3.1, Section- 2.12.3). Calcium deposition after 3 weeks by differentiated osteoblasts was detected by Alizarin Red staining (Figure 4.2A) and the differentiated osteoblasts were positive for osteocalcin (Figure 4.2G). Fat globules produced by differentiated adipocytes were stained with Oil Red O (Figure 4.2B). The adipocytes were also positive for the specific marker FABP-4 (Figure 4.2H). GAG production by chondrogenic nodules was determined by Alcian Blue staining (Figure 4.2C) and aggrecan was detected by immunocytochemistry (Figure 4.2I).

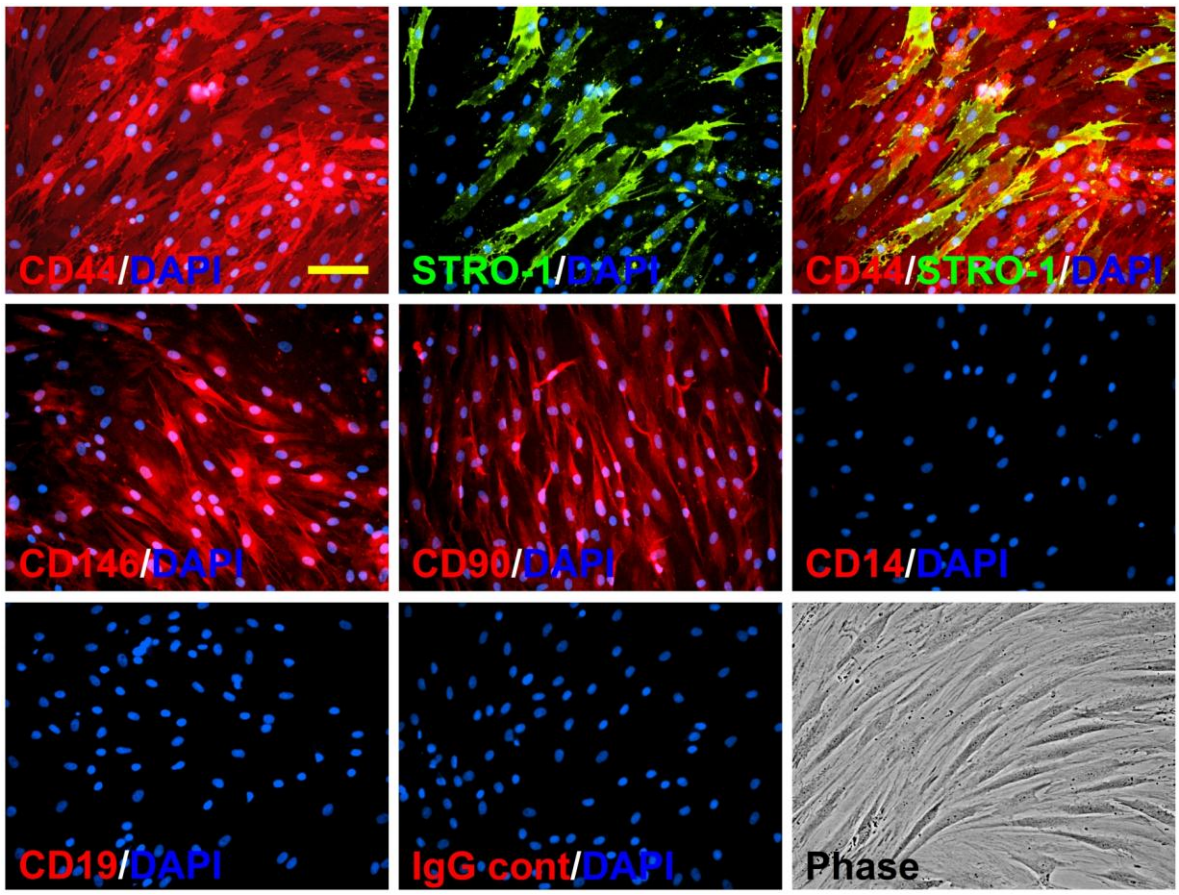

Figure 4.1: Immunophenotyping of hMSC on isolated MSC.

hMSC were positive for surface antigens CD44, STRO-1, CD146, and CD90 and negative for haematopoietic markers CD14 and CD19. DAPI was used for nuclear counter staining. Image magnification for fluorescence and phase was 200X. Scale bar, 100 µm.

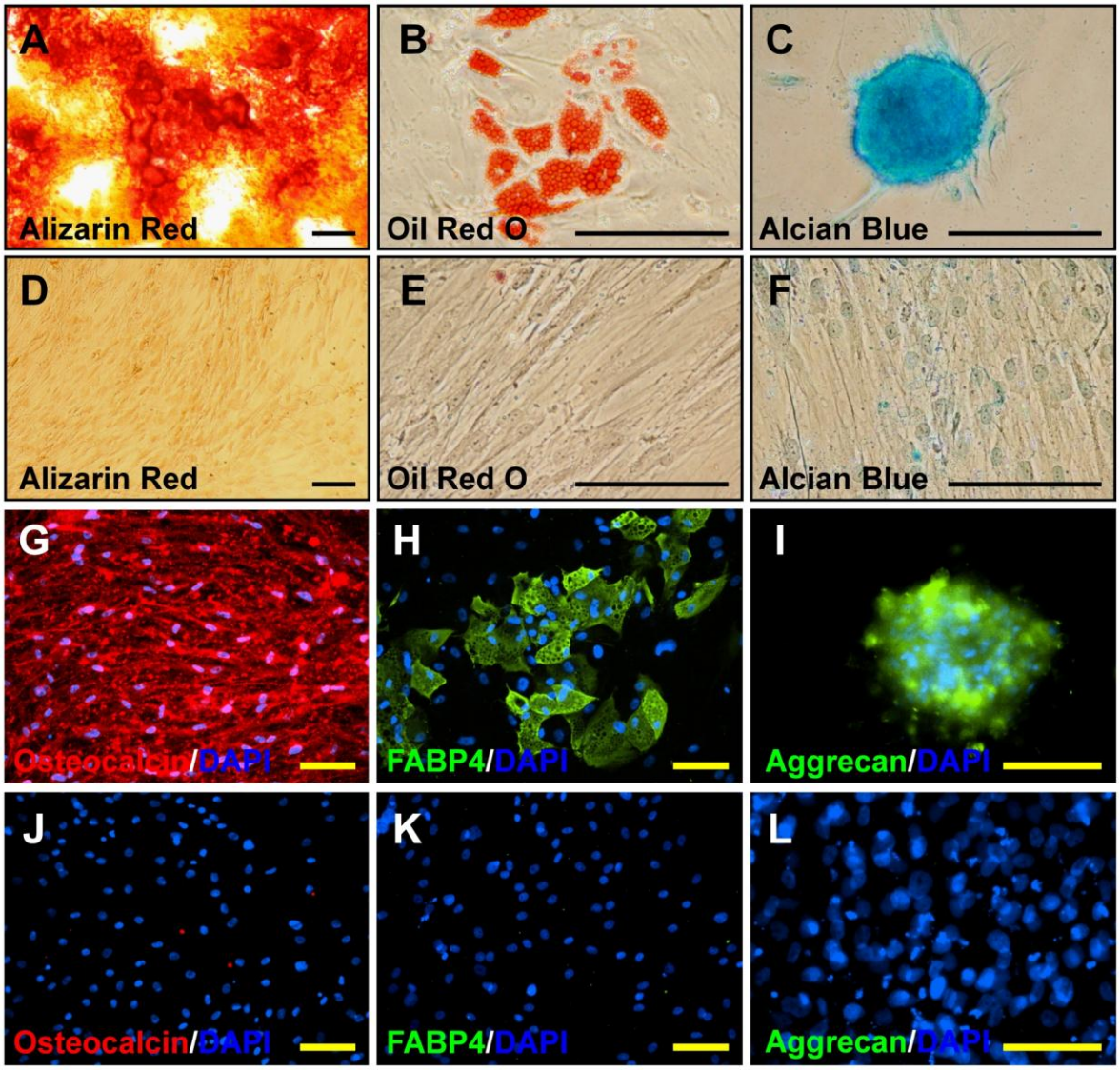

Figure 4.2: Classical tri-lineage differentiation of hMSC.

(**A**) Calcium deposition by differentiated osteoblasts was stained with Alizarin Red and (**G**) osteocalcin detected by immunofluorescence (G). **D** and **J** indicate respective control images. (**B**) Differentiated adipocytes produce triglyceride as indicated by Oil Red O stain and express FABP4 as indicated by positive immunofluorescence (H). **E** and **K** indicate respective control images (**C**) Chondrogenic nodules stained positive with Alcian Blue and aggrecan immunofluorescence (I). **F** and **L** indicate respective controls. Scale bar, 150 µm (A, B, C, D, E, F); 100 µm (G, H, I, J, K, L).

4.3.2 hMSC secretome stimulates alveolar epithelial cell wound repair in a co-factor dependent manner

To investigate the role of the hMSC secretome on AEC and SAEC wound repair, human MSC-derived serum-free conditioned media was tested on *pro*SP-C expressing human type II AEC line A549 cells (Figure 3.2) and primary human SAEC utilising the established *in vitro* scratch wound repair model. Aberrant alveolar repair processes resulting in denuded alveolar walls are thought to be among the key elements required for pathogenesis of IPF. (Selman et al., 2001). The use of the scratch wound repair model replicates, at least in a part, the wounds and, through the controlled experimentation I describe, allows replication of the inability to repair and a platform to test novel factors in repair stimulation (Section- 2.7, Section- 2.7.1, Section- 2.7.4). hMSC serum-free conditioned media (SF-MSC CM^{DMEM}) did not show any stimulatory effect on alveolar A549 cell wound repair after 24 hours (36 ± 9.84% SF-MSC CM^{DMEM} vs. 35 ± 6.57% SF-DMEM (negative control)); whereas, SAEC wound repair was enhanced with SF-MSC CM^{SABM} (94 ± 7.59% SF-MSC CM^{SABM} vs. 67 ± 6.63% SF-SABM (negative control); $p<0.001$) (Figure 4.3A, 4.3C) (Section- 2.4.2, Section- 2.7.4).

Surprisingly, supplementation of SF-MSC CM^{DMEM} with trace amounts of FBS improved the rate of alveolar A549 cell wound repair stimulation (Figure 4.3B) (Section- 2.7.4). A maximal effect was observed with the addition of 0.2% FBS in SF-MSC CM^{DMEM} over its corresponding control (0.2% FBS supplemented DMEM) (66 ± 7.39% vs. 36 ± 9.48%; $p<0.001$) (Figures 4.3B, 4.3D). The correlation between wound repair rate and increase in FBS addition was poor, though consistent, when FBS concentrations of <1% were examined. This was noted for both SF-MSC CM^{DMEM} and DMEM (Figure 4.3B).

SF-MSC CM^{DMEM} without additional FBS supplementation did not increase the alveolar A549 cell wound repair rate. However, when exposed to SF-MSC CM^{DMEM} for 24 hours, isolated alveolar A549 cells migrated from their wound margins towards wound gaps with an accompanying migratory morphology which was not seen in the control where cells were treated with SF-DMEM (Figure 4.4A). Inter-nuclear distances, a measure of migration (Atabai et al., 2002, Geiser et al., 2000), in SF-MSC CM^{DMEM} treated alveolar A549 cells were significantly higher than that observed in SF-DMEM treated wounded A549 cells (44.57 ± 3.66 µm vs. 30.61 ± 3.02 µm; $p<0.001$) (Figure 4.4B) (Section- 2.8).

Next, I investigated the influences of 0.2% FBS supplementation with SF-MSC CM^{DMEM} or SF-DMEM on A549 cell proliferation during *in vitro* wound repair. The MTT assay, an established method for determination of cell proliferation (Plumb et al., 1989), demonstrated that supplementation of SF-MSC CM^{DMEM} or SF-DMEM with 0.2% FBS did not increase alveolar A549 cell proliferation after 24 hours of wound repair; whereas, supplementation of 10% FBS with DMEM significantly increased A549 cell proliferation in comparison to both SF-DMEM and SF-MSC CM^{DMEM} ($p<0.001$) (Figure 4.5) (Section- 2.9). Taken together, serum-free MSC conditioned media alone can stimulate migratory behaviour of AEC during attempted wound repair but does not induce sufficient wound repair without supplementation of additional co-factor(s) at trace levels. However, SAEC wound repair required SF-MSC CM^{SABM} only. These findings demonstrate a phenotype-dependant and anatomical compartment-specific diverse paracrine response to hMSC secretome on distal airway and AEC wound repair where, at least for the AEC, the reparative process was accomplished by stimulation of cell migration.

On the contrary, serum-free or 0.2% FBS supplemented conditioned media obtained from normal human lung fibroblasts CCD-8Lu (CCD-8Lu CM) neither enhanced alveolar A549 cell wound repair (Figure 4.6A, 4.6C) nor stimulated AEC cell proliferation (Figure 4.6B) (Section- 2.4.3, Section- 2.7.4, Section- 2.9). This observation suggests a distinct influence of hMSC and normal human lung fibroblasts on alveolar epithelial wound repair *in vitro*.

4.3.3. hMSC migrate into wounded A549 cell layers in response to injury

hMSC migration to the site of injury is proposed as an important element of alveolar wound repair and regeneration in animal models of pulmonary fibrosis (Rojas et al., 2005). To investigate the migratory properties of hMSC, I developed a two-cell direct-contact co-culture wound repair model (Figure 4.7A) (Section- 2.7.2, Section- 2.7.8.2). In response to alveolar A549 cell injury, hMSC migrated into the A549 cell wound and completely closed the wound gap (Figure 4.7B and 4.7C). A549 cell wound repair was significantly lower in both the negative and positive control than in the A549-MSC direct contact co-culture (28 ± 6.54% negative control (A549 upper PET surface mono-culture in SF-DMEM), 72 ± 6.90% positive control (AEC upper PET surface mono-culture in 10% FBS DMEM) and 100% A549-MSC direct-contact in SF-DMEM respectively; $p<0.001$ vs A549-MSC direct-contact) (Figure 4.7C).

Cell migration assessment demonstrated a 5-fold higher hMSC migration into wound gaps over the juxta-wound monolayers after 24 hours of direct-contact co-culture (308 ± 13.96 MSC/field (wound gap) vs. 66 ± 13.44 MSC/field (juxta-wound margin); $p<0.001$) (Figure 4.7D) (Section- 2.7.8.2). In the absence of A549 cell, hMSC did not migrate to the contra-lateral surface of the porous transwell membrane (Figure S4.1, Appendix-2).

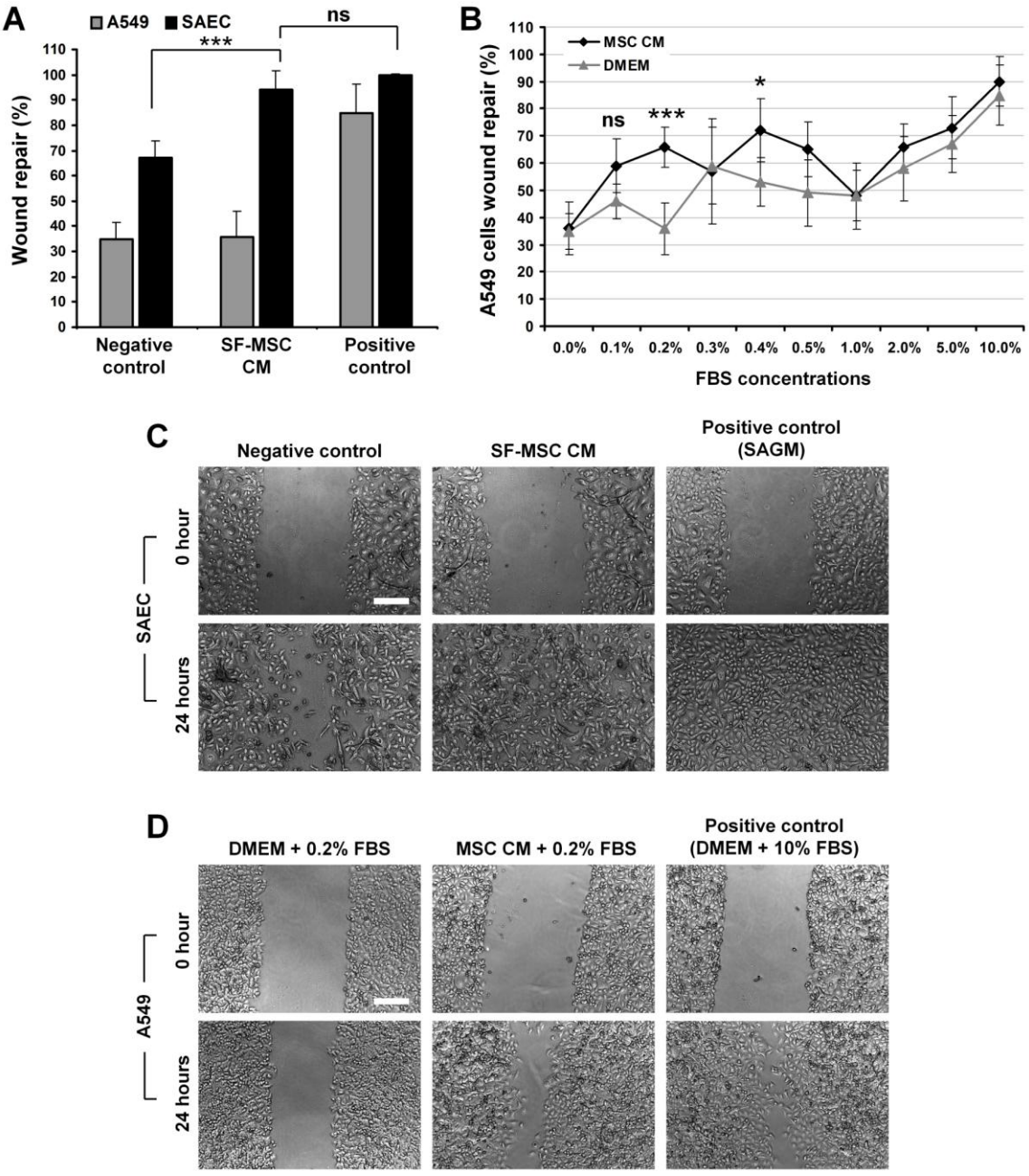

Figure 4.3: hMSC paracrine stimulation of A549 cell and SAEC wound repair *in vitro*.

(**A**) Alveolar A549 cell (grey bars) and SAEC (black bars) wound repair after 24 hours with SF-MSC CM^{DMEM} and SF-MSC CM^{SABM} respectively. Negative controls indicates SF-DMEM for A549 cell and SF-SABM basal media for SAEC; Positive control indicates DMEM + 10% FBS for A549 and SAGM for SAEC. (A549, n = 8 independent experiments; SAEC, n = 6 independent experiments, ***$p<0.001$). (**B**) A549 cell wound repair after 24 hours with hMSC conditioned media and DMEM supplemented with different concentration of FBS (n = 8 independent experiments; ***$p<0.001$ vs DMEM). (**C**) Inverted light microscopic images of SAEC wound repair. (**D**) Inverted light microscopic images of A549 cell wound repair. Data presented as mean ± SD; ns = not significant. Scale bars, 200 µm.

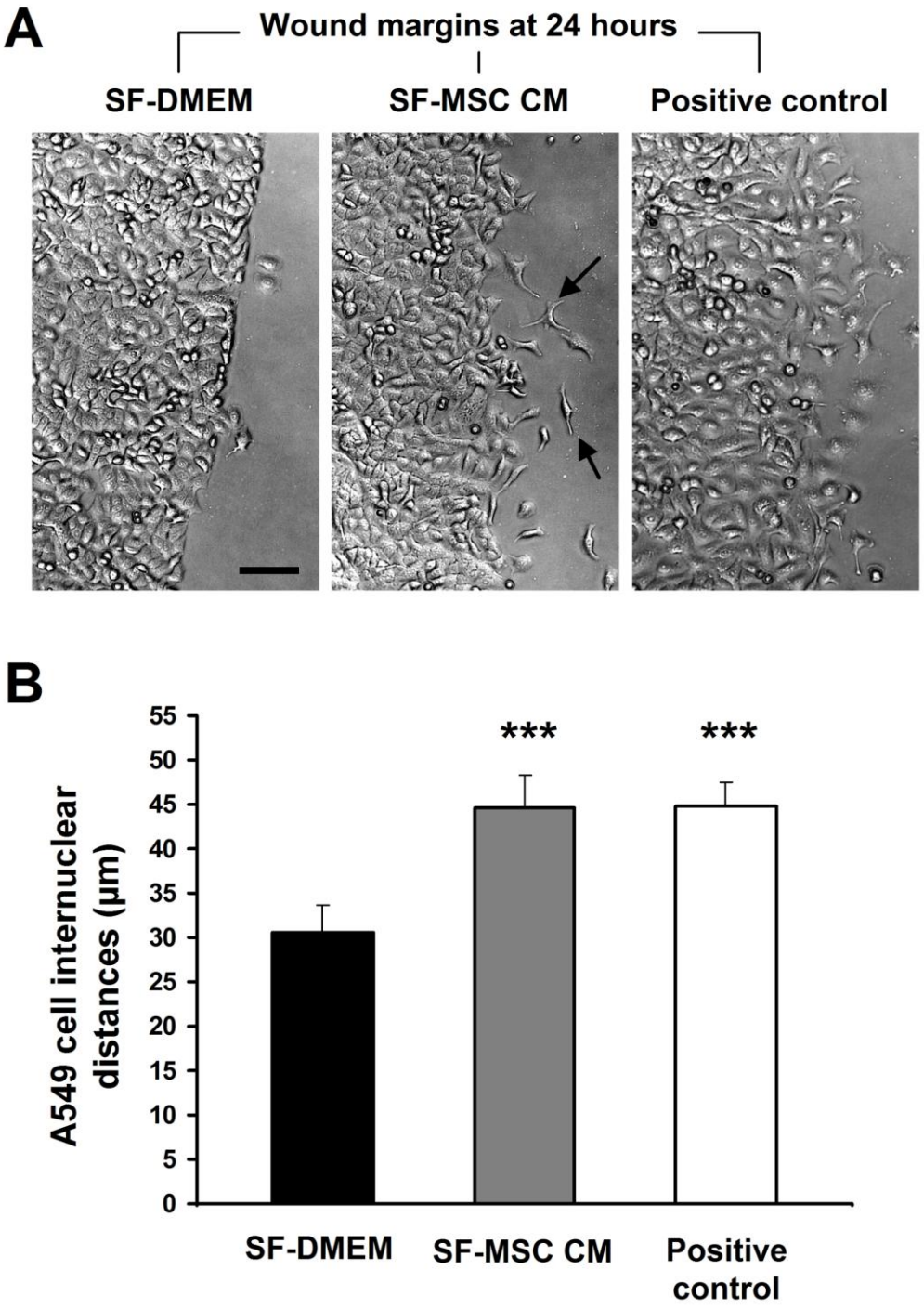

Figure 4.4: Assessment of internuclear distance of alveolar A549 cell.

(**A**) Representative inverted light microscopic images of alveolar A549 cell wound margins after 24 hours in SF-DMEM (Negative control), SF-MSC CM^{DMEM} and 10% FBS supplemented DMEM (Positive control). Numbers of migrating AEC were observed at the wound margins of SF-MSC CM (arrows) and DMEM+10% FBS treated samples. (**B**) The internuclear distances of A549 cells at wound margins after 24 hours; SF-MSC CM^{DMEM} (grey bar), Positive control (DMEM+10% FBS) (open bar) and SF-DMEM (black bar) (n = 6 independent experiments). ***$p<0.001$ vs SF-DMEM. Data presented as mean ± SD; ns = not significant. Scale bars, 100 µm.

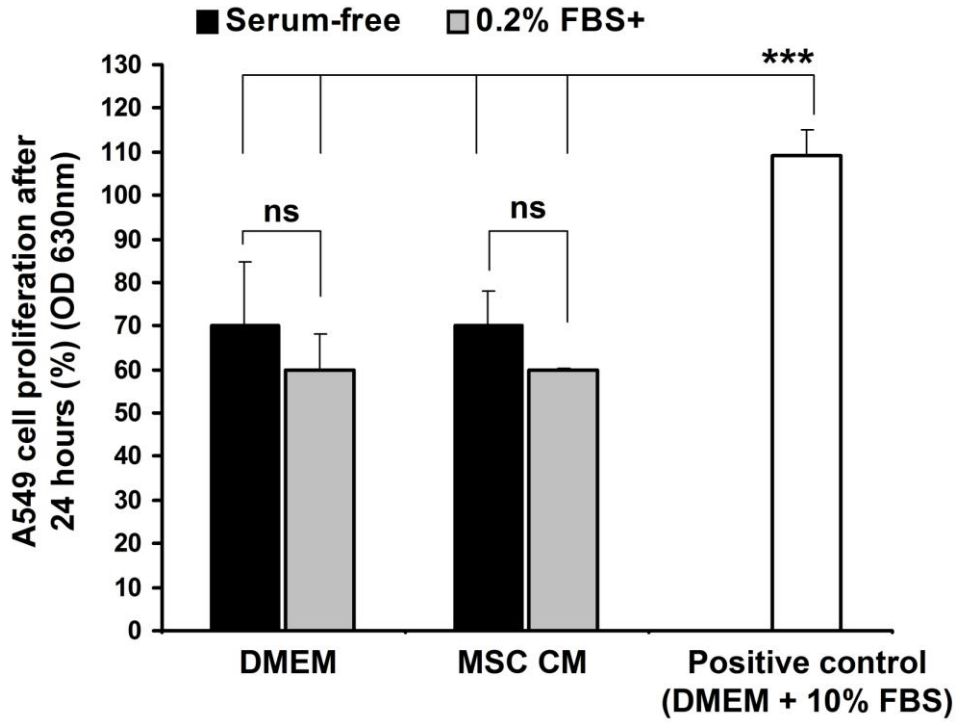

Figure 4.5: MTT cell proliferation assay on alveolar A549 cell wound repair with hMSC CM. SF-MSC CM (black bar) or MSC CM supplemented with 0.2% FBS (grey bar) did not increase A549 cell proliferation comparing corresponding controls SF-DMEM (black bar) and DMEM supplemented with 0.2% FBS (grey bar) after 24 hours during *in vitro* wound repair. Positive control was DMEM supplemented with 10% FBS (open bar) which significantly increased A549 cell proliferation after 24 hours comparing all other samples during wound repair *in vitro* (n = 4 independent experiments). ***$p<0.001$, ns = not significant.

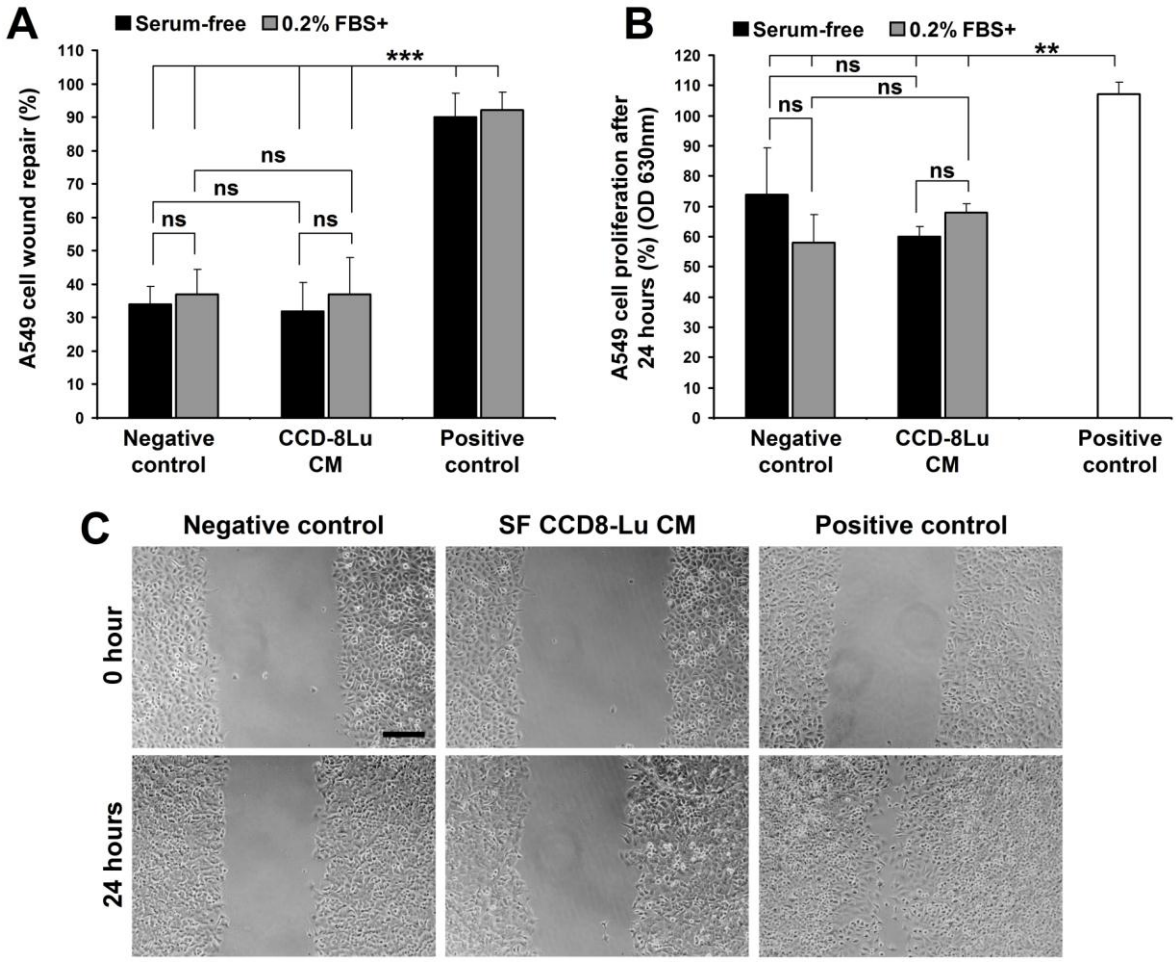

Figure 4.6: CCD-8Lu paracrine stimulation of alveolar A549 cell wound repair *in vitro*.

(**A**) A549 cell wound repair after 24 hours with serum-free (SF) (black bar) and 0.2% FBS supplemented (grey bar) CCD-8Lu CM. Negative controls represent wound repair with SF-DMEM (black bar) and 0.2% FBS supplemented DMEM (grey bar). Positive control represents wound repair with 10% FBS supplemented DMEM (black bar = positive control for SF-media treated samples; grey bar = positive control for 0.2% FBS supplemented treated samples). (n = 4 independent experiments). (**B**) Alveolar A549 cell proliferation (by MTT assay) after 24 hours of wounding treated with SF (black bars) and 0.2% FBS supplemented CCD-8Lu CM (grey bars). Negative controls represent A549 cell proliferation after 24 hours with SF or 0.2% FBS supplemented DMEM and positive control represents A549 cell proliferation with 10% FBS supplemented DMEM (open bar). (n = 4 independent experiments). (**C**) Representative inverted light microscopic images of A549 cell wound repair. Negative control = SF-DMEM, Positive control = 10% FBS supplemented DMEM. Data presented as mean ± SD. ***$p<0.001$. ns = not significant. Scale bar, 200 μm.

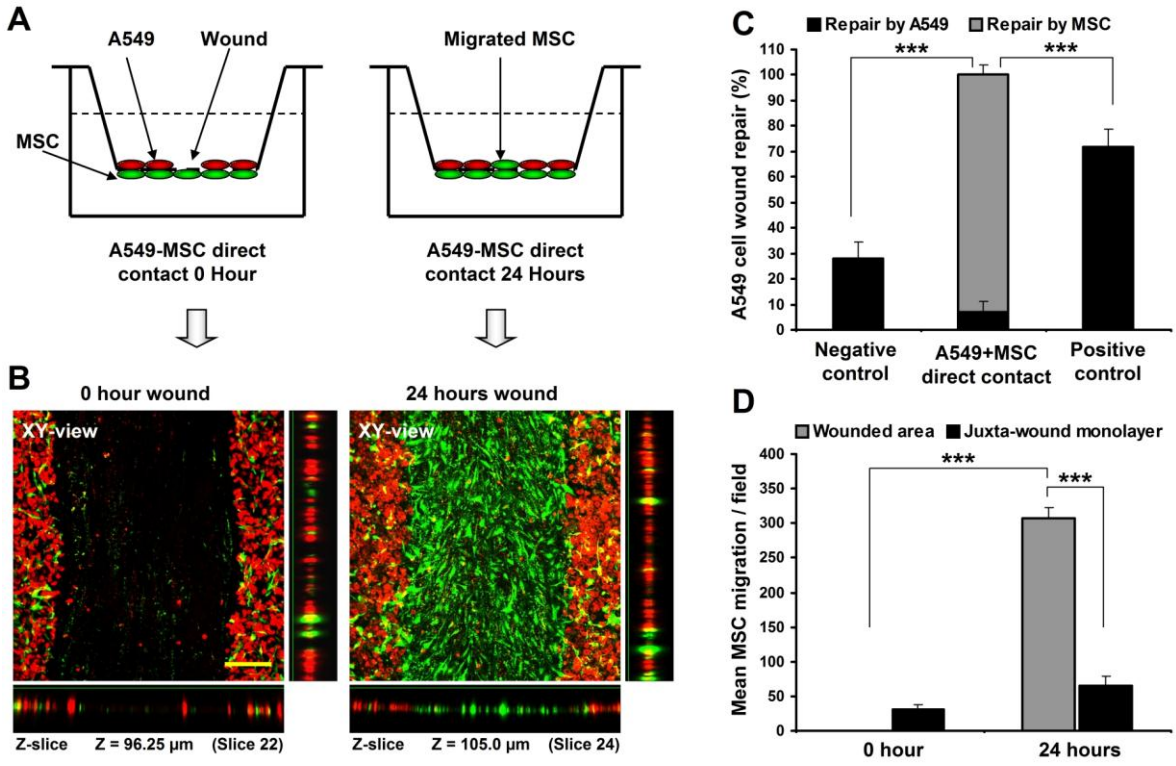

Figure 4.7: hMSC migrate to the A549 cell wound sites and close wound gaps.

(**A**) Schematic diagram showing two-cell direct-contact co-culture wound repair model using 3 µm porous transwell system. (**B**) Laser scanning confocal micrographs of A549-MSC direct-contact co-culture wound repair model at 0 and 24 hours. Red cells are DiI-labelled A549 cells and green cells are DiO-labelled hMSC. Horizontal panels are the Z-slicing through the wound gaps and the vertical panels are Z-slicing through the corresponding juxta-wound monolayers. Appearance of green signals in the same plane of red signals in the in the Z-slice after 24 hours confirms hMSC migration to the A549 cell wound site. (**C**) A549-MSC direct-contact co-culture vs. negative and positive controls wound repair. Black and grey bars indicate A549 cell and hMSC contribution to repair, respectively. Negative control represents A549 cell wound repair in SF-DMEM in mono-culture setting on upper surface of transwell PET membrane. Positive control represents A549 cell wound repair in 10% FBS supplemented DMEM in mono-culture setting on upper surface of transwell PET membrane. (n = 6 independent experiments). (**D**) hMSC migration in a direct-contact co-culture wound repair system (n = 6 independent experiments). Data presented as mean ± SD. ***p<0.001. Scale bar, 150 µm.

4.3.4. Proteins detected in MSC conditioned media show differential wound repair potential

hMSC conditioned media enhanced alveolar A549 cell migration and wound repair (with trace FBS supplementation). I hypothesised that candidate molecules within the hMSC secretome could enhance alveolar epithelial cell wound repair. To test this hypothesis, I first evaluated the composition of the SF-MSC CM^{DMEM} secretome from hMSC isolated from three donor independent marrow samples using LC-MS/MS mass spectrometry (Table 4.1) (Section- 2.5). The composition of CCD-8Lu CM was also evaluated to compare with that of SF-MSC CM^{DMEM} (Table S4.1, Appendix-2). Based on biological relevance to epithelial wound repair Fibronectin, Lumican, Periostin, IGFBP-7 and MMP-2 candidate proteins were chosen from the list of the whole MSC secretome (Table 4.1) to evaluate their reparative effects on *in vitro* AEC wound. My primary target cell type was alveolar A549 cell; however, I replicated equivalent experiments on SAEC to compare and contrast the wound repair responses to the paracrine stimuli of above mentioned commonly identified hMSC-secreted candidate proteins (Table 2.3, 4.1) (Section- 2.7.7).

Fibronectin displayed no effect on alveolar A549 cell wound repair rate when added to serum-free medium; however, when supplemented with 0.2% FBS, it significantly increased A549 cell wound repair (Figure 4.8A and 4.8C). Fibronectin-induced wound repair was maximal at a concentration of 100 ng/ml when compared to the corresponding control medium (NC) (51 ± 6.73% vs. 34 ± 6.26% NC (0.2% FBS supplemented DMEM); $p<0.001$) (Figure 4.8A). On the other hand, Fibronectin significantly increased SAEC wound repair without an additional serum supplementation requirement (Figure 4.8B and 4.8D). Fibronectin displayed a maximal wound repair effect on SAEC with a 100 ng/ml concentration (73 ± 12.90% vs. 49 ± 8.54% NC (SABM); $p<0.05$) (Figure 4.8B).

Lumican also displayed no effect on A549 cell wound repair in serum-free medium; however, when supplemented with 0.2% FBS they significantly increased A549 cell wound repair after 24 hours (Figure 4.9A and 4.9C). Lumican displayed maximal A549 cell wound repair effect at 1 ng/ml concentration (59 ± 9.09% vs. 30 ± 3.55% NC (0.2% FBS supplemented DMEM); $p<0.001$) (Figure 4.9A). Like Fibronectin, Lumican significantly increased SAEC wound repair without an additional serum supplementation requirement (Figure 4.9B, 4.9D) where it displayed significant wound repair effect at a concentration of 100 ng/ml (92 ± 6.55% vs. 54 ± 12.39% NC (SABM); $p<0.001$) (Figure 4.9B, 4.9D). However, a significant SAEC wound repair response was observed at a minimum concentration of 1ng/ml Lumican (73 ± 11.83% vs. 54 ± 12.39% NC (SABM); $p<0.01$) (Figure 4.9B).

Unlike Fibronectin and Lumican, Periostin significantly enhanced alveolar A549 cell wound repair without any additional supplementation where a maximal effect was observed with a 100 ng/ml concentration in serum-free medium (50 ± 4.50% vs. 29 ± 2.43% NC (SF-DMEM); $p<0.01$) (Figure 4.10A, 4.10C). Periostin also enhanced alveolar A549 cell wound repair when supplemented with 0.2% FBS, where a minimum concentration of Periostin at 10 ng/ml elicited significant wound repair response (53 ± 6.48% vs. 32 ± 2.06% NC (0.2% FBS supplemented DMEM); $p<0.01$) (Figure 4.10A, 4.10C). A maximum wound repair response, however, observed at a concentration of 1 µg/ml Periostin when supplemented with 0.2% FBS (61 ± 11.00% vs. 32 ± 2.06% NC (0.2% FBS supplemented DMEM); $p<0.001$) (Figure 4.10A, 4.10C). Periostin also enhanced SAEC wound repair in serum-free basal medium (90 ± 5.20% vs. 62 ± 15.97% NC (SABM); $p<0.05$) (Figure 4.10B).

On the other hand, IGFBP-7 (Insulin-like growth factor binding protein-7) showed no significant effect on A549 cell wound repair (Figure 4.11A); whereas, SAEC wound repair was significantly stimulated by all tested concentrations of IGFBP-7 in serum-free basal media where a maximum effect was observed with 100 ng/ml concentration (95 ± 3.51% vs. 53 ± 13.38% (SABM); $p<0.001$) (Figure 4.11B, 4.11C). A significant SAEC wound repair effect was observed at a minimum concentration of 1 ng/ml IGFBP-7 comparing control (85 ± 6.30% vs. 53 ± 13.38% NC (SABM); $p<0.01$) (Figure 4.11B, 4.11C). Gelatinase A (MMP2) had no discernable effect on A549 cell wound repair irrespective of the presence of 0.2% FBS in the media (Figure 4.12).

Table 4.1: Protein components of SF-MSC CM detected by LC-MS/MS mass spectrometry. SF-MSC CM preparation was as described in Section- 2.4.2, 2.5. Proteins selected for investigations in wound repair and migration are indicated in bold. Accession numbers are derived from MS/MS data searches against non-redundant Human NCBI Protein Database. Average peptide count from 3 biologically independent replicates of hMSC secretome profiles.

Protein name	Accession number	Peptide count
Fibronectin 1, isoform CRA	**gi|119590945**	**39.0**
Collagen alpha-2(I) chain	gi|124056488	30.0
Collagen alpha 1 chain precursor variant	gi|62088774	23.5
Pro alpha 1(I) collagen	gi|186893270	23.5
Alpha 1 (I) chain propeptide	gi|180392	21.3
Collagen, type VI, alpha 1 precursor	gi|87196339	11.0
Precursor polypeptide (AA -31 to 1139)	gi|37465	7.5
Actin, gamma 1 propeptide	gi|4501887	7.0
Gelatinase A	**gi|5822007**	**6.7**
Keratin 1	gi|7331218	6.5
Tumor necrosis factor	gi|339992	6.3
Osteoblast specific factor 2 (Periostin)	**gi|393319**	**6.0**
Chain A, Crystal Structure Of The Thrombospondin-1	gi|88191917	5.5
Biglycan	gi|179433	4.7
Lumican	**gi|642534**	**4.7**
Collagen alpha 1(V) chain precursor	gi|219510	4.5
Insulin-like growth factor binding protein 7	**gi|119625925**	**4.5**
CALU	gi|49456627	4.0
Thrombospondin 2 precursor	gi|40317628	4.0
Fructose-bisphosphate aldolase A	gi|4557305	3.5
Heparan sulfate proteoglycan	gi|184427	3.5
Pigment epithelium-derived factor	gi|1144299	3.5
Profilin Binds Proline	gi|5822002	3.0
Protein disulfide isomerase	gi|860986	3.0
Versican isoform 3 precursor	gi|255918077	3.0
Decorin	gi|181519	2.7
The Antigenic Identity Of Peptide(Slash)mhc Complexes	gi|442989	2.5
COL1A1 and PDGFB fusion transcript	gi|3288487	2.5
Peptidylprolyl isomerase A	gi|10863927	2.5
Fibrillin	gi|306746	2.0
Similar to cardiac leiomodin	gi|51095092	2.0
Solution Structure Of Calcium-Calmodulin N-Terminal Domain	gi|16974825	1.7
Myosin, light chain 6, alkali, smooth muscle and non-muscle isoform 1	gi|17986258	1.5
Protein disulfide-isomerase A3	gi|729433	1.5
Insulin-like growth factor binding protein 6	gi|183894	1.0

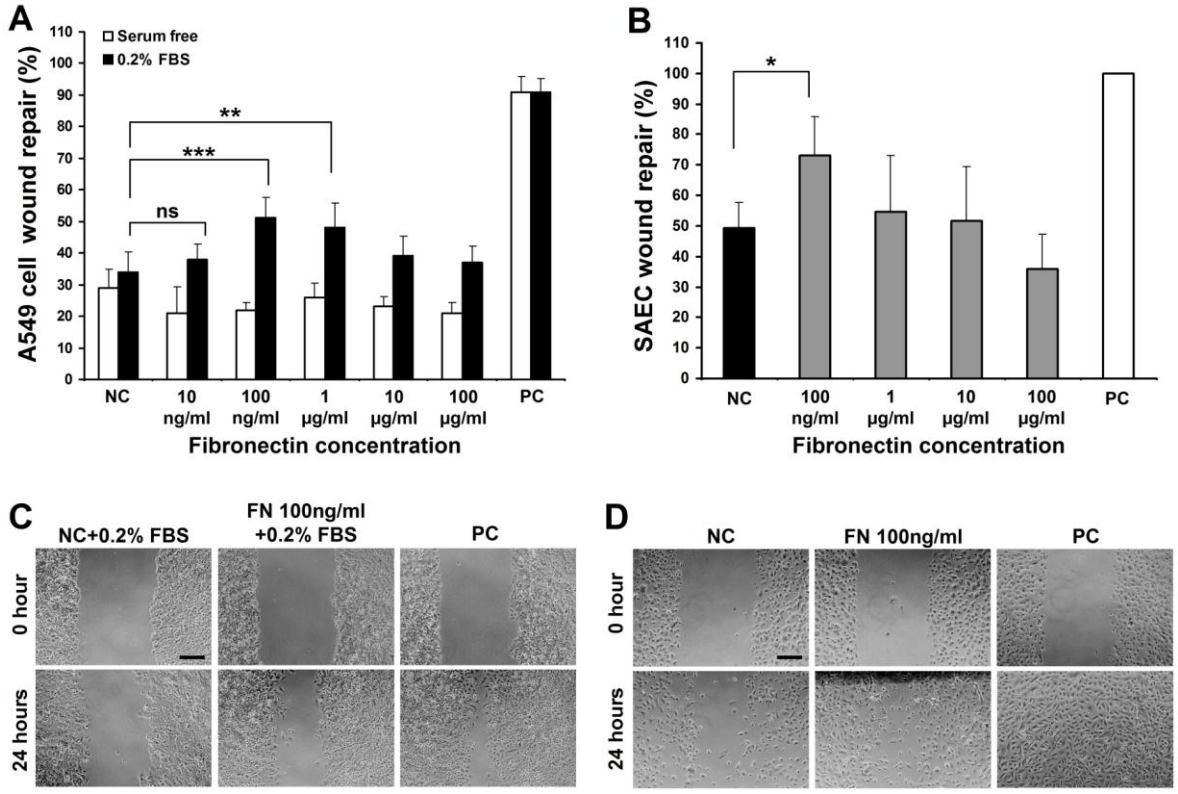

Figure 4.8: Alveolar A549 cell and SAEC wound repair assay with Fibronectin.

(**A**) Alveolar A549 cell wound repair after 24 hours with recombinant human plasma Fibronectin in serum-free condition (open bars) and with 0.2% FBS supplementation (black bars) (n = 6 independent experiments). Negative control (NC) and Positive control (PC) indicate wound repair with SF-DMEM and DMEM + 10% FBS respectively. (**B**) SAEC wound repair after 24 hours with recombinant human plasma Fibronectin in SF-SABM (grey bar). Negative control (NC) (black bar) and Positive control (PC) (open bar) indicate wound repair with SF-SABM and SAGM respectively. (n = 6 independent experiments). (**C**) Inverted light microscopic images of alveolar A549 cell wound repair with 100 ng/ml Fibronectin (FN) in 0.2% FBS supplemented media. (**D**) Inverted light microscopic images of SAEC wound repair with 100 ng/ml Fibronectin (FN) in serum-free SABM. Data presented as mean ± SD. *p<0.05, **p<0.01, ***p<0.001. ns = not significant. Scale bar, 200 µm.

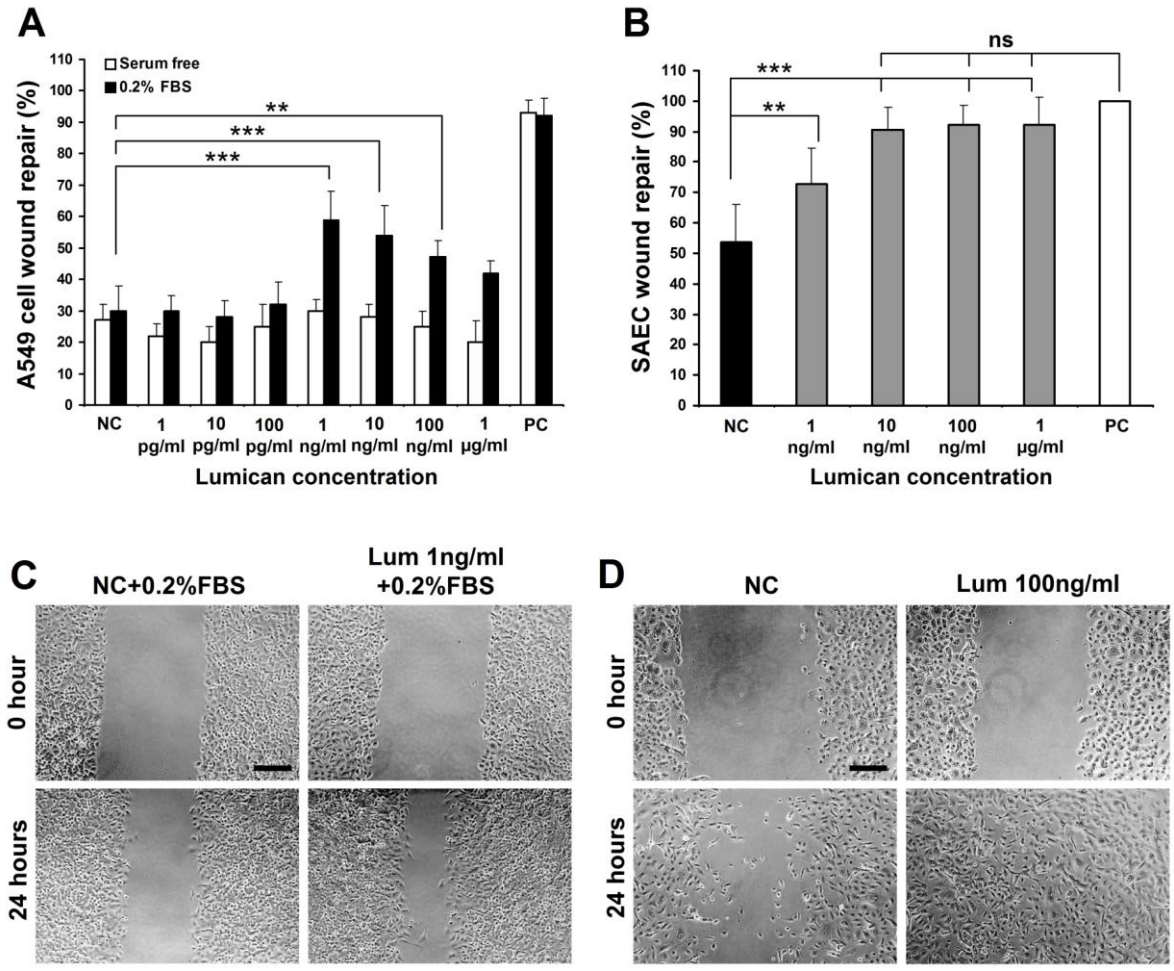

Figure 4.9: Alveolar A549 cell and SAEC wound repair assay with Lumican.

(**A**) Alveolar A549 cell wound repair after 24 hours with recombinant human Lumican in serum-free condition (open bars) and with 0.2% FBS supplementation (black bars). Negative control (NC) and Positive control (PC) indicate wound repair with SF-DMEM and DMEM + 10% FBS respectively. (n = 3 independent experiments, 3 replicates per n). (**B**) SAEC wound repair after 24 hours with recombinant human Lumican. Negative control (NC) (black bar) and Positive control (PC) (open bar) indicate wound repair with SF-SABM and SAGM respectively. (n = 3 independent experiments, duplicate per n). (**C**) Inverted light microscopic images of alveolar A549 cell wound repair with 1 ng/ml Lumican (Lum) in 0.2% FBS supplemented media. (**D**) Inverted light microscopic images of SAEC wound repair with 100 ng/ml Lumican (Lum) in serum-free SABM. Data presented as mean ± SD. **p<0.01, ***p<0.001. ns = not significant. Scale bar, 200 µm.

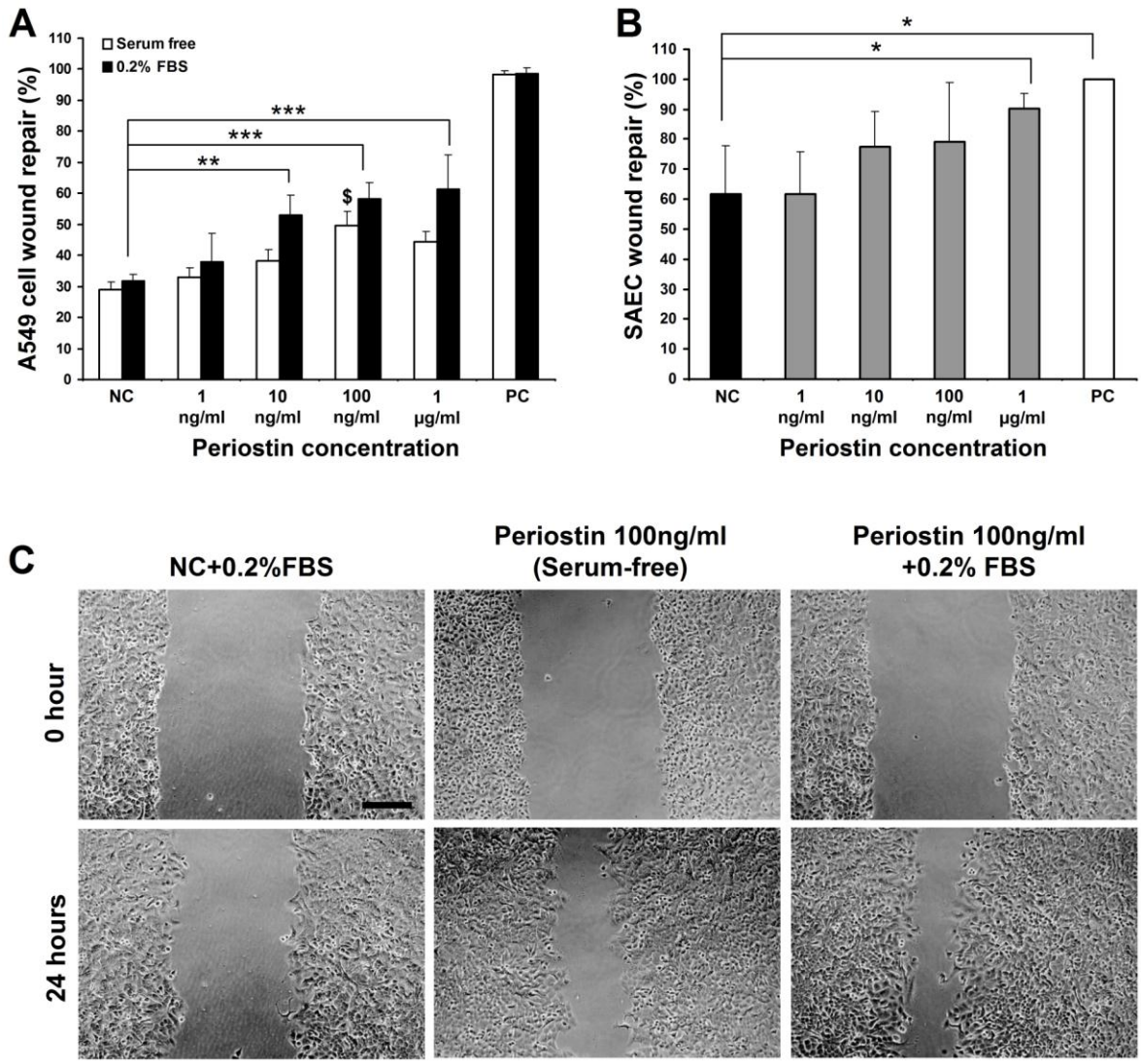

Figure 4.10: Alveolar A549 cell and SAEC wound repair assay with Periostin.

(**A**) Alveolar A549 cell wound repair after 24 hours with recombinant human Periostin in serum-free condition (open bars) and with 0.2% FBS supplementation (black bars). Negative control (NC) and Positive control (PC) indicate wound repair with SF-DMEM and DMEM + 10% FBS respectively. (n = 4, ≥2 replicates per n, $^{\$}p<0.001$ vs corresponding serum-free NC). (**B**) SAEC wound repair after 24 hours with recombinant human Periostin in SF-SABM. Negative control (NC) (black bar) and Positive control (PC) (open bar) indicate wound repair with SF-SABM and SAGM respectively. (n = 6 independent experiments). (**C**) Inverted light microscopic images of alveolar A549 cell wound repair with 100 ng/ml Periostin in serum-free and 0.2% FBS supplemented media. Data presented as mean ± SD. *p<0.05, **p<0.01, ***p<0.001. ns = not significant. Scale bar, 200 µm.

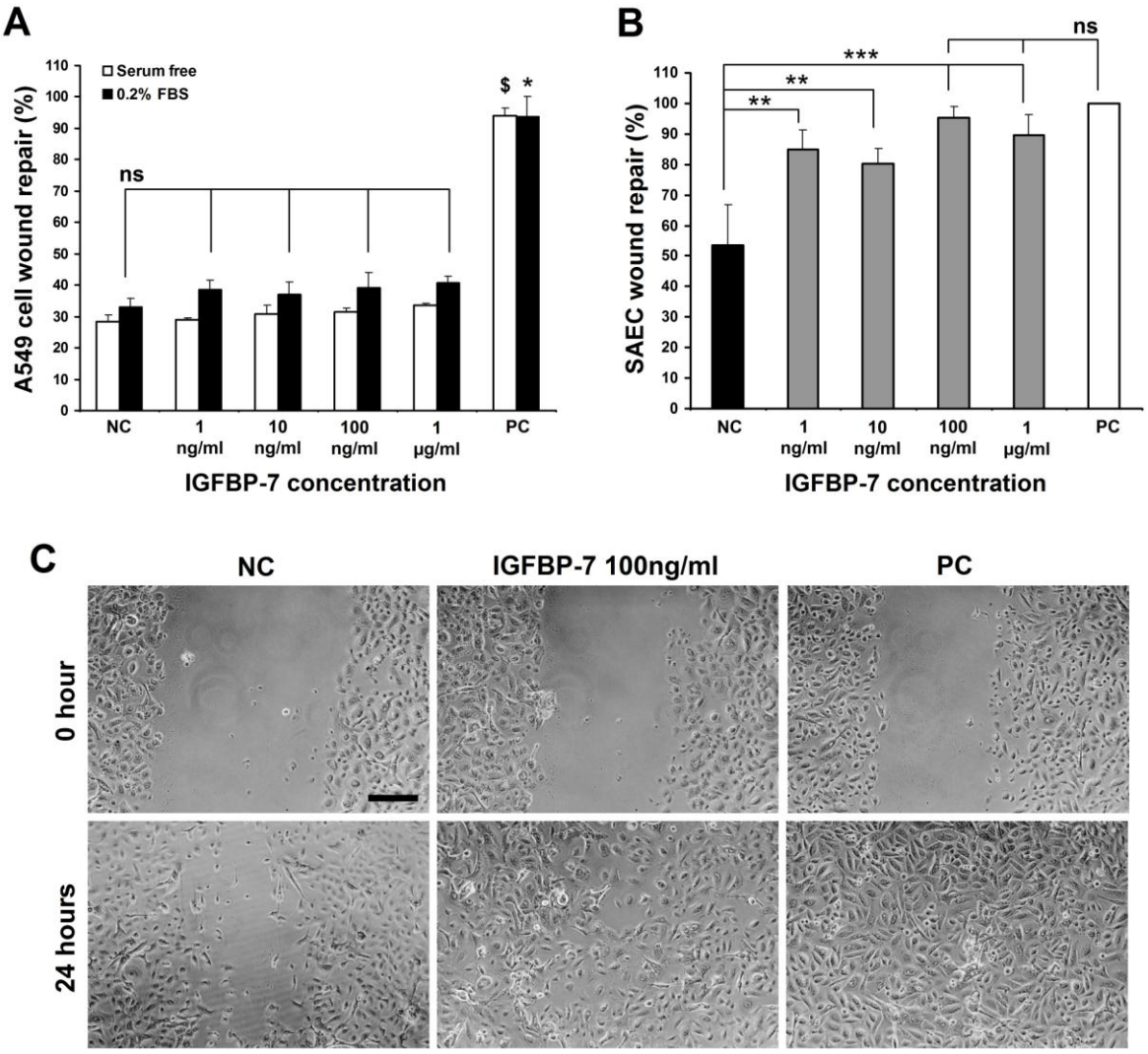

Figure 4.11: Alveolar A549 cell and SAEC wound repair assay with IGFBP-7.

(**A**) Alveolar A549 cell wound repair after 24 hours with recombinant human IGFBP-7 in serum-free (open bars) and with 0.2% FBS supplementation (black bars). Negative control (NC) and Positive control (PC) indicate wound repair with SF-DMEM and DMEM + 10% FBS respectively. (n = 3 independent experiments, 3 replicates per n; *$p<0.001$ vs 0.2% FBS supplemented NC, $^{\$}p<0.001$ vs serum-free NC). (**B**) SAEC wound repair after 24 hours with recombinant human IGFBP-7 in SF-SABM. Negative control (NC) (black bar) and Positive control (PC) (open bar) indicate wound repair with SF-SABM and SAGM respectively. (n = 6 independent experiments; **$p<0.01$, ***$p<0.001$). (**C**) Inverted light microscopic images of SAEC wound repair with 100 ng/ml IGFBP-7 in serum-free SABM. Data presented as mean ± SD. ns = not significant. Scale bar, 200 µm.

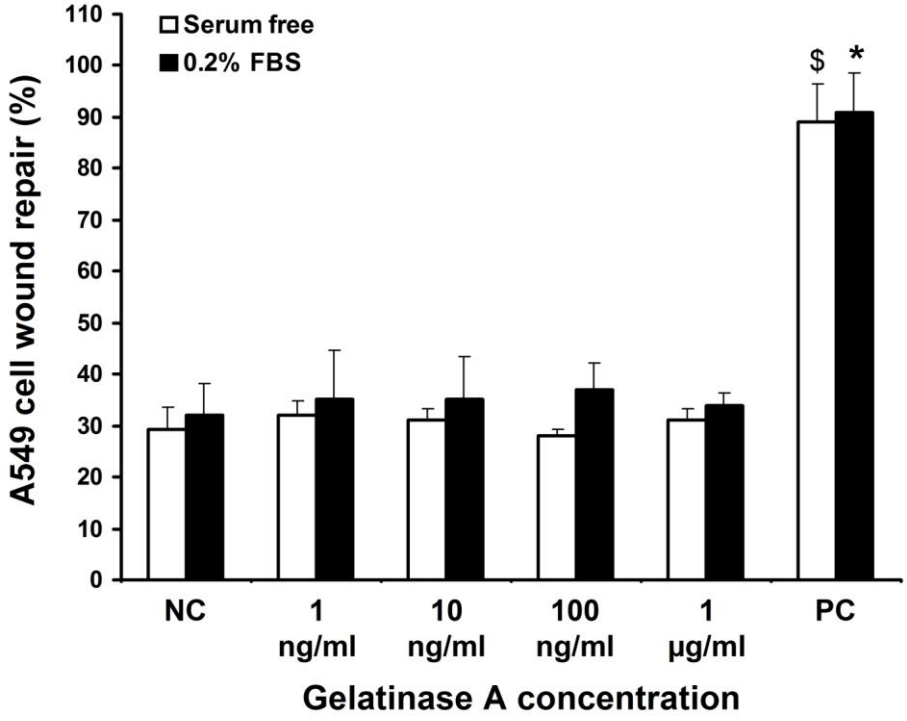

Figure 4.12: Alveolar A549 cell wound repair assay with Gelatinase A.

Alveolar A549 cell wound repair after 24 hours with recombinant human Gelatinase A (MMP-2) in serum-free (open bars) and with 0.2% FBS supplementation (black bars). Negative control (NC) and Positive control (PC) indicate wound repair with SF-DMEM and DMEM + 10% FBS respectively. (n = 3 independent experiments). Data presented as mean ± SD. *$p<0.001$ vs 0.2% FBS supplemented NC, \$$p<0.001$ vs serum-free NC.

4.3.5. Fibronectin, Lumican and Periostin-mediated alveolar A549 cell wound repair occurs through cell migration

Earlier, I demonstrated that Fibronectin and Lumican required 0.2% FBS to stimulate A549 cell wound repair; whereas, Periostin enhanced wound repair in serum-free condition. Here, by performing the MTT assay, I investigated whether this observed wound repair was driven by cell proliferation or migration (Section 2.9). The MTT data showed that none of the tested candidate proteins (Fibronectin, 100 ng/ml; Lumican, 1 ng/ml; Periostin, 100 ng/ml; IGFBP-7, 100 ng/ml) increased A549 cell proliferation after 24 hours during wound repair (Figure 4.13). In addition, supplementation of 0.2% FBS with the candidate proteins also did not show any significant effect on cell proliferation (Figure 4.13). However, the A549 cell proliferation was significantly higher in positive control (PC) when compared with negative control and all other groups ($p<0.05$ vs. all other groups) (Figure 4.13). In this assessment, the tested dose of individual protein was the effective wound repair dose that was determined in previous separate experiment (Section 4.3.4). Taken together, it concludes that Fibronectin, Lumican and Periostin stimulate alveolar epithelial wound repair through cell migration but not by cell proliferation.

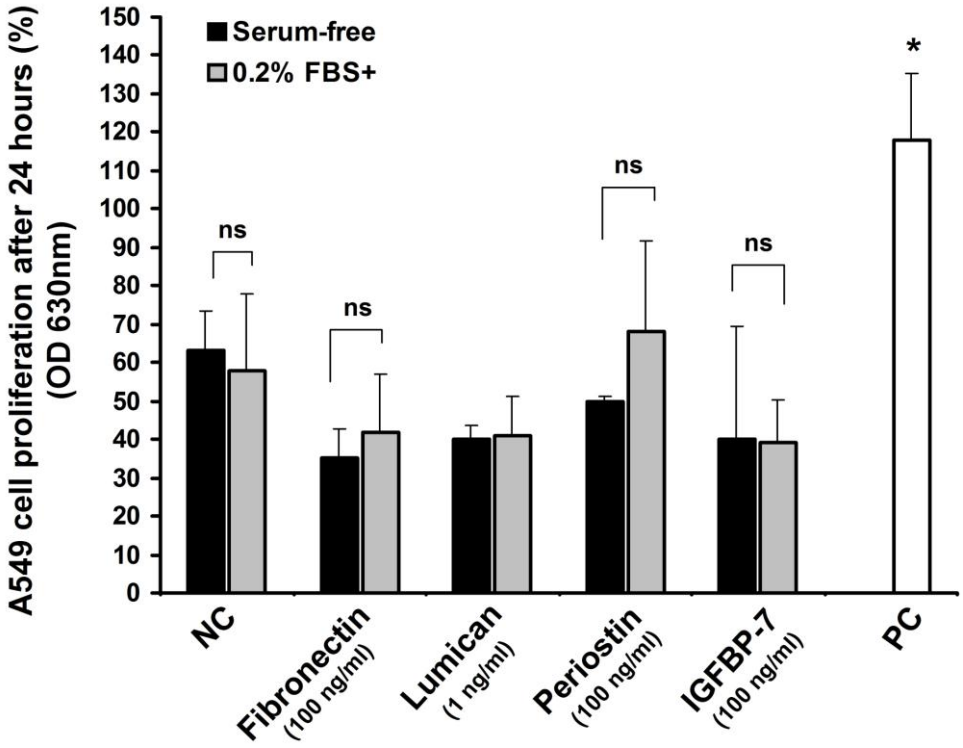

Figure 4.13: MTT cell proliferation assay on A549 cell wound repair with candidate proteins. Recombinant human proteins Fibronectin, Lumican, Periostin and IGFBP-7 did not stimulate A549 cell proliferation in serum free (black bars) or in 0.2% FBS supplemented media (grey bars) after 24 hours of wound repair. NC (Negative control) represents serum-free (black bar) or 0.2% FBS supplemented (grey bar) DMEM treated sample. PC (Positive control) was DMEM supplemented with 10% FBS (open bar) treated sample that significantly increased A549 cell proliferation after 24 hours of wounding comparing all other samples (n = 3 independent experiments). Data presented as mean ± SD. *$p<0.05$ vs all other groups, ns=not significant.

4.3.6. Periostin and Lumican display a significant correlation in alveolar epithelial cell and SAEC wound repair response

The correlation between concentrations of the above tested proteins and their wound repair responses were evaluated by non-parametric Spearman correlation coefficient assessment (Moine et al., 1997, Park et al., 2011) (Section- 2.14). Periostin enhanced alveolar A549 cell wound repair in both serum-free and 0.2% FBS supplemented media; however, a strong correlation between the concentrations and wound repair rate was observed when this protein was applied in 0.2% FBS supplemented media (Spearman correlation coefficient, r = 1.000; p=0.016) (Figure 4.14A; Table 4.2). Periostin also showed a strong correlation with SAEC wound repair in serum-free basal medium (Spearman r = 0.9747; p=0.0176) (Figure 4.14B; Table 4.2).

A strong correlation between Lumican and its wound repair effect on SAEC was noted (Spearman r = 0.9747; p=0.0167) (Figure 4.14C; Table 4.2). However, although Fibronectin and Lumican displayed a critical optimal concentration for maximal A549 cell wound repair response, no significant concentration-response correlation was established; similarly, Fibronectin failed to show the significant correlation on SAEC wound repair (Table 4.2). IGFBP-7 displayed significant SAEC wound repair across all tested concentrations (1 ng/ml to 1µg/ml) (Figure 4.11B) without any demonstrable correlation (Table 4.2).

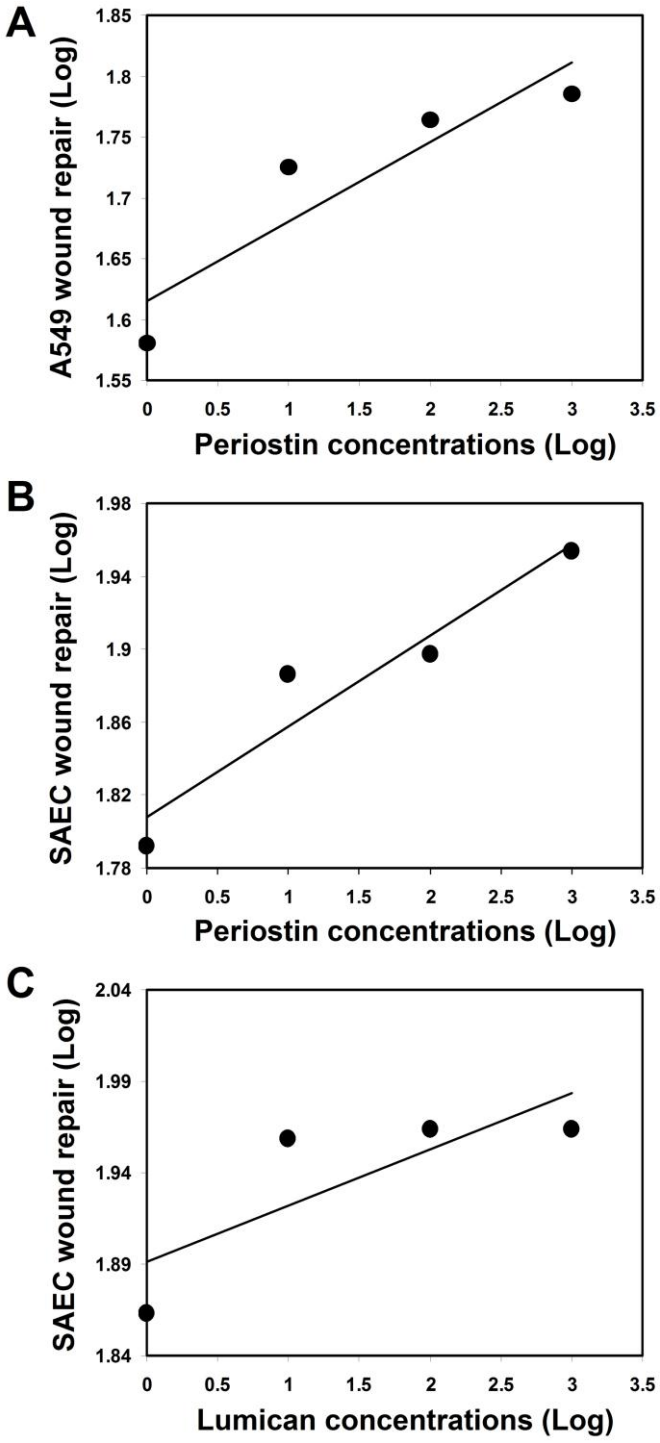

Figure 4.14: Correlation effects of proteins on wound repair rate.

(**A**) Correlation between Periostin concentrations and A549 cell wound repair responses in 0.2% FBS supplemented DMEM. Spearman correlation coefficient, r = 1.000; p=0.016. (**B**) Correlation between Periostin concentrations and SAEC wound repair responses. Spearman r = 0.9747; p=0.0176. (**C**) Correlation between Lumican concentrations and SAEC wound repair responses. Spearman r = 0.9747; p=0.0167. Data are plotted on logarithmic-logarithmic scale to allow better representation.

Table 4.2: Determination of correlation coefficient between recombinant human protein treatment and *in vitro* wound repair responses of alveolar A549 and SAEC wounds.

A549 SAEC wound repair were performed in 0.2% FBS supplemented DMEM and serum-free SABM. Correlation coefficient was determined by non-parametric Spearman analysis.

Protein	Cell type	Spearman 'r'	P value	Is correlation significant
Fibronectin	A549	0.2000	0.7139	No
	SAEC	-0.4000	0.5167	No
Lumican	A549	0.0000	1.0500	No
	SAEC	**0.9747**	**0.0167**	**Yes**
Periostin	**A549**	**1.0000**	**0.0167**	**Yes**
	SAEC	**0.9747**	**0.0167**	**Yes**
IGFBP-7	A549	N/A	N/A	N/A
	SAEC	0.8000	0.1333	No

4.3.7. Fibronectin and Lumican but not Periostin stimulate alveolar A549 cell migration as substrate components

Fibronectin, Lumican and Periostin induced alveolar A549 cell wound repair when delivered as a culture medium supplement. As these proteins are abundant within the ECM, I hypothesised that these proteins could influence A549 cell migration as substrate components. Immediate relevance to fibrotic lung disease is evidenced by the abrogation of effective AEC migration over denuded alveolar epithelium. To test this hypothesis, I developed a 'collagen drop' cell migration assay, where an aggregated population of alveolar A549 cells were resuspended in a drop of collagen which was 'dropped' onto a culture surface coated with Fibronectin, Lumican, or Periostin (Section- 2.13) (Figure 2.13). To provide an additional 'positive' bias to A549 cell migration, the collagen drop contained 0.2% FBS whereas the external serum concentration was 20% (Figure 2.13).

Optimal cell migration was observed on either Fibronectin or Lumican coated surfaces at a concentration of 10 ng/ml (Fibronectin 28 ± 11.10 cells/mm vs. 7 ± 1.52 cells/mm (uncoated surface), $p<0.001$; Lumican 31 ± 6.85 cells/mm vs. 6 ± 1.38 cells/mm (uncoated surface), $p<0.001$) (Figure 4.15A, 4.15B, 4.15C, 4.15F). On the other hand, Periostin did not stimulate A549 cell migration (Figure 4.15A, 4.15D). Taken together, this data indicates that Fibronectin and Lumican stimulate alveolar A549 cell wound repair as both soluble factors and as a substrate component; whereas, Periostin stimulates A549 cell wound repair as a soluble factor only.

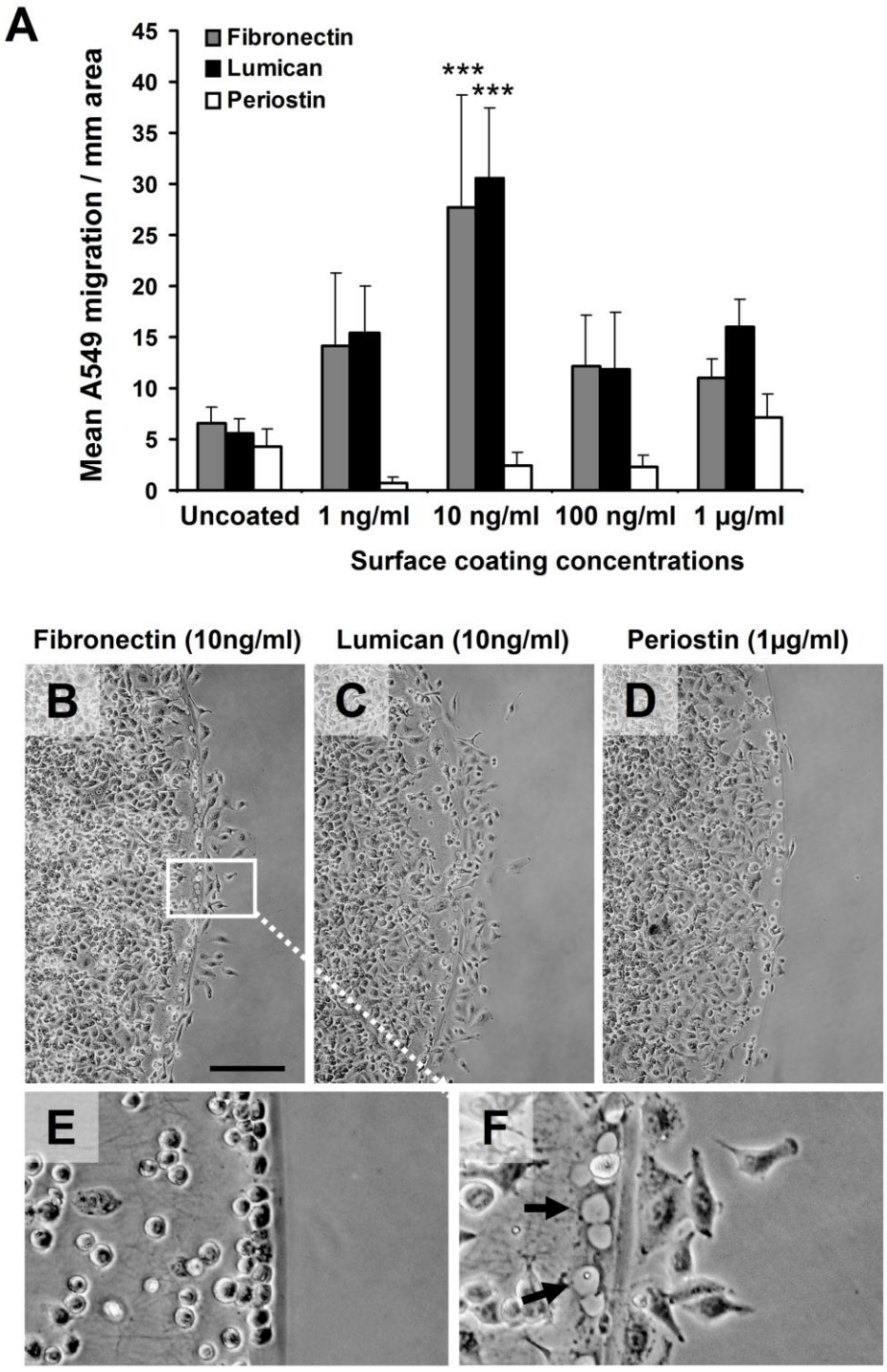

Figure 4.15: Collagen drop alveolar A549 cell migration assay

(**A**) Fibronectin and Lumican coating at various concentration stimulate alveolar A549 cell migration (Fibronectin, n = 3 independent experiments; Lumican, n = 6 independent experiments). Periostin coating did not stimulate A549 cell migration (n = 6 independent experiments). (**B, C, D**) Inverted light microscopic images of A549 cell migration across the collagen-drop barrier on protein coated surfaces. (**E, F**) Enlarged images of cell migration on Fibronectin coated surface at 0 hr and 24 hrs respectively showing impression of cells in collagen (arrows). Data presented as mean ± SD. ***$p<0.001$. Scale bar, 250 µm.

4.4. Discussion

Human mesenchymal stem cells are in current clinical trials for diseases including osteogenesis imperfecta, graft-versus-host disease, chronic ischemic heart disease, and chronic obstructive pulmonary disease (www.clinicaltrials.gov) and are the focus of many other clinical applications. Studies on animal pulmonary fibrosis models demonstrate that intravenous and endotracheal administration of MSC attenuate lung injury and fibrosis suggesting a potential clinical application of MSC for the treatment of IPF (Rojas et al., 2005, Ortiz et al., 2003, Moodley et al., 2009). However, the mechanism of MSC-mediated amelioration of pulmonary fibrosis is not clear and an active participation of MSC through differentiation into AEC and lung regeneration is under debate (Ortiz et al., 2003, Neuringer & Randell, 2006). Bleomycin-induced mouse lung fibrosis models have demonstrated an MSC-stimulated reduction in pulmonary fibrosis via inhibition of pro-fibrotic cytokines TNF-α and IL-1 through a paracrine mechanism (Ortiz et al., 2007). Furthermore, rat models of pulmonary emphysema demonstrated that MSC reduce AEC apoptosis through paracrine mechanism via up-regulation of anti-apoptotic Bcl-2 gene (Zhen et al., 2008). Here, I demonstrate that in response to injury hMSC display site-specific migration into alveolar epithelial wounds and that in response to SF-MSC CM migration and wound repair (A549 cell and SAEC) occur with distinct trace serum augmentation requirements. I also provide evidence supporting specific hMSC-secreted paracrine components for effective alveolar and small airway epithelial wound repair.

hMSC secrete a myriad of proteins that include growth factors, cytokines and ECM proteins (Chen et al., 2008a, Estrada et al., 2009). Many of these secretory proteins are biologically active with anti-inflammatory, anti-fibrotic and immunomodulatory functions (Meirelles et al., 2009, Nauta & Fibbe, 2007). Previous and current studies are mostly

focused on evaluation of MSC-secreted growth factors and their effects on tissue repair. Here, in line with others, my mass spectrometry-mediated hMSC secretome analyses indicate the presence of a high abundance of ECM/matricellular protein components with diverse biological activities on wound healing and tissue repair (Estrada et al., 2009, Walter et al., 2010). Fibronectin (a multifunctional glycoprotein), Lumican (collagen-binding keratin sulfate proteoglycan), Periostin (matricellular N-glycoprotein), and IGFBP-7 (IGF-I, -II low affinity binding protein) were identified as major components of SF-MSC CM through high peptide counts and ion score confidence intervals (Table 4.1). Data supportive of a role for these factors in alveolar wound repair is relatively scarce though implied in previous studies. Fibronectin up-regulation is implicated in abdominal wall, corneal, and skin *in vivo* and *ex vivo* wound repair and migration where values ranging from 100 ng/ml to 60µg/ml of Fibronectin have been evaluated (Fujikawa et al., 1981, Grinnell et al., 1981, Nishida et al., 1983, Cheng et al., 1988, Kwon et al., 2007). *In vitro* models including corneal epithelial cells, corneal fibroblasts, keratinocyte, dermal fibroblast, nasal airway epithelial cells, gingival fibroblast, and SAEC have further demonstrated that fibronectin stimulated wound repair and cell migration as either soluble factor or substrate component frequently through integrin signaling activation (Dean & Blankenship, 1997, Herard et al., 1996, Hocking & Chang, 2003, Nishida et al., 1992, Schmidinger et al., 2003, Yamada, 2000).

Lumican, a small leucine-rich proteoglycan (SLRP) family member, is a major component of the proteoglycan-based ECM. Lumican displays a heterogeneous, diffuse, staining profile in the alveolar walls and peripheral regions of adult human lung and its sub-epithelial deposition is implicated in airway remodeling and counteracting the severity of asthma (Dolhnikoff et al., 1998, Pini et al., 2007). *In vivo* and *ex vivo* studies indicate that

Lumican is essential for corneal epithelial cell, skin, and oral mucosa wound repair and promotion of chemotactic migration (Honardoust et al., 2008, Lee et al., 2009b, Saika et al., 2000, Yeh et al., 2010). *In vitro* migration and wound healing of corneal epithelial cells was also induced by Lumican (Seomun & Joo, 2008, Yeh et al., 2005). Circulating plasma and cellular Fibronectin concentrations (300 µg/ml and 2.46 µg/ml, respectively) are substantially in excess of those required to induce wound repair and migration in my, and previously described (see above), *in vitro* models; whereas, physiological levels of Lumican are yet to be defined (Ylatupa et al., 1995). In support and extension of these previous reports, I have now demonstrated that both Fibronectin and Lumican facilitated alveolar A549 cell and SAEC wound repair as soluble factors (with trace serum supplementation for A549 cell only) and migration of A549 cells as a substrate component.

Periostin (or OSF-2, Osteoblast Specific Factor-2) is a matricellular protein with a poorly defined role in wound repair and a physiological serum level of approximately 39 ng/ml (Hamilton, 2008, Okamoto et al., 2011). *In vivo* studies revealed an association of Periostin with fracture healing, wound-derived blood vessels, acute myocardial infarction response, skin wounds, and ligament repair (Chamberlain et al., 2011, Jackson-Boeters et al., 2009, Nakazawa et al., 2004, Nishiyama et al., 2011, Shimazaki et al., 2008, Zhou et al., 2010). In addition to those above, low levels of Periostin expression are common in normal lung while high levels of Periostin are detected in IPF lungs and patient serum, although the role of this protein in the pathogenesis of lung fibrosis has not been clarified (Okamoto et al., 2011). A relationship between Periostin and wound repair across multiple tissues is immediately apparent though little is known, at this time, of mechanism of action. A solitary report describes exogenous overexpression of Periostin in A549 cells, as used in our study, which enhanced both proliferation and migration in routine culture (Hong et al.,

2010). I have, herein, reported that Periostin has a role in alveolar A549 cell and SAEC wound repair and migration as a soluble factor and identified a putative hMSC source of wound associated Periostin.

IGFBP-7 (also known as IGFBP-rP1) is an IGFBP-related protein (IGFBP-rPs) superfamily member. IGFBP-rPs have less binding affinity to IGF (insulin growth factor) and are involved in diverse biological activities in an IGF-independent manner (Hwa et al., 1999). IGFBP-rP2 (CTGF, connective tissue growth factor), another IGFBP-rP family member, plays a critical role during fibrogenesis in IPF (Allen et al., 1999, Pan et al., 2001). However, the role of IGFBP-7, which has a normal serum concentration of 33 ng/ml (Kutsukake et al., 2008), in pulmonary fibrosis is unknown. IGFBP-7 is up-regulated in the fibrotic regions of IPF lung tissue as well as in isolated IPF fibroblasts though absent from controls (Hsu et al., 2011). Here, I have demonstrated that recombinant human IGFBP-7 significantly increased human primary SAEC wound repair when applied in serum-free basal media; whereas, alveolar A549 cells were non-responsive to this protein. The mechanism behind these divergent responses remains to be clarified. The development of transferable and accessible primary human AEC cultures (which replicate *in vivo* characteristics; i.e. monolayer formation) will be necessary before clarification can be achieved. However, at this time I cannot preclude the possibility that the distinct response is due tissue source or phenotypic background of the AEC and SAEC used in this study. However, this distinction in response provides strong support for broad therapeutic applicability across multiple clinical applications for the hMSC secretome. Characterization of these cell-specific responses will underpin the continuing development of the stem cell-driven regenerative medicine industry.

The protein composition of ECM is variable, tissue specific, and provides essential scaffold and biochemical signals required for cell growth, tissue homeostasis, development and wound repair (Hamilton, 2008, Frantz et al., 2010). My *in vitro* alveolar A549 cell wound repair data encouraged us to investigate the substrate roles of Fibronectin, Lumican and Periostin on A549 cell migration. The *in vitro* scratch wound repair system is not suitable to test the effectiveness of individual substrate components as the wounding process would disrupt the protein coating. Therefore, I developed a novel 'collagen drop' cell migration assay to evaluate individual substrate component capacity to support or inhibit migration (Section- 2.13). Normal basement membrane architecture provides a favourable substrate for AEC migration; whereas, disrupted alveolar basement membrane and aberrant ECM remodeling play a crucial role in the abrogation of alveolar re-epithelialisation in pulmonary fibrosis (Selman et al., 2001). Data from my 'collagen drop' cell migration assay has identified that both Fibronectin and Lumican are supportive of cell migration as substrate component. This has potential implications in strategy development to address repair of the disrupted alveolar basement membrane in pulmonary fibrosis.

These data provide insight into potential hMSC paracrine influences on epithelial wound repair during alveolar injury repair. Aberrant alveolar re-epithelialisation is believed to be one of the major contributing factors for uncontrolled fibrogenesis in IPF (Selman et al., 2001). Therefore, stimulation of re-epithelialisation within the alveolar regions could be a potential active vector for alleviation of the pro-fibrogenic processes as a curative therapeutic measure for IPF. Previous animal model-based studies demonstrated that MSC-paracrine factors attenuate pulmonary fibrosis through modulation of inflammation, suppression of fibrogenesis and stimulation of angiogenesis (Ortiz et al., 2007, Chen et al., 2008a, Estrada et al., 2009, Moodley et al., 2009). Here, I have demonstrated the

efficacious influence of the hMSC secretome in the modulation of alveolar and small airway epithelial cell dynamics resulting in stimulation of wound repair. In-depth understanding of the humoral mechanisms of hMSC in epithelial wound repair and regeneration will provide extended therapeutic options for clinical application of hMSC or their secretory products for fibrotic lung diseases, such as IPF.

Chapter 5

Activin-directed differentiation of hESC enhances alveolar epithelial wound repair via distinct paracrine mechanisms *in vitro*

5.1. Background

Embryonic stem cells (ESC) are self-renewing pluripotent stem cells derived from the inner cell mass of a 5-6 day-old blastocyst of an early mammalian embryo and are capable of unlimited, undifferentiated proliferation *in vitro*. Unlike adult stem cells, ESC are capable of differentiating into tissues of all three germ layers (Evans & Kaufman, 1981, Kaufman et al., 1983) (Martin, 1981). Pluripotent hESC lines express a set of antigens including SSEA-3, SSEA-4, TRA-1-60, TRA-1-81, the enzyme alkaline phosphatase (ALP), transcription factors Oct-4 and Nanog, and display high levels of telomerase activity (Thomson et al., 1998, Reubinoff et al., 2000, Henderson et al., 2002, Laslett et al., 2003).

hESC lines maintain a pluripotent differentiation potential enabling formation of cell types representative of all three embryonic germ layers. The pluripotency of hESC is demonstrated *in vivo* through teratoma development after injection into the SCID (severe combined immunodeficient) mice (Thomson et al., 1998). Teratoma is a germ layer benign tumour comprised of endodermal derivatives, such as gut epithelium; mesodermal derivatives, such as bone, cartilage, smooth muscle, striated muscle and ectodermal derivatives such as neural epithelium, embryonic ganglia, and stratified squamous epithelium (Thomson et al., 1998). Embryonic stem cells also can differentiate into derivatives of all three germ layers when allowed to undergo spontaneous differentiation in *in vitro* culture, either as adherent monolayer or EB suspension culture (Itskovitz-Eldor et al., 2000, Heo et al., 2005). However, differentiation of ESC into definitive ectodermal, mesodermal and endodermal lineages is difficult. Successful derivation of cardiomyocytes or neuronal cells from ESC has already been described (Mummery et al., 2002, Mummery et al., 2003, Ying et al., 2003, Shin et al., 2005, Abranches et al., 2009). Meanwhile,

definitive endodermal lineage differentiation has appeared to be more challenging and the protocols are currently evolving. The definitive endoderm forms during gastrulation, in which pluripotent epiblast cells are localised to the three principle embryonic germ layers- ectoderm, mesoderm and definitive endoderm. The definitive endoderm gives rise to the epithelium of lung, intestine, liver, pancreas, thyroid glands and thymus (D'Amour et al., 2005) (Figure 5.1).

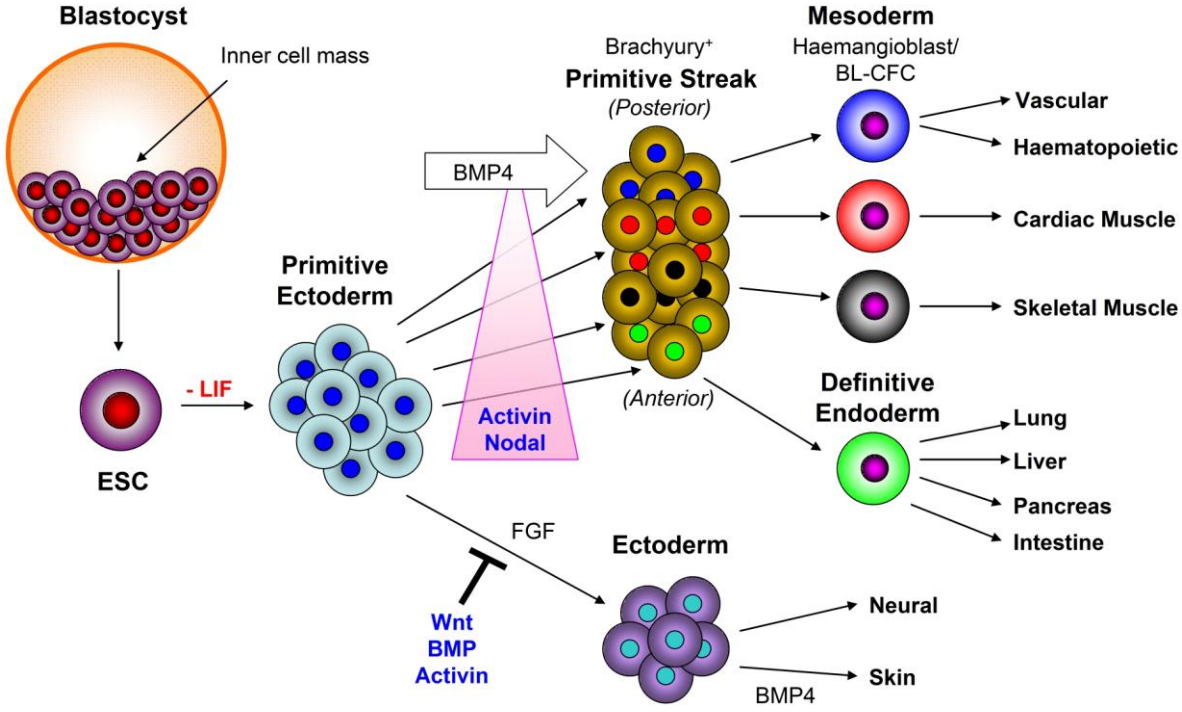

Figure 5.1: ESC differentiation into ectodermal, mesodermal and endodermal derivatives. Wnt, BMP and Activin inhibit ectodermal differentiation from primitive ectoderm. High concentrations of Activin or Nodal directs definitive endodermal differentiation; whereas, low concentrations of Activin directs mesodermal differentiation from brachyury-expressing cells of primitive streak. BMP4 is shown can induce posterior mesoderm and skin. FGF is involved in neural induction (Modified from Keller, 2005).

Serum plays a critical role in endodermal differentiation of ESC during *in vitro* culture. Restricted exposure of EBs to serum followed by serum-free culture enhances endodermal differentiation and suppresses development of mesodermal derivatives within the EBs (Kubo et al., 2004). Work performed on mouse ESC demonstrated that stimulation of EBs with serum for 2.5 days followed by a serum-free culture for further 3.5 days increased expression of endodermal genes, *Foxa2* and *Sox17* and simultaneously decreased expression of mesodermal gene, *Gata1* and brachyury; whereas, continuous exposure of EBs to serum reduced endodermal gene expression (Kubo et al., 2004). Activin A has also been suggested to have a strong role in directing differentiation of hESC into definitive endoderm (D'Amour et al., 2005, Kubo et al., 2004, McLean et al., 2007).

Activin A, a member of the TGF-β super-family, has a dual role in ESC differentiation. Different concentrations of Activin A induce different developmental programs in EB. High concentrations stimulate an endodermal differentiation programme and low concentration stimulate mesodermal differentiation (Kubo et al., 2004) (Figure 5.1). Differentiation of mouse ESC in EB culture with Activin A at a concentration of 100 ng/ml in a serum-free condition significantly increased expression of definitive endodermal genes, *Foxa2* and *Sox17* where more than 50% of differentiated EB cell population expressed the Foxa2 protein. On the other hand, when EBs were differentiated with 1-3 ng/ml concentration of Activin A, expression of mesodermal gene brachyury was high and *Foxa2* and *Sox17* were undetectable (Kubo et al., 2004). In addition, high concentrations of Activin completely suppressed expression of neuroectoderm-specific gene *Pax6* (Kubo et al., 2004). The generation of endodermal derivatives from ESC has been demonstrated through differentiation of pancreatic islets (Colman, 2004, Stoffel et al., 2004), hepatocytes

(Hamazaki et al., 2001, Jones et al., 2002, Yamada et al., 2002a), intestinal cells (Yamada et al., 2002b) and lung epithelial cells (Ali et al., 2002, Rippon et al., 2006).

ESCs have been suggested as a suitable tool for application in regenerative cell therapy for lung repair and regeneration due to their differentiation potential into lung epithelial cells (Weiss & Finck, 2010). For IPF, ESC could be utilised to replace damaged AEC to facilitate alveolar wound repair. Type II AEC have been successfully differentiated from human (Wang et al., 2007) and mouse (Ali et al., 2002, Rippon et al., 2006, Roszell et al., 2009) ESC. More recently, Wang and colleagues have demonstrated that intratracheal administration of ESC-derived type II AEC improved survival and ameliorated pulmonary inflammation and fibrosis in a bleomycin-induced experimental lung injury model (Wang et al., 2010). In this study, structural engraftment of transplanted ESC-derived type II AEC and their differentiation into type I AEC were also noted (Wang et al., 2010). However, attenuation of bleomycin-induced fibrotic responses occurred as early as 24 to 48 hours post ESC-derived type II AEC administration which indicated a putative paracrine mechanism involved in the amelioration of pulmonary fibrosis. The notion of a paracrine influence of stem cells in the repair of lung injury has been widely demonstrated utilising adult stem cells such as MSC and HSC, as discussed in chapter 4. However, data supportive of an ESC-paracrine influence in lung injury repair is limited. The current hypothesis suggests that failure or delay of alveolar re-epithelialisation following injury plays a major role in propagation of fibrogenesis in IPF (Selman et al., 2001). Thereby, stimulation of an alveolar re-epithelialisation process by stem cells or their secretory product(s) could have potential clinical benefits in the development of novel regenerative therapies for IPF where efficacious treatment is currently absent.

5.1.1. Aim of this study

The primary objective of this study was to explore the paracrine effects of hESC on alveolar epithelial cell wound repair.

5.2. Study design

The *in vitro* scratch wound repair system was implemented to test the paracrine influences of undifferentiated and differentiated hESC on alveolar A549 cell wound repair as described in Section- 2.7.6 (See Chart 5.1). Conditioned media (CM) was obtained from the undifferentiated adherent culture of hESC cell line SHEF-2 (Section- 2.4.4.1). To collect CM from differentiated hESC, SHEF-2 cells were differentiated with Activin A (Section- 2.4.4.2). CM was collected during various time points (stages) of differentiation. Collected CM from undifferentiated and differentiated hESC were tested on A549 cell wound repair (Section- 2.7.6). To determine whether the A549 cell wound repair occurred due to the stimulation of cell proliferation or migration or both, the internuclear distances between A549 cells at wound margin was measured (Section- 2.8), and MTT cell proliferation assay was performed (Section- 2.9). hESC differentiation was confirmed by the evaluation of lineage-specific gene expression by RT-PCR (Section- 2.11) and pluripotent marker protein expression by immunocytochemistry (Section- 2.12.5). LC-MS/MS mass spectrometry analysis was performed to identify the secretory proteins of differentiated hESC (Section- 2.5). The experimental data was analysed using the Excel programme of Microsoft Office XP. The statistical analysis was performed using the software GraphPad Prism v5.00 (Section- 2.14). A conclusion was drawn according to the outcome of the experimental results (See Chart 5.1).

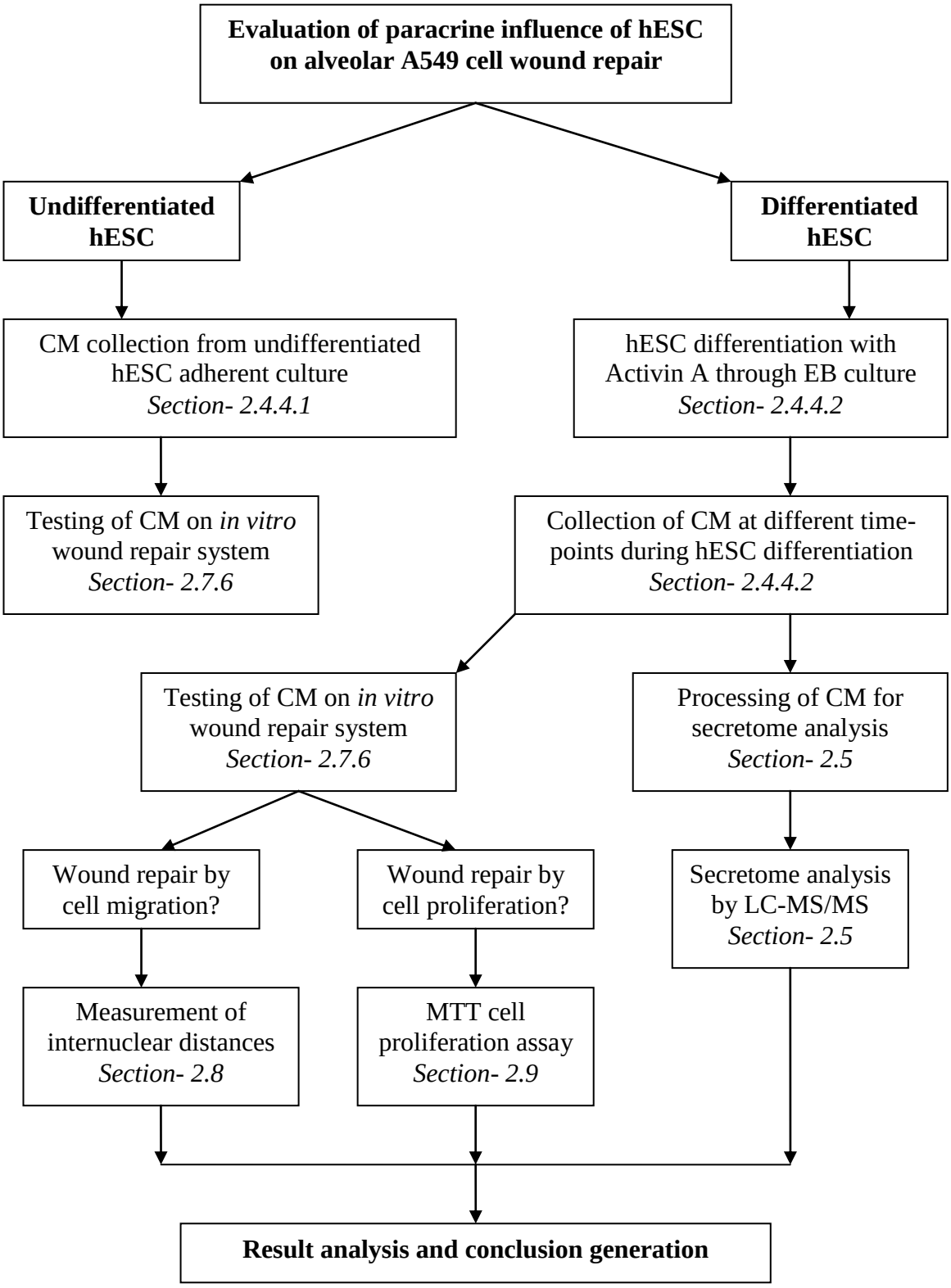

Chart 5.1: Experimental plan flowchart.

5.3. Results

5.3.1. SHEF-2 cell line retains the hESC criteria

hESC cell line SHEF-2 was utilised for my experiments and cultured in a feeder-free, culture condition using MEFs-CM media following the established protocol described in the Section- 2.2.4 (Xu et al., 2001). SHEF-2 cells readily formed distinct colonies in adherent culture and were capable of forming EBs in suspension culture, which are described as the specific morphological criteria of human embryonic stem cells (Thomson et al., 1998) (Figure 5.2A, 5.2C). SHEF-2 cells had a high nucleus to cytoplasm ratio and prominent nucleoli (Figure 5.2B). Throughout the culture period, SHEF-2 cells grew in a steady manner and did not show any apparent sign of senescence. SHEF-2 cells displayed high levels of *hTERT* gene expression as detected by RT-PCR (Figure 5.2D) (Section-2.11), a common criterion for hESC (Thomson et al., 1998). Cells were also positive for pluripotent nuclear markers Octamer-binding protein-4 (Oct-4) (also know as POU domain, class 5, transcription factor 1, POU5F1) and Nanog (also know as Homeobox protein NANOG) again detected by RT-PCR (Figure 5.2D) and immunocytochemistry (Figure 5.3) (Section- 2.12.4) (Reubinoff et al., 2000, Chambers et al., 2003, Mitsui et al., 2003). SHEF-2 cells were highly positive for alkaline phosphatase (ALP) and stage-specific embryonic antigen-4 (SSEA-4) markers and negative for SSEA-1 (Thomson et al., 1998, Reubinoff et al., 2000).

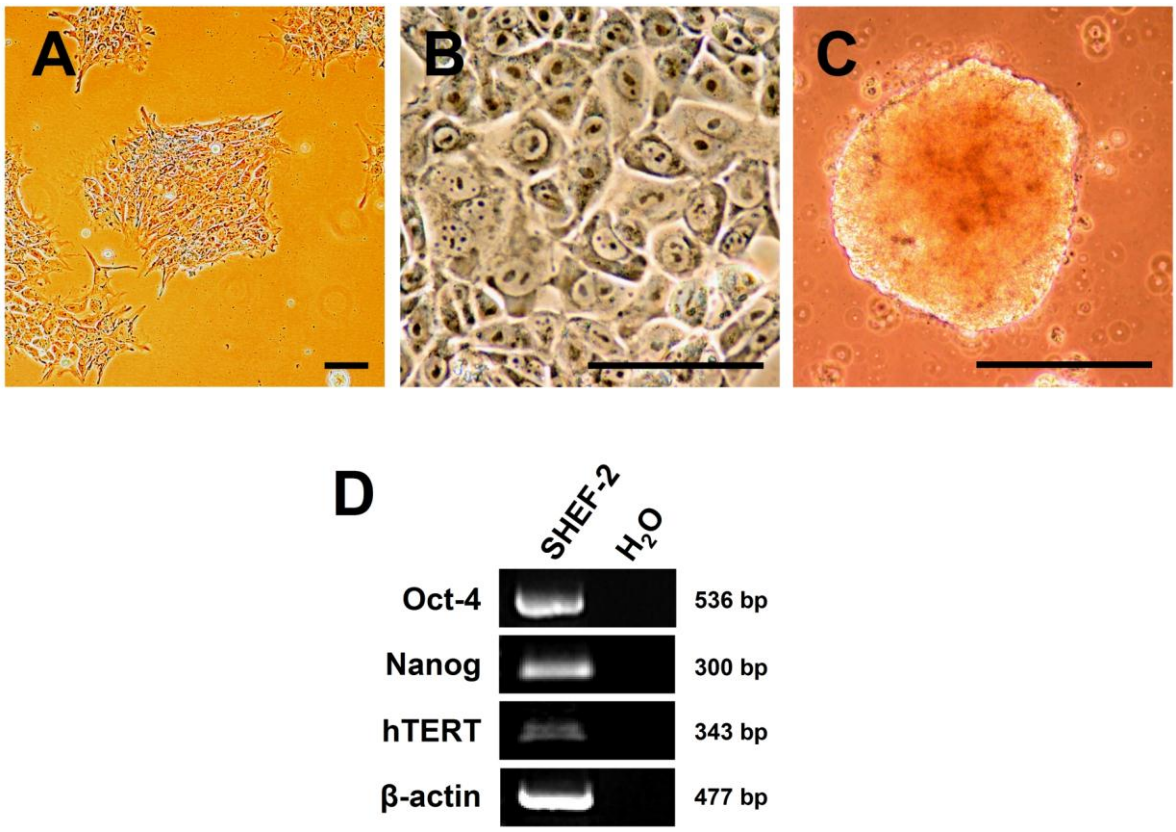

Figure 5.2: Pluripotent ESC criteria of SHEF-2 cell line.

Inverted light microscopic images show (**A**) SHEF-2 colonies on matrigel coated culture surfaces in adherent culture (100X magnification), (**B**) High ratio of nucleus to cytoplasm with prominent nucleoli (400X magnification) and (**C**) Formation of EB in suspension culture (400X magnification). (**D**) mRNA expression for Oct-4, Nanog and *hTERT* was detected in hESC cell line, SHEF-2 by RT-PCR. β-actin was run as a house-keeping gene. Scale bar, 100 µm.

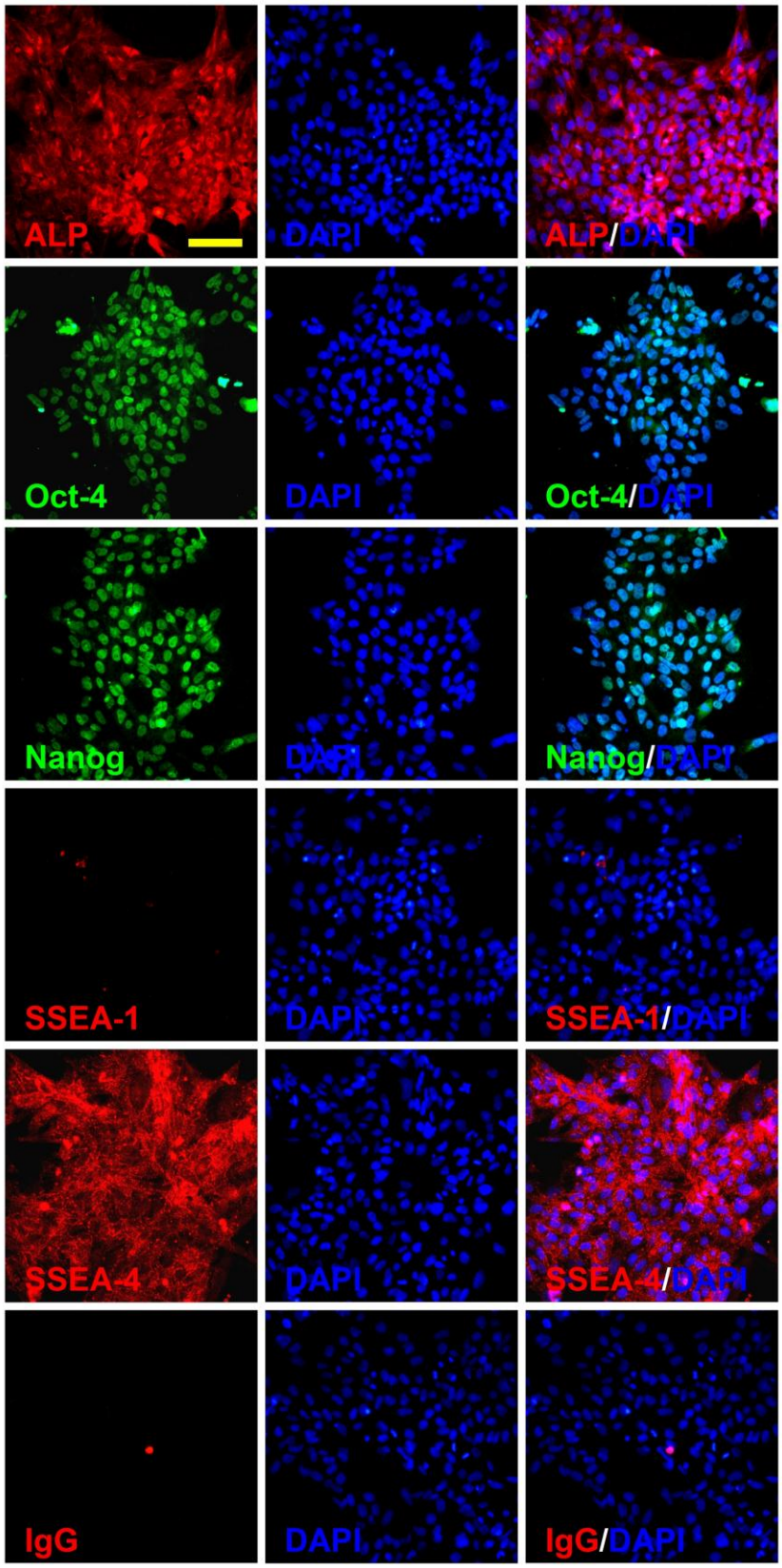

Figure 5.3: hESC Pluripotent markers profile in SHEF-2 detected by immunocytochemistry. SHEF-2 cells were positive for ALP, Oct-4, Nanog and SSEA-4 and negative for SSEA-1. Nuclear counter staining with DAPI. Scale bar, 100 µm.

5.3.2. Undifferentiated hESC secretome inhibits alveolar A549 cell wound repair

To investigate the effect of secretory factors of undifferentiated hESC on A549 cell wound repair, I prepared conditioned media (CM) from adherent cultures of undifferentiated SHEF-2 cells (Section- 2.4.4.1) and tested these with the *in vitro* wound repair system (Section- 2.7.6). Three sets of CM were prepared with KO-DMEM based on presence of KO-SR and bFGF in the media composition as tabulated below (Table 5.1). Each type of CM was paired with its own control where composition was identical to that of the CM excepting that it was not conditioned (Un-CM). $^{+SR+bFGF}$CM from undifferentiated SHEF-2 significantly inhibited alveolar A549 cell wound repair after 24 hours in comparison to its control $^{+SR+bFGF}$Un-CM (83 ± 6.56% vs 99 ± 2.38% control; $p<0.01$) (Figure 5.4A, 5.4B). A similar effect was observed in $^{+SR-bFGF}$CM treated samples when compared to control $^{+SR-bFGF}$Un-CM (82 ± 5.12% vs 99 ± 0.5% control; $p<0.001$) (Figure 5.4A, 5.4B). Whereas, no significant difference was observed in wound repair rate between $^{-SR-bFGF}$CM and $^{-SR-bFGF}$Un-CM treated samples (35 ± 4.79% vs 42 ± 8.29% control) (Figure 5.4A). This data indicates that presence or absence of bFGF (4 ng/ml) in the media did not influence A549 cell wound repair; however, absence of KO-SR in the media significantly inhibited wound repair after 24 hours when compared to KO-SR containing CM or Un-CM treated samples ($p<0.001$; Figure 5.4A). Taken together, the secretome of undifferentiated hESC is inhibitory to the A549 cell wounds *in vitro*.

Table 5.1: Composition of culture media for CM preparation from undifferentiated hESC

Media name	Composition
$^{+SR\ +bFGF}$**CM**	KO-DMEM supplemented with 20% KO-SR, 4 ng/ml bFGF
$^{+SR\ -bFGF}$**CM**	KO-DMEM supplemented with 20% KO-SR
$^{-SR\ -bFGF}$**CM**	KO-DMEM
All above mentioned media were supplemented with 1% L-glutamine, 1% NEAA and 0.1 mM β-mercaptoethanol.	

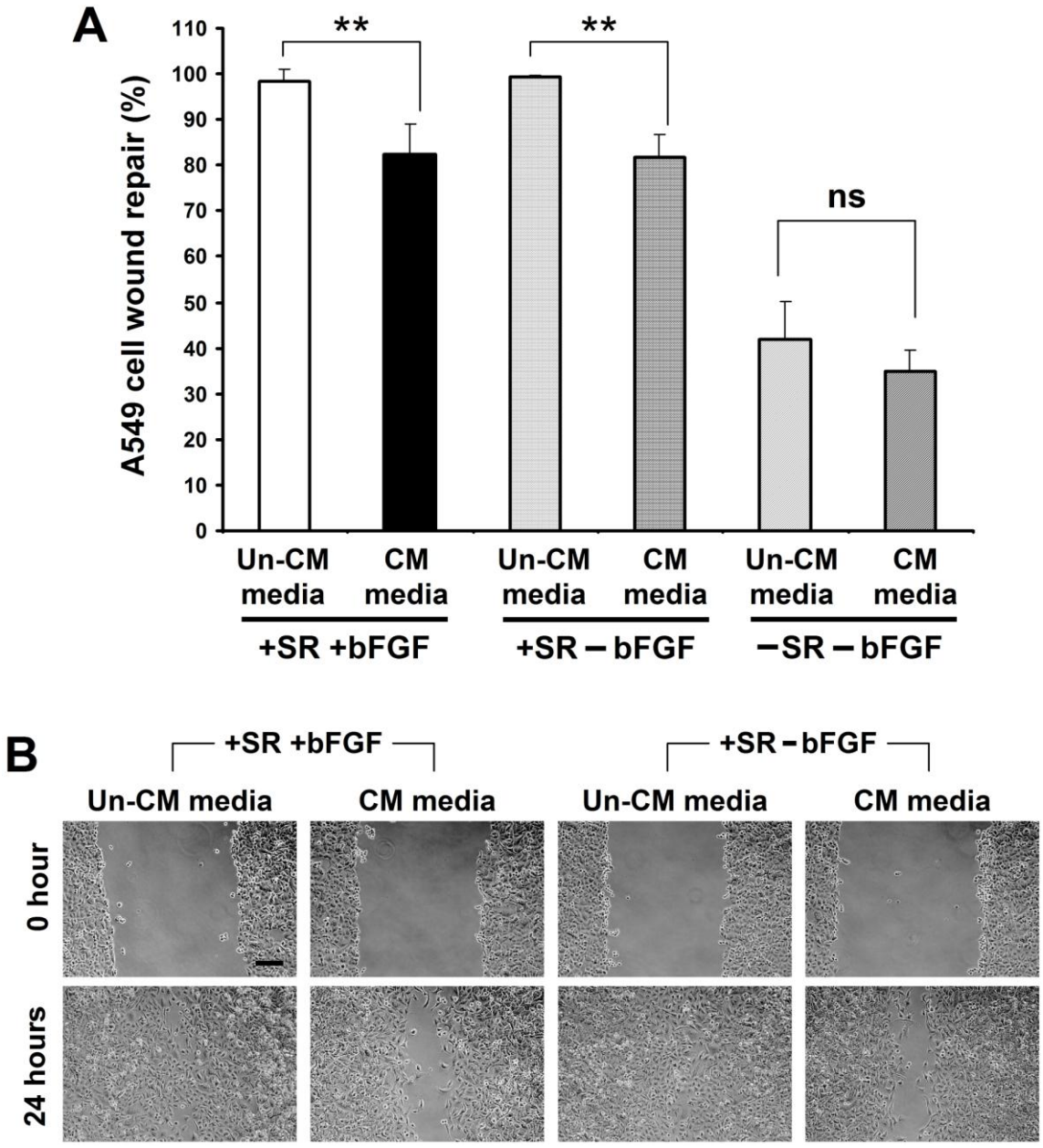

Figure 5.4: Alveolar A549 cell wound repair with CM obtained from undifferentiated hESC. (**A**) A549 cell wound repair with 3 different sets of conditioned (CM) and un-conditioned (Un-CM) media after 24 hours. (**B**) Inverted light microscopy representative images of A549 cell wound repair with conditioned and un-conditioned media obtained from undifferentiated hESC. Data presented as mean ± SD. n = 4 independent experiments. **p<0.01. ns = not significant. Scale bar, 200 μm.

5.3.3. Differentiated hESC secretome displays differential alveolar epithelial cell wound repair effects *in vitro*

To evaluate the role of secretory factors of differentiated hESC on alveolar A549 cell wound repair, SHEF-2 cells were differentiated towards endodermal lineages by Activin A (100 ng/ml) (Rippon et al., 2006, Kubo et al., 2004) through an EB suspension culture method (Section- 2.4.4.2). During differentiation, CM was collected at different time-points from a continuous EB-suspension culture (Figure 5.5). The composition of media for conditioning/culture is tabulated below (Table 5.2). Collected CM was tested on A549 cell wound repair system (Section- 2.7.6). CM collected on day 8 (3.5-8 day-CM) significantly inhibited A549 cell wound repair after 24 hours when compared to its corresponding control (positive control) (62 ± 15.17% vs 90 ± 14.66% positive control; $p<0.05$) (Figure 5.6A, 5.6B). 11-16 day-CM and 16-22 day-CM also inhibited A549 cell wound repair compared to the positive control (63 ± 6.95%, 11-16 day-CM and 52 ± 6.24%, 16-22 day-CM vs 90 ± 14.66%, positive control; $p<0.05$ for 11-16 day-CM and $p<0.01$ for 16-22 day-CM) (Figure 5.6A, 5.6B). In contrast, 8-11 day-CM did not inhibit alveolar A549 cell wound repair after 24 hours in comparison to the positive control (86 ± 10.07% vs 90 ± 14.66% positive control) (Figure 5.6A, 5.6B). Although the starting media composition of 8-11 day-CM, 11-16 day-CM and 16-22 day-CM were identical the wound repair rate was significantly higher in 8-11 day-CM treated sample compared to 11-16 day-CM ($p<0.01$) and 16-22-day CM ($p<0.01$) (Figure 5.6A, 5.6B). The wound repair rate was significantly higher in 8-11 day-CM treated sample compared to 3.5-8 day-CM as well ($p<0.05$; Figure 5.6A, 5.6B).

Next, I performed a separate set of similar wound repair experiment with CM collected from non-Activin-directed differentiating hESC (Section- 2.4.4.2). To compare and

contrast, wound repair with CM collected from Activin-directed differentiation protocol was performed in parallel. The overall observation was that A549 cell wound repair with CM collected from different stages of Activin-directed or non-Activin directed differentiating EBs were not significantly different (Figure 5.7). However, a contrasting effect was observed when comparing wound repair rate induction with 16-22 day-CM from either Activin-treated or un-treated EBs. 16-22 day-CM collected from non-Activin treated differentiating EBs did not show any significant inhibitory effect on A549 cell wound repair comparing 8-11 day-CM of un-treated group (70 ± 14.9%, 16-22 day-CM vs 71 ± 14.64%, 8-11 day-CM) (Figure 5.7); whereas, 16-22 day-CM of Activin-treated differentiating EBs significantly suppressed A549 cell wound repair (Figure 5.6, 5.7). Activin A (100 ng/ml) itself, when present in 3.5-8 day-CM, did not influence A549 wound repair (Figure 5.7). Taken together, it can be concluded that during Activin-directed hESC differentiation, differentiated ESC secrete factors on day 8-11 which stimulate alveolar epithelial cell wound repair; whereas, secreted factors earlier or later than 8-11 days of differentiation are wound repair-inhibitory in nature.

Table 5.2: Composition of culture media for CM preparation from differentiating hESC through EB suspension culture.

Media name	Composition
3.5-8 day-CM	KO-DMEM supplemented with 10% KO-SR, Activin A (100 ng/ml)
8-11 day-CM	KO-DMEM supplemented with 10% KO-SR
11-16 day-CM	KO-DMEM supplemented with 10% KO-SR
16-22 day-CM	KO-DMEM supplemented with 10% KO-SR
Positive control	KO-DMEM supplemented with 10% KO-SR (Un-conditioned)
Negative control	KO-DMEM (Un-conditioned)

All above mentioned media were additionally supplemented with 1% L-glutamine, 1% NEAA and 0.1 mM β-mercaptoethanol. Positive and Negative controls were not conditioned but all others were conditioned in EB culture.

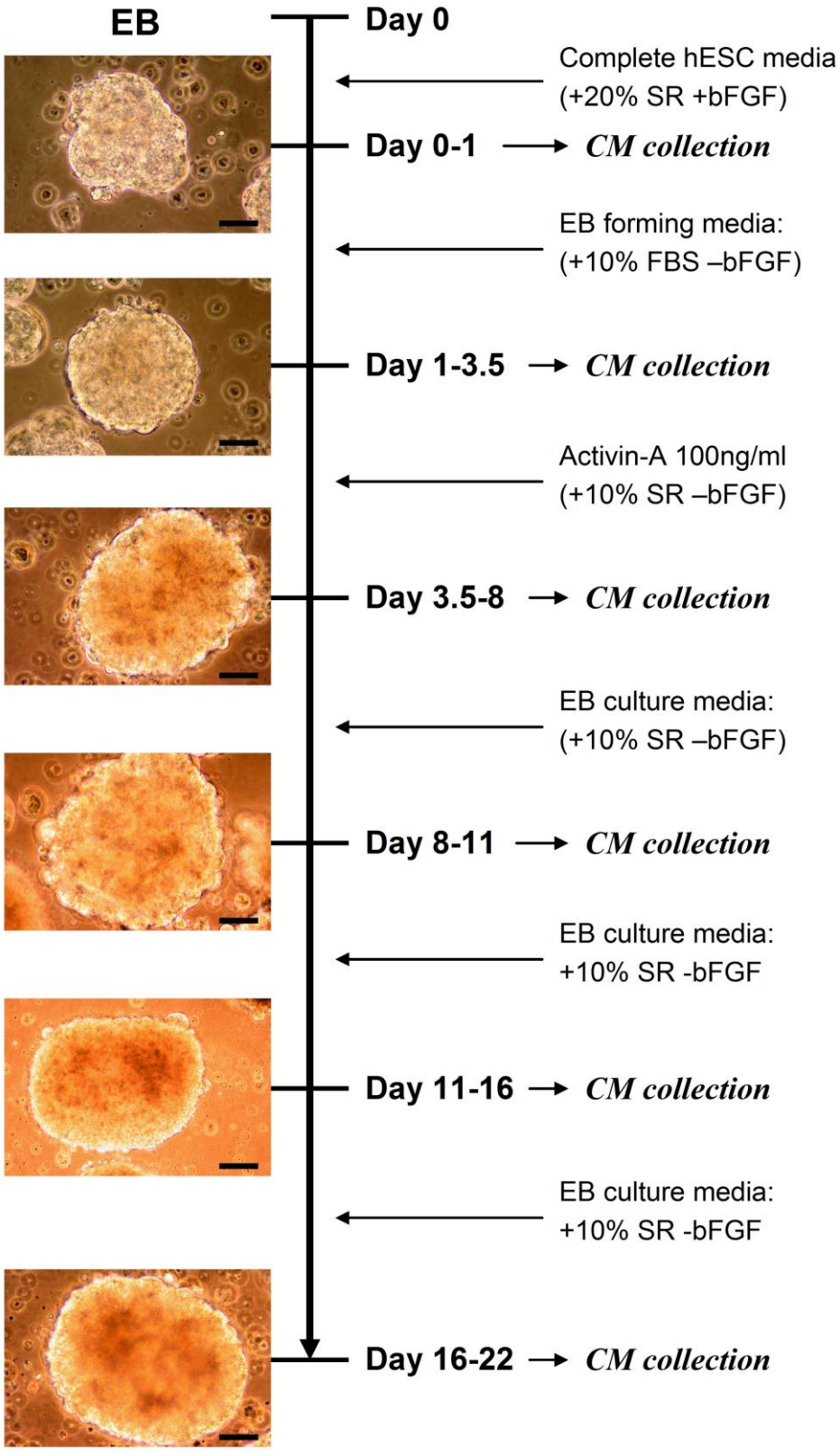

Figure 5.5: CM preparation and collection from different stages of hESC differentiation with Activin A through EB suspension culture. CM were collected on 1st, 3.5th, 8th, 11th, 16th and 22nd day of differentiation. Colour images were captured on an inverted light microscope with attached CCD camera. Scale bar, 50 µm.

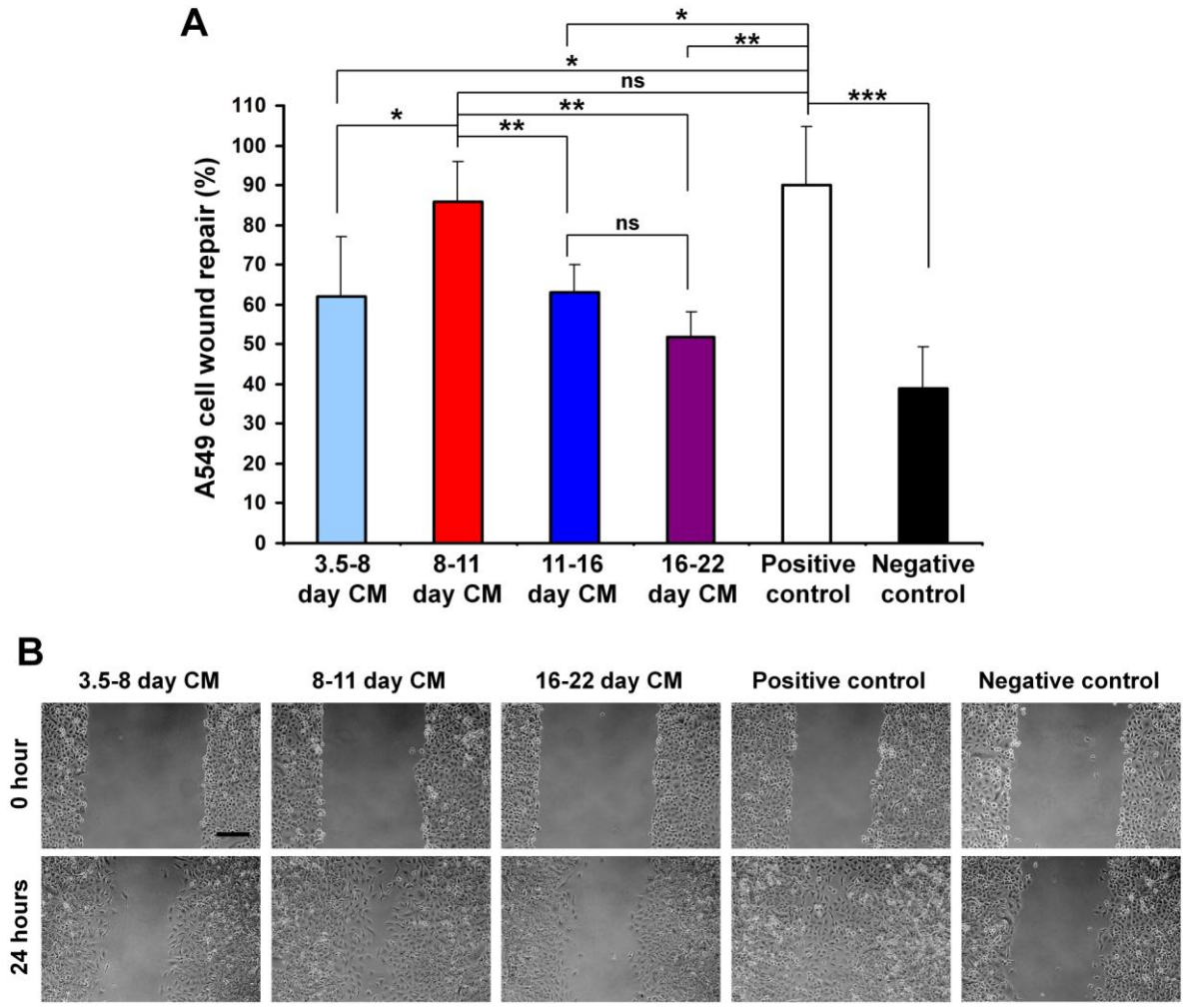

Figure 5.6: Alveolar A549 cell wound repair with CM collected from different stages of hESC differentiation in Activin A-directed differentiation protocol. (**A**) A549 cell wound repair after 24 hours with CM obtained from differentiating hESC through EB culture. 3.5-8 day-CM contains 100 ng/ml concentration of Activin A. Other CM from day 8 to day 22 were Activin A free (post-treatment stages) and the media composition was identical. Positive and negative controls represent A549 cell wound repair with 10% KO-SR supplemented KO-DMEM and KO-SR-free KO-DMEM respectively; both of these control media were un-conditioned. (**B**) Inverted light microscopic representative images of A549 cell wound repair with CM obtained from different stages of hESC differentiation. Data presented as mean ± SD. (n = 4 independent experiments, triplicate per n). *p<0.05, **p<0.01, ***p<0.001. ns = not significant (Newman-Keuls Multiple Comparison Posthoc Analysis). Scale bar, 200 µm.

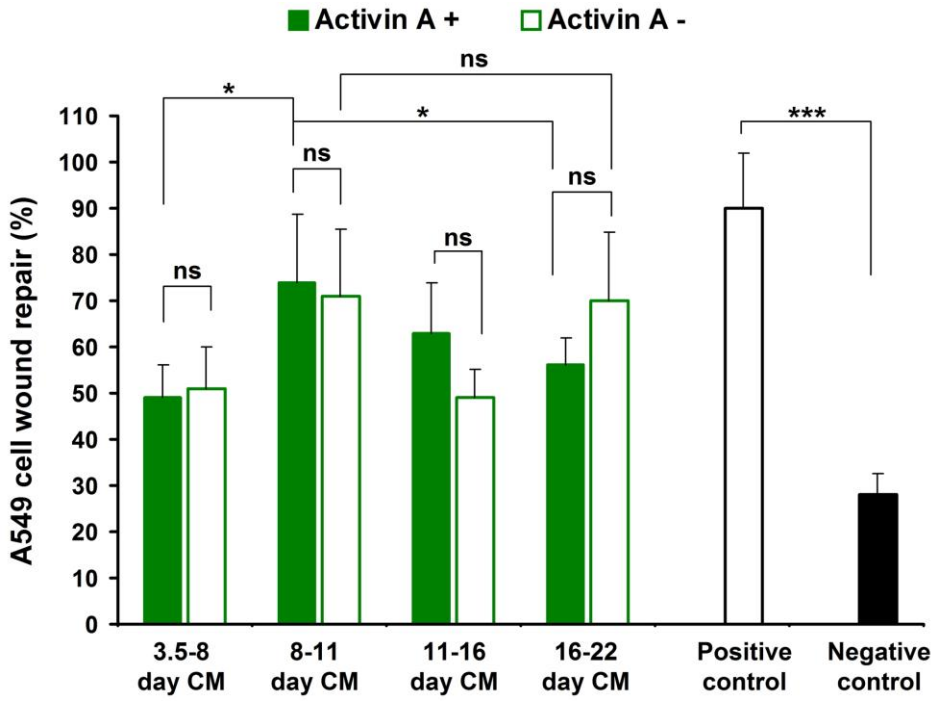

Figure 5.7: Alveolar A549 cell wound repair with CM collected from different stages of hESC differentiation. A549 cell wound repair with CM collected from different stages of Activin A directed (green bars) or Activin-free (open green bars) hESC differentiation through EB suspension culture after 24 hours. Positive and negative control represent A549 cell wound repair with 10% KO-SR supplemented KO-DMEM or KO-SR free KO-DMEM respectively. Both positive and negative controls were un-conditioned. Data presented as mean ± SD. n = 4 independent experiments. *p<0.05, ***p<0.001. ns = not significant.

5.3.4. Day 8-11 CM of hESC differentiation promotes alveolar A549 cell wound repair via cell migration and proliferation when compared with other CM groups

A successful epithelial wound repair is reported as requiring cell spreading, migration and proliferation (Zahm et al., 1991, Puchelle et al., 2006). As seen above, in general, CM obtained from differentiated hESC was inhibitory to A549 cell wound repair except 8-11 day-CM which was comparatively stimulatory (Figure 5.6). Here, I first evaluated the influence of CM collected from different time-points of Activin A-directed differentiated hESC on A549 cell migration during wound repair by measuring internuclear distance, an established method for assessment of cell migration (Geiser et al., 2000, Atabai et al., 2002) (Section- 2.8). The internuclear distances between A549 cells at the wound margins of 8-11 day-CM treated samples were significantly higher than that of 3.5-8 day-CM and 16-22 day-CM treated samples after 24 hours of wounding (57.26 ± 5.87 µm, 8-11 day-CM vs 47.41 ± 2.84 µm, 3.5-8 day-CM; $p<0.05$ and 45.80 ± 2.80 µm, 16-22 day-CM; $p<0.01$) (Figure 5.8A, 5.8B). The internuclear distances between A549 cells at the wound margins of 8-11 day-CM treated samples were significantly higher than that of positive control as well (57.26 ± 5.87 µm, 8-11 day-CM vs 49.01 ± 4.52 µm; $p<0.05$) (Figure 5.8A, 5.8B). The mean internuclear distances in positive control was significantly higher than that of negative control (49.01 ± 4.52 µm vs 31.68 ± 2.95 µm, $p<0.001$) (Figure 5.8A, 5.8B). However, no statistical significance was determined between internuclear distances of positive control and other CM-treated wound repair groups (day 3.5-8 CM and day 16-22 CM) (Figure 5.8A).

Next, I evaluated the influences of above mentioned CM on A549 cell proliferation during wound repair by conducting an MTT cell proliferation assay (Section- 2.9). 8-11 day-CM significantly stimulated A549 cell proliferation during wound repair when compared to other CM-treated wound repair groups, 3.5-8 day-CM and 16-22 day-CM treated samples

(104 ± 27.95%, 8-11 day-CM vs 51 ± 23.97%, 3.5-8 day-CM and 45 ± 3.87%, 16-22 day-CM; $p<0.05$) (Figure 5.9). A549 cell proliferation was significantly higher in day 8-11 CM-treated samples when compared with positive control (104 ± 27.95%, 8-11 day-CM vs 69 ± 6.21%, positive control) (Figure 5.9). A significant inhibition of A549 cell proliferation was also noted in 16-22 day-CM treated wound repair samples when compared with positive control (16-22 day CM vs positive control, $p<0.05$) (Figure 5.9). Taken together, conditioned media obtained from day 8-11 of differentiated hESC enhances alveolar epithelial cell wound repair through stimulation of both cell migration and proliferation.

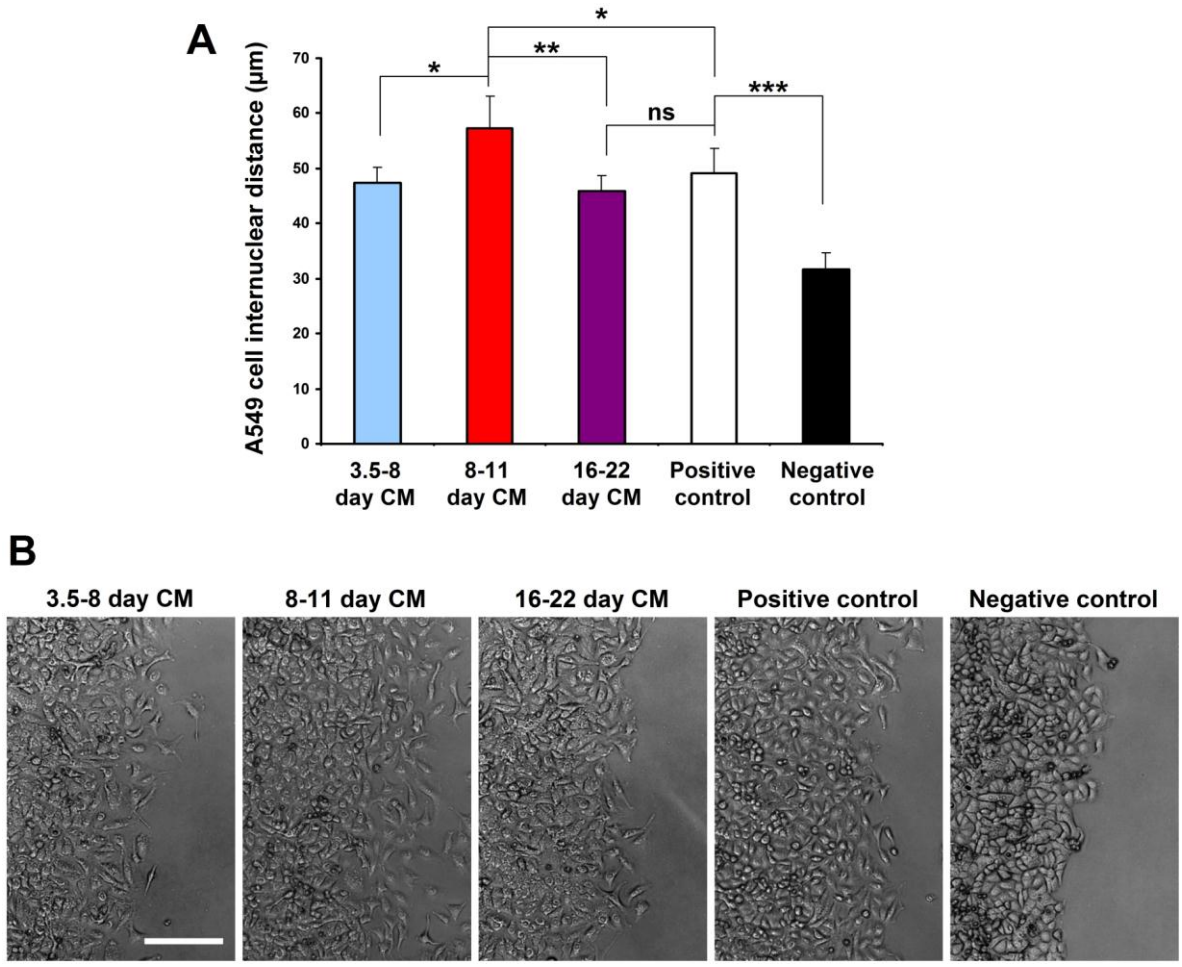

Figure 5.8: Internuclear distances of A549 cells at wound margins after 24 hours of wounding. (**A**) Internuclear distance of A549 cells at the wound margins after 24 hours of wound repair with different CM obtained from different stages of Actin-directed differentiated hESC through EB culture. Positive and negative controls represent A549 cell wound repair with 10% KO-SR supplemented KO-DMEM and KO-SR-free KO-DMEM respectively; both control media were un-conditioned. (**B**) Representative inverted light microscopy images of A549 cell wound margins after 24 hours of treatment with CM and control media. Data presented as mean ± SD. (n = 4 independent experiments, a minimum of 40 measurements were recorded for each sample each time). *p<0.05, **p<0.01, ***p<0,001. ns = not significant (Newman-Keuls Multiple Comparison Posthoc Analysis). Scale bar, 200 µm.

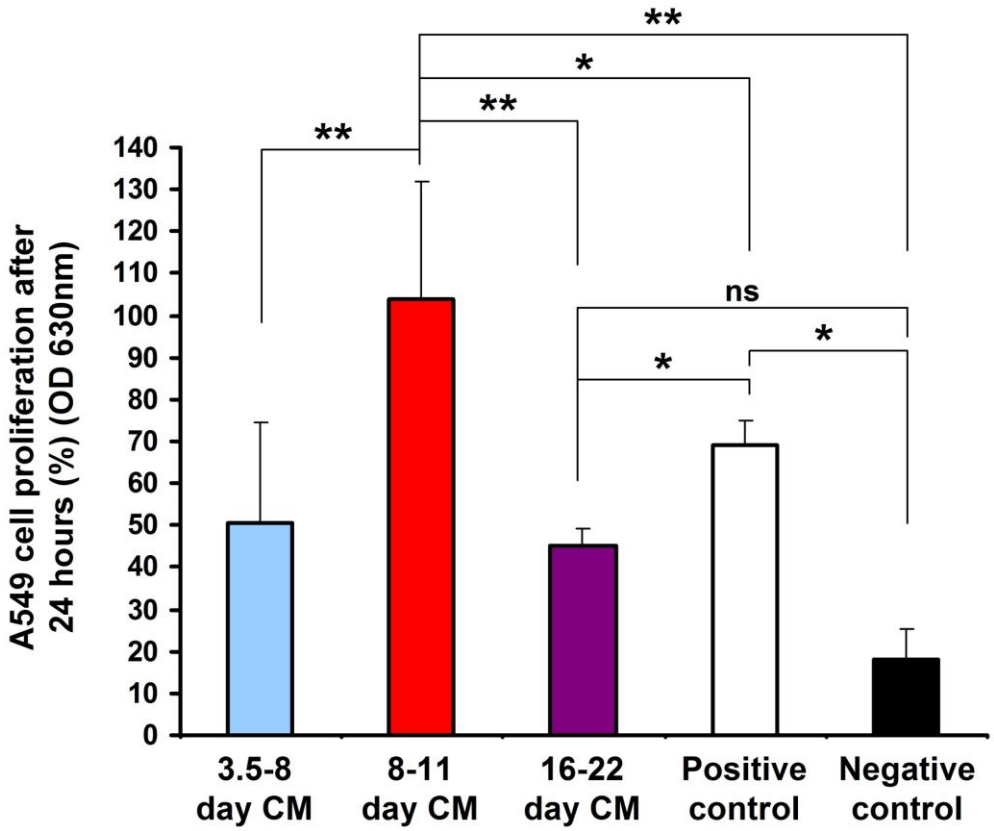

Figure 5.9: MTT cell proliferation assay on A549 cell wound repair.

A549 cell proliferation was determined by the colorimetric MTT assay on different conditioned media obtained from Activin A directed hESC differentiation treated wound repair samples after 24 hours. Positive and negative controls represent A549 cell wound repair with 10% KO-SR supplemented KO-DMEM and KO-SR-free KO-DMEM respectively; both these control media were un-conditioned. Data presented as mean ± SD. (n = 3 independent experiments). *$p<0.05$, **$p<0.01$. ns = not significant (Newman-Keuls Multiple Comparison Posthoc Analysis).

5.3.5. Day 8-11 CM was collected from a mixed population of endodermal and mesodermal differentiated hESC

High concentration of Activin directs ESC differentiation into endodermal and mesodermal derivatives and suppresses ectodermal differentiation (Kubo et al., 2004, Rippon et al., 2006). Earlier, I have shown that CM obtained form 8-11 day of Activin-directed hESC differentiation enhanced alveolar epithelial cell wound repair (Figure 5.6). Here, I sought to investigate whether the CM of this stage of differentiation was from differentiated hESC. I performed semi-quantitative RT-PCR (Section- 2.11) and immunocytochemistry (Section- 2.12.5) to determine the differentiation status of the Activin-treated hESC. RT-PCR analysis showed that the differentiated cell population within the EBs of day-11 expressed endodermal lineage-specific gene, *AFP* (α-Fetoprotein) (Abe et al., 1996) (Figure 5.10, lane-3). *AFP* expression was also noted in EBs of day-22 of differentiation (Lane-4). However, undifferentiated hESC from adherent cultures and spontaneously differentiated hESC did not express *AFP* (Figure 5.10; lane-1, 5 respectively). hESC were spontaneously differentiated in adherent culture with 10% FBS in KO-DMEM for 20 days. *ACTC1* (actin, alpha, cardiac muscle 1), a gene specific to mesodermal lineage (Bruce et al., 2007), was expressed in both Activin-directed and spontaneously differentiated hESC (Figure 5.10). Unexpectedly, slight expression of *ACTC1* was noted in undifferentiated hESC. On the other hand, neuro-ectodermal lineage-specific gene, *SOX1* (sex determining region Y-box 1) (Pevny et al., 1998) expression was not detected any of the differentiated samples (Figure 5.10). Previous studies also showed that differentiation of ESC with high concentration of Activin A (100 ng/ml) completely suppressed neuro-ectodermal gene expression (Kubo et al., 2004).

Next, I performed immunocytochemistry on differentiated EBs to evaluate their pluripotent marker expression (Section- 2.12.5). EBs from day 1 of differentiation was strongly positive for ALP, Oct-4, Nanog and SSEA-4; and weakly positive for SSEA-1 (Figure 5.11). On the other hand, the expression of above marker proteins was very low (or negative) in the day 11 EBs (Figure 5.12). Taken together, I conclude that 8-11 day-CM EBs contain endodermal and mesodermal cell population and therefore, 8-11 day-CM contains secretory products of a mixed population of endodermal and mesodermal differentiated derivatives.

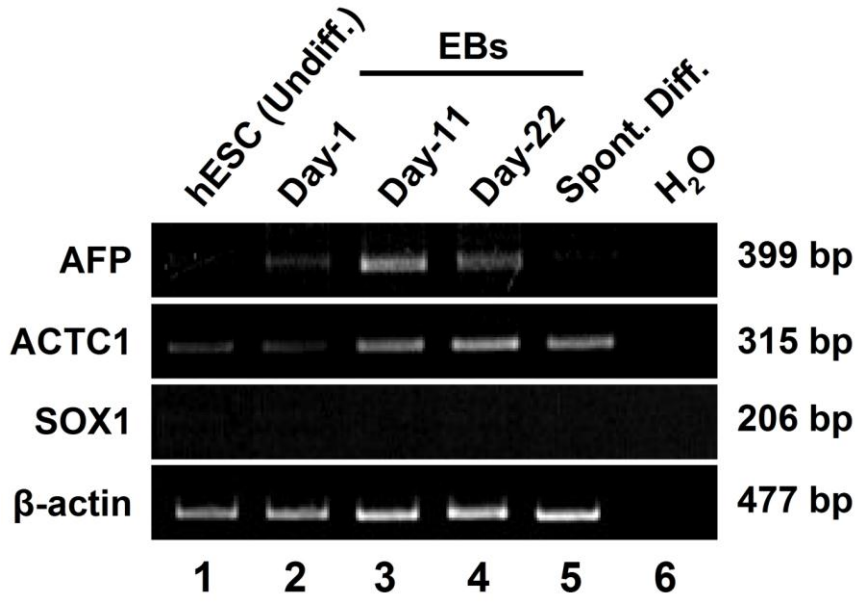

Figure 5.10: Semi-quantitative RT-PCR on differentiated hESC.

Endodermal lineage-specific gene, *AFP* expression was detected on day-11 differentiated EBs (lane-3). *AFP* expression was not detected in undifferentiated hESC (lane-1) or spontaneously differentiated hESC (lane-5). Differentiated hESC on day-11 (lane-3) and day-22 (lane-4) expressed mesodermal specific gene, *ACTC1*. *SOX1*, an ectodermal specific gene, expression was not detected in our tested samples. β-actin was used as a house-keeping gene.

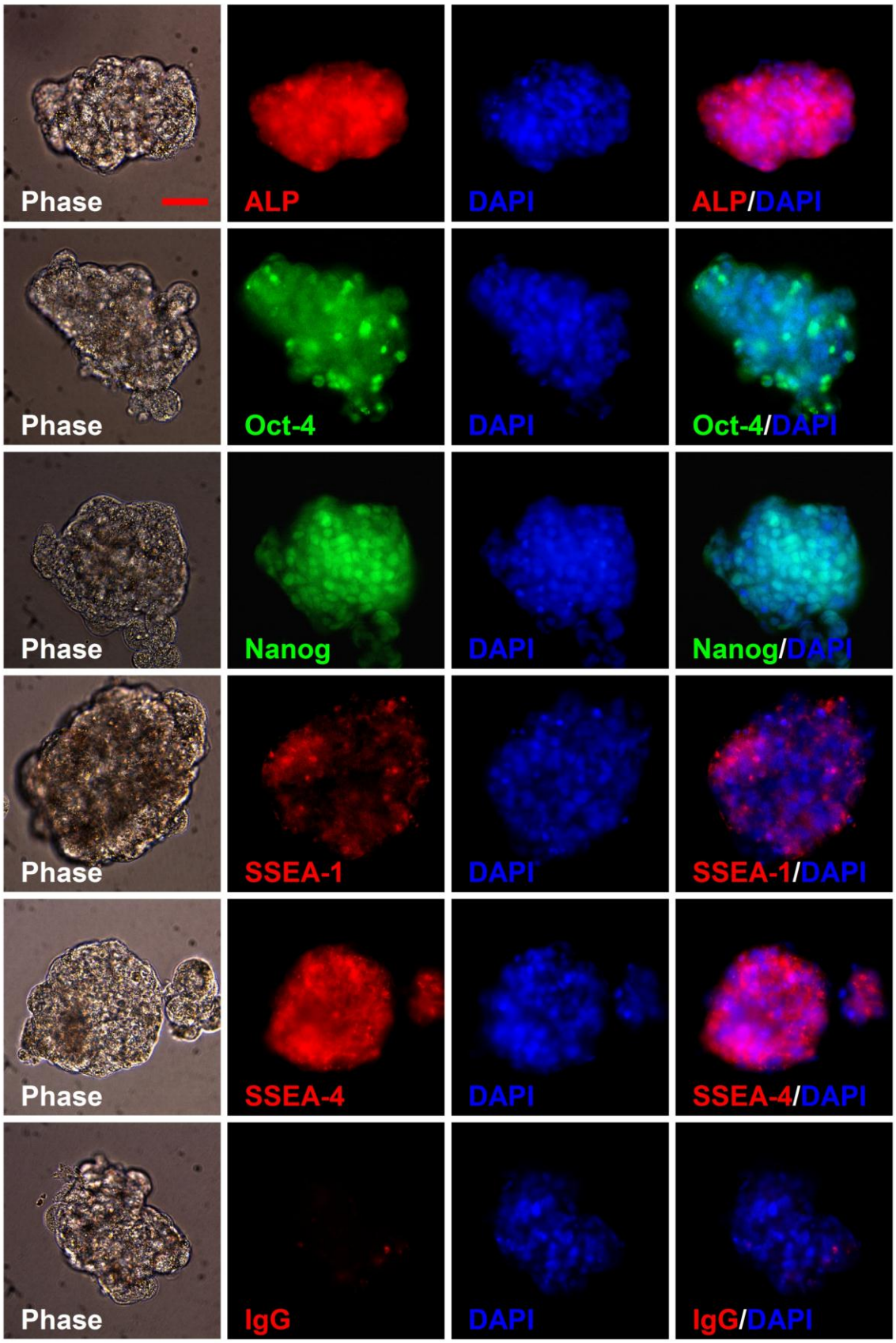

Figure 5.11: Evaluation of hESC pluripotent markers on day 1 EBs.

IgG is for secondary antibody control. DAPI used for nuclear counterstaining. Scale bar, 50 µm.

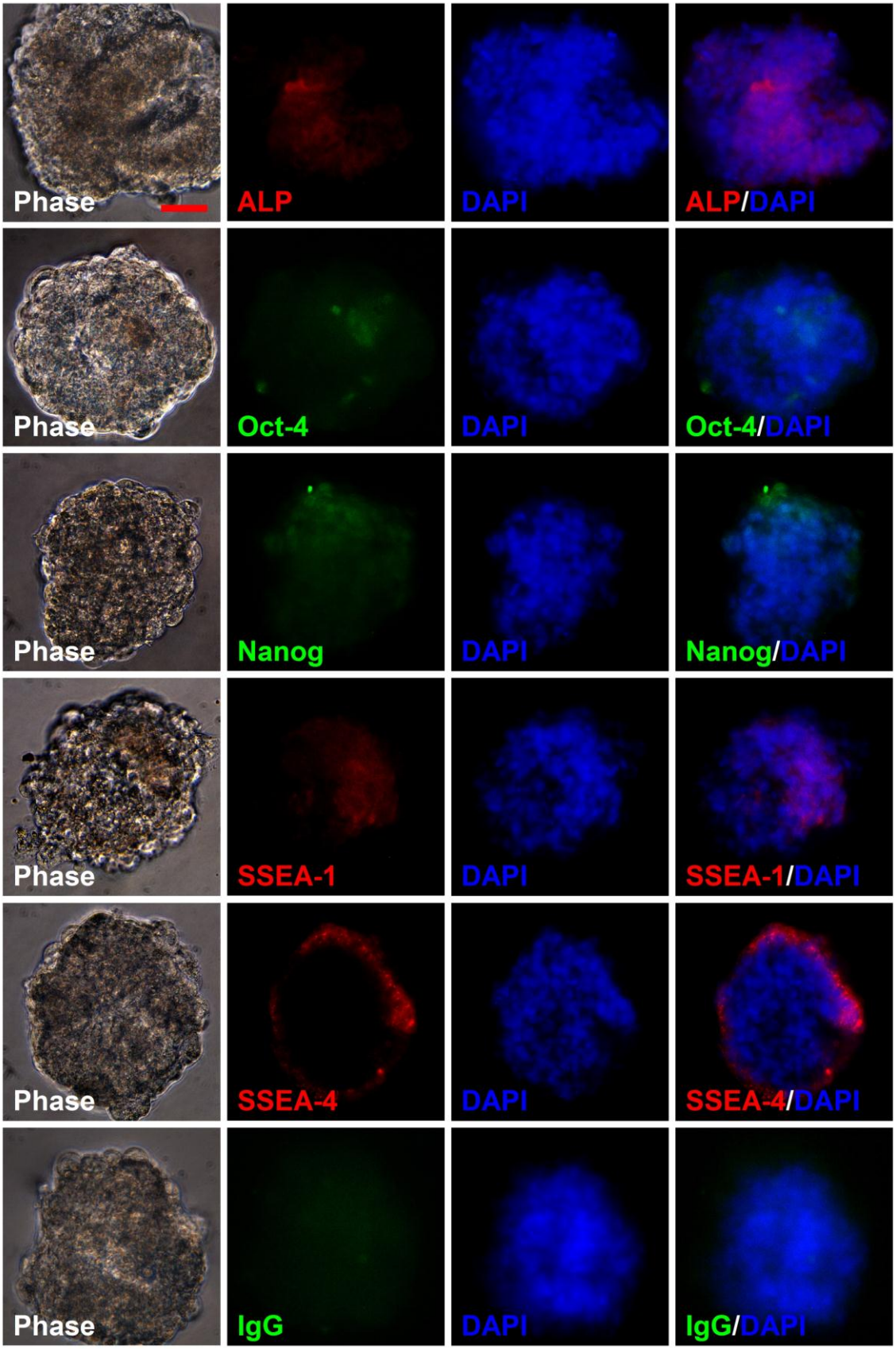

Figure 5.12: Evaluation of hESC pluripotent markers on day 11 EBs.

IgG is for secondary antibody control. DAPI used for nuclear counterstaining. Scale bar, 50 µm.

5.3.6: Secretome analysis CM obtained from differentiated hESC

As 8-11 day-CM and 16-22 day-CM have shown contrasting alveolar epithelial wound repair effects; I hypothesised that the secretome composition of these two CM would differ. To test this hypothesis and to identify the proteins responsible for the differential wound repair, LC-MS/MS mass spectrometry was performed on CM (Section- 2.5). Immediately, I experienced difficulties of determining proteins in the above mentioned conditioned media, possibly due to presence of high KO-SR content (10%) in the CM. Two approaches were taken to identify secretory human proteins in the CM by this method. It detected comparatively high abundance of human proteins in 8-11 day-CM; whereas, only one human protein was so far significantly detected in 16-22 day-CM (Table 5.3). A large numbers of mammalian proteins were although detected in the 10% KO-SR supplemented KO-DMEM. The source of these mammalian proteins was mostly bovine in origin (Table S4.2, Appendix 2). 10% KO-SR supplemented KO-DMEM was used for preparation of CM from differentiating hESC from Day 3.5 to 22.

Table 5.3: Activin-directed differentiated hESC secretome detected in 8-11 day-CM and 16-22 day-CM by LC-MS/MS MALDI TOF/TOF mass spectrometry.

Detected proteins	Accession No	Peptide count
8-11 day-CM		
Actin, gamma 1 propeptide	gi|4501887	3
Actin-like protein	gi|62421069	2
Alpha 2 globin	gi|4504345	4
Albumin preproprotein	gi|4502027	3
Actin, beta-like 2	gi|63055057	3
Apolipoprotein C-III precursor	gi|4557323	1
Chain A, Apolipoprotein E3 22kd Fragment Lys146glu Mutant	gi|15826264	1
Chain B, Nmr Structure Of Human Insulin Mutant His-B10-Asp, Val-B12- Aba, Pro-B28-Lys, Lys-B29-Pro	gi|159163040	2
Chain D, Human Insulin Hexamers With Chain B His Mutated To Tyr Complexed With Phenol	gi|5542375	1
Kininogen L, high MW	gi|225724	2
Heterogeneous nuclear ribonucleoprotein A2/B1 isoform B1	gi|14043072	1
16-22 day-CM		
Chain A, Apolipoprotein E3 22kd Fragment Lys146glu Mutant	gi|15826264	1

Human proteins were tabulated with total Ion score C.I. 100% to >95% in a descending manner. Accession numbers are of NCBI protein database.

5.4. Discussion

Regenerative cell therapy for incurable lung diseases continues to evolve at a rapid pace. Preliminary studies suggested that adult stem cells, such as bone marrow-derived MSC might engraft to the injured lung, replace damaged epithelium and potentiate lung repair in animal models of COPD/emphysema, cystic fibrosis and IPF. However, it is now recognised that structural engraftment of MSC in lung is generally a rare occurrence with an uncertain fate of differentiation into alveolar epithelial cells (Weiss & Finck, 2010). A growing body of evidence suggests that the MSC-mediated lung repair effect largely occurs through paracrine mechanisms (Ortiz et al., 2007, Zhen et al., 2008, Burdon et al., 2011, Baber et al., 2007, Nemeth et al., 2010). Unlike adult stem cells, ESC have enormous potential to differentiate into wide variety of cell types. Therefore, ESC have been suggested as a suitable source of lung epithelial/progenitor cells for cell-based regenerative therapy for lung diseases. Numerous approaches have been taken to differentiate human and mouse ESC into lung epithelial cells (Wang et al., 2007, Ali et al., 2002, Rippon et al., 2006, Roszell et al., 2009). More recently, it has been reported that intratracheal administration of ESC-derived type II AEC ameliorated pulmonary inflammation and fibrosis in a bleomycin-induced experimental lung injury model; where, minimally, the early reparative response was mediated by a paracrine mechanism, although this paracrine effect has yet to be confirmed (Wang et al., 2010, Banerjee et al., 2012). Here, I demonstrate that secretome of differentiated hESC (8-11 day CM) promotes alveolar epithelial cell wound repair via stimulation of cell migration and proliferation. This paracrine effect of cell-secretory products is specific to a particular stage of ESC differentiation, where the secretome of 8-11 day of differentiation is only found to be effective in the repair of alveolar epithelial wound *in vitro*.

Data supportive of ESC-mediated paracrine influence in lung injury repair is lacking. However, a rat model of cardiac ischemia demonstrated that infusion of mouse-ESC or ESC-conditioned media attenuated myocardial ischemia and improved cardiac function through a paracrine mechanism by ESC-secretory anti-inflammatory and cytoprotective cytokines, IL-10 and VEGF. In addition, transplantation of ESC suppressed pro-inflammatory cytokines TNF-α, IL-1 and IL-6 production by the injured cardiomyocytes (Crisostomo et al., 2008). Moreover, Crisostomo and colleagues demonstrated that the ESC paracrine protective mechanism in cardiac ischemia was superior to those of adult stem cells (Crisostomo et al., 2008). An *in vitro* study demonstrated that conditioned media obtained from undifferentiated pluripotent human ESC stimulated neonatal cardiomyocyte proliferation through secretory growth factors (LaFramboise et al., 2010). ESC paracrine-mediated anti-apoptotic effects have also been demonstrated in cardiomyocytes and corneal endothelial cells in the *in vitro* culture system (Singla & McDonald, 2007, Singla et al., 2008, Lu et al., 2010). Conditioned media obtained from undifferentiated mouse ESC was shown to be capable of inhibiting H_2O_2-induced apoptosis in rat cardiomyocyte cell line H9c2 through ESC-secretory anti-apoptotic proteins cystatin c, osteopontin, clusterin and tissue inhibitor of metalloproteinase-1 (TIMP-1) via activation of PI3K/Akt signalling pathway (Singla & McDonald, 2007, Singla et al., 2008).

To date, ESC-paracrine effects were evaluated mostly by using undifferentiated ESC. In my study, approaches were taken to evaluate the paracrine effects of both undifferentiated and differentiated hESC on alveolar A549 cell wound repair. My data demonstrates that the conditioned media obtained from undifferentiated hESC inhibits alveolar cell wound repair. Indirectly, it can be speculated that cell proliferation is not likely to be stimulated when an *in vitro* wound repair is inhibited. In support of this, I observed that conditioned

media obtained from day 16-22 of hESC differentiation significantly inhibited alveolar epithelial cell wound repair which was also associated with suppression of cell proliferation. Considering the LaFramboise et al. 2010 finding coupled to my observation, it suggests that secretome of undifferentiated hESC may have a phenotype-specific effect, particularly on cell proliferation.

Here, I have demonstrated that after 8-11 days of Activin-directed hESC differentiation, the differentiated cell population secrete factors which can stimulate alveolar A549 cell wound repair. This wound repair effect was accompanied by cell proliferation and migration stimulation. I investigated the effects of stage-specific secretome of differentiating hESC separately in the *in vitro* wound repair system. The comparative data analysis reveals an interesting observation that the paracrine effects of differentiating hESC on alveolar wound repair is heterogeneous. Unlike day 8-11, the secretome of day 3.5-8 and 16-22 stage of hESC differentiation appeared to be inhibitory to cell proliferation and migration resulting in an inhibition of alveolar epithelial cell wound repair.

Delay or failure of alveolar re-epithelialisation is thought to play a major role in aberrant alveolar wound healing and fibrogenesis in IPF (Selman et al., 2001). Type II AEC are the progenitors for type I AEC. Type II AEC participate in the injury repair by proliferation and differentiation into type I AEC promoting re-epithelialisation of denuded alveolar wall and restore the alveolar function (Uhal, 1997, Fehrenbach, 2001). Histopathological findings show features of type II AEC hyperplasia, which are presumably due to reparative response. A recent study showed that targeted injury of type II AEC induced pulmonary fibrosis (Sisson et al., 2010). Therapeutic intervention to facilitate type II AEC migration, proliferation and differentiation, therefore could augment the reparative process of injured

alveoli. More recently, it has been demonstrated that the milieu of damaged type II alveolar epithelial cells stimulates alveolar wound repair by autocrine and paracrine mechanism (Buckley et al., 2011). Herein, I report that *ex vivo* manipulation of hESC towards differentiation into endodermal and mesodermal derivatives provides a biological cue supportive of alveolar epithelial wound repair.

In this study, hESC were differentiated by restricted exposure of serum (FBS) followed by treatment with high concentration of recombinant human Activin A which, according to previous published data, generates prominently cells of endodermal origin (Kubo et al., 2004, Rippon et al., 2006). However, in my protocol, differentiated cells within the EBs, particularly on day 11 and 22, expressed both endodermal and mesodermal specific genes. The similarity of this gene expression profile in differentiating EBs is also supported by the work of Rippon and colleagues (Rippon et al., 2006). Using a similar differentiation protocol but on mouse-ESC, Rippon et al. demonstrated that endodermal lineage-specific genes *Foxa2* and *Sox17* appeared to be highly expressed between 10 and 15 days of differentiation, whereas, distal lung progenitor marker *TTF-1* and type II AEC-specific marker *SPC* gene expression appeared after 15 days of EB differentiation (Rippon et al., 2006). The mesodermal gene expression spiked on and afterwards the 7^{th} day of differentiation. The Rippon et al findings combined with my data, suggest that the secretome of day 8-11 hESC differentiation is originated from a mixed population of endodermal and mesodermal derivatives.

Identification of ESC-secretory proteins and understanding their biological function in alveolar wound repair and regeneration is important for *ex vivo* optimal differentiation of ESC towards regenerative therapeutic application. I explored LC-MS/MS mass

spectrometry to identify secretory proteins in 8-11 day-CM of differentiated hESC. However, I was not successful in detection of well-documented wound repair-associated secretory proteins of *H. sapiens* origin by this method. Mass spectrometry is a high throughput technique and, a wide range of proteins from cell lysates of undifferentiated and differentiated ESC have been identified by this method before (Van Hoof et al., 2006). Difficulties are apparent in identification of secretory proteins in high serum-containing cell culture conditioned media via a LC-MS/MS approach without any immediately identified reason (Thorsell et al., 2008). Thereby, a complete secretory profile of the day 8-11 differentiated hESC remains unknow. By using multiple antibody/ELISA techniques myriads of secretory proteins were identified in undifferentiated hESC, among them some have proven cell proliferation and differentiation effects (LaFramboise et al., 2010). Adaptation of suitable technique(s) will reveal the secretome profile of our specified stage of ESC differentiation which preliminarily has shown potential for alveolar epithelial repair.

Idiopathic pulmonary fibrosis is a terminal lung disease with poor prognosis. Alveolar epithelial cell damage (apoptosis) and failure of re-epithelialisation underpin the pathogenesis. ESC has been shown to have anti-apoptotic and anti-fibrotic effects, and here I demonstrate their re-epithelialisation stimulatory effect. Due to enormous differentiation potential, ESC has been proposed for clinical application of incurable lungs disease (Weiss & Finck, 2010). However, potential risk of teratoma formation and graft rejection in post transplantation period are the major obstacles in the ESC-mediated cell therapy. Herein, alternatively, I propose an acellular ESC-mediated intervention where secretory products from an optimised *ex vivo*-differentiated hESC could be utilised for regenerative therapy for IPF or other lung diseases avoiding direct cellular application. Development of a xeno-

free ESC differentiation culture condition and the identification of their secretome are the next steps towards achieving the goal.

Chapter 6

General discussion and conclusion

6.1. General discussion

The aim of this thesis was to explore two aspects of idiopathic pulmonary fibrosis; one was related to the pathogenesis of this disease and another was associated with its regenerative therapeutics. Despite intense research, the pathophysiological process of IPF remains largely unknown. Although many aspects of this disease have been studied, many aspects remain widely unexplored. One of the relatively unexplored pathognomic entities is the alveolar bronchiolisation and its effect on fibrogenesis. Using *in vitro* models and *ex vivo* studies, efforts have been made to understand the role of bronchiolar Clara cells on alveolar epithelial wound repair in the context of alveolar bronchiolisation (Chilosi et al., 2002, Odajima et al., 2007, Plantier et al., 2011).

Currently, there is no effective/curative treatment for IPF other than lung transplantation. Due to insufficient donor lungs and post-transplantation complication/failure, a new and effective curative therapy needs to be developed. It is now recognised that anti-inflammatory agents and steroids are ineffective to halt this disease progression. Recent unsatisfactory outcomes from newly developed anti-fibrotic drugs warrant an alternative stem cell-mediated regenerative approach for the treatment of IPF. In this thesis, experiments have been conducted to explore, particularly, the paracrine aspects of hMSC and hESC in alveolar epithelial wound repair. IPF is a disease of aberrant alveolar epithelial wound repair where inflammation is not the pivotal pathological player (Selman et al., 2001). Therefore, a therapeutic measure to facilitate alveolar epithelial restitution is likely to be an effective approach. My studies have demonstrated that hMSC and hESC stimulate alveolar epithelial wound repair via a paracrine mechanism. Of itself, this preliminary finding is important to support future development of stem cell-mediated

regenerative therapy for IPF, and highlights why this approach may work. In the following sections the major findings of this thesis have been discussed in general.

6.1.1. Clara cells inhibit alveolar epithelial wound repair via TRAIL-depended apoptosis mechanism, a new hypothesis has been proposed for the pathogenesis of IPF.

Currently the understanding of IPF pathogenesis is based on several hypotheses as discussed in the Chapter 1. While the inflammatory hypothesis is no longer valid, the evolving hypothesis implies that IPF develops due to multiple alveolar epithelial injuries, failure of alveolar epithelial restitution and abnormal epithelial-mesenchymal cross-talk. Type II AEC hyperplasia and fibroblastic foci within the active lesions are consistent pathognomic features of IPF. Numerous studies have been performed to explore the mechanism of fibroblastic foci formation and the source of myofibroblasts. Besides, the feature of alveolar epithelial cell hyperplasia has been explained as an overt-reparative response (Panos et al., 1990). Hyperplasia causes remodelling of the alveoli with cuboidalised epithelium leading to impaired gaseous exchange, which is the major function of the lung. The alveolar cuboidalisation seen in human IPF lungs and animal lung fibrosis models is contributed by both alveolar and bronchiolar epithelial cells (Odajima et al., 2007, Chilosi et al., 2002, Betsuyaku et al., 2000); this alveolar remodelling process is called alveolar bronchiolisation. However, the extent of bronchiolar epithelial cell contribution in alveolar bronchiolisation in IPF lung was hitherto unknown. Through this current study, we now know that 15% of cuboidalised epithelial cells within the alveolar bronchiolised area are phenotypically Clara cells, as shown in the Chapter 3 of this thesis.

Alveolar bronchiolisation is a part of the pathological process of IPF (Odajima et al., 2007, Chilosi et al., 2002, Betsuyaku et al., 2000). However, the effect of Clara cells on alveolar epithelial wound repair remains unknown. In this thesis, experiments were undertaken to investigate the consequence of Clara-AEC cross-talk during alveolar wound repair in IPF. The first challenge was to develop a suitable *in vitro* model which could be utilised to investigate the direct-contact effects of Clara cells on AEC wound repair, as no such model existed. A transwell system was utilised. Transwell provides an infrastructure of two compartments which are separated by a porous PET membrane. Alveolar epithelial cells were grown in monolayer on the upper surface of the PET membrane to make an alveolar compartment. Whereas, H441 Clara cells were grown in monolayer on the opposite surface to provide a bronchiolar compartment, where the porous PET membrane allowed cell migration from one compartment to another. Mechanical injury was made on alveolar A549 cells and responses of Clara and A549 cells were monitored. This model was replicable and transferable to other cell types as demonstrated through successful implementation in SAEC-H441, A549-CCD8Lu and A549-hMSC direct-contact co-culture wound repair settings, as shown in the Chapter 3 and Chapter 4. Therefore, this model offers a valuable tool for the investigation of interactive cell behaviour of one cell type onto another.

The mechanism of Clara cell migration into the affected alveoli is not clearly understood. Study on the animal model of lung fibrosis suggests that up-regulation of MMP-9 facilitates bronchiolar/Clara cell migration to the affected alveoli (Betsuyaku et al., 2000). Our *in vitro* model has demonstrated a distinct type of Clara cell migration, where the majority of cells localise to the alveolar epithelial wound margins but not within the wound gaps. This migration apparently occurred through a chemotactic-dependent mechanism, as

in the absence of AEC, Clara cells were unable to migrate. However, due to time and resource limitations, the chemokine(s) responsible for this phenomenon has (have) not been identified and remains as an important subject for future study.

According to the current hypothesis, multiple injuries take place in the alveolar epithelial cells but does not indicate if there is any direct injury-stimulation to the bronchiolar epithelium (Selman et al., 2001, Kaminski *et al*., 2003). Following alveolar injury, fibroblastic response is a part of the normal healing process; however, the bronchiolar/Clara cell response in IPF remains hitherto unexplained. Down-regulation of caveolin-1 in bronchiolar cells which causes hyperproliferation of Clara cells (bronchiolisation) has been reported in IPF (Odajima et al., 2007). Ectopic mucous cell differentiation has also been reported, which is involved in the process of bronchiolisation in IPF (Plantier et al., 2011). The ectopic differentiation takes place in a NRG1-α dependent manner where AEC do not contribute to this differentiation (Plantier et al., 2011). The evidence above is suggestive of an active involvement of Clara or other bronchiolar cells in the pathogenesis of IPF.

Clara cells are the progenitors of bronchiolar epithelium but do not take part in alveolar wound repair (Evans et al., 1976, Rawlins et al., 2009, Reynolds & Malkinson, 2010). The *in vitro* data shown in the Chapter 3 of this thesis suggests an inhibitory influence of Clara cells on AEC wound repair that is driven *via* a TRAIL-mediated apoptosis pathway. The *ex vivo* findings on IPF lung tissues also supports the *in vitro* observation by showing the evidence of TRAIL-expressing Clara cells within the bronchiolised alveoli with an association of AEC apoptosis, as shown in the Chapter 3. This first report suggests a

putative involvement of TRAIL-expressing Clara cells in the pathogenesis of IPF, which occurs more likely through the induction of AEC apoptosis.

This study has also demonstrated an anatomical compartment-specific distribution of epithelial TRAIL expression profile in the normal healthy lung. TRAIL expression has been observed in bronchiolar/Clara cells but not in the alveolar epithelium in health. A similar TRAIL expression pattern has been observed in cultured Clara cell line H441 cells and type II AEC line A549 cells, where H441 cells were strongly positive to TRAIL but A549 cells were negative. The reason for this compartment-specific differential TRAIL expression in normal lung epithelium is not clear; however, it is possible that bronchiolar cells require TRAIL for normal tissue homeostasis whereas AEC follow a different pathway. However, in disease states, this phenotype-specific TRAIL expression alters, where AEC express TRAIL along with bronchiolar cells as shown in the Chapter 3. A recent study however showed contrasting findings, demonstrating high levels of TRAIL expression in AEC of normal healthy lung compared to IPF counterparts (McGrath et al., 2012). The reason for these opposing findings is as yet unclear. But this reason can be methodological. McGrath et al. utilised resected lung tissues from primary lung cancer as control subjects where their smoking status was undisclosed. There is a possibility that existing disease condition or cigarette smoking can alter TRAIL expression in healthy lung. Moreover, they presented non-quantitative data from three control cases, which is, I think, inadequate number of control subjects to make a concrete conclusion in this regard.

It has been reported that administration of bleomycin in the lung of TRAIL-knock out mice decreases apoptosis in inflammatory cells that exacerbate inflammation and collagen deposition (McGrath et al., 2012). Another report however has shown that, application of

recombinant TRAIL stimulates collagen secretion by the lung fibroblasts (Yurovsky, 2003). TRAIL involvement in the pathogenesis of bronchial asthma has also been reported (Weckmann et al., 2007). Administration of recombinant TRAIL induces asthma-like pathological features in animal models. High levels of TRAIL have also been detected in the sputum of asthmatic patients (Weckmann et al., 2007). In addition, both soluble TRAIL and TRAIL-expressing Clara cells are capable of inducing apoptosis in alveolar and small airway epithelial cells and, application of TRAIL-receptor blocker mAbs reverses Clara cell direct-contact induced inhibition of AEC wound repair *in vitro*, as shown in the Chapter 3 of this thesis.

In this thesis, a set of experimental protocols has been designed to clarify the role of Clara cells on AEC wound repair. The generated data provide a novel concept for IPF pathogenesis. Considering the *in vitro* and *ex vivo* findings, I propose that the extensive pro-fibrotic remodelling observed in IPF lungs is, at least in part, driven by the TRAIL-expressing Clara cells through induction of alveolar epithelial cell apoptosis via a TRAIL-dependent mechanism. However, further experimentation is required to consolidate this hypothesis; possible future studies are suggested below (Section 6.2).

6.1.2. hMSC enhance lung epithelial wound repair through paracrine mechanisms

Due to the lack of effective anti-IPF treatment to date, an MSC-mediated strategy has been suggested. Pre-clinical studies on animal models of acute lung injury (ALI) and pulmonary fibrosis have shown some promise for clinical application of hMSC in idiopathic pulmonary fibrosis. The MSC-mediated regenerative therapy for IPF is still in its infancy. However, a recent small scale Phase I clinical trials of adipose-derived MSC on 12 IPF patients has shown promising safety profile (Tzouvelekis et al., 2011), which is

encouraging for future broader multicenter clinical trials. The reparative mechanism of MSC is largely mediated by paracrine mechanisms in injured lung (Weiss & Finck, 2010). More recently, this notion has been further supported by the work of Curley et al., where they demonstrate that MSC themselves and the conditioned media obtained from MSC exert similar wound repair effects on a ventilator induced murine model of ALI and alveolar A549 cell wound repair (Curley et al., 2012).

Anti-inflammatory effects of MSC have been demonstrated through murine models of ALI and pulmonary fibrosis (Ortiz et al., 2007, Gupta et al., 2007, Curley et al., 2012). However, the effect of MSC or their secretory product on injured AEC remains widely unexplored. The animal model is not suitable for monitoring the AEC migration. An *in vitro* wound repair model can be a suitable alternative for this purpose, where the epithelial cell migration and proliferation in response to given stimuli can be monitored. Using this method, a recent study has demonstrated that serum-free MSC conditioned media enhances alveolar A549 cell wound repair (Curley et al., 2012). Following a similar model, the experiments in this thesis show that the serum-free MSC conditioned alone is unable to enhance A549 cell wound repair but requires trace serum supplementation (0.2% FBS). The reason for this different pattern of A549 cell response to hMSC CM is not clear, but it is possible that this happens due to the donor variation of hMSC secretome profile. Another possible cause can be the source of the A549 cell lines. Curley et al. obtained A549 cell line from Porton Down, UK; whereas, our study used ATCC, USA originated A549 cell line which expressed type II AEC marker, *pro*SP-C. However, in this study, serum-free MSC CM alone was capable of SAEC wound repair, as shown in the Chapter 4.

Understanding the function of the hMSC secretome on AEC wound repair is important, as delayed or failure of AEC restitution is the likely cause of uncontrolled fibrosis in IPF. Hyperplasia of type II AEC within the IPF lung, as seen in histopathological tissue samples, indicates a presence of sufficient cells for repair. Therefore, modulation of type II AEC migration and/or differentiation can be an effective measure for appropriate wound repair. This study demonstrates the paracrine stimulatory effects of hMSC secretome on pulmonary epithelial wound repair.

Identification and characterisation of the individual component of hMSC secretome were the next steps of my investigation protocol. Myriads of secretory proteins have been identified in the hMSC conditioned media in previous studies. However, published hMSC secretome profiles largely vary depending on the detection techniques (Chen et al., 2008a, Estrada et al., 2009, Walter et al., 2010). The antibody based techniques have identified mostly growth factors and cytokine (Parekkadan et al., 2007, Chen et al., 2008a); on the other hand, the mass spectrometry based technique identified proteins which are mostly ECM proteins (Estrada et al., 2009, Walter et al., 2010, Scheibe et al., 2012). The reason for this difference is not clear, possibly, secretory growth factors and cytokines present in the conditioned media at a very low concentration which is beyond the lowest detection limit of LC-MS/MS mass spectrometry. Moreover, it is recognised that the adoption of ELISA-based approaches carries with it an inherent bias towards identification only of those constituents that one may wish to detect. I therefore, specifically elected to adopt an approach that would minimise such a potential bias, which admittedly in turn generates a methodological bias away from proteins present at lower abundance levels. However, considering my findings and those of others, it can be concluded that hMSC effectively

secrete a wide and varied spectrum of growth factors, cytokines and ECM/matricellular proteins with diverse biological and functional properties.

Using antibody depletion technique, a recent study has shown that hMSC-CM enhances alveolar A549 cell wound repair through secreted KGF (Curley et al., 2012). In line with other studies, KGF was not detected in hMSC-CM or lung fibroblast-CM in our study (Parekkadan et al., 2007, Estrada et al., 2009, Walter et al., 2010, Scheibe et al., 2012). However, we have consistently detected Fibronectin, Lumican, and Periostin in the hMSC-CM which appear to be capable of stimulating alveolar and small airway epithelial cells wound repair with or without supplementation of trace serum. The alveolar epithelial cell wound repair occurs through stimulation of cell migration but not by cell proliferation with hMSC-CM or secretory individual protein components, as shown in the Chapter 4. Growth factors such as KGF, HGF have an established role in epithelial restitution during injury repair. It is now recognised that ECM proteins not only provide the structural support of the tissue but also provide biological cues for cell growth, proliferation, migration and differentiation (Frantz et al., 2010). Previous studies have demonstrated that Fibronectin, Lumican and Periostin are crucial for epithelial wound repair. This study has not confirmed that hMSC conditioned media enhances alveolar or small airway epithelial wound repair through their secretory Fibronectin or Lumican or Periostin, but demonstrated an abundant presence in hMSC secretome which are capable of pulmonary epithelial wound repair. Therefore, it is not unlikely that these secretory proteins contribute, at least in a part, to the hMSC-mediated pulmonary epithelial cell wound repair.

6.1.3. Differentiated hESC displays both positive and negative regulatory effects of alveolar epithelial wound repair depending on their stage of differentiation through paracrine mechanisms

hESC are pluripotent stem cells with the capacity to differentiate into derivatives of all three germ layers including alveolar epithelial cells. Due to this enormous differential potential, hESC have been suggested for the regenerative therapy for lung injury and pulmonary fibrosis. Numerous protocols have been developed for the differentiation of type II AEC from human and mouse ESC (Ali et al., 2002, Rippon et al., 2006, Wang et al., 2007, Roszell et al., 2009). However, data supportive of ESC-mediated healing effect in pulmonary fibrosis is limited.

Intratracheal administration of ESC-derived type II AEC has shown amelioration of pulmonary inflammation and fibrosis in a bleomycin-induced experimental lung injury model, where, the early reparative response was thought to be mediated via paracrine mechanisms (Wang et al., 2010, Banerjee et al., 2012). The paracrine effect of differentiated hESC on alveolar epithelial cell wound repair is, to date, unexplored. Through this study the paracrine role of undifferentiated and differentiated hESC have been investigated on *in vitro* alveolar epithelial wound repair system. The data that generated through this study is an important addition to our understanding of the paracrine role of hESC on alveolar wound repair.

The secretome of undifferentiated pluripotent hESC inhibits alveolar epithelial wound repair, as shown in the Chapter 5; whereas, the secretome of Activin-directed differentiated hESC has shown differential alveolar epithelial cell wound repair effects. Overall, the conditioned media obtained from differentiated hESC appeared to be inhibitory to alveolar

epithelial wound repair comparing control except the Day 8-11 CM. Conditioned media obtained from day 8-11 of differentiation significantly stimulated wound repair comparing that were observed with CM collected from before and after the specific differentiation window of 8-11 days. Subsequent studies clarify that the alveolar epithelial wound repair inhibition by CM obtained from 3.5-8 and 16-22 days differentiated hESC occurs through inhibition of cell migration and proliferation.

The anti-inflammatory and cytoprotective functions of ESC or ESC-conditioned media have already been demonstrated in animal models of cardiac ischemia and pulmonary fibrosis (Wang et al., 2010, Crisostomo et al., 2008). My study data demonstrated human ESC-paracrine mediated pulmonary epithelial wound repair stimulation which is albeit a differentiation-stage specific. The next step was to identify the hESC secretory molecules that were responsible for this observed effect. After successful detection of the hMSC secretory proteins, as shown in the Chapter 4, LC-MS/MS mass spectrometry was attempted. However, despite the repetitive efforts, the mass spectrometry technique was unable to identify any well-known biologically relevant secretory proteins in differentiated hESC conditioned media. Mass spectrometry is a high throughput technique and a wide range of proteins from cell lysates of undifferentiated and differentiated ESC have been identified previously by this method (Van Hoof et al., 2006). Due to consecutive failures, I concluded that the LC-MS/MS mass spectrometry approach may not be suitable for identification of secretory proteins from a high serum-containing culture media. An antibody-based growth factor/cytokine array kit can be used instead.

Although this study and previous reports provide supportive evidence for the clinical application of ESC, there are certain concerns including potential risk of teratoma

formation and graft-rejection during post transplantation period. As ESC have potential paracrine-mediated healing effects, through this study I propose an acellular ESC-mediated intervention, where secretory products from an optimised *in vitro*-differentiated hESC could be utilised for regenerative therapy in various lung diseases including IPF to avoid direct application of cellular components. However, there is still a long way to go and many other issues need to be explored before development of such acellular regenerative modalities for the treatment of IPF.

6.2. Recommendations for future studies

1. Due to the unavailability of primary and IPF Clara cells, human Clara cell line, H441 cells have been utilised in this study to evaluate the role of Clara cells on AEC wound repair. Similar experiments can be replicated using primary alveolar epithelial cells and Clara cells isolated from IPF and healthy control lungs. Anatomically, Clara cells and AEC are situated in close proximity; therefore, it is difficult to isolate a homogeneously pure population of type II AEC and Clara cells. These two cell populations can be separated from each other and from lung fibroblasts by using antibody coated magnetic micro-bids, such as MACS® Cell Separation Technology. Magnetic micro-bids will be conjugated with antibody *pro*SP-C specific for type II AEC and antibody CC10 specific for Clara cell isolation. The next challenge is the optimisation of appropriate culture conditions for AEC and Clara cells. As primary human small airway epithelial cells (SAEC) grew well in SAGM (Small airway growth media, Lonza). SAGM can be used for AEC and Clara cell culture initially and subsequently media could be optimised by adding suitable growth factors if required.

2. My thesis has explored the TRAIL expression profile in IPF and normal healthy lung tissues. TRAIL has an equal binding affinity to its four cell membrane receptors TRAIL-R1, TRAIL-R2, TRAIL-R3 (DcR1) and TRAIL-R4 (DcR2). Up-regulation of TRAIL-R1 and TRAIL-R2 sensitises cells to undergo TRAIL-mediated apoptosis; conversely, up-regulation of decoy receptors TRAIL-R3 and TRAIL-R4 makes cells resistant to TRAIL-induced apoptosis. Therefore, a complete expression profile of these four receptors in IPF and normal healthy lung tissue samples needs to be evaluated. Evidence of TRAIL-R1 and TRAIL-R2 up-regulation along with TRAIL-R3 and TRAIL-R4 down-regulation in AEC of IPF lungs will further support the hypothesis proposed here.

3. In this thesis, the paracrine influences of hMSC on alveolar A549 cell and primary small airway epithelial cell wound repair have been investigated. It would be interesting to replicate similar sets of experiments on alveolar epithelial cells isolated from IPF lung to see if hMSC elicit the same response.

4. My studies have not confirmed that hMSC CM stimulates pulmonary epithelial cell wound repair through secretory Fibronectin, Lumican or Periostin. This study suggests a possibility of hMSC CM-mediated wound repair effects may be driven by the above secretory protein(s). Further studies can be done to confirm if this is the case. A depletion method could be adopted using neutralising antibodies specific to Fibronectin, Lumican and Periostin in hMSC conditioned media in similar or adapted wound repair systems.

5. In my study, 10% KO-SR has been used for the hESC differentiation protocol and hESC-CM preparation as an initial step. Adaptation of a similar xeno-free ESC differentiation culture protocol by withdrawal of serum and addition of recombinant

growth factor(s) is the next step towards development of hESC-mediated acellular regenerative therapeutic modalities. The identification of hESC secretory proteins in the CM of different stages of differentiation remains elusive. A suitable technique, such as, protein array method can be approached for precise profiling of the hESC secretome.

6. I have proposed a possible TRAIL-mediated apoptosis mechanism for the alveolar epithelial cell apoptosis during the pathogenesis of IPF. As anti-apoptotic paracrine effects of MSC and ESC have been shown (Zhen et al., 2008, Singla & McDonald, 2007), it would be important to dissect this further through further exploration to seek whether the hMSC CM or hESC CM could abrogate the TRAIL-mediate AEC apoptosis.

6.3. CONCLUSION

In the UK, 4000 new IPF cases are being diagnosed each year and amongst them more than two-third die within 3-5 years of diagnosis. Therefore, a better understanding and clarification of critical pathogenic events in IPF and exploration of novel therapeutic approaches are timely. Through this thesis, I have suggested a new aspect of pathogenesis which implies that the TRAIL-expressing Clara cells are likely to be involved in the aberrant alveolar wound repair and subsequent fibrogenesis in IPF, which occurs possibly through induction of alveolar epithelial cell apoptosis via a TRAIL-medicated mechanism. This finding unravels critical targets for further investigative dissection towards development of novel therapeutic agents for IPF. The study of this thesis has also demonstrated the paracrine role of hMSC and hESC in the alveolar epithelial wound repair. hMSC conditioned media and a cohort of secretory proteins, namely, Fibronectin, Lumican and Periostin have shown some promise in pulmonary epithelial wound repair. As a preliminary step, I have also demonstrated the paracrine healing capacity of differentiated

hESC which has opened a new horizon for future study. Further identification and characterisation of hESC and hMSC secretome on alveolar wound repair are the next steps towards development of novel acellular stem cell-mediated regenerative therapeutic intervention for IPF and other incurable lung diseases.

References

American Thoracic Society/European Respiratory Society. (2002). International Multidisciplinary Consensus Classification of the Idiopathic Interstitial Pneumonias. This joint statement of the American Thoracic Society (ATS), and the European Respiratory Society (ERS) was adopted by the ATS board of directors, June 2001 and by the ERS Executive Committee, June 2001. *American Journal Of Respiratory And Critical Care Medicine.* 165 (2): 277-304.

American Thoracic Society (ATS), and the European Respiratory Society (ERS). (2000). American Thoracic Society. Idiopathic pulmonary fibrosis: diagnosis and treatment. International consensus statement.. *American Journal Of Respiratory And Critical Care Medicine.* 161 (2): 646-664.

Abranches, E., Silva, M., Pradier, L., Schulz, H., Hummel, O., Henrique, D. & Bekman, E. (2009). Neural differentiation of embryonic stem cells in vitro: a road map to neurogenesis in the embryo. *Plos One.* 4 (7): e6286-e6286.

Adamson, I.Y., Young, L. & King, G.M. (1991). Reciprocal epithelial: fibroblast interactions in the control of fetal and adult rat lung cells in culture. *Experimental lung research.* 17 (4): 821-835.

Adamson, I.Y., Hedgecock, C. & Bowden, D.H. (1990). Epithelial cell-fibroblast interactions in lung injury and repair. *The American journal of pathology.* 137 (2): 385-392.

Adamson, I.Y., Young, L. & Bowden, D.H. (1988). Relationship of alveolar epithelial injury and repair to the induction of pulmonary fibrosis. *The American journal of pathology.* 130 (2): 377-383.

Aguilar, S., Scotton, C.J., McNulty, K., Nye, E., Stamp, G., Laurent, G., Bonnet, D. & Janes, S.M. (2009). Bone marrow stem cells expressing keratinocyte growth factor via an inducible lentivirus protects against bleomycin-induced pulmonary fibrosis. *PloS one.* 4 (11): e8013.

Akram, K.M., Samad, S., Spiteri, M. & Forsyth, N.R. (2012). Mesenchymal Stem Cell Therapy and Lung Diseases. *Advances in Biochemical Engineering/Biotechnology.* [Epub ahead of print]

Alder, J.K., Chen, J.J., Lancaster, L., Danoff, S., Su, S.C., Cogan, J.D., Vulto, I., Xie, M., Qi, X., Tuder, R.M., Phillips, J.A.,3rd, Lansdorp, P.M., Loyd, J.E. & Armanios, M.Y. (2008). Short telomeres are a risk factor for idiopathic pulmonary fibrosis. *Proceedings of the National Academy of Sciences of the United States of America.* 105 (35): 13051-13056.

Ali, N.N., Edgar, A.J., Samadikuchaksaraei, A., Timson, C.M., Romanska, H.M., Polak, J.M. & Bishop, A.E. (2002). Derivation of type II alveolar epithelial cells from murine embryonic stem cells. *Tissue engineering.* 8 (4): 541-550.

Allen, J.T., Knight, R.A., Bloor, C.A. & Spiteri, M.A. (1999). Enhanced insulin-like growth factor binding protein-related protein 2 (Connective tissue growth factor) expression in patients with idiopathic pulmonary fibrosis and pulmonary sarcoidosis. *American journal of respiratory cell and molecular biology.* 21 (6): 693-700.

Antoniades, H.N., Bravo, M.A., Avila, R.E., Galanopoulos, T., Neville-Golden, J., Maxwell, M. & Selman, M. (1990). Platelet-derived growth factor in idiopathic pulmonary fibrosis. *The Journal of clinical investigation.* 86 (4): 1055-1064.

Antoniou, K.M., Hansell, D.M., Rubens, M.B., Marten, K., Desai, S.R., Siafakas, N.M., Nicholson, A.G., du Bois, R.M. & Wells, A.U. (2008). Idiopathic pulmonary fibrosis: outcome in relation to smoking status. *American journal of respiratory and critical care medicine.* 177 (2): 190-194.

Antoniou, K.M., Papadaki, H.A., Soufla, G., Kastrinaki, M.C., Damianaki, A., Koutala, H., Spandidos, D.A. & Siafakas, N.M. (2010). Investigation of bone marrow mesenchymal stem cells (BM MSCs) involvement in Idiopathic Pulmonary Fibrosis (IPF). *Respiratory medicine.* 104 (10): 1535-1542.

Armanios, M.Y., Chen, J.J., Cogan, J.D., Alder, J.K., Ingersoll, R.G., Markin, C., Lawson, W.E., Xie, M., Vulto, I., Phillips, J.A.,3rd, Lansdorp, P.M., Greider, C.W. & Loyd, J.E. (2007). Telomerase mutations in families with idiopathic pulmonary fibrosis. *The New England journal of medicine.* 356 (13): 1317-1326.

Arnhold, S., Absenger, Y., Klein, H., Addicks, K. & Schraermeyer, U. (2007). Transplantation of bone marrow-derived mesenchymal stem cells rescue photoreceptor cells in the dystrophic retina of the rhodopsin knockout mouse. *Graefe's archive for clinical and experimental ophthalmology = Albrecht von Graefes Archiv fur klinische und experimentelle Ophthalmologie.* 245 (3): 414-422.

Ashino, Y., Ying, X., Dobbs, L.G. & Bhattacharya, J. (2000). [Ca(2+)](i) oscillations regulate type II cell exocytosis in the pulmonary alveolus. *American Journal Of Physiology.Lung Cellular And Molecular Physiology.* 279 (1): L5-L13.

Atabai, K., Ishigaki, M., Geiser, T., Ueki, I., Matthay, M.A. & Ware, L.B. (2002). Keratinocyte growth factor can enhance alveolar epithelial repair by nonmitogenic mechanisms. *American journal of physiology.Lung cellular and molecular physiology.* 283 (1): L163-9.

Azuma, A., Nukiwa, T., Tsuboi, E., Suga, M., Abe, S., Nakata, K., Taguchi, Y., Nagai, S., Itoh, H., Ohi, M., Sato, A. & Kudoh, S. (2005). Double-blind, placebo-controlled trial of pirfenidone in patients with idiopathic pulmonary fibrosis. *American journal of respiratory and critical care medicine.* 171 (9): 1040-1047.

Baber, S.R., Deng, W., Master, R.G., Bunnell, B.A., Taylor, B.K., Murthy, S.N., Hyman, A.L. & Kadowitz, P.J. (2007). Intratracheal mesenchymal stem cell administration attenuates monocrotaline-induced pulmonary hypertension and endothelial dysfunction. *American journal of physiology.Heart and circulatory physiology.* 292 (2): H1120-8.

Bajada, S., Mazakova, I., Richardson, J.B. & Ashammakhi, N. (2008). Updates on stem cells and their applications in regenerative medicine. *Journal of tissue engineering and regenerative medicine.* 2 (4): 169-183.

Baksh, D., Yao, R. & Tuan, R.S. (2007). Comparison of proliferative and multilineage differentiation potential of human mesenchymal stem cells derived from umbilical cord and bone marrow. *Stem cells (Dayton, Ohio).* 25 (6): 1384-1392.

Banerjee, E.R., Laflamme, M.A., Papayannopoulou, T., Kahn, M., Murry, C.E. & Henderson,William R.,,Jr (2012). Human embryonic stem cells differentiated to lung lineage-specific cells ameliorate pulmonary fibrosis in a xenograft transplant mouse model. *Plos One.* 7 (3): e33165-e33165.

Barbas-Filho, J.V., Ferreira, M.A., Sesso, A., Kairalla, R.A., Carvalho, C.R. & Capelozzi, V.L. (2001). Evidence of type II pneumocyte apoptosis in the pathogenesis of idiopathic pulmonary fibrosis (IFP)/usual interstitial pneumonia (UIP). *Journal of clinical pathology.* 54 (2): 132-138.

Baumgartner, K.B., Samet, J.M., Stidley, C.A., Colby, T.V. & Waldron, J.A. (1997). Cigarette smoking: a risk factor for idiopathic pulmonary fibrosis. *American Journal Of Respiratory And Critical Care Medicine.* 155 (1): 242-248.

Begue, B., Wajant, H., Bambou, J.C., Dubuquoy, L., Siegmund, D., Beaulieu, J.F., Canioni, D., Berrebi, D., Brousse, N., Desreumaux, P., Schmitz, J., Lentze, M.J., Goulet, O., Cerf-Bensussan, N. & Ruemmele, F.M. (2006). Implication of TNF-

related apoptosis-inducing ligand in inflammatory intestinal epithelial lesions. *Gastroenterology.* 130 (7): 1962-1974.

Belperio, J.A., Dy, M., Murray, L., Burdick, M.D., Xue, Y.Y., Strieter, R.M. & Keane, M.P. (2004). The role of the Th2 CC chemokine ligand CCL17 in pulmonary fibrosis. *Journal of immunology (Baltimore, Md.: 1950).* 173 (7): 4692-4698.

Berry, M.F., Engler, A.J., Woo, Y.J., Pirolli, T.J., Bish, L.T., Jayasankar, V., Morine, K.J., Gardner, T.J., Discher, D.E. & Sweeney, H.L. (2006). Mesenchymal stem cell injection after myocardial infarction improves myocardial compliance. *American journal of physiology.Heart and circulatory physiology.* 290 (6): H2196-203.

Betsuyaku, T., Fukuda, Y., Parks, W.C., Shipley, J.M. & Senior, R.M. (2000). Gelatinase B is required for alveolar bronchiolization after intratracheal bleomycin. *The American journal of pathology.* 157 (2): 525-535.

Bishop, A.E. (2004). Pulmonary epithelial stem cells. *Cell proliferation.* 37 (1): 89-96.

Bjoraker, J.A., Ryu, J.H., Edwin, M.K., Myers, J.L., Tazelaar, H.D., Schroeder, D.R. & Offord, K.P. (1998). Prognostic significance of histopathologic subsets in idiopathic pulmonary fibrosis. *American journal of respiratory and critical care medicine.* 157 (1): 199-203.

Borok, Z., Gillissen, A., Buhl, R., Hoyt, R.F., Hubbard, R.C., Ozaki, T., Rennard, S.I. & Crystal, R.G. (1991). Augmentation of functional prostaglandin E levels on the respiratory epithelial surface by aerosol administration of prostaglandin E. *The American Review of Respiratory Disease.* 144 (5): 1080-1084.

Bozelka, B.E., Sestini, P., Gaumer, H.R., Hammad, Y., Heather, C.J. & Salvaggio, J.E. (1983). A murine model of asbestosis. *The American Journal Of Pathology.* 112 (3): 326-337.

Brody, J.S. &Williams, M.C. (1992). Pulmonary alveolar epithelial cell differentiation. *Annual Review of Physiology.* 54 : 351-371.

Brost, S., Koschny, R., Sykora, J., Stremmel, W., Lasitschka, F., Walczak, H. & Ganten, T.M. (2010). Differential expression of the TRAIL/TRAIL-receptor system in patients with inflammatory bowel disease. *Pathology, research and practice.* 206 (1): 43-50.

Bruce, S.J., Gardiner, B.B., Burke, L.J., Gongora, M.M., Grimmond, S.M. & Perkins, A.C. (2007). Dynamic transcription programs during ES cell differentiation towards mesoderm in serum versus serum-freeBMP4 culture. *BMC Genomics.* 8 : 365-365.

Buckley, S., Shi, W., Barsky, L. & Warburton, D. (2008). TGF-beta signaling promotes survival and repair in rat alveolar epithelial type 2 cells during recovery after hyperoxic injury. *American journal of physiology.Lung cellular and molecular physiology.* 294 (4): L739-48.

Buckley, S., Shi, W., Carraro, G., Sedrakyan, S., Da Sacco, S., Driscoll, B.A., Perin, L., De Filippo, R.E. & Warburton, D. (2011). The milieu of damaged alveolar epithelial type 2 cells stimulates alveolar wound repair by endogenous and exogenous progenitors. *American journal of respiratory cell and molecular biology.* 45 (6): 1212-1221.

Budinger, G.R.S., Mutlu, G., Eisenbart, J., Fuller, A.C., Bellmeyer, A.A., Baker, C.M., Wilson, M., Ridge, K., Barrett, T.A., Lee, V.Y. & Chandel, N.S. (2006). Proapoptotic Bid is required for pulmonary fibrosis. *Proceedings of the National Academy of Sciences of the United States of America.* 103 (12): 4604-4609.

Burdon, T.J., Paul, A., Noiseux, N., Prakash, S. & Shum-Tim, D. (2011). Bone marrow stem cell derived paracrine factors for regenerative medicine: current perspectives and therapeutic potential. *Bone marrow research.* 2011 : 207326.

Cantin, A.M., Hubbard, R.C. & Crystal, R.G. (1989). Glutathione deficiency in the epithelial lining fluid of the lower respiratory tract in idiopathic pulmonary fibrosis. *The American Review of Respiratory Disease.* 139 (2): 370-372.

Chamberlain, C.S., Brounts, S.H., Sterken, D.G., Rolnick, K.I., Baer, G.S. & Vanderby, R. (2011). Gene profiling of the rat medial collateral ligament during early healing using microarray analysis. *Journal of applied physiology (Bethesda, Md.: 1985).* 111 (2): 552-565.

Chambers, I., Colby, D., Robertson, M., Nichols, J., Lee, S., Tweedie, S. & Smith, A. (2003). Functional expression cloning of Nanog, a pluripotency sustaining factor in embryonic stem cells. *Cell.* 113 (5): 643-655.

Chang, W., Wei, K., Jacobs, S.S., Upadhyay, D., Weill, D. & Rosen, G.D. (2010). SPARC suppresses apoptosis of idiopathic pulmonary fibrosis fibroblasts through constitutive activation of beta-catenin. *The Journal of biological chemistry.* 285 (11): 8196-8206.

Checa, M., Ruiz, V., Montano, M., Velazquez-Cruz, R., Selman, M. & Pardo, A. (2008). MMP-1 polymorphisms and the risk of idiopathic pulmonary fibrosis. *Human genetics.* 124 (5): 465-472.

Chen, H., Matsumoto, K. & Stripp, B.R. (2009). Bronchiolar progenitor cells. *Proceedings Of The American Thoracic Society.* 6 (7): 602-606.

Chen, L., Tredget, E.E., Wu, P.Y. & Wu, Y. (2008a). Paracrine factors of mesenchymal stem cells recruit macrophages and endothelial lineage cells and enhance wound healing. *PloS one.* 3 (4): e1886.

Chen, P., McGuire, J.K., Hackman, R.C., Kim, K.H., Black, R.A., Poindexter, K., Yan, W., Liu, P., Chen, A.J., Parks, W.C. & Madtes, D.K. (2008b). Tissue inhibitor of metalloproteinase-1 moderates airway re-epithelialization by regulating matrilysin activity. *The American journal of pathology.* 172 (5): 1256-1270.

Cheng, C.Y., Martin, D.E., Leggett, C.G., Reece, M.C. & Reese, A.C. (1988). Fibronectin enhances healing of excised wounds in rats. *Archives of Dermatology.* 124 (2): 221-225.

Chilosi, M., Poletti, V., Murer, B., Lestani, M., Cancellieri, A., Montagna, L., Piccoli, P., Cangi, G., Semenzato, G. & Doglioni, C. (2002). Abnormal re-epithelialization and lung remodeling in idiopathic pulmonary fibrosis: the role of deltaN-p63. *Laboratory investigation; a journal of technical methods and pathology.* 82 (10): 1335-1345.

Collins, J.F., Orozco, C.R., McCullough, B., Coalson, J.J. & Johanson, W.G.,Jr (1982). Pulmonary fibrosis with small-airway disease: a model in nonhuman primates. *Experimental lung research.* 3 (2): 91-108.

Colman, A. (2004). Making new beta cells from stem cells. *Seminars in cell & developmental biology.* 15 (3): 337-345.

Colter, D.C., Sekiya, I. & Prockop, D.J. (2001). Identification of a subpopulation of rapidly self-renewing and multipotential adult stem cells in colonies of human marrow stromal cells. *Proceedings of the National Academy of Sciences of the United States of America.* 98 (14): 7841-7845.

Conconi, M.T., Burra, P., Di Liddo, R., Calore, C., Turetta, M., Bellini, S., Bo, P., Nussdorfer, G.G. & Parnigotto, P.P. (2006). CD105(+) cells from Wharton's jelly show in vitro and in vivo myogenic differentiative potential. *International journal of molecular medicine.* 18 (6): 1089-1096.

Corrin, B., Dewar, A., Rodriguez-Roisin, R. & Turner-Warwick, M. (1985). Fine structural changes in cryptogenic fibrosing alveolitis and asbestosis. *The Journal of pathology.* 147 (2): 107-119.

Crisostomo, P.R., Abarbanell, A.M., Wang, M., Lahm, T., Wang, Y. & Meldrum, D.R. (2008). Embryonic stem cells attenuate myocardial dysfunction and inflammation after surgical global ischemia via paracrine actions. *American journal of physiology.Heart and circulatory physiology.* 295 (4): H1726-35.

Crosby, L.M. &Waters, C.M. (2010). Epithelial repair mechanisms in the lung. *American Journal Of Physiology.Lung Cellular And Molecular Physiology.* 298 (6): L715-L731.

Curley, G.F., Hayes, M., Ansari, B., Shaw, G., Ryan, A., Barry, F., O'Brien, T., O'Toole, D. & Laffey, J.G. (2012). Mesenchymal stem cells enhance recovery and repair following ventilator-induced lung injury in the rat. *Thorax.* 67 (6): 496-501.

Daar, A.S. &Greenwood, H.L. (2007). A proposed definition of regenerative medicine. *Journal of tissue engineering and regenerative medicine.* 1 (3): 179-184.

Dacic, S. &Yousem, S.A. (2003). Histologic classification of idiopathic chronic interstitial pneumonias. *American Journal Of Respiratory Cell And Molecular Biology.* 29 (3): S5-S9.

D'Amour, K.A., Agulnick, A.D., Eliazer, S., Kelly, O.G., Kroon, E. & Baetge, E.E. (2005). Efficient differentiation of human embryonic stem cells to definitive endoderm. *Nature biotechnology.* 23 (12): 1534-1541.

Daniels, R.A., Turley, H., Kimberley, F.C., Liu, X.S., Mongkolsapaya, J., Ch'En, P., Xu, X.N., Jin, B.Q., Pezzella, F. & Screaton, G.R. (2005). Expression of TRAIL and TRAIL receptors in normal and malignant tissues. *Cell research.* 15 (6): 430-438.

Danjo, Y. &Gipson, I.K. (1998). Actin 'purse string' filaments are anchored by E-cadherin-mediated adherens junctions at the leading edge of the epithelial wound, providing coordinated cell movement. *Journal of cell science.* 111 (Pt 22) (Pt 22): 3323-3332.

Darby, I., Skalli, O. & Gabbiani, G. (1990). Alpha-smooth muscle actin is transiently expressed by myofibroblasts during experimental wound healing. *Laboratory investigation; a journal of technical methods and pathology.* 63 (1): 21-29.

Davis, G.S., Leslie, K.O. & Hemenway, D.R. (1998). Silicosis in mice: effects of dose, time, and genetic strain. *Journal of environmental pathology, toxicology and oncology : official organ of the International Society for Environmental Toxicology and Cancer.* 17 (2): 81-97.

Dean, J.W.,3rd &Blankenship, J.A. (1997). Migration of gingival fibroblasts on fibronectin and laminin. *Journal of periodontology.* 68 (8): 750-757.

Deb, A., Wang, S., Skelding, K.A., Miller, D., Simper, D. & Caplice, N.M. (2003). Bone marrow-derived cardiomyocytes are present in adult human heart: A study of gender-mismatched bone marrow transplantation patients. *Circulation.* 107 (9): 1247-1249.

Delorme, B., Ringe, J., Pontikoglou, C., Gaillard, J., Langonne, A., Sensebe, L., Noel, D., Jorgensen, C., Haupl, T. & Charbord, P. (2009). Specific lineage-priming of bone marrow mesenchymal stem cells provides the molecular framework for their plasticity. *Stem cells (Dayton, Ohio).* 27 (5): 1142-1151.

Desmoulière, A., Geinoz, A., Gabbiani, F. & Gabbiani, G. (1993). Transforming growth factor-beta 1 induces alpha-smooth muscle actin expression in granulation tissue myofibroblasts and in quiescent and growing cultured fibroblasts. *The Journal of cell biology.* 122 (1): 103-111.

Desmouliere, A., Redard, M., Darby, I. & Gabbiani, G. (1995). Apoptosis mediates the decrease in cellularity during the transition between granulation tissue and scar. *The American journal of pathology.* 146 (1): 56-66.

Dezawa, M., Kanno, H., Hoshino, M., Cho, H., Matsumoto, N., Itokazu, Y., Tajima, N., Yamada, H., Sawada, H., Ishikawa, H., Mimura, T., Kitada, M., Suzuki, Y. & Ide, C. (2004). Specific induction of neuronal cells from bone marrow stromal cells and application for autologous transplantation. *The Journal of clinical investigation.* 113 (12): 1701-1710.

Diaz de Leon, A., Cronkhite, J.T., Katzenstein, A.L., Godwin, J.D., Raghu, G., Glazer, C.S., Rosenblatt, R.L., Girod, C.E., Garrity, E.R., Xing, C. & Garcia, C.K. (2010). Telomere lengths, pulmonary fibrosis and telomerase (TERT) mutations. *PloS one.* 5 (5): e10680.

D'Ippolito, G., Diabira, S., Howard, G.A., Menei, P., Roos, B.A. & Schiller, P.C. (2004). Marrow-isolated adult multilineage inducible (MIAMI) cells, a unique population of postnatal young and old human cells with extensive expansion and differentiation potential. *Journal of cell science.* 117 : 2971-2981.

Dissanayake, S.K., Wade, M., Johnson, C.E., O'Connell, M.P., Leotlela, P.D., French, A.D., Shah, K.V., Hewitt, K.J., Rosenthal, D.T., Indig, F.E., Jiang, Y., Nickoloff, B.J., Taub, D.D., Trent, J.M., Moon, R.T., Bittner, M. & Weeraratna, A.T. (2007). The Wnt5A/protein kinase C pathway mediates motility in melanoma cells via the inhibition of metastasis suppressors and initiation of an epithelial to mesenchymal transition. *The Journal of biological chemistry.* 282 (23): 17259-17271.

Dolhnikoff, M., Morin, J., Roughley, P.J. & Ludwig, M.S. (1998). Expression of lumican in human lungs. *American journal of respiratory cell and molecular biology.* 19 (4): 582-587.

Dominici, M., Le Blanc, K., Mueller, I., Slaper-Cortenbach, I., Marini, F., Krause, D., Deans, R., Keating, A., Prockop, D. & Horwitz, E. (2006). Minimal criteria for defining multipotent mesenchymal stromal cells. The International Society for Cellular Therapy position statement. *Cytotherapy.* 8 (4): 315-317.

Egan, J.J., Stewart, J.P., Hasleton, P.S., Arrand, J.R., Carroll, K.B. & Woodcock, A.A. (1995). Epstein-Barr virus replication within pulmonary epithelial cells in cryptogenic fibrosing alveolitis. *Thorax.* 50 (12): 1234-1239.

Ennis, J., Sarugaser, R., Gomez, A., Baksh, D. & Davies, J.E. (2008). Isolation, characterization, and differentiation of human umbilical cord perivascular cells (HUCPVCs). *Methods in cell biology.* 86 : 121-136.

Epperly, M.W., Guo, H., Gretton, J.E. & Greenberger, J.S. (2003). Bone marrow origin of myofibroblasts in irradiation pulmonary fibrosis. *American journal of respiratory cell and molecular biology.* 29 (2): 213-224.

Estrada, R., Li, N., Sarojini, H., An, J., Lee, M. & Wang, E. (2009). Secretome from mesenchymal stem cells induces angiogenesis via Cyr61. *Journal of cellular physiology.* 219 (3): 563-571.

Evans, M.J., Cabral, L.J., Stephens, R.J. & Freeman, G. (1975). Transformation of alveolar type 2 cells to type 1 cells following exposure to NO2. *Experimental and molecular pathology.* 22 (1): 142-150.

Evans, M.J., Johnson, L.V., Stephens, R.J. & Freeman, G. (1976). Renewal of the terminal bronchiolar epithelium in the rat following exposure to NO2 or O3. *Laboratory investigation; a journal of technical methods and pathology.* 35 (3): 246-257.

Evans, M.J. &Kaufman, M.H. (1981). Establishment in culture of pluripotential cells from mouse embryos. *Nature.* 292 (5819): 154-156.

Falschlehner, C., Schaefer, U. & Walczak, H. (2009). Following TRAIL's path in the immune system. *Immunology.* 127 (2): 145-154.

Fehrenbach, H. (2001). Alveolar epithelial type II cell: defender of the alveolus revisited. *Respiratory Research.* 2 (1): 33-46.

Fehrenbach, H., Kasper, M., Tschernig, T., Pan, T., Schuh, D., Shannon, J.M., Muller, M. & Mason, R.J. (1999). Keratinocyte growth factor-induced hyperplasia of rat alveolar type II cells in vivo is resolved by differentiation into type I cells and by apoptosis. *The European respiratory journal : official journal of the European Society for Clinical Respiratory Physiology.* 14 (3): 534-544.

Fenteany, G., Janmey, P.A. & Stossel, T.P. (2000). Signaling pathways and cell mechanics involved in wound closure by epithelial cell sheets. *Current biology : CB.* 10 (14): 831-838.

Finder, J., Stark, W.W., J., Nakayama, D.K., Geller, D., Wasserloos, K., Pitt, B.R. & Davies, P. (1995). TGF-beta regulates production of NO in pulmonary artery smooth muscle cells by inhibiting expression of NOS. *The American Journal of Physiology.* 268 (5): L862-L867.

Frantz, C., Stewart, K.M. & Weaver, V.M. (2010). The extracellular matrix at a glance. *Journal of cell science.* 123 : 4195-4200.

Friedenstein, A.J., Chailakhjan, R.K. & Lalykina, K.S. (1970). The development of fibroblast colonies in monolayer cultures of guinea-pig bone marrow and spleen cells. *Cell and tissue kinetics.* 3 (4): 393-403.

Fujikawa, L.S., Foster, C.S., Harrist, T.J., Lanigan, J.M. & Colvin, R.B. (1981). Fibronectin in healing rabbit corneal wounds. *Laboratory investigation; a journal of technical methods and pathology.* 45 (2): 120-129.

Fujino, N., Kubo, H., Suzuki, T., Ota, C., Hegab, A.E., He, M., Suzuki, S., Suzuki, T., Yamada, M., Kondo, T., Kato, H. & Yamaya, M. (2011). Isolation of alveolar epithelial type II progenitor cells from adult human lungs. *Laboratory investigation; a journal of technical methods and pathology.* 91 (3): 363-378.

Fukuda, Y., Takemura, T. & Ferrans, V.J. (1989). Evolution of metaplastic squamous cells of alveolar walls in pulmonary fibrosis produced by paraquat. An ultrastructural and immunohistochemical study. *Virchows Archiv.B, Cell pathology including molecular pathology.* 58 (1): 27-43.

Furuyama, A. &Mochitate, K. (2004). Hepatocyte growth factor inhibits the formation of the basement membrane of alveolar epithelial cells in vitro. *American Journal Of Physiology.Lung Cellular And Molecular Physiology.* 286 (5): L939-L946.

Galiacy, S., Planus, E., Lepetit, H., Fereol, S., Laurent, V., Ware, L., Isabey, D., Matthay, M., Harf, A. & d'Ortho, M.P. (2003). Keratinocyte growth factor promotes cell motility during alveolar epithelial repair in vitro. *Experimental cell research.* 283 (2): 215-229.

Gazdar, A.F., Linnoila, R.I., Kurita, Y., Oie, H.K., Mulshine, J.L., Clark, J.C. & Whitsett, J.A. (1990). Peripheral airway cell differentiation in human lung cancer cell lines. *Cancer research.* 50 (17): 5481-5487.

Geiser, T., Ishigaki, M., van Leer, C., Matthay, M.A. & Broaddus, V.C. (2004). H(2)O(2) inhibits alveolar epithelial wound repair in vitro by induction of apoptosis. *American journal of physiology.Lung cellular and molecular physiology.* 287 (2): L448-53.

Geiser, T., Jarreau, P.H., Atabai, K. & Matthay, M.A. (2000). Interleukin-1beta augments in vitro alveolar epithelial repair. *American journal of physiology.Lung cellular and molecular physiology.* 279 (6): L1184-90.

Geiser, T. (2003). Idiopathic pulmonary fibrosis--a disorder of alveolar wound repair? *Swiss Medical Weekly.* 133 (29-30): 405-411.

Gharaee-Kermani, M., Gyetko, M.R., Hu, B. & Phan, S.H. (2007). New insights into the pathogenesis and treatment of idiopathic pulmonary fibrosis: a potential role for stem cells in the lung parenchyma and implications for therapy. *Pharmaceutical research.* 24 (5): 819-841.

Giaid, A., Michel, R.P., Stewart, D.J., Sheppard, M., Corrin, B. & Hamid, Q. (1993). Expression of endothelin-1 in lungs of patients with cryptogenic fibrosing alveolitis. *Lancet.* 341 (8860): 1550-1554.

Gnecchi, M., Zhang, Z., Ni, A. & Dzau, V.J. (2008). Paracrine mechanisms in adult stem cell signaling and therapy. *Circulation research.* 103 (11): 1204-1219.

Gribbin, J., Hubbard, R. & Smith, C. (2009). Role of diabetes mellitus and gastro-oesophageal reflux in the aetiology of idiopathic pulmonary fibrosis. *Respiratory medicine.* 103 (6): 927-931.

Gribbin, J., Hubbard, R.B., Le Jeune, I., Smith, C.J., West, J. & Tata, L.J. (2006). Incidence and mortality of idiopathic pulmonary fibrosis and sarcoidosis in the UK. *Thorax.* 61 (11): 980-985.

Griffith, T.S., Brunner, T., Fletcher, S.M., Green, D.R. & Ferguson, T.A. (1995). Fas ligand-induced apoptosis as a mechanism of immune privilege. *Science (New York, N.Y.).* 270 (5239): 1189-1192.

Grinnell, F., Billingham, R.E. & Burgess, L. (1981). Distribution of fibronectin during wound healing in vivo. *The Journal of investigative dermatology.* 76 (3): 181-189.

Grutters, J.C. &du Bois, R.M. (2005). Genetics of fibrosing lung diseases. *The European respiratory journal : official journal of the European Society for Clinical Respiratory Physiology.* 25 (5): 915-927.

Guilak, F., Lott, K.E., Awad, H.A., Cao, Q., Hicok, K.C., Fermor, B. & Gimble, J.M. (2006). Clonal analysis of the differentiation potential of human adipose-derived adult stem cells. *Journal of cellular physiology.* 206 (1): 229-237.

Guo, J., Yi, E.S., Havill, A.M., Sarosi, I., Whitcomb, L., Yin, S., Middleton, S.C., Piguet, P. & Ulich, T.R. (1998). Intravenous keratinocyte growth factor protects against experimental pulmonary injury. *The American Journal of Physiology.* 275 (4 Pt 1): L800-5.

Gupta, N., Su, X., Popov, B., Lee, J.W., Serikov, V. & Matthay, M.A. (2007). Intrapulmonary delivery of bone marrow-derived mesenchymal stem cells improves survival and attenuates endotoxin-induced acute lung injury in mice. *Journal of immunology (Baltimore, Md.: 1950).* 179 (3): 1855-1863.

Gustafson, T., Dahlman-Höglund, A., Nilsson, K., Ström, K., Tornling, G. & Torén, K. (2007). Occupational exposure and severe pulmonary fibrosis. *Respiratory medicine.* 101 (10): 2207-2212.

Hagimoto, N., Kuwano, K., Miyazaki, H., Kunitake, R., Fujita, M., Kawasaki, M., Kaneko, Y. & Hara, N. (1997a). Induction of apoptosis and pulmonary fibrosis in mice in response to ligation of Fas antigen. *American journal of respiratory cell and molecular biology.* 17 (3): 272-278.

Hagimoto, N., Kuwano, K., Nomoto, Y., Kunitake, R. & Hara, N. (1997b). Apoptosis and expression of Fas/Fas ligand mRNA in bleomycin-induced pulmonary fibrosis in mice. *American journal of respiratory cell and molecular biology.* 16 (1): 91-101.

Hamazaki, T., Iiboshi, Y., Oka, M., Papst, P.J., Meacham, A.M., Zon, L.I. & Terada, N. (2001). Hepatic maturation in differentiating embryonic stem cells in vitro. *FEBS letters.* 497 (1): 15-19.

Hamilton, D.W. (2008). Functional role of periostin in development and wound repair: implications for connective tissue disease. *Journal of cell communication and signaling.* 2 (1-2): 9-17.

Harrison, J.H.,Jr &Lazo, J.S. (1987). High dose continuous infusion of bleomycin in mice: a new model for drug-induced pulmonary fibrosis. *The Journal of pharmacology and experimental therapeutics.* 243 (3): 1185-1194.

Hartman, T.E., Primack, S.L., Swensen, S.J., Hansell, D., McGuinness, G. & Muller, N.L. (1993). Desquamative interstitial pneumonia: thin-section CT findings in 22 patients. *Radiology.* 187 (3): 787-790.

Hasel, C., Durr, S., Rau, B., Strater, J., Schmid, R.M., Walczak, H., Bachem, M.G. & Moller, P. (2003). In chronic pancreatitis, widespread emergence of TRAIL receptors in epithelia coincides with neoexpression of TRAIL by pancreatic stellate cells of early fibrotic areas. *Laboratory investigation; a journal of technical methods and pathology.* 83 (6): 825-836.

Hashimoto, N., Jin, H., Liu, T., Chensue, S.W. & Phan, S.H. (2004). Bone marrow-derived progenitor cells in pulmonary fibrosis. *The Journal of clinical investigation.* 113 (2): 243-252.

Haston, C.K. &Travis, E.L. (1997). Murine susceptibility to radiation-induced pulmonary fibrosis is influenced by a genetic factor implicated in susceptibility to bleomycin-induced pulmonary fibrosis. *Cancer research.* 57 (23): 5286-5291.

Henderson, J.K., Draper, J.S., Baillie, H.S., Fishel, S., Thomson, J.A., Moore, H. & Andrews, P.W. (2002). Preimplantation human embryos and embryonic stem cells show comparable expression of stage-specific embryonic antigens. *Stem cells (Dayton, Ohio).* 20 (4): 329-337.

Heo, J., Lee, J., Chu, I., Takahama, Y. & Thorgeirsson, S.S. (2005). Spontaneous differentiation of mouse embryonic stem cells in vitro: characterization by global gene expression profiles. *Biochemical and biophysical research communications.* 332 (4): 1061-1069.

Herard, A.L., Pierrot, D., Hinnrasky, J., Kaplan, H., Sheppard, D., Puchelle, E. & Zahm, J.M. (1996). Fibronectin and its alpha 5 beta 1-integrin receptor are involved in the wound-repair process of airway epithelium. *The American Journal of Physiology.* 271 (5 Pt 1): L726-33.

Hirano, A., Kanehiro, A., Ono, K., Ito, W., Yoshida, A., Okada, C., Nakashima, H., Tanimoto, Y., Kataoka, M., Gelfand, E.W. & Tanimoto, M. (2006). Pirfenidone modulates airway responsiveness, inflammation, and remodeling after repeated challenge. *American Journal Of Respiratory Cell And Molecular Biology.* 35 (3): 366-377.

Hocking, D.C. &Chang, C.H. (2003). Fibronectin matrix polymerization regulates small airway epithelial cell migration. *American journal of physiology.Lung cellular and molecular physiology.* 285 (1): L169-79.

Honardoust, D., Eslami, A., Larjava, H. & Hakkinen, L. (2008). Localization of small leucine-rich proteoglycans and transforming growth factor-beta in human oral mucosal wound healing. *Wound repair and regeneration : official publication of the Wound Healing Society [and] the European Tissue Repair Society.* 16 (6): 814-823.

Hong, L., Sun, H., Lv, X., Yang, D., Zhang, J. & Shi, Y. (2010). Expression of periostin in the serum of NSCLC and its function on proliferation and migration of human lung adenocarcinoma cell line (A549) in vitro. *Molecular biology reports.* 37 (5): 2285-2293.

Horiba, K. &Fukuda, Y. (1994). Synchronous appearance of fibronectin, integrin alpha 5 beta 1, vinculin and actin in epithelial cells and fibroblasts during rat tracheal wound healing. *Virchows Archiv : an international journal of pathology.* 425 (4): 425-434.

Horowitz, J.C. &Thannickal, V.J. (2006). Idiopathic pulmonary fibrosis : new concepts in pathogenesis and implications for drug therapy. *Treatments in respiratory medicine.* 5 (5): 325-342.

Hsu, E., Shi, H., Jordan, R.M., Lyons-Weiler, J., Pilewski, J.M. & Feghali-Bostwick, C.A. (2011). Lung tissues in patients with systemic sclerosis have gene expression patterns unique to pulmonary fibrosis and pulmonary hypertension. *Arthritis and Rheumatism.* 63 (3): 783-794.

Huaux, F., Louahed, J., Hudspith, B., Meredith, C., Delos, M., Renauld, J.C. & Lison, D. (1998). Role of interleukin-10 in the lung response to silica in mice. *American journal of respiratory cell and molecular biology.* 18 (1): 51-59.

Hubbard, R., Lewis, S., Richards, K., Johnston, I. & Britton, J. (1996). Occupational exposure to metal or wood dust and aetiology of cryptogenic fibrosing alveolitis. *Lancet.* 347 (8997): 284-289.

Hunninghake, G.W., Lynch, D.A., Galvin, J.R., Gross, B.H., Müller, N., Schwartz, D.A., King,Talmadge E.,,Jr, Lynch,Joseph P.,,3rd, Hegele, R., Waldron, J., Colby, T.V. & Hogg, J.C. (2003). Radiologic findings are strongly associated with a pathologic diagnosis of usual interstitial pneumonia. *Chest.* 124 (4): 1215-1223.

Hutyrova, B., Pantelidis, P., Drabek, J., Zurkova, M., Kolek, V., Lenhart, K., Welsh, K.I., Du Bois, R.M. & Petrek, M. (2002). Interleukin-1 gene cluster polymorphisms in sarcoidosis and idiopathic pulmonary fibrosis. *American journal of respiratory and critical care medicine.* 165 (2): 148-151.

Hwa, V., Oh, Y. & Rosenfeld, R.G. (1999). The insulin-like growth factor-binding protein (IGFBP) superfamily. *Endocrine reviews.* 20 (6): 761-787.

Isakson, B.E., Lubman, R.L., Seedorf, G.J. & Boitano, S. (2001). Modulation of pulmonary alveolar type II cell phenotype and communication by extracellular matrix and KGF. *American journal of physiology.Cell physiology.* 281 (4): C1291-9.

Isakson, B.E., Seedorf, G.J., Lubman, R.L. & Boitano, S. (2002). Heterocellular cultures of pulmonary alveolar epithelial cells grown on laminin-5 supplemented matrix. *In vitro cellular & developmental biology.Animal.* 38 (8): 443-449.

Ishii, G., Sangai, T., Sugiyama, K., Ito, T., Hasebe, T., Endoh, Y., Magae, J. & Ochiai, A. (2005). In vivo characterization of bone marrow-derived fibroblasts recruited into fibrotic lesions. *Stem cells (Dayton, Ohio).* 23 (5): 699-706.

Itskovitz-Eldor, J., Schuldiner, M., Karsenti, D., Eden, A., Yanuka, O., Amit, M., Soreq, H. & Benvenisty, N. (2000). Differentiation of human embryonic stem cells into embryoid bodies compromising the three embryonic germ layers. *Molecular medicine (Cambridge, Mass.).* 6 (2): 88-95.

Iwai, K., Mori, T., Yamada, N., Yamaguchi, M. & Hosoda, Y. (1994). Idiopathic pulmonary fibrosis. Epidemiologic approaches to occupational exposure. *American journal of respiratory and critical care medicine.* 150 (3): 670-675.

Iyer, S.N., Gurujeyalakshmi, G. & Giri, S.N. (1999). Effects of pirfenidone on procollagen gene expression at the transcriptional level in bleomycin hamster model of lung fibrosis. *The Journal of pharmacology and experimental therapeutics.* 289 (1): 211-218.

Iyer, S.N., Margolin, S.B., Hyde, D.M. & Giri, S.N. (1998). Lung fibrosis is ameliorated by pirfenidone fed in diet after the second dose in a three-dose bleomycin-hamster model. *Experimental lung research.* 24 (1): 119-132.

Iyer, S.N., Gurujeyalakshmi, G. & Giri, S.N. (1999). Effects of pirfenidone on transforming growth factor-beta gene expression at the transcriptional level in bleomycin hamster model of lung fibrosis. *The Journal of pharmacology and experimental therapeutics.* 291 (1): 367-373.

Iyer, S.N., Wild, J.S., Schiedt, M.J., Hyde, D.M., Margolin, S.B. & Giri, S.N. (1995). Dietary intake of pirfenidone ameliorates bleomycin-induced lung fibrosis in hamsters. *The Journal of laboratory and clinical medicine.* 125 (6): 779-785.

Jackson-Boeters, L., Wen, W. & Hamilton, D.W. (2009). Periostin localizes to cells in normal skin, but is associated with the extracellular matrix during wound repair. *Journal of cell communication and signaling.* 3 (2): 125-133.

Jain, R., Shaul, P.W., Borok, Z. & Willis, B.C. (2007). Endothelin-1 induces alveolar epithelial-mesenchymal transition through endothelin type A receptor-mediated production of TGF-beta1. *American Journal Of Respiratory Cell And Molecular Biology.* 37 (1): 38-47.

Jemal, A., Siegel, R., Ward, E., Murray, T., Xu, J. & Thun, M.J. (2007). Cancer statistics, 2007. *CA: A Cancer Journal For Clinicians.* 57 (1): 43-66.

Johnson, M.A., Kwan, S., Snell, N.J., Nunn, A.J., Darbyshire, J.H. & Turner-Warwick, M. (1989). Randomised controlled trial comparing prednisolone alone with cyclophosphamide and low dose prednisolone in combination in cryptogenic fibrosing alveolitis. *Thorax.* 44 (4): 280-288.

Jones, E.A., Tosh, D., Wilson, D.I., Lindsay, S. & Forrester, L.M. (2002). Hepatic differentiation of murine embryonic stem cells. *Experimental cell research.* 272 (1): 15-22.

Jordana, M., Schulman, J., McSharry, C., Irving, L.B., Newhouse, M.T., Jordana, G. & Gauldie, J. (1988). Heterogeneous proliferative characteristics of human adult lung fibroblast lines and clonally derived fibroblasts from control and fibrotic tissue. *The American Review of Respiratory Disease.* 137 (3): 579-584.

Jorens, P.G., Van Overveld, ,F.J., Vermeire, P.A., Bult, H. & Herman, A.G. (1992). Synergism between interleukin-1 beta and interferon-gamma, an inducer of nitric oxide synthase, in rat lung fibroblasts. *European journal of pharmacology.* 224 (1): 7-12.

Kajstura, J., Rota, M., Hall, S.R., Hosoda, T., D'Amario, D., Sanada, F., Zheng, H., Ogorek, B., Rondon-Clavo, C., Ferreira-Martins, J., Matsuda, A., Arranto, C., Goichberg, P., Giordano, G., Haley, K.J., Bardelli, S., Rayatzadeh, H., Liu, X., Quaini, F., Liao, R., Leri, A., Perrella, M.A., Loscalzo, J. & Anversa, P. (2011). Evidence for human lung stem cells. *The New England journal of medicine.* 364 (19): 1795-1806.

Kaminski, N. (2003). Microarray analysis of idiopathic pulmonary fibrosis. *American journal of respiratory cell and molecular biology.* 29 (3 Suppl): S32-6.

Kaminski N. *et al*. Idiopathic Pulmonary Fibrosis. (2003). *Am. J. Respir. Cell Mol. Biol.* Vol. 29: S1–S105.

Kanki-Horimoto, S., Horimoto, H., Mieno, S., Kishida, K., Watanabe, F., Furuya, E. & Katsumata, T. (2006). Implantation of mesenchymal stem cells overexpressing endothelial nitric oxide synthase improves right ventricular impairments caused by pulmonary hypertension. *Circulation.* 114 (1 Suppl): I181-5.

Kapanci, Y., Desmouliere, A., Pache, J.C., Redard, M. & Gabbiani, G. (1995). Cytoskeletal protein modulation in pulmonary alveolar myofibroblasts during idiopathic pulmonary fibrosis. Possible role of transforming growth factor beta and tumor necrosis factor alpha. *American journal of respiratory and critical care medicine.* 152 (6 Pt 1): 2163-2169.

Kasai, H., Allen, J.T., Mason, R.M., Kamimura, T. & Zhang, Z. (2005). TGF-beta1 induces human alveolar epithelial to mesenchymal cell transition (EMT). *Respiratory research.* 6 : 56.

Kasper, M. &Haroske, G. (1996). Alterations in the alveolar epithelium after injury leading to pulmonary fibrosis. *Histology and histopathology.* 11 (2): 463-483.

Katzenstein, A.L. &Myers, J.L. (1998). Idiopathic pulmonary fibrosis: clinical relevance of pathologic classification. *American journal of respiratory and critical care medicine.* 157 (4 Pt 1): 1301-1315.

Kaufman, M.H., Robertson, E.J., Handyside, A.H. & Evans, M.J. (1983). Establishment of pluripotential cell lines from haploid mouse embryos. *Journal of embryology and experimental morphology.* 73 : 249-261.

Kawamoto, M. &Fukuda, Y. (1990). Cell proliferation during the process of bleomycin-induced pulmonary fibrosis in rats. *Acta Pathologica Japonica.* 40 (4): 227-238.

Kawanami, O., Ferrans, V.J. & Crystal, R.G. (1982). Structure of alveolar epithelial cells in patients with fibrotic lung disorders. *Laboratory investigation; a journal of technical methods and pathology.* 46 (1): 39-53.

Keane M.P. The role of chemokines and cytokines in lung fibrosis. (2008). *Eur Respir Rev*. 17: 109, 151-156.

Keller, G. (2005). Embryonic stem cell differentiation: emergence of a new era in biology and medicine. *Genes & development.* 19 (10): 1129-1155.

Kelly, B.G., Lok, S.S., Hasleton, P.S., Egan, J.J. & Stewart, J.P. (2002). A rearranged form of Epstein-Barr virus DNA is associated with idiopathic pulmonary fibrosis. *American journal of respiratory and critical care medicine.* 166 (4): 510-513.

Khalil, N., O'Connor, R.N., Unruh, H.W., Warren, P.W., Flanders, K.C., Kemp, A., Bereznay, O.H. & Greenberg, A.H. (1991). Increased production and immunohistochemical localization of transforming growth factor-beta in idiopathic pulmonary fibrosis. *American journal of respiratory cell and molecular biology.* 5 (2): 155-162.

Kheradmand, F., Folkesson, H.G., Shum, L., Derynk, R., Pytela, R. & Matthay, M.A. (1994). Transforming growth factor-alpha enhances alveolar epithelial cell repair in a new in vitro model. *The American Journal of Physiology.* 267 (6): L728-L738.

Kim, C.F., Jackson, E.L., Woolfenden, A.E., Lawrence, S., Babar, I., Vogel, S., Crowley, D., Bronson, R.T. & Jacks, T. (2005). Identification of bronchioalveolar stem cells in normal lung and lung cancer. *Cell.* 121 (6): 823-835.

Kim, D.S., Collard, H.R. & King, T.E.,Jr (2006). Classification and natural history of the idiopathic interstitial pneumonias. *Proceedings of the American Thoracic Society.* 3 (4): 285-292.

Kim, H.J., Henke, C.A., Savik, S.K. & Ingbar, D.H. (1997). Integrin mediation of alveolar epithelial cell migration on fibronectin and type I collagen. *The American Journal of Physiology.* 273 (1 Pt 1): L134-41.

Kim, K.K., Kugler, M.C., Wolters, P.J., Robillard, L., Galvez, M.G., Brumwell, A.N., Sheppard, D. & Chapman, H.A. (2006). Alveolar epithelial cell mesenchymal transition develops in vivo during pulmonary fibrosis and is regulated by the extracellular matrix. *Proceedings of the National Academy of Sciences of the United States of America.* 103 (35): 13180-13185.

Konigshoff, M., Balsara, N., Pfaff, E.M., Kramer, M., Chrobak, I., Seeger, W. & Eickelberg, O. (2008). Functional Wnt signaling is increased in idiopathic pulmonary fibrosis. *PloS one.* 3 (5): e2142.

Korfei, M., Ruppert, C., Mahavadi, P., Henneke, I., Markart, P., Koch, M., Lang, G., Fink, L., Bohle, R.M., Seeger, W., Weaver, T.E. & Guenther, A. (2008). Epithelial endoplasmic reticulum stress and apoptosis in sporadic idiopathic pulmonary fibrosis. *American journal of respiratory and critical care medicine.* 178 (8): 838-846.

Kotton, D.N., Ma, B.Y., Cardoso, W.V., Sanderson, E.A., Summer, R.S., Williams, M.C. & Fine, A. (2001). Bone marrow-derived cells as progenitors of lung alveolar epithelium. *Development (Cambridge, England).* 128 (24): 5181-5188.

Kubo, A., Shinozaki, K., Shannon, J.M., Kouskoff, V., Kennedy, M., Woo, S., Fehling, H.J. & Keller, G. (2004). Development of definitive endoderm from embryonic stem cells in culture. *Development (Cambridge, England).* 131 (7): 1651-1662.

Kuhbier, J.W., Weyand, B., Radtke, C., Vogt, P.M., Kasper, C. & Reimers, K. (2010). Isolation, characterization, differentiation, and application of adipose-derived stem cells. *Advances in Biochemical Engineering/Biotechnology.* 123 : 55-105.

Kulaksiz, H., Schmid, A., Honscheid, M., Ramaswamy, A. & Cetin, Y. (2002). Clara cell impact in air-side activation of CFTR in small pulmonary airways. *Proceedings of the National Academy of Sciences of the United States of America.* 99 (10): 6796-6801.

Kutsukake, M., Ishihara, R., Momose, K., Isaka, K., Itokazu, O., Higuma, C., Matsutani, T., Matsuda, A., Sasajima, K., Hara, T. & Tamura, K. (2008). Circulating IGF-binding protein 7 (IGFBP7) levels are elevated in patients with endometriosis or undergoing diabetic hemodialysis. *Reproductive Biology And Endocrinology: RB&E.* 6 : 54-54.

Kuwano, K., Miyazaki, H., Hagimoto, N., Kawasaki, M., Fujita, M., Kunitake, R., Kaneko, Y. & Hara, N. (1999). The involvement of Fas-Fas ligand pathway in fibrosing lung diseases. *American journal of respiratory cell and molecular biology.* 20 (1): 53-60.

Kwon, A.H., Qiu, Z. & Hiraon, Y. (2007). Effect of plasma fibronectin on the incisional wound healing in rats. *Surgery.* 141 (2): 254-261.

LaFramboise, W.A., Petrosko, P., Krill-Burger, J.M., Morris, D.R., McCoy, A.R., Scalise, D., Malehorn, D.E., Guthrie, R.D., Becich, M.J. & Dhir, R. (2010). Proteins secreted by embryonic stem cells activate cardiomyocytes through ligand binding pathways. *Journal of proteomics.* 73 (5): 992-1003.

Lama, V.N. &Phan, S.H. (2006). The extrapulmonary origin of fibroblasts: stem/progenitor cells and beyond. *Proceedings of the American Thoracic Society.* 3 (4): 373-376.

Laslett, A.L., Filipczyk, A.A. & Pera, M.F. (2003). Characterization and culture of human embryonic stem cells. *Trends in cardiovascular medicine.* 13 (7): 295-301.

Lavnikova, N. &Laskin, D.L. (1995). Unique patterns of regulation of nitric oxide production in fibroblasts. *Journal of leukocyte biology.* 58 (4): 451-458.

Lawson, W.E., Cheng, D.S., Degryse, A.L., Tanjore, H., Polosukhin, V.V., Xu, X.C., Newcomb, D.C., Jones, B.R., Roldan, J., Lane, K.B., Morrisey, E.E., Beers, M.F., Yull, F.E. & Blackwell, T.S. (2011). Endoplasmic reticulum stress enhances fibrotic remodeling in the lungs. *Proceedings of the National Academy of Sciences of the United States of America.* 108 (26): 10562-10567.

Lawson, W.E., Grant, S.W., Ambrosini, V., Womble, K.E., Dawson, E.P., Lane, K.B., Markin, C., Renzoni, E., Lympany, P., Thomas, A.Q., Roldan, J., Scott, T.A., Blackwell, T.S., Phillips, J.A.,3rd, Loyd, J.E. & du Bois, R.M. (2004). Genetic mutations in surfactant protein C are a rare cause of sporadic cases of IPF. *Thorax.* 59 (11): 977-980.

LeBlanc, H.N. &Ashkenazi, A. (2003). Apo2L/TRAIL and its death and decoy receptors. *Cell death and differentiation.* 10 (1): 66-75.

Lee, C.G., Kang, H.R., Homer, R.J., Chupp, G. & Elias, J.A. (2006). Transgenic modeling of transforming growth factor-beta(1): role of apoptosis in fibrosis and alveolar remodeling. *Proceedings of the American Thoracic Society.* 3 (5): 418-423.

Lee, E.H. &Hui, J.H.P. (2006). The potential of stem cells in orthopaedic surgery. *The Journal Of Bone And Joint Surgery.British Volume.* 88 (7): 841-851.

Lee, J.W., Fang, X., Gupta, N., Serikov, V. & Matthay, M.A. (2009a). Allogeneic human mesenchymal stem cells for treatment of E. coli endotoxin-induced acute lung injury in the ex vivo perfused human lung. *Proceedings of the National Academy of Sciences of the United States of America.* 106 (38): 16357-16362.

Lee, S., Bowrin, K., Hamad, A.R. & Chakravarti, S. (2009b). Extracellular matrix lumican deposited on the surface of neutrophils promotes migration by binding to beta2 integrin. *The Journal of biological chemistry.* 284 (35): 23662-23669.

Legrand, C., Polette, M., Tournier, J.M., de Bentzmann, S., Huet, E., Monteau, M. & Birembaut, P. (2001). uPA/plasmin system-mediated MMP-9 activation is implicated in bronchial epithelial cell migration. *Experimental cell research.* 264 (2): 326-336.

Leslie, C.C., McCormick-Shannon, K., Shannon, J.M., Garrick, B., Damm, D., Abraham, J.A. & Mason, R.J. (1997). Heparin-binding EGF-like growth factor is a mitogen for rat alveolar type II cells. *American journal of respiratory cell and molecular biology.* 16 (4): 379-387.

Lesur, O., Arsalane, K. & Lane, D. (1996). Lung alveolar epithelial cell migration in vitro: modulators and regulation processes. *The American Journal of Physiology.* 270 (3 Pt 1): L311-9.

Li, X., Rayford, H. & Uhal, B.D. (2003). Essential roles for angiotensin receptor AT1a in bleomycin-induced apoptosis and lung fibrosis in mice. *The American journal of pathology.* 163 (6): 2523-2530.

Liechty, K.W., MacKenzie, T.C., Shaaban, A.F., Radu, A., Moseley, A.M., Deans, R., Marshak, D.R. & Flake, A.W. (2000). Human mesenchymal stem cells engraft and demonstrate site-specific differentiation after in utero transplantation in sheep. *Nature medicine.* 6 (11): 1282-1286.

Lok, S.S., Stewart, J.P., Kelly, B.G., Hasleton, P.S. & Egan, J.J. (2001). Epstein-Barr virus and wild p53 in idiopathic pulmonary fibrosis. *Respiratory medicine.* 95 (10): 787-791.

Lomas, N.J., Watts, K.L., Akram, K.M., Forsyth, N.R. & Spiteri, M.A. (2012). Idiopathic pulmonary fibrosis: immunohistochemical analysis provides fresh insights into lung tissue remodelling with implications for novel prognostic markers. *International Journal Of Clinical And Experimental Pathology.* 5 (1): 58-71.

Lorz, C., Benito-Martin, A., Boucherot, A., Ucero, A.C., Rastaldi, M.P., Henger, A., Armelloni, S., Santamaria, B., Berthier, C.C., Kretzler, M., Egido, J. & Ortiz, A. (2008). The death ligand TRAIL in diabetic nephropathy. *Journal of the American Society of Nephrology : JASN.* 19 (5): 904-914.

Lotz, M.M., Rabinovitz, I. & Mercurio, A.M. (2000). Intestinal restitution: progression of actin cytoskeleton rearrangements and integrin function in a model of epithelial wound healing. *The American Journal Of Pathology.* 156 (3): 985-996.

Loyd J.E. Gene expression profiling: can we identify the right target genes? (2008) *European Respiratory Review*. 17 (109): 163-167.

Lu, X., Chen, D., Liu, Z., Li, C., Liu, Y., Zhou, J., Wan, P., Mou, Y.G. & Wang, Z. (2010). Enhanced survival in vitro of human corneal endothelial cells using mouse embryonic stem cell conditioned medium. *Molecular vision.* 16 : 611-622.

Ma, N., Gai, H., Mei, J., Ding, F.B., Bao, C.R., Nguyen, D.M. & Zhong, H. (2011). Bone marrow mesenchymal stem cells can differentiate into type II alveolar epithelial cells in vitro. *Cell biology international.* 35 (12): 1261-1266.

MacNee, W. & Rahman, I. (1995). Oxidants/antioxidants in idiopathic pulmonary fibrosis. *Thorax.* 50 Suppl 1 : S53-S58.

Madonna, R., Geng, Y.J. & De Caterina, R. (2009). Adipose tissue-derived stem cells: characterization and potential for cardiovascular repair. *Arteriosclerosis, Thrombosis, and Vascular Biology.* 29 (11): 1723-1729.

Maeyama, T., Kuwano, K., Kawasaki, M., Kunitake, R., Hagimoto, N., Matsuba, T., Yoshimi, M., Inoshima, I., Yoshida, K. & Hara, N. (2001). Upregulation of Fas-signalling molecules in lung epithelial cells from patients with idiopathic pulmonary fibrosis. *The European respiratory journal : official journal of the European Society for Clinical Respiratory Physiology.* 17 (2): 180-189.

Maher, T.M., Wells, A.U. & Laurent, G.J. (2007). Idiopathic pulmonary fibrosis: multiple causes and multiple mechanisms? *The European respiratory journal : official journal of the European Society for Clinical Respiratory Physiology.* 30 (5): 835-839.

Mapel, D.W., Samet, J.M. & Coultas, D.B. (1996). Corticosteroids and the treatment of idiopathic pulmonary fibrosis. Past, present, and future. *Chest.* 110 (4): 1058-1067.

Martin, G.R. (1981). Isolation of a pluripotent cell line from early mouse embryos cultured in medium conditioned by teratocarcinoma stem cells. *Proceedings of the National Academy of Sciences of the United States of America.* 78 (12): 7634-7638.

Mason, R.J., Leslie, C.C., McCormick-Shannon, K., Deterding, R.R., Nakamura, T., Rubin, J.S. & Shannon, J.M. (1994). Hepatocyte growth factor is a growth factor for rat alveolar type II cells. *American Journal Of Respiratory Cell And Molecular Biology.* 11 (5): 561-567.

Mattey, D.L., Dawes, P.T., Nixon, N.B. & Slater, H. (1997). Transforming growth factor beta 1 and interleukin 4 induced alpha smooth muscle actin expression and myofibroblast-like differentiation in human synovial fibroblasts in vitro: modulation by basic fibroblast growth factor. *Annals of the Rheumatic Diseases.* 56 (7): 426-431.

McGrath, E.E., Lawrie, A., Marriott, H.M., Mercer, P., Cross, S.S., Arnold, N., Singleton, V., Thompson, A.A., Walmsley, S.R., Renshaw, S.A., Sabroe, I., Chambers, R.C., Dockrell, D.H. & Whyte, M.K. (2012). Deficiency of tumour necrosis factor-related apoptosis-inducing ligand exacerbates lung injury and fibrosis. *Thorax.* 67(9):796-803

McLean, A.B., D'Amour, K.,A., Jones, K.L., Krishnamoorthy, M., Kulik, M.J., Reynolds, D.M., Sheppard, A.M., Liu, H., Xu, Y., Baetge, E.E. & Dalton, S. (2007). Activin a efficiently specifies definitive endoderm from human embryonic stem cells only when phosphatidylinositol 3-kinase signaling is suppressed. *Stem cells (Dayton, Ohio).* 25 (1): 29-38.

Medici, D., Hay, E.D. & Olsen, B.R. (2008). Snail and Slug promote epithelial-mesenchymal transition through beta-catenin-T-cell factor-4-dependent expression of transforming growth factor-beta3. *Molecular biology of the cell.* 19 (11): 4875-4887.

Meirelles Lda, S., Fontes, A.M., Covas, D.T. & Caplan, A.I. (2009). Mechanisms involved in the therapeutic properties of mesenchymal stem cells. *Cytokine & growth factor reviews.* 20 (5-6): 419-427.

Meliconi, R., Andreone, P., Fasano, L., Galli, S., Pacilli, A., Miniero, R., Fabbri, M., Solforosi, L. & Bernardi, M. (1996). Incidence of hepatitis C virus infection in Italian patients with idiopathic pulmonary fibrosis. *Thorax.* 51 (3): 315-317.

Misumi, S. &Lynch, D.A. (2006). Idiopathic pulmonary fibrosis/usual interstitial pneumonia: imaging diagnosis, spectrum of abnormalities, and temporal progression. *Proceedings Of The American Thoracic Society.* 3 (4): 307-314.

Mitsui, K., Tokuzawa, Y., Itoh, H., Segawa, K., Murakami, M., Takahashi, K., Maruyama, M., Maeda, M. & Yamanaka, S. (2003). The homeoprotein Nanog is required for maintenance of pluripotency in mouse epiblast and ES cells. *Cell.* 113 (5): 631-642.

Miyake, Y., Sasaki, S., Yokoyama, T., Chida, K., Azuma, A., Suda, T., Kudoh, S., Sakamoto, N., Okamoto, K., Kobashi, G., Washio, M., Inaba, Y. & Tanaka, H.

(2005). Occupational and environmental factors and idiopathic pulmonary fibrosis in Japan. *The Annals of Occupational Hygiene.* 49 (3): 259-265.

Mohler, K.M., Torrance, D.S., Smith, C.A., Goodwin, R.G., Stremler, K.E., Fung, V.P., Madani, H. & Widmer, M.B. (1993). Soluble tumor necrosis factor (TNF) receptors are effective therapeutic agents in lethal endotoxemia and function simultaneously as both TNF carriers and TNF antagonists. *Journal of immunology (Baltimore, Md.: 1950).* 151 (3): 1548-1561.

Moine, P., Mazoit, J.X., Bedos, J.P., Vallee, E. & Azoulay-Dupuis, E. (1997). Correlation between in vitro and in vivo activity of amoxicillin against Streptococcus pneumoniae in a murine pneumonia model. *The Journal of pharmacology and experimental therapeutics.* 280 (1): 310-315.

Moodley, Y., Atienza, D., Manuelpillai, U., Samuel, C.S., Tchongue, J., Ilancheran, S., Boyd, R. & Trounson, A. (2009). Human umbilical cord mesenchymal stem cells reduce fibrosis of bleomycin-induced lung injury. *The American journal of pathology.* 175 (1): 303-313.

Moore, B.B. &Hogaboam, C.M. (2008). Murine models of pulmonary fibrosis. *American Journal Of Physiology.Lung Cellular And Molecular Physiology.* 294 (2): L152-L160.

Mori, M., Morishita, H., Nakamura, H., Matsuoka, H., Yoshida, K., Kishima, Y., Zhou, Z., Kida, H., Funakoshi, T., Goya, S., Yoshida, M., Kumagai, T., Tachibana, I., Yamamoto, Y., Kawase, I. & Hayashi, S. (2004). Hepatoma-derived growth factor is involved in lung remodeling by stimulating epithelial growth. *American journal of respiratory cell and molecular biology.* 30 (4): 459-469.

Morigi, M., Imberti, B., Zoja, C., Corna, D., Tomasoni, S., Abbate, M., Rottoli, D., Angioletti, S., Benigni, A., Perico, N., Alison, M. & Remuzzi, G. (2004). Mesenchymal stem cells are renotropic, helping to repair the kidney and improve function in acute renal failure. *Journal of the American Society of Nephrology : JASN.* 15 (7): 1794-1804.

Morrison, C.D., Papp, A.C., Hejmanowski, A.Q., Addis, V.M. & Prior, T.W. (2001). Increased D allele frequency of the angiotensin-converting enzyme gene in pulmonary fibrosis. *Human pathology.* 32 (5): 521-528.

Mummery, C., Ward, D., van den Brink, ,C.E., Bird, S.D., Doevendans, P.A., Opthof, T., Brutel de, l.R., Tertoolen, L., van, d.H. & Pera, M. (2002). Cardiomyocyte differentiation of mouse and human embryonic stem cells. *Journal of anatomy.* 200 : 233-242.

Mummery, C., Ward-van Oostwaard, D., Doevendans, P., Spijker, R., van, d.B., Hassink, R., van, d.H., Opthof, T., Pera, M., de, l.R., Passier, R. & Tertoolen, L. (2003). Differentiation of human embryonic stem cells to cardiomyocytes: role of coculture with visceral endoderm-like cells. *Circulation.* 107 (21): 2733-2740.

Munger, J.S., Huang, X., Kawakatsu, H., Griffiths, M.J., Dalton, S.L., Wu, J., Pittet, J.F., Kaminski, N., Garat, C., Matthay, M.A., Rifkin, D.B. & Sheppard, D. (1999). The integrin alpha v beta 6 binds and activates latent TGF beta 1: a mechanism for regulating pulmonary inflammation and fibrosis. *Cell.* 96 (3): 319-328.

Nagai, S., Hamada, K., Shigematsu, M., Taniyama, M., Yamauchi, S. & Izumi, T. (2002). Open-label compassionate use one year-treatment with pirfenidone to patients with chronic pulmonary fibrosis. *Internal medicine (Tokyo, Japan).* 41 (12): 1118-1123.

Nakagawa, H., Akita, S., Fukui, M., Fujii, T. & Akino, K. (2005). Human mesenchymal stem cells successfully improve skin-substitute wound healing. *The British journal of dermatology.* 153 (1): 29-36.

Nakazato, H., Oku, H., Yamane, S., Tsuruta, Y. & Suzuki, R. (2002). A novel anti-fibrotic agent pirfenidone suppresses tumor necrosis factor-alpha at the translational level. *European journal of pharmacology.* 446 (1-3): 177-185.

Nakazawa, T., Nakajima, A., Seki, N., Okawa, A., Kato, M., Moriya, H., Amizuka, N., Einhorn, T.A. & Yamazaki, M. (2004). Gene expression of periostin in the early stage of fracture healing detected by cDNA microarray analysis. *Journal of orthopaedic research : official publication of the Orthopaedic Research Society.* 22 (3): 520-525.

Narasaraju, T.A., Chen, H., Weng, T., Bhaskaran, M., Jin, N., Chen, J., Chen, Z., Chinoy, M.R. & Liu, L. (2006). Expression profile of IGF system during lung injury and recovery in rats exposed to hyperoxia: a possible role of IGF-1 in alveolar epithelial cell proliferation and differentiation. *Journal of cellular biochemistry.* 97 (5): 984-998.

Nash, J.R., McLaughlin, P.J., Butcher, D. & Corrin, B. (1993). Expression of tumour necrosis factor-alpha in cryptogenic fibrosing alveolitis. *Histopathology.* 22 (4): 343-347.

Nauta, A.J. &Fibbe, W.E. (2007). Immunomodulatory properties of mesenchymal stromal cells. *Blood.* 110 (10): 3499-3506.

Nemeth, K., Leelahavanichkul, A., Yuen, P.S., Mayer, B., Parmelee, A., Doi, K., Robey, P.G., Leelahavanichkul, K., Koller, B.H., Brown, J.M., Hu, X., Jelinek, I., Star, R.A. & Mezey, E. (2009). Bone marrow stromal cells attenuate sepsis via prostaglandin E(2)-dependent reprogramming of host macrophages to increase their interleukin-10 production. *Nature medicine.* 15 (1): 42-49.

Nemeth, K., Keane-Myers, A., Brown, J.M., Metcalfe, D.D., Gorham, J.D., Bundoc, V.G., Hodges, M.G., Jelinek, I., Madala, S., Karpati, S. & Mezey, E. (2010). Bone marrow stromal cells use TGF-beta to suppress allergic responses in a mouse model of ragweed-induced asthma. *Proceedings of the National Academy of Sciences of the United States of America.* 107 (12): 5652-5657.

Neuringer, I.P. &Randell, S.H. (2006). Lung stem cell update: promise and controversy. *Monaldi archives for chest disease = Archivio Monaldi per le malattie del torace / Fondazione clinica del lavoro, IRCCS [and] Istituto di clinica tisiologica e malattie apparato respiratorio, Universita di Napoli, Secondo ateneo.* 65 (1): 47-51.

Nguyen, B.K., Maltais, S., Perrault, L.P., Tanguay, J.F., Tardif, J.C., Stevens, L.M., Borie, M., Harel, F., Mansour, S. & Noiseux, N. (2010). Improved function and myocardial repair of infarcted heart by intracoronary injection of mesenchymal stem cell-derived growth factors. *Journal of cardiovascular translational research.* 3 (5): 547-558.

Nishida, T., Nakagawa, S., Awata, T., Ohashi, Y., Watanabe, K. & Manabe, R. (1983). Fibronectin promotes epithelial migration of cultured rabbit cornea in situ. *The Journal of cell biology.* 97 (5 Pt 1): 1653-1657.

Nishida, T., Nakamura, M., Mishima, H. & Otori, T. (1992). Interleukin 6 promotes epithelial migration by a fibronectin-dependent mechanism. *Journal of cellular physiology.* 153 (1): 1-5.

Nishiyama, T., Kii, I., Kashima, T.G., Kikuchi, Y., Ohazama, A., Shimazaki, M., Fukayama, M. & Kudo, A. (2011). Delayed re-epithelialization in periostin-deficient mice during cutaneous wound healing. *PloS one.* 6 (4): e18410.

Noble, P.W., Albera, C., Bradford, W.Z., Costabel, U., Glassberg, M.K., Kardatzke, D., King,Talmadge E.,,Jr, Lancaster, L., Sahn, S.A., Szwarcberg, J., Valeyre, D. & du Bois, R.,M. (2011). Pirfenidone in patients with idiopathic pulmonary fibrosis (CAPACITY): two randomised trials. *Lancet.* 377 (9779): 1760-1769.

Noble, P.W. Epithelial fibroblast triggering and interaction in pulmonary fibrosis. (2008). *Eur Respir Rev.* 17: 109, 123-129.

Nogee, L.M., Dunbar, A.E., 3, Wert, S.E., Askin, F., Hamvas, A. & Whitsett, J.A. (2001). A mutation in the surfactant protein C gene associated with familial interstitial lung disease. *The New England journal of medicine.* 344 (8): 573-579.

O'Brien, A.D., Standiford, T.J., Christensen, P.J., Wilcoxen, S.E. & Paine, R.,3rd (1998). Chemotaxis of alveolar macrophages in response to signals derived from alveolar epithelial cells. *The Journal of laboratory and clinical medicine.* 131 (5): 417-424.

Odajima, N., Betsuyaku, T., Nasuhara, Y. & Nishimura, M. (2007). Loss of caveolin-1 in bronchiolization in lung fibrosis. *The journal of histochemistry and cytochemistry : official journal of the Histochemistry Society.* 55 (9): 899-909.

Oedayrajsingh-Varma, M.J., van Ham, S.M., Knippenberg, M., Helder, M.N., Klein-Nulend, J., Schouten, T.E., Ritt, M.J. & van Milligen, F.J. (2006). Adipose tissue-derived mesenchymal stem cell yield and growth characteristics are affected by the tissue-harvesting procedure. *Cytotherapy.* 8 (2): 166-177.

Okamoto, M., Hoshino, T., Kitasato, Y., Sakazaki, Y., Kawayama, T., Fujimoto, K., Ohshima, K., Shiraishi, H., Uchida, M., Ono, J., Ohta, S., Kato, S., Izuhara, K. & Aizawa, H. (2011). Periostin, a matrix protein, is a novel biomarker for idiopathic interstitial pneumonias. *The European respiratory journal : official journal of the European Society for Clinical Respiratory Physiology.* 37 (5): 1119-1127.

Oku, H., Nakazato, H., Horikawa, T., Tsuruta, Y. & Suzuki, R. (2002). Pirfenidone suppresses tumor necrosis factor-alpha, enhances interleukin-10 and protects mice from endotoxic shock. *European journal of pharmacology.* 446 (1-3): 167-176.

Olsen, C.O., Isakson, B.E., Seedorf, G.J., Lubman, R.L. & Boitano, S. (2005). Extracellular matrix-driven alveolar epithelial cell differentiation in vitro. *Experimental lung research.* 31 (5): 461-482.

Olson, A.L., Swigris, J.J., Lezotte, D.C., Norris, J.M., Wilson, C.G. & Brown, K.K. (2007). Mortality from pulmonary fibrosis increased in the United States from 1992 to 2003. *American journal of respiratory and critical care medicine.* 176 (3): 277-284.

Ortiz, L.A., Dutreil, M., Fattman, C., Pandey, A.C., Torres, G., Go, K. & Phinney, D.G. (2007). Interleukin 1 receptor antagonist mediates the antiinflammatory and antifibrotic effect of mesenchymal stem cells during lung injury. *Proceedings of the National Academy of Sciences of the United States of America.* 104 (26): 11002-11007.

Ortiz, L.A., Gambelli, F., McBride, C., Gaupp, D., Baddoo, M., Kaminski, N. & Phinney, D.G. (2003). Mesenchymal stem cell engraftment in lung is enhanced in response to bleomycin exposure and ameliorates its fibrotic effects. *Proceedings of the National Academy of Sciences of the United States of America.* 100 (14): 8407-8411.

O'Toole, D., Hassett, P., Contreras, M., Higgins, B.D., McKeown, S.T., McAuley, D.F., O'Brien, T. & Laffey, J.G. (2009). Hypercapnic acidosis attenuates pulmonary epithelial wound repair by an NF-kappaB dependent mechanism. *Thorax.* 64 (11): 976-982.

Pan, G., O'Rourke, K., Chinnaiyan, A.M., Gentz, R., Ebner, R., Ni, J. & Dixit, V.M. (1997). The receptor for the cytotoxic ligand TRAIL. *Science (New York, N.Y.).* 276 (5309): 111-113.

Pan, L.H., Yamauchi, K., Uzuki, M., Nakanishi, T., Takigawa, M., Inoue, H. & Sawai, T. (2001). Type II alveolar epithelial cells and interstitial fibroblasts express connective tissue growth factor in IPF. *The European respiratory journal : official journal of the European Society for Clinical Respiratory Physiology.* 17 (6): 1220-1227.

Panos, R.J., Patel, R. & Bak, P.M. (1996). Intratracheal administration of hepatocyte growth factor/scatter factor stimulates rat alveolar type II cell proliferation in vivo. *American Journal Of Respiratory Cell And Molecular Biology.* 15 (5): 574-581.

Panos, R.J., Bak, P.M., Simonet, W.S., Rubin, J.S. & Smith, L.J. (1995). Intratracheal instillation of keratinocyte growth factor decreases hyperoxia-induced mortality in rats. *The Journal of clinical investigation.* 96 (4): 2026-2033.

Panos, R.J., Rubin, J.S., Csaky, K.G., Aaronson, S.A. & Mason, R.J. (1993). Keratinocyte growth factor and hepatocyte growth factor/scatter factor are heparin-binding growth factors for alveolar type II cells in fibroblast-conditioned medium. *The Journal of clinical investigation.* 92 (2): 969-977.

Panos, R.J., Suwabe, A., Leslie, C.C. & Mason, R.J. (1990). Hypertrophic alveolar type II cells from silica-treated rats are committed to DNA synthesis in vitro. *American journal of respiratory cell and molecular biology.* 3 (1): 51-59.

Pantelidis, P., Fanning, G.C., Wells, A.U., Welsh, K.I. & Du Bois, R.M. (2001). Analysis of tumor necrosis factor-alpha, lymphotoxin-alpha, tumor necrosis factor receptor II, and interleukin-6 polymorphisms in patients with idiopathic pulmonary fibrosis. *American journal of respiratory and critical care medicine.* 163 (6): 1432-1436.

Pardo, A., Gibson, K., Cisneros, J., Richards, T.J., Yang, Y., Becerril, C., Yousem, S., Herrera, I., Ruiz, V., Selman, M. & Kaminski, N. (2005). Up-regulation and profibrotic role of osteopontin in human idiopathic pulmonary fibrosis. *PLoS medicine.* 2 (9): e251.

Parekkadan, B., van Poll, D., Suganuma, K., Carter, E.A., Berthiaume, F., Tilles, A.W. & Yarmush, M.L. (2007). Mesenchymal stem cell-derived molecules reverse fulminant hepatic failure. *PloS one.* 2 (9): e941.

Park, S.B., Lin, C.S., Krishnan, A.V., Goldstein, D., Friedlander, M.L. & Kiernan, M.C. (2011). Dose effects of oxaliplatin on persistent and transient Na+ conductances and the development of neurotoxicity. *PloS one.* 6 (4): e18469.

Parks, W.C., Lopez-Boado, Y.S. & Wilson, C.L. (2001). Matrilysin in epithelial repair and defense. *Chest.* 120 (1 Suppl): 36S-41S.

Perrella, M.A., Yoshizumi, M., Fen, Z., Tsai, J.C., Hsieh, C.M., Kourembanas, S. & Lee, M.E. (1994). Transforming growth factor-beta 1, but not dexamethasone, down-regulates nitric-oxide synthase mRNA after its induction by interleukin-1 beta in rat smooth muscle cells. *The Journal Of Biological Chemistry.* 269 (20): 14595-14600.

Perrio, M.J., Ewen, D., Trevethick, M.A., Salmon, G.P. & Shute, J.K. (2007). Fibrin formation by wounded bronchial epithelial cell layers in vitro is essential for normal epithelial repair and independent of plasma proteins. *Clinical and experimental allergy : journal of the British Society for Allergy and Clinical Immunology.* 37 (11): 1688-1700.

Pevny, L.H., Sockanathan, S., Placzek, M. & Lovell-Badge, R. (1998). A role for SOX1 in neural determination. *Development (Cambridge, England).* 125 (10): 1967-1978.

Phan, S.H. (2002). The myofibroblast in pulmonary fibrosis. *Chest.* 122 (6): 286S-289S.

Phillips, R.J., Burdick, M.D., Hong, K., Lutz, M.A., Murray, L.A., Xue, Y.Y., Belperio, J.A., Keane, M.P. & Strieter, R.M. (2004). Circulating fibrocytes traffic to the lungs in response to CXCL12 and mediate fibrosis. *The Journal of clinical investigation.* 114 (3): 438-446.

Pini, L., Hamid, Q., Shannon, J., Lemelin, L., Olivenstein, R., Ernst, P., Lemiere, C., Martin, J.G. & Ludwig, M.S. (2007). Differences in proteoglycan deposition in the airways of moderate and severe asthmatics. *The European respiratory journal : official journal of the European Society for Clinical Respiratory Physiology.* 29 (1): 71-77.

Pittenger, M.F., Mackay, A.M., Beck, S.C., Jaiswal, R.K., Douglas, R., Mosca, J.D., Moorman, M.A., Simonetti, D.W., Craig, S. & Marshak, D.R. (1999). Multilineage potential of adult human mesenchymal stem cells. *Science (New York, N.Y.).* 284 (5411): 143-147.

Plantier, L., Crestani, B., Wert, S.E., Dehoux, M., Zweytick, B., Guenther, A. & Whitsett, J.A. (2011). Ectopic respiratory epithelial cell differentiation in bronchiolised distal airspaces in idiopathic pulmonary fibrosis. *Thorax.* 66 (8): 651-657.

Planus, E., Galiacy, S., Matthay, M., Laurent, V., Gavrilovic, J., Murphy, G., Clerici, C., Isabey, D., Lafuma, C. & d'Ortho, M.P. (1999). Role of collagenase in mediating in vitro alveolar epithelial wound repair. *Journal of cell science.* 112 (Pt 2) (Pt 2): 243-252.

Plataki, M., Koutsopoulos, A.V., Darivianaki, K., Delides, G., Siafakas, N.M. & Bouros, D. (2005). Expression of apoptotic and antiapoptotic markers in epithelial cells in idiopathic pulmonary fibrosis. *Chest.* 127 (1): 266-274.

Plumb, J.A., Milroy, R. & Kaye, S.B. (1989). Effects of the pH dependence of 3-(4,5-dimethylthiazol-2-yl)-2,5-diphenyl-tetrazolium bromide-formazan absorption on chemosensitivity determined by a novel tetrazolium-based assay. *Cancer research.* 49 (16): 4435-4440.

Pozharskaya, V., Torres-González, E., Rojas, M., Gal, A., Amin, M., Dollard, S., Roman, J., Stecenko, A.A. & Mora, A.L. (2009). Twist: a regulator of epithelial-mesenchymal transition in lung fibrosis. *Plos One.* 4 (10): e7559-e7559.

Puchelle, E., Zahm, J.M., Tournier, J.M. & Coraux, C. (2006). Airway epithelial repair, regeneration, and remodeling after injury in chronic obstructive pulmonary disease. *Proceedings of the American Thoracic Society.* 3 (8): 726-733.

Raghu, G., Brown, K.K., Costabel, U., Cottin, V., du Bois, R.M., Lasky, J.A., Thomeer, M., Utz, J.P., Khandker, R.K., McDermott, L. & Fatenejad, S. (2008). Treatment of idiopathic pulmonary fibrosis with etanercept: an exploratory, placebo-controlled trial. *American journal of respiratory and critical care medicine.* 178 (9): 948-955.

Raghu, G., Collard, H.R., Egan, J.J., Martinez, F.J., Behr, J., Brown, K.K., Colby, T.V., Cordier, J.F., Flaherty, K.R., Lasky, J.A., Lynch, D.A., Ryu, J.H., Swigris, J.J., Wells, A.U., Ancochea, J., Bouros, D., Carvalho, C., Costabel, U., Ebina, M., Hansell, D.M., Johkoh, T., Kim, D.S., King, T.E.,Jr, Kondoh, Y., Myers, J., Muller, N.L., Nicholson, A.G., Richeldi, L., Selman, M., Dudden, R.F., Griss, B.S., Protzko, S.L., Schunemann, H.J. & ATS/ERS/JRS/ALAT Committee on Idiopathic Pulmonary Fibrosis (2011). An official ATS/ERS/JRS/ALAT statement: idiopathic pulmonary fibrosis: evidence-based guidelines for diagnosis and management. *American journal of respiratory and critical care medicine.* 183 (6): 788-824.

Raghu, G., Freudenberger, T.D., Yang, S., Curtis, J.R., Spada, C., Hayes, J., Sillery, J.K., Pope, C.E.,2nd & Pellegrini, C.A. (2006). High prevalence of abnormal acid gastro-oesophageal reflux in idiopathic pulmonary fibrosis. *The European respiratory journal : official journal of the European Society for Clinical Respiratory Physiology.* 27 (1): 136-142.

Raghu, G., Johnson, W.C., Lockhart, D. & Mageto, Y. (1999). Treatment of idiopathic pulmonary fibrosis with a new antifibrotic agent, pirfenidone: results of a prospective, open-label Phase II study. *American Journal Of Respiratory And Critical Care Medicine.* 159 (4): 1061-1069.

Raghu, G., Weycker, D., Edelsberg, J., Bradford, W.Z. & Oster, G. (2006). Incidence and prevalence of idiopathic pulmonary fibrosis. *American Journal Of Respiratory And Critical Care Medicine.* 174 (7): 810-816.

Rahman, I., Skwarska, E., Henry, M., Davis, M., O'Connor, C.M., FitzGerald, M.X., Greening, A. & MacNee, W. (1999). Systemic and pulmonary oxidative stress in idiopathic pulmonary fibrosis. *Free radical biology & medicine.* 27 (1-2): 60-68.

Ramos, C., Montano, M., Garcia-Alvarez, J., Ruiz, V., Uhal, B.D., Selman, M. & Pardo, A. (2001). Fibroblasts from idiopathic pulmonary fibrosis and normal lungs differ in growth rate, apoptosis, and tissue inhibitor of metalloproteinases expression. *American journal of respiratory cell and molecular biology.* 24 (5): 591-598.

Rawlins, E.L. (2008). Lung epithelial progenitor cells: lessons from development. *Proceedings of the American Thoracic Society.* 5 (6): 675-681.

Rawlins, E.L., Okubo, T., Xue, Y., Brass, D.M., Auten, R.L., Hasegawa, H., Wang, F. & Hogan, B.L.M. (2009). The role of Scgb1a1+ Clara cells in the long-term maintenance and repair of lung airway, but not alveolar, epithelium. *Cell Stem Cell.* 4 (6): 525-534.

Reddy, R., Buckley, S., Doerken, M., Barsky, L., Weinberg, K., Anderson, K.D., Warburton, D. & Driscoll, B. (2004). Isolation of a putative progenitor subpopulation of alveolar epithelial type 2 cells. *American Journal Of Physiology.Lung Cellular And Molecular Physiology.* 286 (4): L658-L667.

Renzoni, E., Lympany, P., Sestini, P., Pantelidis, P., Wells, A., Black, C., Welsh, K., Bunn, C., Knight, C., Foley, P. & du Bois, R.M. (2000). Distribution of novel polymorphisms of the interleukin-8 and CXC receptor 1 and 2 genes in systemic sclerosis and cryptogenic fibrosing alveolitis. *Arthritis and Rheumatism.* 43 (7): 1633-1640.

Reubinoff, B.E., Pera, M.F., Fong, C.Y., Trounson, A. & Bongso, A. (2000). Embryonic stem cell lines from human blastocysts: somatic differentiation in vitro. *Nature biotechnology.* 18 (4): 399-404.

Reynolds, S.D. &Malkinson, A.M. (2010). Clara cell: progenitor for the bronchiolar epithelium. *The international journal of biochemistry & cell biology.* 42 (1): 1-4.

Riha, R.L., Yang, I.A., Rabnott, G.C., Tunnicliffe, A.M., Fong, K.M. & Zimmerman, P.V. (2004). Cytokine gene polymorphisms in idiopathic pulmonary fibrosis. *Internal Medicine Journal.* 34 (3): 126-129.

Rimondi, E., Secchiero, P., Quaroni, A., Zerbinati, C., Capitani, S. & Zauli, G. (2006). Involvement of TRAIL/TRAIL-receptors in human intestinal cell differentiation. *Journal of cellular physiology.* 206 (3): 647-654.

Rippon, H.J., Polak, J.M., Qin, M. & Bishop, A.E. (2006). Derivation of distal lung epithelial progenitors from murine embryonic stem cells using a novel three-step differentiation protocol. *Stem cells (Dayton, Ohio).* 24 (5): 1389-1398.

Rock, J.R., Onaitis, M.W., Rawlins, E.L., Lu, Y., Clark, C.P., Xue, Y., Randell, S.H. & Hogan, B.L. (2009). Basal cells as stem cells of the mouse trachea and human airway epithelium. *Proceedings of the National Academy of Sciences of the United States of America.* 106 (31): 12771-12775.

Rojas, M., Xu, J., Woods, C.R., Mora, A.L., Spears, W., Roman, J. & Brigham, K.L. (2005). Bone marrow-derived mesenchymal stem cells in repair of the injured lung. *American journal of respiratory cell and molecular biology.* 33 (2): 145-152.

Roszell, B., Mondrinos, M.J., Seaton, A., Simons, D.M., Koutzaki, S.H., Fong, G.H., Lelkes, P.I. & Finck, C.M. (2009). Efficient derivation of alveolar type II cells from embryonic stem cells for in vivo application. *Tissue engineering.Part A.* 15 (11): 3351-3365.

Roy, S.G., Nozaki, Y. & Phan, S.H. (2001). Regulation of alpha-smooth muscle actin gene expression in myofibroblast differentiation from rat lung fibroblasts. *The international journal of biochemistry & cell biology.* 33 (7): 723-734.

Ryan, R.M., Mineo-Kuhn, M.M., Kramer, C.M. & Finkelstein, J.N. (1994). Growth factors alter neonatal type II alveolar epithelial cell proliferation. *The American Journal of Physiology.* 266 (1 Pt 1): L17-22.

Saika, S., Shiraishi, A., Liu, C.Y., Funderburgh, J.L., Kao, C.W., Converse, R.L. & Kao, W.W. (2000). Role of lumican in the corneal epithelium during wound healing. *The Journal of biological chemistry.* 275 (4): 2607-2612.

Salazar, K.D., Lankford, S.M. & Brody, A.R. (2009). Mesenchymal stem cells produce Wnt isoforms and TGF-beta1 that mediate proliferation and procollagen expression by lung fibroblasts. *American journal of physiology.Lung cellular and molecular physiology.* 297 (5): L1002-11.

Sallusto, F., Lanzavecchia, A. & Mackay, C.R. (1998). Chemokines and chemokine receptors in T-cell priming and Th1/Th2-mediated responses. *Immunology today.* 19 (12): 568-574.

Sato, Y., Araki, H., Kato, J., Nakamura, K., Kawano, Y., Kobune, M., Sato, T., Miyanishi, K., Takayama, T., Takahashi, M., Takimoto, R., Iyama, S., Matsunaga, T., Ohtani, S., Matsuura, A., Hamada, H. & Niitsu, Y. (2005). Human mesenchymal stem cells xenografted directly to rat liver are differentiated into human hepatocytes without fusion. *Blood.* 106 (2): 756-763.

Savla, U. &Waters, C.M. (1998). Mechanical strain inhibits repair of airway epithelium in vitro. *The American Journal of Physiology.* 274 (6 Pt 1): L883-92.

Scheibe, F., Klein, O., Klose, J. & Priller, J. (2012). Mesenchymal stromal cells rescue cortical neurons from apoptotic cell death in an in vitro model of cerebral ischemia. *Cellular and molecular neurobiology.* 32 (4): 567-576.

Schmidinger, G., Hanselmayer, G., Pieh, S., Lackner, B., Kaminski, S., Ruhswurm, I. & Skorpik, C. (2003). Effect of tenascin and fibronectin on the migration of human corneal fibroblasts. *Journal of cataract and refractive surgery.* 29 (2): 354-360.

Selman, M., Carrillo, G., Salas, J., Padilla, R.P., Perez-Chavira, R., Sansores, R. & Chapela, R. (1998). Colchicine, D-penicillamine, and prednisone in the treatment of idiopathic pulmonary fibrosis: a controlled clinical trial. *Chest.* 114 (2): 507-512.

Selman, M., King, T.E., Pardo, A., American Thoracic Society, European Respiratory Society & American College of Chest Physicians (2001). Idiopathic pulmonary fibrosis: prevailing and evolving hypotheses about its pathogenesis and implications for therapy. *Annals of Internal Medicine.* 134 (2): 136-151.

Selman, M. &Pardo, A. (2002). Idiopathic pulmonary fibrosis: an epithelial/fibroblastic cross-talk disorder. *Respiratory research.* 3 : 3.

Selman, M., Pardo, A., Barrera, L., Estrada, A., Watson, S.R., Wilson, K., Aziz, N., Kaminski, N. & Zlotnik, A. (2006). Gene expression profiles distinguish idiopathic pulmonary fibrosis from hypersensitivity pneumonitis. *American journal of respiratory and critical care medicine.* 173 (2): 188-198.

Selman, M., Ruiz, V., Cabrera, S., Segura, L., Ramirez, R., Barrios, R. & Pardo, A. (2000). TIMP-1, -2, -3, and -4 in idiopathic pulmonary fibrosis. A prevailing nondegradative lung microenvironment? *American journal of physiology.Lung cellular and molecular physiology.* 279 (3): L562-74.

Selman, M., Lin, H., Montaño, M., Jenkins, A.L., Estrada, A., Lin, Z., Wang, G., DiAngelo, S.L., Guo, X., Umstead, T.M., Lang, C.M., Pardo, A., Phelps, D.S. & Floros, J. (2003). Surfactant protein A and B genetic variants predispose to idiopathic pulmonary fibrosis. *Human genetics.* 113 (6): 542-550.

Selman, M. &Pardo, A. (2006). Role of epithelial cells in idiopathic pulmonary fibrosis: from innocent targets to serial killers. *Proceedings Of The American Thoracic Society.* 3 (4): 364-372.

Seomun, Y. &Joo, C.K. (2008). Lumican induces human corneal epithelial cell migration and integrin expression via ERK 1/2 signaling. *Biochemical and biophysical research communications.* 372 (1): 221-225.

Sheridan, J.P., Marsters, S.A., Pitti, R.M., Gurney, A., Skubatch, M., Baldwin, D., Ramakrishnan, L., Gray, C.L., Baker, K., Wood, W.I., Goddard, A.D., Godowski, P. & Ashkenazi, A. (1997). Control of TRAIL-induced apoptosis by a family of signaling and decoy receptors. *Science (New York, N.Y.).* 277 (5327): 818-821.

Shimazaki, M., Nakamura, K., Kii, I., Kashima, T., Amizuka, N., Li, M., Saito, M., Fukuda, K., Nishiyama, T., Kitajima, S., Saga, Y., Fukayama, M., Sata, M. & Kudo, A. (2008). Periostin is essential for cardiac healing after acute myocardial infarction. *The Journal of experimental medicine.* 205 (2): 295-303.

Shin, S., Dalton, S. & Stice, S.L. (2005). Human motor neuron differentiation from human embryonic stem cells. *Stem Cells And Development.* 14 (3): 266-269.

Simmons, P.J. &Torok-Storb, B. (1991). Identification of stromal cell precursors in human bone marrow by a novel monoclonal antibody, STRO-1. *Blood.* 78 (1): 55-62.

Simonet, W.S., DeRose, M.L., Bucay, N., Nguyen, H.Q., Wert, S.E., Zhou, L., Ulich, T.R., Thomason, A., Danilenko, D.M. & Whitsett, J.A. (1995). Pulmonary malformation in transgenic mice expressing human keratinocyte growth factor in the lung. *Proceedings of the National Academy of Sciences of the United States of America.* 92 (26): 12461-12465.

Singla, D.K. &McDonald, D.E. (2007). Factors released from embryonic stem cells inhibit apoptosis of H9c2 cells. *American journal of physiology.Heart and circulatory physiology.* 293 (3): H1590-5.

Singla, D.K., Singla, R.D. & McDonald, D.E. (2008). Factors released from embryonic stem cells inhibit apoptosis in H9c2 cells through PI3K/Akt but not ERK pathway. *American Journal Of Physiology.Heart And Circulatory Physiology.* 295 (2): H907-H913.

Sisson, T.H., Mendez, M., Choi, K., Subbotina, N., Courey, A., Cunningham, A., Dave, A., Engelhardt, J.F., Liu, X., White, E.S., Thannickal, V.J., Moore, B.B., Christensen, P.J. & Simon, R.H. (2010). Targeted injury of type II alveolar epithelial cells induces pulmonary fibrosis. *American journal of respiratory and critical care medicine.* 181 (3): 254-263.

Sonar, S.S., Schwinge, D., Kilic, A., Yildirim, A.O., Conrad, M.L., Seidler, K., Muller, B., Renz, H. & Nockher, W.A. (2010). Nerve growth factor enhances Clara cell proliferation after lung injury. *The European respiratory journal : official journal of the European Society for Clinical Respiratory Physiology.* 36 (1): 105-115.

Steele, M.P., Speer, M.C., Loyd, J.E., Brown, K.K., Herron, A., Slifer, S.H., Burch, L.H., Wahidi, M.M., Phillips,John A.,,3rd, Sporn, T.A., McAdams, H.P., Schwarz, M.I. & Schwartz, D.A. (2005). Clinical and pathologic features of familial interstitial pneumonia. *American Journal Of Respiratory And Critical Care Medicine.* 172 (9): 1146-1152.

Stewart, J.P., Egan, J.J., Ross, A.J., Kelly, B.G., Lok, S.S., Hasleton, P.S. & Woodcock, A.A. (1999). The detection of Epstein-Barr virus DNA in lung tissue from patients with idiopathic pulmonary fibrosis. *American journal of respiratory and critical care medicine.* 159 (4 Pt 1): 1336-1341.

Stoffel, M., Vallier, L. & Pedersen, R.A. (2004). Navigating the pathway from embryonic stem cells to beta cells. *Seminars in cell & developmental biology.* 15 (3): 327-336.

Strieter, R.M. (2005). Pathogenesis and natural history of usual interstitial pneumonia: the whole story or the last chapter of a long novel. *Chest.* 128 (5): 526S-532S.

Stripp, B.R. (2008). Hierarchical organization of lung progenitor cells: is there an adult lung tissue stem cell? *Proceedings of the American Thoracic Society.* 5 (6): 695-698.

Stripp, B.R. &Reynolds, S.D. (2008). Maintenance and repair of the bronchiolar epithelium. *Proceedings of the American Thoracic Society.* 5 (3): 328-333.

Strobel, E.S., Gay, R.E. & Greenberg, P.L. (1986). Characterization of the in vitro stromal microenvironment of human bone marrow. *International journal of cell cloning.* 4 (5): 341-356.

Strollo, D.C. (2003). Imaging of idiopathic interstitial lung diseases. Concepts and conundrums. *American Journal Of Respiratory Cell And Molecular Biology.* 29 (3): S10-S18.

Sueblinvong, V. &Weiss, D.J. (2010). Stem cells and cell therapy approaches in lung biology and diseases. *Translational Research: The Journal Of Laboratory And Clinical Medicine.* 156 (3): 188-205.

Suzuki, G., Iyer, V., Lee, T.C. & Canty, J.M.,Jr (2011). Autologous mesenchymal stem cells mobilize cKit+ and CD133+ bone marrow progenitor cells and improve regional function in hibernating myocardium. *Circulation research.* 109 (9): 1044-1054.

Tang, Y.W., Johnson, J.E., Browning, P.J., Cruz-Gervis, R.A., Davis, A., Graham, B.S., Brigham, K.L., Oates, J.A.,Jr, Loyd, J.E. & Stecenko, A.A. (2003). Herpesvirus DNA is consistently detected in lungs of patients with idiopathic pulmonary fibrosis. *Journal of clinical microbiology.* 41 (6): 2633-2640.

Taniguchi, H., Ebina, M., Kondoh, Y., Ogura, T., Azuma, A., Suga, M., Taguchi, Y., Takahashi, H., Nakata, K., Sato, A., Takeuchi, M., Raghu, G., Kudoh, S., Nukiwa, T. & Pirfenidone Clinical Study Group in Japan (2010). Pirfenidone in idiopathic pulmonary fibrosis. *The European respiratory journal : official journal of the European Society for Clinical Respiratory Physiology.* 35 (4): 821-829.

Tanjore, H., Blackwell, T.S. & Lawson, W.E. (2012). Emerging evidence for endoplasmic reticulum stress in the pathogenesis of idiopathic pulmonary fibrosis. *American journal of physiology.Lung cellular and molecular physiology.* 15; 302 (8): L721-9

Thannickal, V.J. &Fanburg, B.L. (1995). Activation of an H2O2-generating NADH oxidase in human lung fibroblasts by transforming growth factor beta 1. *The Journal of biological chemistry.* 270 (51): 30334-30338.

Thannickal, V.J., Toews, G.B., White, E.S., Lynch,Joseph P.,,3rd & Martinez, F.J. (2004). Mechanisms of pulmonary fibrosis. *Annual Review of Medicine.* 55 : 395-417.

Theise, N.D., Henegariu, O., Grove, J., Jagirdar, J., Kao, P.N., Crawford, J.M., Badve, S., Saxena, R. & Krause, D.S. (2002). Radiation pneumonitis in mice: a severe injury model for pneumocyte engraftment from bone marrow. *Experimental hematology.* 30 (11): 1333-1338.

Thiery, J.P. &Sleeman, J.P. (2006). Complex networks orchestrate epithelial-mesenchymal transitions. *Nature reviews.Molecular cell biology.* 7 (2): 131-142.

Thomas, A.Q., Lane, K., Phillips, J.,3rd, Prince, M., Markin, C., Speer, M., Schwartz, D.A., Gaddipati, R., Marney, A., Johnson, J., Roberts, R., Haines, J., Stahlman, M. & Loyd, J.E. (2002). Heterozygosity for a surfactant protein C gene mutation associated with usual interstitial pneumonitis and cellular nonspecific interstitial pneumonitis in one kindred. *American Journal Of Respiratory And Critical Care Medicine.* 165 (9): 1322-1328.

Thomson, J.A., Itskovitz-Eldor, J., Shapiro, S.S., Waknitz, M.A., Swiergiel, J.J., Marshall, V.S. & Jones, J.M. (1998). Embryonic stem cell lines derived from human blastocysts. *Science (New York, N.Y.).* 282 (5391): 1145-1147.

Thorsell, A., Faijerson, J, Blomstrand, F., Nilsson, M., Kaj Blennow, K., Eriksson, P.S & Westman-Brinkmalm, A. (2008). Proteome analysis of serum-containing conditioned medium from primary astrocyte cultures. Journal of Proteomics & Bioinformatics. 1(3) :128-142.

Tobin, R.W., Pope, C.E.,2nd, Pellegrini, C.A., Emond, M.J., Sillery, J. & Raghu, G. (1998). Increased prevalence of gastroesophageal reflux in patients with idiopathic pulmonary fibrosis. *American journal of respiratory and critical care medicine.* 158 (6): 1804-1808.

Toma, C., Pittenger, M.F., Cahill, K.S., Byrne, B.J. & Kessler, P.D. (2002). Human mesenchymal stem cells differentiate to a cardiomyocyte phenotype in the adult murine heart. *Circulation.* 105 (1): 93-98.

Tsakiri, K.D., Cronkhite, J.T., Kuan, P.J., Xing, C., Raghu, G., Weissler, J.C., Rosenblatt, R.L., Shay, J.W. & Garcia, C.K. (2007). Adult-onset pulmonary fibrosis caused by mutations in telomerase. *Proceedings of the National Academy of Sciences of the United States of America.* 104 (18): 7552-7557.

Tsukamoto, K., Hayakawa, H., Sato, A., Chida, K., Nakamura, H. & Miura, K. (2000). Involvement of Epstein-Barr virus latent membrane protein 1 in disease progression in patients with idiopathic pulmonary fibrosis. *Thorax.* 55 (11): 958-961.

Tzouvelekis, A., Koliakos, G., Ntolios, P., Baira, I., Bouros, E., Oikonomou, A., Zissimopoulos, A., Kolios, G., Kakagia, D., Paspaliaris, V., Kotsianidis, I., Froudarakis, M. & Bouros, D. (2011). Stem cell therapy for idiopathic pulmonary fibrosis: a protocol proposal. *Journal of translational medicine.* 9 : 182.

Ueda, T., Ohta, K., Suzuki, N., Yamaguchi, M., Hirai, K., Horiuchi, T., Watanabe, J., Miyamoto, T. & Ito, K. (1992). Idiopathic pulmonary fibrosis and high prevalence of serum antibodies to hepatitis C virus. *The American Review of Respiratory Disease.* 146 (1): 266-268.

Uhal, B.D. (1997). Cell cycle kinetics in the alveolar epithelium. *The American Journal of Physiology.* 272 (6): L1031-L1045.

Uhal, B.D., Joshi, I., True, A.L., Mundle, S., Raza, A., Pardo, A. & Selman, M. (1995). Fibroblasts isolated after fibrotic lung injury induce apoptosis of alveolar epithelial cells in vitro. *The American Journal of Physiology.* 269 (6): L819-L828.

Uhal, B.D., Joshi, I., Hughes, W.F., Ramos, C., Pardo, A. & Selman, M. (1998). Alveolar epithelial cell death adjacent to underlying myofibroblasts in advanced fibrotic human lung. *The American Journal of Physiology.* 275 (6 Pt 1): L1192-9.

Uhal, B.D. The role of apoptosis in pulmonary fibrosis. (2008). *Eur Respir Rev* 17: 109, 138-144.

Ulich, T.R., Yi, E.S., Longmuir, K., Yin, S., Biltz, R., Morris, C.F., Housley, R.M. & Pierce, G.F. (1994). Keratinocyte growth factor is a growth factor for type II pneumocytes in vivo. *The Journal of clinical investigation.* 93 (3): 1298-1306.

Van Hoof, D., Passier, R., Ward-Van Oostwaard, D., Pinkse, M.W.H., Heck, A.J.R., Mummery, C.L. & Krijgsveld, J. (2006). A quest for human and mouse embryonic stem cell-specific proteins. *Molecular & Cellular Proteomics: MCP.* 5 (7): 1261-1273.

Vasakova, M., Striz, I., Slavcev, A., Jandova, S., Dutka, J., Terl, M., Kolesar, L. & Sulc, J. (2007). Correlation of IL-1alpha and IL-4 gene polymorphisms and clinical parameters in idiopathic pulmonary fibrosis. *Scandinavian Journal of Immunology.* 65 (3): 265-270.

Vernet, D., Ferrini, M.G., Valente, E.G., Magee, T.R., Bou-Gharios, G., Rajfer, J. & Gonzalez-Cadavid, N.F. (2002). Effect of nitric oxide on the differentiation of

fibroblasts into myofibroblasts in the Peyronie's fibrotic plaque and in its rat model. *Nitric oxide : biology and chemistry / official journal of the Nitric Oxide Society.* 7 (4): 262-276.

von Plessen, C., Grinde, O. & Gulsvik, A. (2003). Incidence and prevalence of cryptogenic fibrosing alveolitis in a Norwegian community. *Respiratory medicine.* 97 (4): 428-435.

Walczak, H., Degli-Esposti, M.A., Johnson, R.S., Smolak, P.J., Waugh, J.Y., Boiani, N., Timour, M.S., Gerhart, M.J., Schooley, K.A., Smith, C.A., Goodwin, R.G. & Rauch, C.T. (1997). TRAIL-R2: a novel apoptosis-mediating receptor for TRAIL. *The EMBO journal.* 16 (17): 5386-5397.

Walker, N.M., Badri, L.N., Wadhwa, A., Wettlaufer, S., Peters-Golden, M. & Lama, V.N. (2012). Prostaglandin E2 as an inhibitory modulator of fibrogenesis in human lung allografts. *American journal of respiratory and critical care medicine.* 185 (1): 77-84.

Walter, M.N., Wright, K.T., Fuller, H.R., MacNeil, S. & Johnson, W.E. (2010). Mesenchymal stem cell-conditioned medium accelerates skin wound healing: an in vitro study of fibroblast and keratinocyte scratch assays. *Experimental cell research.* 316 (7): 1271-1281.

Walter, N., Collard, H.R. & King, T.E.,Jr (2006). Current perspectives on the treatment of idiopathic pulmonary fibrosis. *Proceedings of the American Thoracic Society.* 3 (4): 330-338.

Wang, D., Morales, J.E., Calame, D.G., Alcorn, J.L. & Wetsel, R.A. (2010). Transplantation of human embryonic stem cell-derived alveolar epithelial type II cells abrogates acute lung injury in mice. *Molecular therapy : the journal of the American Society of Gene Therapy.* 18 (3): 625-634.

Wang, D., Haviland, D.L., Burns, A.R., Zsigmond, E. & Wetsel, R.A. (2007). A pure population of lung alveolar epithelial type II cells derived from human embryonic stem cells. *Proceedings of the National Academy of Sciences of the United States of America.* 104 (11): 4449-4454.

Wang, R., Ghahary, A., Shen, Y.J., Scott, P.G. & Tredget, E.E. (1997). Nitric oxide synthase expression and nitric oxide production are reduced in hypertrophic scar tissue and fibroblasts. *The Journal of investigative dermatology.* 108 (4): 438-444.

Wang, R., Ramos, C., Joshi, I., Zagariya, A., Pardo, A., Selman, M. & Uhal, B.D. (1999). Human lung myofibroblast-derived inducers of alveolar epithelial apoptosis identified as angiotensin peptides. *The American Journal of Physiology.* 277 (6): L1158-L1164.

Wang, Y., Kuan, P.J., Xing, C., Cronkhite, J.T., Torres, F., Rosenblatt, R.L., DiMaio, J.M., Kinch, L.N., Grishin, N.V. & Garcia, C.K. (2009). Genetic defects in surfactant protein A2 are associated with pulmonary fibrosis and lung cancer. *American Journal of Human Genetics.* 84 (1): 52-59.

Wangoo, A., Shaw, R.J., Diss, T.C., Farrell, P.J., du Bois, R.M. & Nicholson, A.G. (1997). Cryptogenic fibrosing alveolitis: lack of association with Epstein-Barr virus infection. *Thorax.* 52 (10): 888-891.

Weckmann, M., Collison, A., Simpson, J.L., Kopp, M.V., Wark, P.A., Smyth, M.J., Yagita, H., Matthaei, K.I., Hansbro, N., Whitehead, B., Gibson, P.G., Foster, P.S. & Mattes, J. (2007). Critical link between TRAIL and CCL20 for the activation of TH2 cells and the expression of allergic airway disease. *Nature medicine.* 13 (11): 1308-1315.

Weiss, D.J. &Finck, C. (2010). Embryonic stem cells and repair of lung injury. *Molecular therapy : the journal of the American Society of Gene Therapy.* 18 (3): 460-461.

Whittington, H.A., Freeburn, R.W., Godinho, S.I., Egan, J., Haider, Y. & Millar, A.B. (2003). Analysis of an IL-10 polymorphism in idiopathic pulmonary fibrosis. *Genes and immunity.* 4 (4): 258-264.

Wilborn, J., Crofford, L.J., Burdick, M.D., Kunkel, S.L., Strieter, R.M. & Peters-Golden, M. (1995). Cultured lung fibroblasts isolated from patients with idiopathic pulmonary fibrosis have a diminished capacity to synthesize prostaglandin E2 and to express cyclooxygenase-2. *The Journal of clinical investigation.* 95 (4): 1861-1868.

Willis, B.C. &Borok, Z. (2007). TGF-beta-induced EMT: mechanisms and implications for fibrotic lung disease. *American journal of physiology.Lung cellular and molecular physiology.* 293 (3): L525-34.

Willis, B.C., duBois, R.M. & Borok, Z. (2006). Epithelial origin of myofibroblasts during fibrosis in the lung. *Proceedings of the American Thoracic Society.* 3 (4): 377-382.

Willis, B.C., Liebler, J.M., Luby-Phelps, K., Nicholson, A.G., Crandall, E.D., du Bois, R.M. & Borok, Z. (2005). Induction of epithelial-mesenchymal transition in alveolar epithelial cells by transforming growth factor-beta1: potential role in idiopathic pulmonary fibrosis. *The American journal of pathology.* 166 (5): 1321-1332.

Wimpenny, I., Hampson, K., Yang, Y., Ashammakhi, N. & Forsyth, N.R. (2010). One-step recovery of marrow stromal cells on nanofibers. *Tissue engineering.Part C, Methods.* 16 (3): 503-509.

Wong, P.S., Vogel, C.F., Kokosinski, K. & Matsumura, F. (2010). Arylhydrocarbon receptor activation in NCI-H441 cells and C57BL/6 mice: possible mechanisms for lung dysfunction. *American journal of respiratory cell and molecular biology.* 42 (2): 210-217.

Wynes, M.W., Frankel, S.K. & Riches, D.W. (2004). IL-4-induced macrophage-derived IGF-I protects myofibroblasts from apoptosis following growth factor withdrawal. *Journal of leukocyte biology.* 76 (5): 1019-1027.

Xaubet, A., Marin-Arguedas, A., Lario, S., Ancochea, J., Morell, F., Ruiz-Manzano, J., Rodriguez-Becerra, E., Rodriguez-Arias, J.M., Inigo, P., Sanz, S., Campistol, J.M., Mullol, J. & Picado, C. (2003). Transforming growth factor-beta1 gene polymorphisms are associated with disease progression in idiopathic pulmonary fibrosis. *American journal of respiratory and critical care medicine.* 168 (4): 431-435.

Xu, C., Inokuma, M.S., Denham, J., Golds, K., Kundu, P., Gold, J.D. & Carpenter, M.K. (2001). Feeder-free growth of undifferentiated human embryonic stem cells. *Nature biotechnology.* 19 (10): 971-974.

Yaguchi, T., Fukuda, Y., Ishizaki, M. & Yamanaka, N. (1998). Immunohistochemical and gelatin zymography studies for matrix metalloproteinases in bleomycin-induced pulmonary fibrosis. *Pathology international.* 48 (12): 954-963.

Yamada, K.M. (2000). Fibronectin peptides in cell migration and wound repair. *The Journal of clinical investigation.* 105 (11): 1507-1509.

Yamada, T., Yoshikawa, M., Kanda, S., Kato, Y., Nakajima, Y., Ishizaka, S. & Tsunoda, Y. (2002a). In vitro differentiation of embryonic stem cells into hepatocyte-like cells identified by cellular uptake of indocyanine green. *Stem cells (Dayton, Ohio).* 20 (2): 146-154.

Yamada, T., Yoshikawa, M., Takaki, M., Torihashi, S., Kato, Y., Nakajima, Y., Ishizaka, S. & Tsunoda, Y. (2002b). In vitro functional gut-like organ formation from mouse embryonic stem cells. *Stem cells (Dayton, Ohio).* 20 (1): 41-49.

Yan, X., Liu, Y., Han, Q., Jia, M., Liao, L., Qi, M. & Zhao, R.C. (2007). Injured microenvironment directly guides the differentiation of engrafted Flk-1(+) mesenchymal stem cell in lung. *Experimental hematology.* 35 (9): 1466-1475.

Yano, T., Mason, R.J., Pan, T., Deterding, R.R., Nielsen, L.D. & Shannon, J.M. (2000). KGF regulates pulmonary epithelial proliferation and surfactant protein gene expression in adult rat lung. *American journal of physiology.Lung cellular and molecular physiology.* 279 (6): L1146-58.

Yee, M., Vitiello, P.F., Roper, J.M., Staversky, R.J., Wright, T.W., McGrath-Morrow, S.A., Maniscalco, W.M., Finkelstein, J.N. & O'Reilly, M.A. (2006). Type II epithelial cells are critical target for hyperoxia-mediated impairment of postnatal lung development. *American journal of physiology.Lung cellular and molecular physiology.* 291 (5): L1101-11.

Yeh, J.T., Yeh, L.K., Jung, S.M., Chang, T.J., Wu, H.H., Shiu, T.F., Liu, C.Y., Kao, W.W. & Chu, P.H. (2010). Impaired skin wound healing in lumican-null mice. *The British journal of dermatology.* 163 (6): 1174-1180.

Yeh, L.K., Chen, W.L., Li, W., Espana, E.M., Ouyang, J., Kawakita, T., Kao, W.W., Tseng, S.C. & Liu, C.Y. (2005). Soluble lumican glycoprotein purified from human amniotic membrane promotes corneal epithelial wound healing. *Investigative ophthalmology & visual science.* 46 (2): 479-486.

Ying, Q., Stavridis, M., Griffiths, D., Li, M. & Smith, A. (2003). Conversion of embryonic stem cells into neuroectodermal precursors in adherent monoculture. *Nature biotechnology.* 21 (2): 183-186.

Ylatupa, S., Haglund, C., Mertaniemi, P., Vahtera, E. & Partanen, P. (1995). Cellular fibronectin in serum and plasma: a potential new tumour marker? *British journal of cancer.* 71 (3): 578-582.

Yu, H., Konigshoff, M., Jayachandran, A., Handley, D., Seeger, W., Kaminski, N. & Eickelberg, O. (2008). Transgelin is a direct target of TGF-beta/Smad3-dependent epithelial cell migration in lung fibrosis. *FASEB journal : official publication of the Federation of American Societies for Experimental Biology.* 22 (6): 1778-1789.

Yurchenco, P.D. &Schittny, J.C. (1990). Molecular architecture of basement membranes. *FASEB Journal: Official Publication Of The Federation Of American Societies For Experimental Biology.* 4 (6): 1577-1590.

Yurovsky, V.V. (2003). Tumor necrosis factor-related apoptosis-inducing ligand enhances collagen production by human lung fibroblasts. *American journal of respiratory cell and molecular biology.* 28 (2): 225-231.

Zahm, J.M., Chevillard, M. & Puchelle, E. (1991). Wound repair of human surface respiratory epithelium. *American Journal Of Respiratory Cell And Molecular Biology.* 5 (3): 242-248.

Zamò, A., Poletti, V., Reghellin, D., Montagna, L., Pedron, S., Piccoli, P. & Chilosi, M. (2005). HHV-8 and EBV are not commonly found in idiopathic pulmonary fibrosis. *Sarcoidosis, Vasculitis, And Diffuse Lung Diseases: Official Journal Of WASOG / World Association Of Sarcoidosis And Other Granulomatous Disorders.* 22 (2): 123-128.

Zeng, R., Wang, L.W., Hu, Z.B., Guo, W.T., Wei, J.S., Lin, H., Sun, X., Chen, L.X. & Yang, L.J. (2011). Differentiation of human bone marrow mesenchymal stem cells into neuron-like cells in vitro. *Spine.* 36 (13): 997-1005.

Zhang, H.Y., Gharaee-Kermani, M. & Phan, S.H. (1997). Regulation of lung fibroblast alpha-smooth muscle actin expression, contractile phenotype, and apoptosis by IL-1beta. *Journal Of Immunology (Baltimore, Md.: 1950).* 158 (3): 1392-1399.

Zhen, G., Liu, H., Gu, N., Zhang, H., Xu, Y. & Zhang, Z. (2008). Mesenchymal stem cells transplantation protects against rat pulmonary emphysema. *Frontiers in bioscience : a journal and virtual library.* 13 : 3415-3422.

Zhou, H.M., Wang, J., Elliott, C., Wen, W., Hamilton, D.W. & Conway, S.J. (2010). Spatiotemporal expression of periostin during skin development and incisional wound healing: lessons for human fibrotic scar formation. *Journal of cell communication and signaling.* 4 (2): 99-107.

Zhou, L., Lim, L., Costa, R.H. & Whitsett, J.A. (1996). Thyroid transcription factor-1, hepatocyte nuclear factor-3beta, surfactant protein B, C, and Clara cell secretory protein in developing mouse lung. *The journal of histochemistry and cytochemistry : official journal of the Histochemistry Society.* 44 (10): 1183-1193.

Zissel, G., Ernst, M., Rabe, K., Papadopoulos, T., Magnussen, H., Schlaak, M. & Muller-Quernheim, J. (2000). Human alveolar epithelial cells type II are capable of regulating T-cell activity. *Journal of investigative medicine : the official publication of the American Federation for Clinical Research.* 48 (1): 66-75.

Zuo, F., Kaminski, N., Eugui, E., Allard, J., Yakhini, Z., Ben-Dor, A., Lollini, L., Morris, D., Kim, Y., DeLustro, B., Sheppard, D., Pardo, A., Selman, M. & Heller, R.A. (2002). Gene expression analysis reveals matrilysin as a key regulator of pulmonary fibrosis in mice and humans. *Proceedings of the National Academy of Sciences of the United States of America.* 99 (9): 6292-6297.

Appendix 1:

Table S1: Media and other supplements for cell culture.

Name	Description	Cat No	Company
DMEM	Dulbeco's Modified Eagle Medium	21969	Gibco, Invitrogen, Paisley, UK
KO-DMEM	Knock Out DMEM	10829	Gibco, Invitrogen, Paisley, UK
FBS	Fetal Bovine Serum	DE14-870F	Lonza, Belgium
KO-SR	Knock Out Serum Replacement	10828	Gibco, Invitrogen, Paisley, UK
PBS	Phosphate Buffered Saline	BE17-516F	Lonza, Belgium
SABM	Small Airway Basal Medium	CC-3119	Lonza, USA
Trypsin/EDTA	Trypsin 10X with Versene	BE02-007E	Lonza, Belgium
DMSO	Dimethyl Sulphoxide	D2650	Sigma-Aldrich, UK
L-glutamine	L-Glutamine	BE17-605E	Lonza, Belgium
NEAA	Non Essential Amino Acid	BE13-114	Lonza, Belgium
Matrigel	BD Matrigel Matrix	354234	BD, Bedford, MA, USA
Collagen I	Rat tail Collagen Type I	354249	BD Bioscience, Bedford, MA, USA
bFGF	Human FGF-basic	100-18B	PeproTech, London
PSA	Penicillin-Streptomycin-Amphotericin B	17-745E	Lonza, MD, USA
β-mercaptoethanol	2-Mercaptoethanol	31350-010	Gibco, Invitrogen, Auckland, NZ
Activin A	Human Activin-A	120-14	PeproTech, Inc., Rocky Hill, NJ, USA

Table S2: Panel of primary antibodies used for immunocytochemistry and immunohistochemistry.

Antibody	Description	Dilution	Company
*pro*SP-C	Anti-ProSurfactant Protein C antibody. Rabbit polyclonal (IgG)	1:250 cell 1:1500 tissue	Abcam Cat No- ab40879
CC10	Anti-Uteroglobin antibody Rabbit polyclonal (IgG)	1:200	Abcam Cat No- ab40873
TRAIL	Anti-TRAIL antibody Rabbit polyclonal (IgG)	1:100, cell 1:80, tissue	Abcam Cat No- ab2435
TRAIL-R1	Recombinant anti-TRAIL-R1 antibody. Mouse monoclonal (IgG_1)	10µg/ml	Enzo Life Science Cat No- ALX-804-297A-C100
TRAIL-R2	Recombinant anti-TRAIL-R2 antibody. Mouse monoclonal (IgG_1)	10µg/ml	Enzo Life Science Cat No- ALX-804-298A-C100
CD44	Anti-H-CAM antibody Mouse monoclonal (IgG_{2a})	1:500	Millipore, USA Cat No- CBL154-20UL, Component of Cat No-SCR067
CD90	Anti-THY-1 antibody Mouse monoclonal (IgG_1)	1:500	Millipore, USA Cat No- CBL415-20UL, Component of Cat No-SCR067
CD146	Anti-MCAM antibody Mouse monoclonal (IgG_1)	1:500	Millipore, USA Cat No- MAB16985-20UL, Component of Cat No-SCR067
CD14	Anti-CD14 antibody Mouse monoclonal (IgG_1)	1:500	Millipore, USA Cat No- MAB1219-20UL, Component of Cat No-SCR067
CD19	Anti-CD19 antibody Mouse monoclonal (IgG_1)	1:500	Millipore, USA Cat No- MAB1794-20UL, Component of Cat No-SCR067
STRO-1	Anti-STRO-1 antibody Mouse monoclonal (IgM)	1:500	Millipore, USA Cat No- MAB4315-20UL, Component of Cat No-SCR067

Continued

Osteocalcin	Anti-Osteocalcin antibody Mouse monoclonal	1 µg/100µl	R & D System Part No- 962645, Component of Cat No- SC006
Aggrecan	Anti-Aggrecan antibody Goat polyclonal	1 µg/100µl	R & D System Part No- 962644, Component of Cat No- SC006
FABP-4	Anti-FABP-4 antibody Goat polyclonal	1 µg/100µl	R & D System Part No- 962643, Component of Cat No- SC006
ALP	Anti-Alkaline phosphatase antibody. Mouse monoclonal (IgG_1)	1 µg/100µl	R & D System Part No- 962647, Component of Cat No- SC008
Oct-4	Anti-Oct-3/4 antibody Goat polyclonal	1 µg/100µl	R & D System Part No- 962649, Component of Cat No- SC008
Nanog	Anti-Nanog antibody Goat polyclonal	1 µg/100µl	R & D System Part No- 963488, Component of Cat No- SC008
SSEA-1	Anti-SSEA-1 antibody Mouse monoclonal (IgM)	1 µg/100µl	R & D System Part No- 963489, Component of Cat No- SC008
SSEA-4	Anti-SSEA-4 antibody Mouse monoclonal (IgG_3)	1 µg/100µl	R & D System Part No- 962648, Component of Cat No- SC008

All primary antibodies are anti-human except FABP-4 which is anti-mouse.

Appendix 2

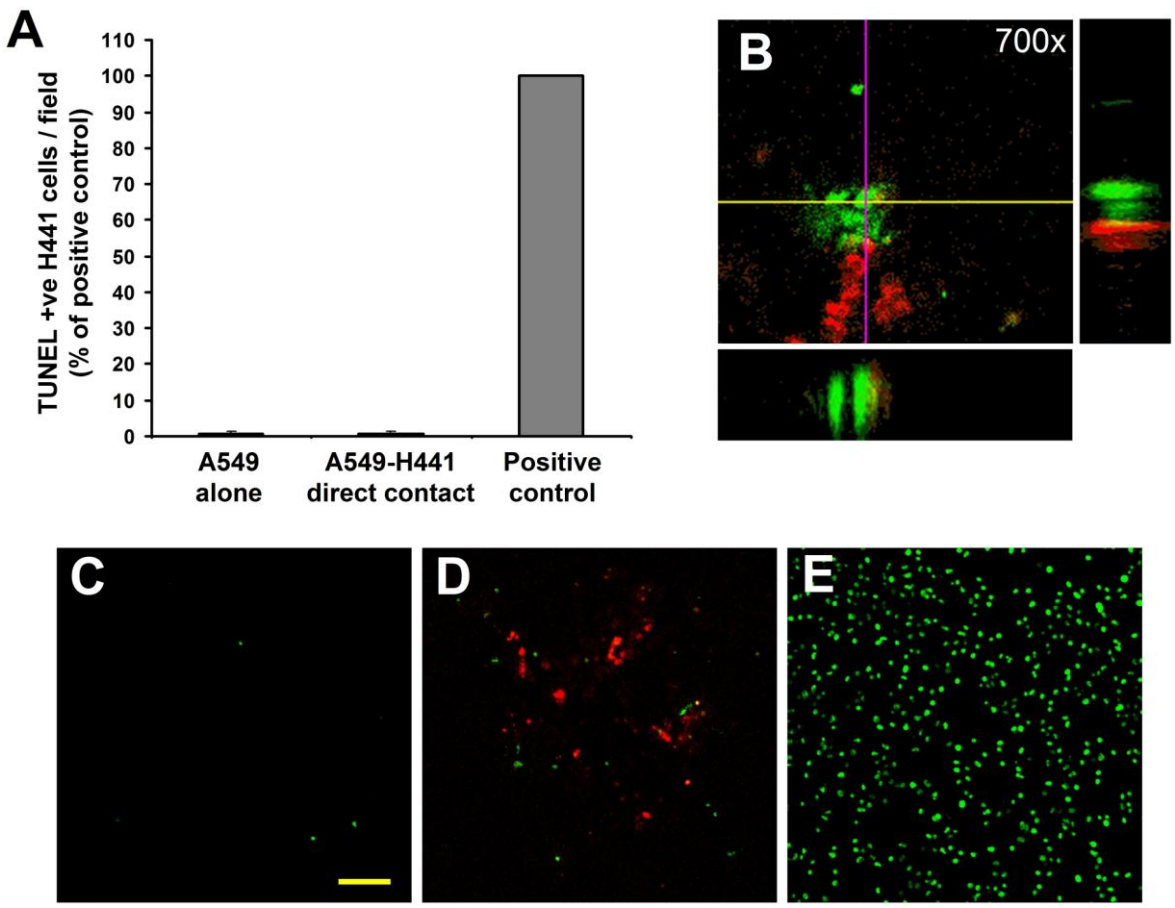

Figure S3.1: Assessment of apoptosis in migrated H441 cells in A549-H441 direct contact co-culture wound repair.

(**A**) Apoptosis in migrated H441 cells at juxta-wound monolayers after 24 hours of direct contact co-culture (n = 3 independent experiments). Negative control: apoptosis in A549 wounded monolayers cultured in SF-DMEM and positive control: apoptosis in A549 wounded monolayers cultured in 200 µM H_2O_2 for 24 hours. (**B**) Confocal laser Z-scanning shows juxta-position of cluster of TUNEL-positive nuclei of un-labelled A549 cells (Green nuclei) and TUNEL-negative migrated DiI-labelled H441 cells (Red) (image magnification, 700x). (**C**) Laser scanning confocal microscopic image show TUNEL positive un-labelled A549 cells in negative control. (**D**) Red cells are DiI-labelled migrated H441 cells and green nuclei are TUNEL positive nuclei in A549-H441 direct contact co-culture wound repair system after 24 hours. (**E**) Positive control. Scale bar, 100 µm (C, D, E).

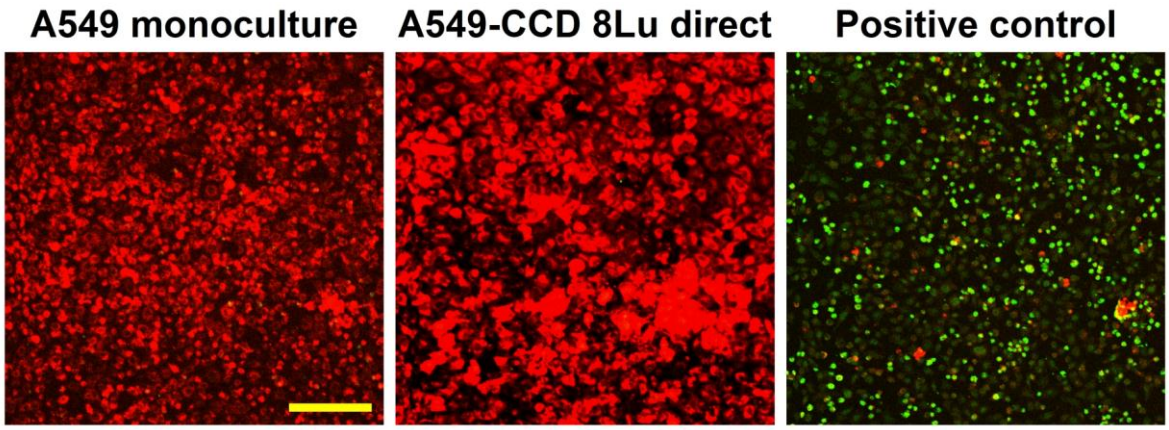

Figure S3.2: TUNEL assay on A549-CCD 8Lu direct-contact co-culture wound repair system. TUNEL positive cells were not observed in A549 cell population (Red) in the A549-CCD 8Lu direct-contact co-culture wound repair system and A549 monoculture (negative control). In positive control, apoptosis was induced in A549 cell monoculture with 200 µM H_2O_2 for 24 hours. A549 cells were labelled with DiI and green signal indicate TUNEL positive apoptotic nuclei. Scale bar, 200 µm.

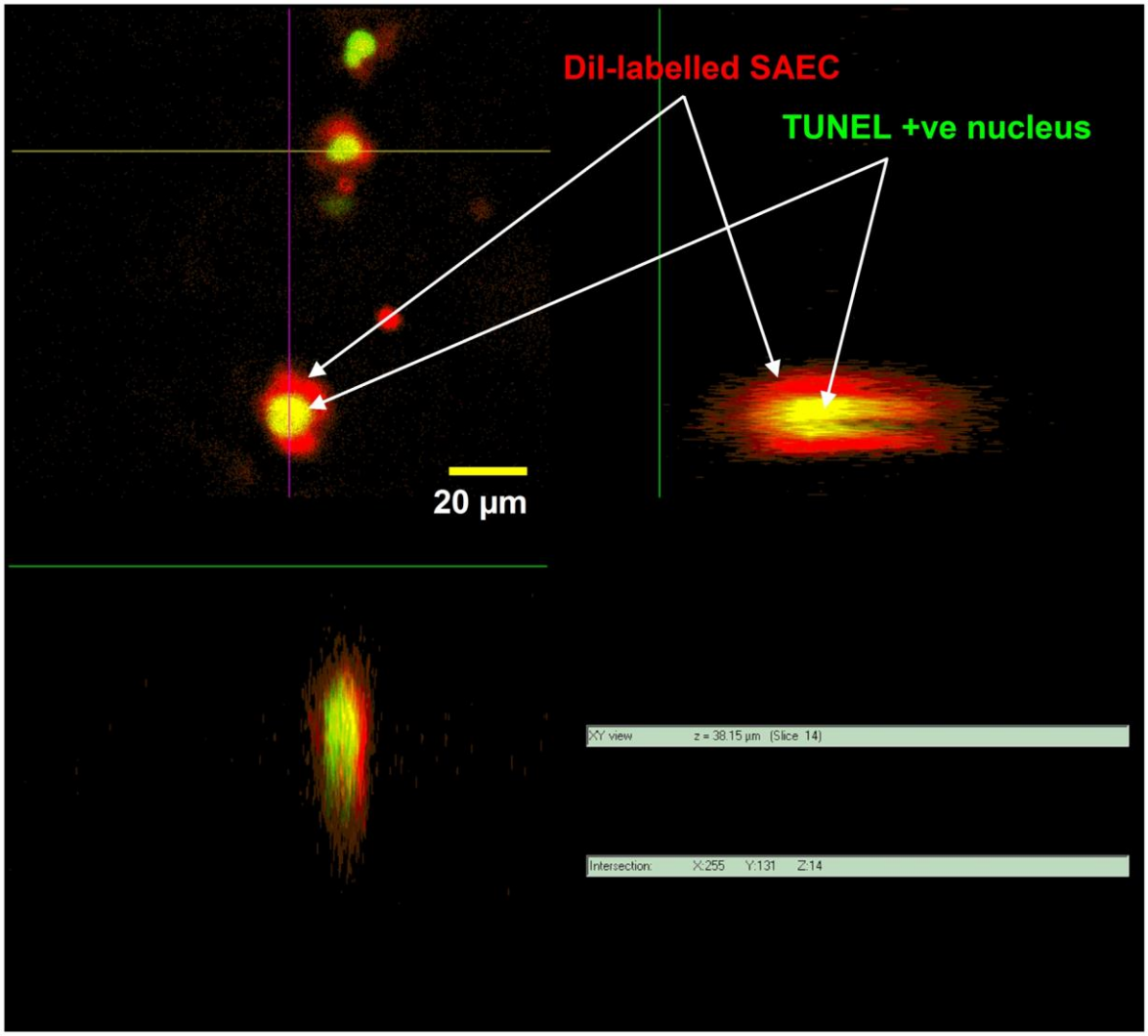

Figure S3.3: SAEC apoptosis in SAEC-H441 direct contact co-culture wound repair model. Laser scanning confocal Z-slicing demonstrates that TUNEL positive nuclei were confined within the DiI-labelled cells and hence confirms the apoptotic cells are SAECs. Image magnification 1000x.

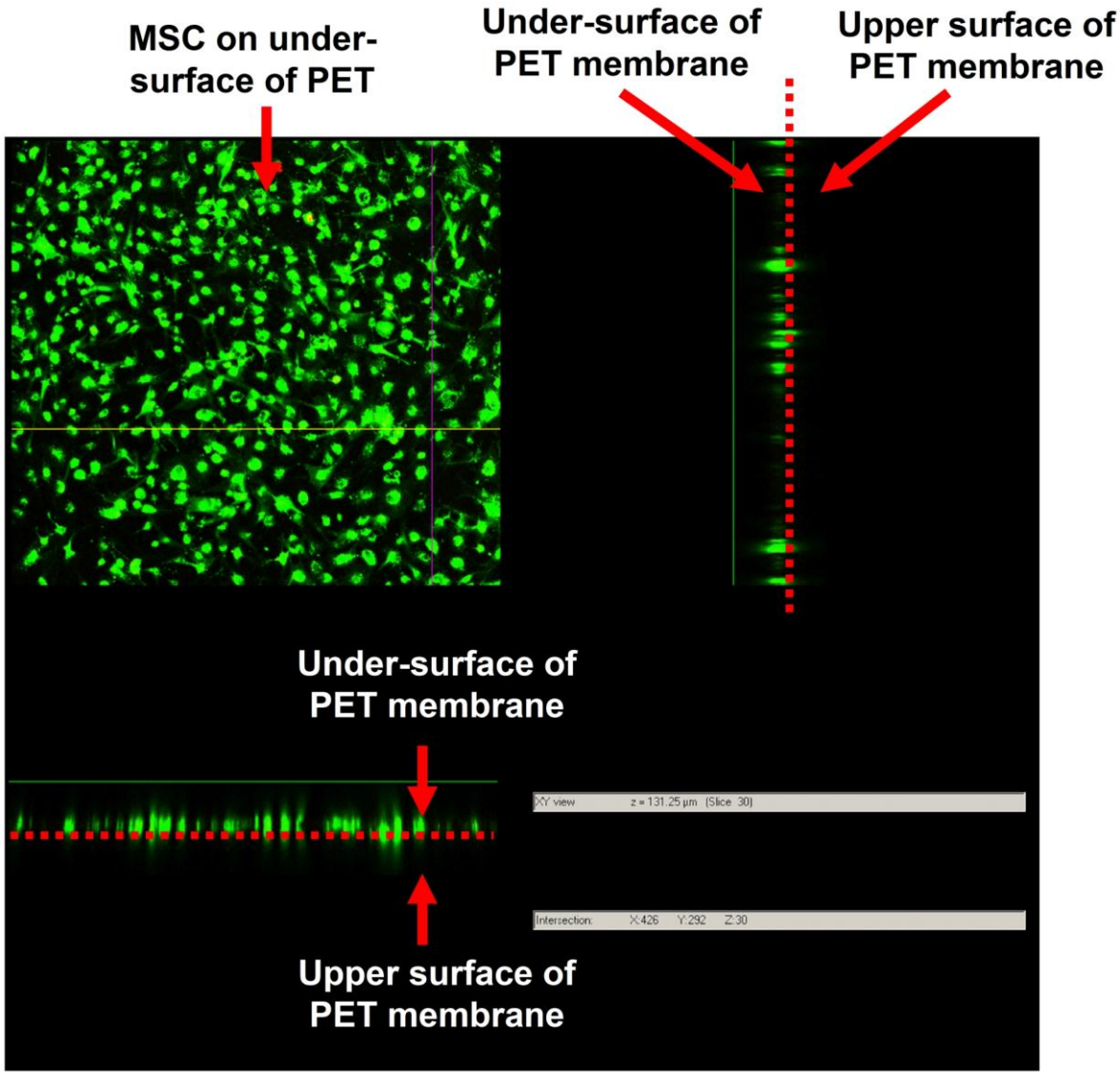

Figure S4.1: Migration of MSC towards contra-lateral surface of transwell PET membrane after 24 hours of culture in absence of A549 cells.

Table S4.1: Protein components of serum-free CCD-8Lu CM detected by LC-MS/MS mass spectrometry.

CCD-8Lu CM preparation was as described in the Section- 2.4.3, 2.5. Accession numbers are derived from MS/MS data searches against the non-redundant Human NCBI Protein Database.

Protein Name	Accession Number	Peptide Count	Ion Score C.I. %
Keratin, type II cytoskeletal 1	gi|1346343	4	99.99374889
Albumin preproprotein [Homo sapiens]	gi|4502027	5	99.99759033
Unnamed protein product [Homo sapiens]	gi|28317	5	99.76069218
Keratin 2 [Homo sapiens]	gi|47132620	3	99.99695241
Keratin 6B, isoform CRA_a [Homo sapiens]	gi|119617032	2	99.98225986
Alpha2-HS glycoprotein [Homo sapiens]	gi|2521981	2	99.96394569
Fibronectin precursor [Homo sapiens]	gi|31397	2	99.89359627
Keratin type II	gi|908801	2	98.12086939
Chain A, Structure Of Human Apolactoferrin	gi|4699853	1	99.5147597
Nebulin	gi|19856971	1	96.50089446

Table S4.2: Protein components detected in 10% KO-SR supplemented KO-DMEM by LC-MS/MS MALDI TOF/TOF mass spectrometry.

Detected proteins	Accession No	Peptide count
10% KO-SR in KO-DMEM (Un-conditioned media)		
Apolipoprotein A-I, apoA-1	gi|245563	11
Serum albumin	gi|1351907	7
Apolipoprotein C-III precursor [Bos Taurus]	gi|47564119	4
Chain A, Crystal Structure Of The First Active Autolysate Form Of The Porcine Alpha Trypsin	gi|1942351	3
Haemoglobin subunit alpha [Bos Taurus]	gi|116812902	3
Chain A, The Crystal Structure Of Modified Bovine Fibrinogen	gi|6980814	2
Complement C4	gi|31563307	2
Alpha-2-HS-glycoprotein precursor [Bos Taurus]	gi|27806751	1
Albumin [Felis catus]	gi|30962111	3
Haemoglobin subunit alpha [Homo sapiens]	gi|4504345	3
Haemoglobin subunit alpha-3	gi|122299	3
Haemoglobin alpha	gi|122413	2
Serotransferrin	gi|2501351	2
Chain D, Human Insulin Hexamers With Chain B His Mutated To Tyr Complexed With Phenol	gi|5542375	2
Kininogen L, high MW	gi|225724	3
Complement component 3 [Bos taurus]	gi|4093220	1
Haemoglobin subunit alpha-1/2	gi|122449	1
Hepatocyte growth factor activator preproprotein [Homo sapiens]	gi|4504383	1
Complement C3	gi|116597	1
Chain B, Structural Properties Of The B25tyr-Nme-B26phe Insulin Mutant.	gi|61680182	2
Haemoglobin subunit alpha	gi|122500	2
Alpha-1-globin [Mus musculus]	gi|553919	2
Angiotensinogen	gi|113876	1
Serum amyloid A2 [Pongo abelii]	gi|197101992	2
Serum amyloid A protein [Canis lupus familiaris]	gi|164060	2
Insulin precursor [Felis catus]	gi|57163807	2
Serpin A3-1 precursor [Bos taurus]	gi|31340900	3

Proteins were tabulated with total Ion score C.I. 100% to >95% in a descending manner. Accession numbers are of NCBI protein database.